2012

Protein Phosphatase 1 at the Kinetochore Regulates Chromosome Segregation

Jessica Scott Rosenberg

PROTEIN PHOSPHATASE 1 AT THE KINETOCHORE REGULATES CHROMOSOME SEGREGATION

A Thesis Presented to the Faculty of

The Rockefeller University

in Partial Fulfillment of the Requirements for

the degree of Doctor of Philosophy

by

Jessica Scott Rosenberg

June 2012

PROTEIN PHOSPHATASE 1 AT THE KINETOCHORE REGULATES CHROMOSOME SEGREGATION

Jessica Scott Rosenberg, Ph.D.

The Rockefeller University 2012

Two regulatory mechanisms exist to ensure proper chromosome segregation in mitosis. First, improper kinetochore-microtubule attachments are destabilized through the error correction machinery. Second, the spindle assembly checkpoint (SAC) delays anaphase onset until all kinetochores have achieved bioriented microtubule attachments. Both of these mechanisms are mediated by several centromeric and kinetochore kinases, including Aurora B. Protein Phosphatase 1 (PP1) plays a counteracting role to Aurora B to stabilize kinetochore-microtubule attachments and silence the SAC. The regulation of PP1 to modulate these functions, however, remains enigmatic.

Using the biochemical tools available in the *Xenopus* egg extract system, I show here that PP1 binds to the protein KNL1 (Spc105, Blinkin, CASC5) through an evolutionarily conserved RVxF motif. KNL1 is a member of the KMN network that forms the microtubule binding interface at the kinetochore. Using the genetic tools of *Saccharomyces cerevisiae*, I show that this interaction is essential for silencing the SAC, but has only a minimal effect on kinetochore-microtubule stability. Although phosphorylation of KNL1 by Aurora B can abrogate the KNL1-

PP1 interaction, constitutive recruitment of PP1 by KNL1 is insufficient to prematurely silence the SAC. However, the amount of PP1 recruited to the kinetochore is tightly tuned, as targeting just one extra copy of PP1 to KNL1 is lethal.

The data presented here leads to a model in which the KNL1-PP1 interaction acts to couple microtubule attachment with SAC signaling. Specific properties of the N-terminus of KNL1 may modulate this coupling, possibly though conformational changes upon microtubule attachment. In addition, there have been several other proteins found to recruit PP1 to the kinetochore, and how these regulatory subunits might cooperate to mediate the functions of PP1 will be discussed.

ACKNOWLEDGMENTS

First and foremost I would like to express my deep gratitude to my graduate advisors, Dr. Hiro Funabiki and Dr. Fred Cross. They have taught me how to think critically, scrutinize every assumption, and generally think like a good scientist. Through them I have learned that if you are passionate about your work and life you will always be successful.

I would also like to thank all the members of the Funabiki and Cross labs, both past and present. Alex Kelly helped me begin my project and taught me all the frog-whispering techniques necessary to make “good” extract. Boo Shan Tseng always gave me a pat on the back when I needed it. Jon Robbins taught me that graduate school is not about success, but rather momentary lack of failure that eventually adds up to a thesis. John “RC” Xue, with his infinite worldly wisdom, was the best bay-mate I could ask for. And of course the fabulous technicians, Kresti Pecani, Nina Soares, and Adriana Garzon, have made everything run smoothly and created a great environment in which to work.

All of my friends at Rockefeller, in New York City, and beyond have provided invaluable emotional support throughout my life. My family has always been behind me, even when they didn’t quite understand what I was thinking. Finally, my deepest love and gratitude goes to my partner, Akash Kumar, for the life we have together.

TABLE OF CONTENTS

LIST OF FIGURES

LIST OF TABLES

LIST OF ABBREVIATIONS

ab	antibody
APC/C	anaphase promoting complex/cyclosome
ATP	Adenosine-5'-triphosphate
BB	binding buffer
BSA	bovine serum albumin
cat	catalytic mutant
CCAN	constitutively centromere-associated network
CDK	cyclin dependent kinase
c-Mad2	closed Mad2
CPC	chromosomal passenger complex
CSF	cytosolic factor
DAPI	4',6-diamidino-2-phenylindole
DTT	dithiothreitol
DMSO	dimethyl sulfoxide
dox	doxycycline
EDTA	ethylenediaminetetraacetic acid
FPLC	fast protein liquid chromatography

FWHM	Full-width half maximum
GFP	green fluorescent protein
GST	glutathione *S*-transferase
HEPES	4-(2-hydroxyethyl)-1-piperazineethanesulfonic acid
HGR	HO-induced gene replacement
IF	immunofluorescence
IgG	immunoglobulin G
IP	immunoprecipitation
IPL	increase in ploidy
KLH	keyhole limpet hemocyanin
KMN	KNL1, MIS12, and NDC80
MBP	maltose binding protein
MCC	mitotic checkpoint complex
noc	nocodazole
OA	okadaic acid
OD	optical density
o-Mad2	open Mad2
PBS	phosphate buffered saline
PCR	polymerase chain reaction

PKA	protein kinase A
pNPP	*p*-nitrophenyl phosphate
PP1	Protein Phosphatase 1
PP2A	Protein Phosphatase 2A
RBM	RVxF binding mutant
SAC	spindle assembly checkpoint
SCA	single cell colony assay
SDS	sodium dodecyl sulfate
SP FF	SP sepharose fast flow
TBS	tris-buffered saline
TCEP	*tris*(2-carboxyethyl)phosphine
tet^R	tetracycline repressable
TRIS	tris(hydroxymethyl)aminomethane
WB	Western blot
WT	wild type
YEPD	yeast extract peptone dextrose

CHAPTER 1: BACKGROUND

Cellular division

The cell cycle

One of the most fundamental properties of a cell is the ability to self-replicate through the process of the cell cycle. This cycle consists of an ordered series of events that duplicate the genetic material of the cell and then segregate it to two daughter cells. This process and its regulation are essential for the propagation of all cells, both of single-cell organisms such as yeast and within multi-cellular organisms such as humans.

The cell cycle is broadly broken up into two phase, interphase and mitosis. Interphase is further broken up into two growth phases, G1 and G2, separated by S-phase in which the DNA is replicated. In mitosis, the replicated DNA is segregated and then two separate daughter cells containing the full genomic complement are formed. The duration of all phases, particularly G1 and G2, varies greatly among organisms and cell types; however, the order of events is tightly controlled and conserved in most cells.

A network of kinases called cyclin-dependent kinases (CDKs) and their activators, cyclins, regulate the ordering and timing of cell cycle events (Norbury and Nurse, 1992). Most organisms have between one and four CDKs, but they all must bind a cyclin to be active. Cyclins bind to CDKs to both activate the catalytic activity and confer substrate specificity. The protein levels of cyclins

oscillate with the cell cycle, and cyclins are broadly classified by the cell cycle phase or transition during which they show peak abundance: either G1, G1/S, S, or M. The cyclin/CDK complex that forms during each phase regulates the execution and timing of specific events. The proper production and destruction of cyclins, therefore, is essential to cell cycle control and progression.

The mitotic spindle

The essential function of mitosis, the segregation of duplicated chromosomes, is achieved by the mitotic spindle. The spindle, formed during metaphase, is made up of a network of proteins and microtubules surrounding the DNA. The plus ends of the microtubules attach to the chromosomes, while the minus ends gather together on either side in spindle poles (Figure 1-1A). The duplicated chromosomes, individually referred to as sister chromatids, are connected to each other by a protein complex called cohesin (Michaelis et al., 1997). In order to ensure that each daughter cell gets a full complement of the genome, each sister chromatid must be attached to microtubules emanating from opposite poles (Figure 1-B).

Anaphase

Anaphase is the stage of mitosis during which sister chromatids are pulled to opposite poles. Biochemically, the transition from metaphase to interphase is characterized by the activation of the Anaphase Promoting Complex/Cyclosome

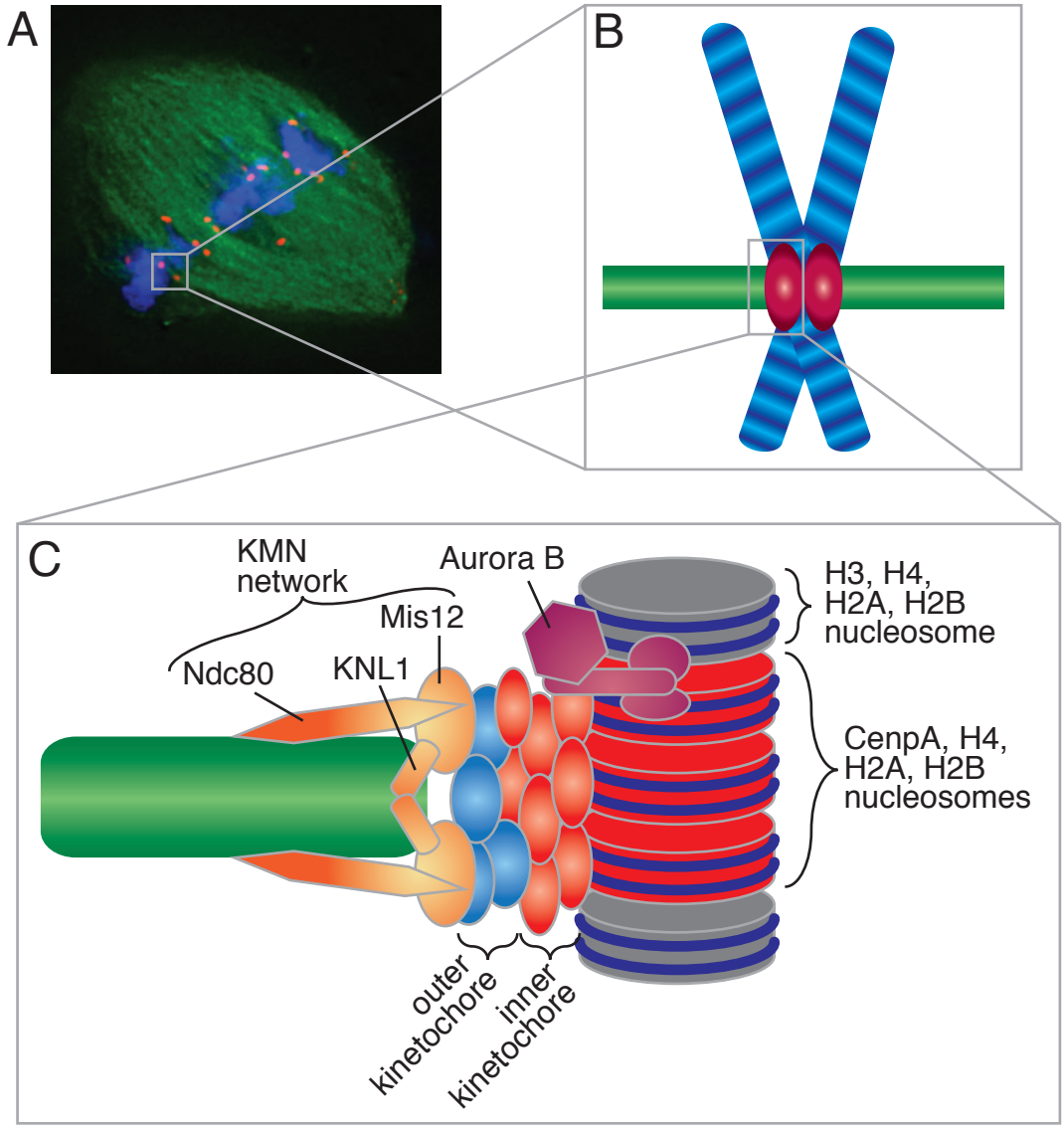

Figure 1-1: Biorientation on the mitotic spindle. (A) Immunoflorescence of a mitotic spindle assembled in *Xenopus laevis* egg extracts. Microtubules are in green, DNA is in blue, and centromeres are in red. (B) Schematic representation of a bioriented chromosome. (C) Schematic representation of the kinetochore components important for this study in the state of microtubule attachment.

(APC/C), an E-3 ubiquitin ligase that targets proteins for destruction. One major target is the mitotic cyclin, Cyclin B. Cyclin B proteolysis in metaphase reduces CDK activity, allowing eventual progression out of metaphase and into the subsequent interphase (Irniger et al., 1995). Another essential target of the APC/C is Pds1/securin, the destruction of which triggers the dissolution of sister chromatid cohesion (Ciosk et al., 1998). This allows sister chromatids to be pulled by spindle microtubules to opposite poles, thus segregating the genome.

Achieving proper genomic segregation

Centromeres

On each chromosome there is a specific region, called the centromere, upon which is built the machinery that facilitates attachment to microtubules (reviewed in Verdaasdonk and Bloom, 2011). Centromeres are distinguished from the rest of the chromosome by the presence of a histone variant, CENP-A, incorporated into the nucleosomes (Sullivan et al., 1994). In budding yeast, the location of the centromere is defined by a specific DNA sequence (Clarke and Carbon, 1980, 1983). In many higher eukaryotes, however, the DNA at the centromere is characterized by arrays of satellite repeats (Choo, 2001; Schueler et al., 2001). DNA sequence alone can contribute, but is not sufficient to determine the location of the functional centromere. There are several histone modifications that are associated with centromeres, and at least one of these marks directly facilitates CENP-A deposition (Bergmann et al., 2011).

Furthermore, it has been hypothesized that there is a "memory" to propagate centromere identification that acts during DNA replication. This could act through epigenetic marks, the presence of licensing factors, or chromatin structure. Definition and maintenance of the centromere, therefore, is a complicated process and still not fully understood.

Kinetochores

The kinetochore is group of proteins that facilitates the interaction between microtubules and the chromosome. A group of proteins called the constitutively centromere-associated network (CCAN) recognizes CENP-A as well as other centromere-defining features and makes up the inner kinetochore. These proteins in turn recruit the machinery that forms attachments to microtubules and comprises the outer kinetochore. The kinetochore as a whole is made up of approximately 80 proteins in humans (Figure 1-1C, reviewed in Cheeseman and Desai, 2008) and there are ongoing efforts that may add more to this list.

Several kinetochore proteins have been specifically identified for their ability to directly interact with microtubules. In fungi, the Dam1 complex forms a ring around microtubules and also facilitates the kinetochore-microtubule attachment (Cheeseman et al., 2001a; Westermann et al., 2005). However, no clear homologue of Dam1 has yet been found in higher eukaryotes. Most organisms studied thus far, however, have a version of the KMN complex, which is comprised of KNL1, and the MIS12 and NDC80 complexes. The KMN network

constitutes the core conserved microtubule binding machinery (Cheeseman et al., 2006; Cheeseman et al., 2004). The MIS12 complex facilitates localization of the KMN network to the kinetochore, while the NDC80 complex and KNL1 directly bind to microtubules. This network forms an attachment to the dynamic plus end of the microtubule, and this attachment must be stable enough to persist when the microtubule is growing or shrinking.

Specifically, KNL1 was first identified in a screen for "kinetochore null" mutants, and RNAi of KNL1 abolishes kinetochore-microtubule interactions (Desai et al., 2003). KNL1 recruitment is downstream of centromere assembly (Cheeseman et al., 2004). KNL1 has the ability to directly bind microtubules *in vitro*, but the binding acts cooperatively with the NDC80 and MIS12 complexes (Cheeseman et al., 2006). Homologues in fission and budding yeast, Spc7 and Spc105 respectively, were identified by functional homology (Kerres et al., 2007; Liu et al., 2005; Nekrasov et al., 2003).

Despite the evolutionary distance and many fundamental cellular and biochemical differences between yeast and mammals, many of the proteins that make up both the inner and outer kinetochore are strikingly conserved. While yeast kinetochores bind a single microtubule (O'Toole et al., 1999; Peterson and Ris, 1976), mammalian kinetochores bind between 15 and 20 (McEwen et al., 1997). However, it is thought that the yeast kinetochore represents a single microtubule-binding unit that is replicated in the larger mammalian structure

(Zinkowski et al., 1991). Therefore, the study of the yeast kinetochore has helped to elucidate the human kinetochore.

Microtubule capture and error correction

The major function of the kinetochore is to attach chromosomes to the microtubules that will ultimately pull them to opposites poles. In order to ensure that each daughter cell gets a full genomic complement, therefore, it is imperative that kinetochores on sister chromatids attach to microtubules emanating from opposite poles, a configuration known as biorientation. However, microtubule capture by kinetochores is a stochastic process. First, chromosomes interact with the lateral surface of microtubules through one of the kinetochores, and are then pulled along the microtubule towards the pole by motor proteins (Hayden et al., 1990; Rieder and Alexander, 1990; Tanaka et al., 2005). In yeast, it appears the motor protein responsible for this movement is Kar3 (Tanaka et al., 2005), while in mammals there is evidence that dynein plays a major role (Echeverri et al., 1996; Howell et al., 2001). It is likely that a combination of motor proteins have varying contributions to the movement. During this pole-ward movement, the kinetochore transitions from lateral to end-on attachment, which is stabilized by the KMN network. The chromosome is then congressed towards the metaphase plate in the middle of the spindle, and at some point during the process, the other kinetochore is also captured by microtubules. The motor protein CENP-E mediates chromosome movement towards the metaphase plate,

and it can cause chromosome movement even when only one kinetochore is attached (Kapoor et al., 2006; Kim et al., 2008).

Throughout this process of chromosome movement, kinetochore-microtubule attachments are dynamic, so it is not inherently obvious how this process would lead to biorientation. The chromatin structure at the centromere does introduce a geometric bias towards biorientation, but this is not enough to ensure that all chromosomes will be bioriented upon initial microtubule capture (Sakuno et al., 2009). Indeed, it has been observed that this process can lead to incorrect kinetochore-microtubule attachments that need to be corrected (Nicklas and Ward, 1994). Two of the three major classes of incorrect kinetochore-microtubule attachment configurations are monotelic and syntelic. In monotelic attachments, only one kinetochore is attached to a microtubule. In syntelic attachments, both kinetochores are attached to microtubules emanating from the same poles. These incorrect attachments can be recognized by the cell as either lacking attachment (monotelic) or lacking tension across centromeres (syntelic) (figure 1-2). All such kinetochore-microtubule attachment configurations would lead to incorrect chromosome segregation once anaphase was initiated.

To overcome this, as attachments are being made, there is a regulatory network promoting “error correction”. The preferential destabilization of incorrect attachments is mediated by the kinase Aurora B, located at the centromere (Cimini et al., 2006a; Hauf et al., 2003). Aurora B achieves this by phosphorylating members of the KMN network, thus decreasing their affinity for

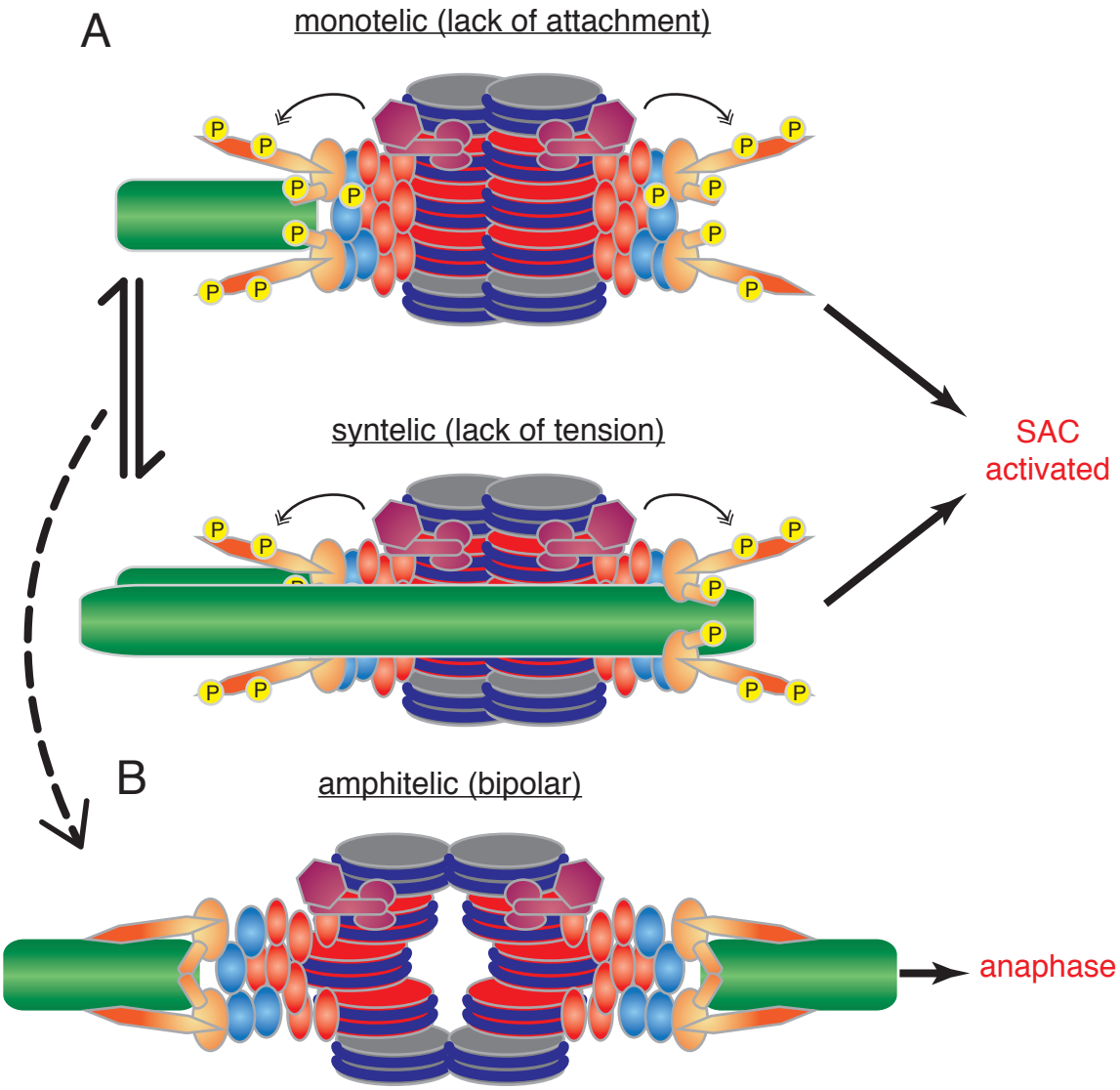

Figure 1-2: Error correction and SAC signaling. (A) Schematic representations of kinetochores in incorrect microtubule attachment configurations. In both cases, the KMN network (orange) is phosphorylated by Aurora B (purple) to promote attachment destabilization, turnover, and correction and to initiate SAC signaling. (B) Only upon amphitelic (bipolar) attachment are kinetochore-microtubule interactions stabilized by dephosphorylation of the KMN network, and is the SAC silenced so that anaphase can proceed.

microtubules (DeLuca et al., 2006; Welburn et al., 2010). In addition, Aurora B phosphorylates Dam1 in budding yeast with similar results (Cheeseman et al., 2002; Keating et al., 2009). Through this destabilization, incorrect attachments can be released and reformed until proper bioriented attachments have been achieved. Once this occurs, the dephosphorylation of the KMN network reverses this process to form stable interactions with microtubules.

The spindle assembly checkpoint

Through careful study of the cell cycle in budding yeast, it was found that cells treated with microtubule poisons arrest in metaphase through a mechanism now known as the spindle assembly checkpoint (SAC) (Jacobs et al., 1988). This arrest persists until all kinetochore pairs have achieved bioriented microtubule attachment (Rieder et al., 1994). The SAC signal originates at the kinetochore (Rieder et al., 1995) and is activated by the same incorrect microtubule attachment configurations discussed above that can initiate the error correction mechanism. These configurations are recognized either as a lack of attachment or a lack of tension across kinetochores (see Figure 1-2). Two seminal studies resulted in a catalogue of the proteins involved in this process (Hoyt et al., 1991; Li and Murray, 1991). Although the mechanisms of the triggering and silencing of the SAC signal remains a complex area of research to be discussed in later sections, the nature of the diffusible signal emanating from

the kinetochore has been elucidated (reviewed in Musacchio and Salmon, 2007, figure 1-3).

The ultimate target of the SAC is the APC/C, which promotes entry into anaphase. The APC/C requires a co-factor, Cdc20, in order to be activated. The SAC functions by forming an inhibitory complex of Mad2, BubR1/Mad3, and Bub3 with Cdc20, called the mitotic checkpoint complex (MCC) (Sudakin et al., 2001). This complex will only form if Mad2 has adopted a conformation change that occurs at the kinetochore (Tipton et al., 2011). This change is mediated by Mad1, which is localized to unattached kinetochores. Mad1 facilitates the conversion of Mad2 from an open to a closed conformation (o-Mad2 to c-Mad2) (Luo et al., 2002; Sironi et al., 2002). c-Mad2 can then diffuse from the kinetochore, where it can bind Cdc20 and complete the MCC. In addition, c-Mad2 can self-propagate, converting other o-Mad2 proteins into c-Mad2, thus creating a diffusible template that propagates the signal from the kinetochore to the pool of free proteins (Nasmyth, 2005). The MCC can only form with the c-Mad2 conformation, thus sequestering Cdc20 and preventing APC/C activation only in the presence of incorrectly attached kinetochores. Interestingly, several of these and other SAC proteins have been implicated in cellular roles independent of SAC signaling, particularly in kinetochore-microtubule attachment stabilization (Gillett et al., 2004; Lampson and Kapoor, 2005; Logarinho and Bousbaa, 2008).

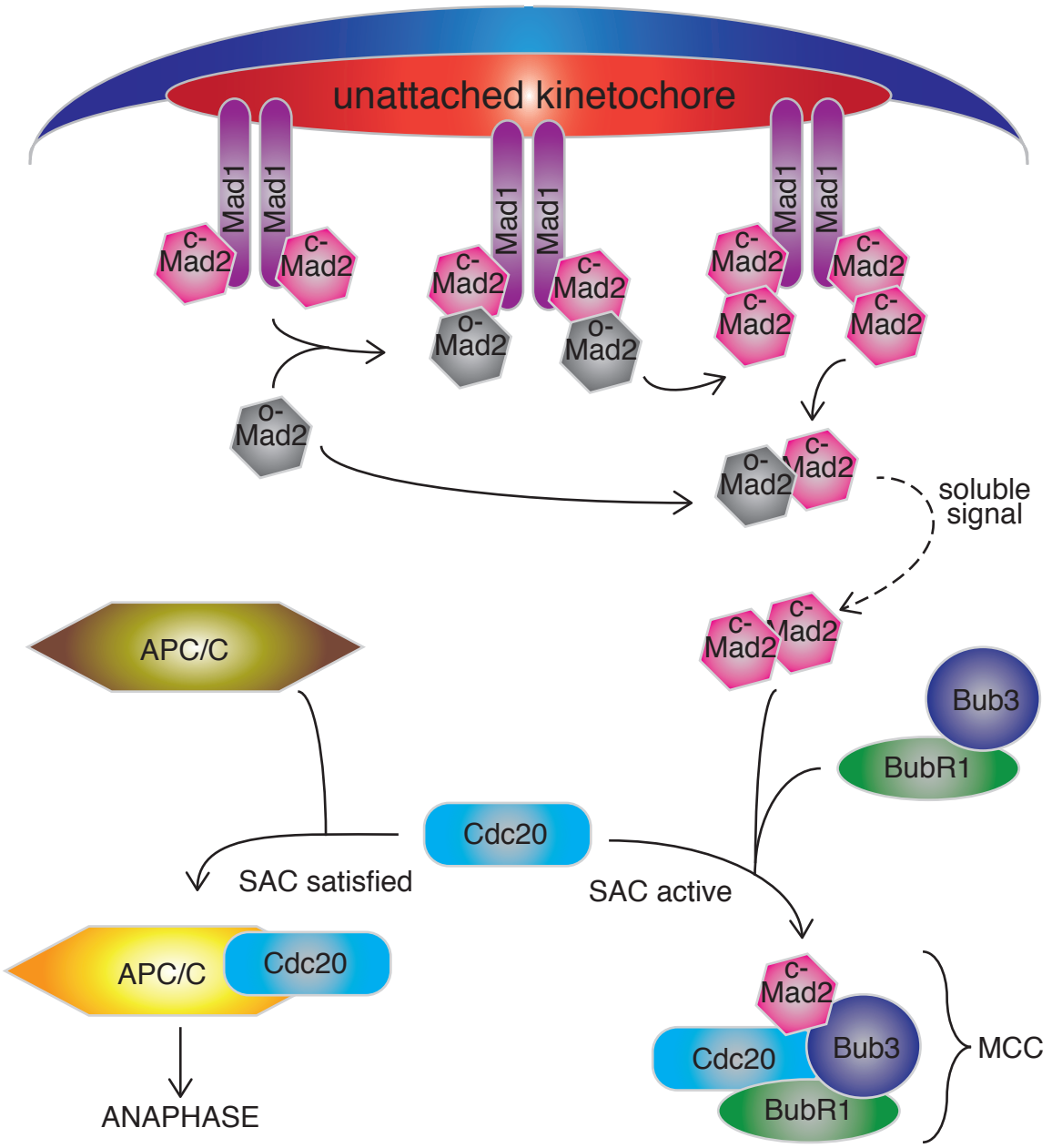

Figure 1-3: The molecular mechanism of SAC signaling. Mad1 bound to c-Mad2 accumulates at unattached kinetochores. This facilitates the conversion of o-Mad2 into c-Mad2, which then becomes a soluble signal by further converting other o-Mad2 into c-Mad2. c-Mad2, but not o-Mad2, can bind Cdc20 along with Bub3 and BubR1 to form the mitotic checkpoint complex (MCC). This sequesters Cdc20 from activating the APC/C when SAC signaling is present, thus preventing the transition into anaphase.

Merotelic attachments

A third class of kinetochore-microtubule attachment configuration, merotelic attachment, occurs when one kinetochore is attached to one pole, but the other kinetochore is attached to both poles. This configuration is unique in that it is fully attached and still produces some level of tension across kinetochores. Consequently, the detection mechanisms discussed above cannot recognize this configuration, and the SAC is not activated. However, it is imperative that merotelic attachments are corrected, as it is a major source of chromosome missegregation and aneuploidy (Cimini et al., 2001).

There is clear evidence that merotelic attachments do get corrected in metaphase (Cimini et al., 2002; Cimini et al., 2003), and that this correction is also dependent on Aurora B-mediated destabilization of kinetochore-microtubule attachments (Cimini et al., 2006b; Knowlton et al., 2006). Additionally, a complex in fungi, the monopolin complex, facilitates correct kinetochore-microtubule attachments by bundling microtubule attachment sites so they have the same orientation. This has been shown to be critical for preventing and correcting merotelic attachments (Corbett et al., 2010; Gregan et al., 2007; Rabitsch et al., 2003). Although no homologues for the monopolin complex proteins have been found in mammals, structural analysis indicates that members of the NDC80 complex may play a similar role (Rumpf et al., 2010).

In addition to mechanisms to correct merotelic attachments in metaphase, there is evidence that spindle forces in anaphase can facilitate the breakage of

the incorrect attachment (Cimini et al., 2004). Microtubule associated motor proteins play a critical role in facilitating this mechanism of correction (Choi and McCollum, 2012). Collectively, these mechanisms correct merotelic attachments by first weakening the incorrect microtubule attachment, and then attachments that have not been fully disconnected will break in anaphase. This apparently two-step process facilitates the correction of these attachments even when they are invisible to the SAC.

Mitotic phosphorylation

Many of the regulatory pathways controlling mitosis are mediated by protein phosphorylation. This modification changes protein properties such as localization, binding partners, or catalytic activity of an enzyme. These property changes facilitate ordering and coordination of events as well as the proper functioning of mitotic cellular structures. In an attempt to elucidate mitotic pathways, massive phospho-proteomic studies have attempted to catalogue all of the phosphorylation events occur in mitosis (Dephoure et al., 2008; Nousiainen et al., 2006). In a different approach, specific pathways have been studied by scrutinizing the kinases involved, examining its mitotic functions and substrates (reviewed Ma and Poon, 2011). Here, I will highlight the kinases that act specifically at the kinetochore in metaphase and our current understanding of their functions and substrates.

Kinases that act at the kinetochore

The fact that the kinase Aurora B plays a critical role at the kinetochore to ensure proper chromosome segregation has long been established. Aurora B acts in a protein complex with Survivin, Incenp, and Dasra/Borealin (hereafter referred to as Dasra) called the chromosomal passenger complex (CPC), named as such for its dynamic localization throughout the course of mitosis (reviewed in Ruchaud et al., 2007). The CPC accumulates on chromosomes in prophase, is concentrated at the centromere in prometaphase and metaphase, then moves to the spindle midzone after initiation of anaphase and to the midbody in telophase. As mentioned above, Aurora B mediates the destabilization of incorrect kinetochore-microtubule attachments and error correction through phosphorylation of members of the KMN network. In addition, Aurora B is necessary for the initiation of SAC signaling and for the preferential localization of SAC proteins to incorrectly attached kinetochores (Vigneron et al., 2004).

Concurrent with the elucidation of the role that Aurora B plays at the kinetochore, a growing list of other kinases have been found to also function similarly within the same processes. Some of these kinases work directly through modulating the localization of Aurora B itself. Haspin kinase phosphorylates histone H3-serine 3 at the centromere, which promotes Aurora B localization (Kelly et al., 2010; Wang et al., 2010; Yamagishi et al., 2010). Cdk1/Cyclin B phosphorylates the CPC member Survivin in fission yeast, which is also required to target Aurora B to the centromere (Tsukahara et al., 2010). In

addition, it phosphorylates Dasra in human cells, although the functional significance of this mark in relation to the activity of the CPC at the kinetochore is unknown (Date et al., 2012).

Other kinases at the kinetochore appear to have similar functions to those of Aurora B. Polo/Plk1 phosphorylates BubR1 (Elowe et al., 2007; Matsumura et al., 2007) and is required both for accumulation of SAC proteins at the kinetochore (Ahonen et al., 2005; Wong and Fang, 2005), and for stabilizing kinetochore-microtubule attachments (Sumara et al., 2004; van Vugt et al., 2004). The kinase Mps1 facilitates SAC signaling (He et al., 1998; Weiss and Winey, 1996) by mediating the localization of the Mad1/Mad2 complex to incorrectly attached kinetochores (Hewitt et al., 2010; Tighe et al., 2008). In addition, Mps1 is required to form stabilized, bioriented attachments and for the error correction mechanism (Jones et al., 2005; Maure et al., 2007). Bub1 and Nek2A are two other kinases that are known to be involved in both SAC signaling and stabilization of kinetochore-microtubule attachments (Du et al., 2008; Meraldi and Sorger, 2005; Wei et al., 2011), and Nek2A is also required for Mad1 localization (Lou et al., 2004). Bub1 is unique in that it also promotes the localization of shugoshin, which protects centromeric cohesion until anapahse through phosphorylation of histone H2A-serine 121 (Kawashima et al., 2010).

Interplay of kinase pathways

Based on current knowledge, there appears to be an excess of kinases over functions at the kinetochore, a "kinase paradox." For two major functions (error correction and SAC activation), we have at least five kinases that appear to be directly involved (figure 1-4). There may be simple redundancy of the pathways, but there is growing evidence that the signaling pathways interact with each other in a more direct way. For example, one of the most well characterized phospho-proteins at the kinetochore is Ndc80, phosphorylation of which is necessary for both error correction and SAC activation. Nek2A (Du et al., 2008; Wei et al., 2011), Aurora B (Akiyoshi et al., 2009a), and Mps1 (Kemmler et al., 2009) all phosphorylate Ndc80 on separate but overlapping sets of residues. In another example, both Aurora B and Polo phosphorylate BubR1 (Rancati et al., 2005). The physiological consequences of multiple pathways converging on a single target have yet to be elucidated.

Aside from converging on a shared target, several kinase pathways are required for the function of others. In addition to Haspin and Cdk1/Cyclin B mentioned above, Plk1 and Mps1 regulate Aurora B activity through other members of the CPC. Plk1 physically interacts with Incenp at the centromere (Carmena et al., 2012; Goto et al., 2006), and Mps1 phosphorylates Dasra (Jelluma et al., 2008). Conversely, Aurora B itself is required for the localization of Mps1 and Bub1 (Vigneron et al., 2004). Finally, Mps1 is required for Plk1 kinetochore targeting (Wong and Fang, 2005). These are just some of the known

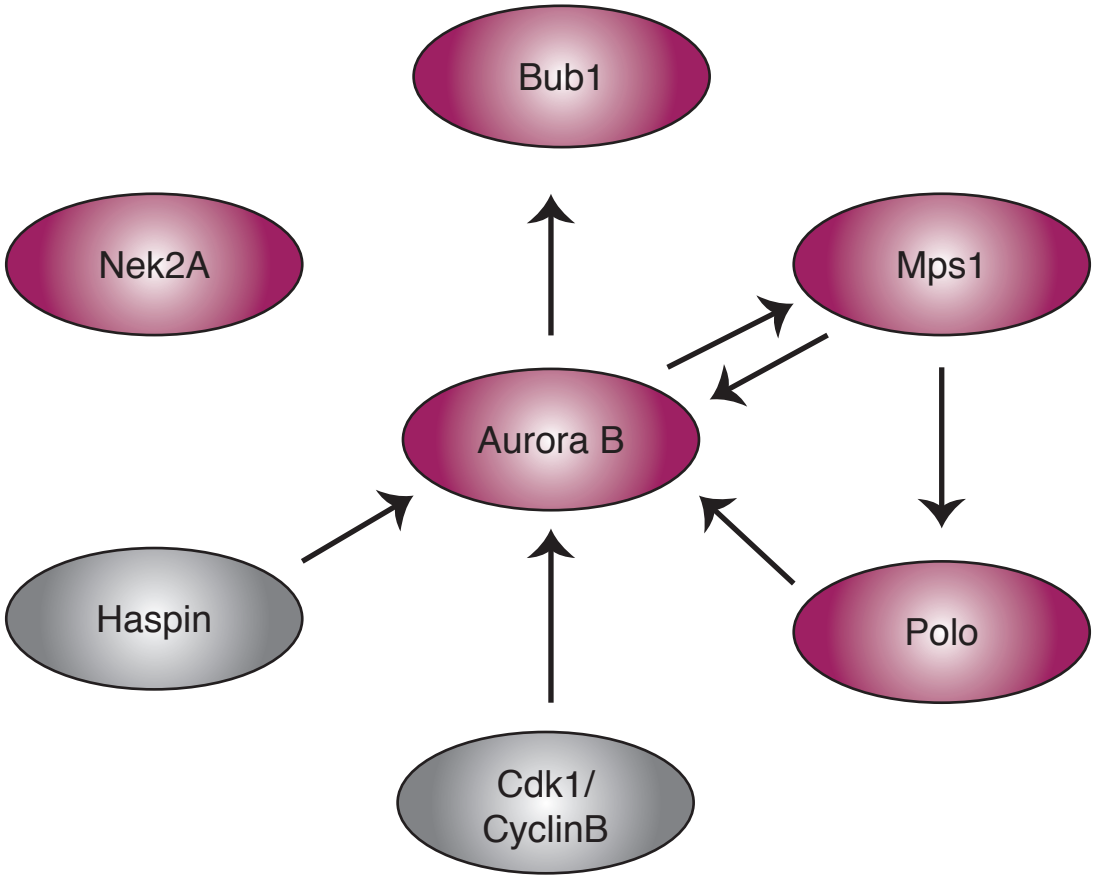

Figure 1-4: Interplay of kinases at the kinetochore. Schematic representation of the relationships between kinases that act at the kinetochore. For kinases in purple, there is evidence of a direct role in SAC activation and error correction. Arrows indicate the requirement of one kinase (base) for the localization of another kinase (arrow head).

functional connections between kinases, and these interdependencies point to a complex regulatory network not yet fully understood.

SAC activation: tension versus attachment

As mentioned above, an established function of several kinetochore kinases is to activate SAC signaling. Specifically, Polo, Aurora B, and Mps1 all appear to be significant for the recruitment of checkpoint proteins to kinetochores, which initiates the signal when the SAC is active. What triggers this signaling and the molecular mechanism of its transduction, however, remains widely enigmatic and fiercely debated.

Early studies of SAC signaling indicated that it could be triggered either by unattached kinetochores (Rieder et al., 1995), or by a lack of tension across kinetochores (Li and Nicklas, 1995). There have been many efforts to distinguish how each mechanical property of the kinetochore is sensed and translated into a SAC signal (reviewed in Pinsky and Biggins, 2005). However, this research is complicated by the fact that tension and attachment are interdependent: an increase in tension across kinetochores clearly stabilizes kinetochore-microtubule attachments (Dewar et al., 2004; King and Nicklas, 2000; Nicklas and Ward, 1994). Conversely, a lack of tension across kinetochores promotes the error correction mechanism that then generates unstable and unattached kinetochores.

At the heart of the SAC signaling mystery is Aurora B (reviewed in Kelly and Funabiki, 2009 and Maresca and Salmon, 2010). It first appeared to be required for signaling the SAC in response to a lack of tension (generated by a lack of sister chromatid cohesion or the microtubule stabilizer taxol) but not in response to lack of attachment (generated by the microtubule depolymerizer nocodazole) (Biggins and Murray, 2001). Combined with the data that Aurora B enables error correction by destabilizing kinetochore-microtubule attachments, a model emerged in which a lack of tension caused Aurora B to create unattached kinetochore, and this was the primary platform for SAC signaling and the convergence of both pathways (Pinsky et al., 2006).

Other data, however, has implicated a direct role for Aurora B in SAC signaling aside from simply creating unattached kinetochores through error correction. First, in mammalian cells and *Xenopus* extracts Aurora B is required for SAC activation in response to both lack of tension and lack of attachment (Ditchfield et al., 2003; Hauf et al., 2003; Kallio et al., 2002). Second, in *Xenopus* egg extracts Aurora B is required for the recruitment of most SAC proteins (Vigneron et al., 2004). Third, a mutant of Incenp has been identified which separates the functions of Aurora B. In the presence of this mutant, Aurora B can effect error correction, creating unstable kinetochore-microtubule attachment, but the SAC response is impaired (Vader et al., 2007). Finally, unattached kinetochores indeed activate the SAC, but this signal cannot be maintained even when all kinetochores are unattached if Aurora B activity is impaired (Santaguida

et al., 2011; Vanoosthuyse and Hardwick, 2009). Similarly, constitutive recruitment of Mad1 to the kinetochore arrests cells through SAC activation, but this also requires Aurora B (Maldonado and Kapoor, 2011). Both of these results indicate that Aurora B actually plays a role downstream of Mad1/Mad2 recruitment in perpetuating SAC signaling. Finally, upon initiation of anaphase Aurora B relocates to the spindle midzone. Preventing this and retaining Aurora B at the centromere in anaphase, when there is no longer tension across the kinetochore, induces recruitment of some SAC signaling proteins, but does not destabilize the kinetochore microtubule attachments (Vázquez-Novelle and Petronczki, 2010). This indicates that lack of tension may signal the SAC without creating unattached kinetochores, and that Aurora B mediates this signal.

Sensing tension

How is tension, or lack thereof, translated from a mechanical to a biochemical signal? Careful studies of the molecular structure of the kinetochore have revealed that the tension generated by bioriented microtubule attachment generates a stretch, both between sister kinetochores and within a single centromere-kinetochore unit (Maresca and Salmon, 2009; Uchida et al., 2009; Wan et al., 2009). The inverse correlation between kinetochore tension and SAC activation led to the hypothesis that the critical SAC-activating substrates of Aurora B, which is localized to the inner centromere, can only be phosphorylated when there is no tension and the substrates are thus close to the kinase. Upon

biorientation, the kinetochore stretch generated by tension pulls the substrates away from the kinase, and thus the SAC signaling cannot be generated (Andrews et al., 2004; Liu et al., 2009; Tanaka et al., 2002) (see figure 1-2). This has been coined the “spatial separation” model.

A related sub-model to explain this mechanism exploits the structure of the non-catalytic members of the CPC complex. Incenp has a long coiled-coil structure, which binds Aurora B at one end and Survivin and Dasra, which are responsible for the localization of the complex, at the other. Thus it was proposed that Incenp acts as a ruler for kinetochore stretch, limiting the activity of Aurora B to a defined region in which the SAC signaling substrates reside when the kinetochores are not under tension but which they are pulled out of upon biorientation (Santaguida and Musacchio, 2009).

One caveat to both of these models is that they rely on Aurora B being stably bound to the inner centromere. However, FRAP analysis reveals that the CPC localization to the centromere is dynamic, and that the dynamicity depends on Aurora B kinase activity and microtubule attachment status (Beardmore et al., 2004). Additionally, recent immunofluorescence studies show that there is at least a small population of active Aurora B associated with the outer kinetochore (Deluca et al., 2011). Supporting an alternative model, work in budding yeast suggests that tension across kinetochores causes a conformational change in the CPC that impairs the catalytic activity of Aurora B (Sandall et al., 2006). These models are not mutually exclusive, and it is likely that many changes of

the kinetochore occur upon biorientation. Disentangling how these changes translate into biochemical signals is challenging.

Protein Phosphatase 1

Clearly, the activation of the SAC and its response to the physical status of the kinetochore is perpetuated by kinases. They phosphorylate critical substrates that then translate into formation of the MCC and inhibition of the APC. Specifically, the lack of tension across kinetochores allows substrate phosphorylation by Aurora B, and then tension generated by biorientation prevents this phosphorylation. Simply preventing further phosphorylation, however, will not change the signal that has already been generated. This is just one example of the essential reversibility of phosphorylation. Thus phosphatases, the enzymes that remove phosphorylation marks, represent an equally critical set of regulators of mitotic events.

Evidence that PP1 acts in mitosis

Protein phosphatase 1 (PP1) was originally isolated from rabbit skeletal muscle (Antoniw and Cohen, 1976) and characterized as involved in glycogen metabolism (Antoniw et al., 1977). More than a decade later, it was isolated in two independent screens for genes involved in segregation defects in fission yeast (Ohkura et al., 1988; Ohkura et al., 1989) and *Aspergillus* (Doonan and Morris, 1989). As it was becoming increasingly clear that phosphatases, working

opposite to kinases, might also be essential mitotic regulators, this led to the re-examining of the functions of PP1 in other organisms, now specifically looking at its potential role in mitosis.

First, in *Drosophila*, a mutant of one of the four genes encoding PP1 isoforms was shown to cause severe mitotic defects in larvae (Axton et al., 1990; Dombrádi et al., 1990). It was then shown in mammalian cells that PP1 localized to chromosomes during mitosis, and that injection of inhibitory antibodies against PP1 into mammalian cells at different stages of mitosis led to either an arrest at metaphase or a defect in cytokinesis (Fernandez et al., 1992). Interestingly, it was first thought in *Xenopus* that the major phosphatase that acted in mitosis was the related enzyme protein phosphatase 2A (PP2A) (Félix et al., 1990), but it was later revealed to be a combination of PP1 and PP2A. Finally, in budding yeast the PP1 homologue Glc7, which was also originally characterized for its role in glycogen metabolism (Feng et al., 1991), was found to function in mitosis as well. A mutant was isolated that caused mitotic defects in the form of chromosome missegregation at permissive temperatures and metaphase arrest at restrictive temperatures (Hisamoto et al., 1994). Thus, in the course of 6 years, there was phenomenological evidence in almost every model system in use that PP1 played an essential role in mitosis. The next set of questions, which persist today, include how PP1 is regulated and what specific mitotic functions it carries out.

Specific functions of PP1 in mitosis

The ubiquitous functions of PP1 make identifying the subcellular localization of the enzyme difficult. However, several experiments have shown that PP1 is dynamic throughout the cell cycle, and particularly in mitosis it localizes to several distinct structures (Bloecher and Tatchell, 2000; Trinkle-Mulcahy et al., 2003; Trinkle-Mulcahy et al., 2001). This localization points to PP1 serving multiple roles in mitosis. Specifically, several chromosome-related roles have been reported, concurrent with localization of PP1 to chromatin in metaphase.

The only established substrate of PP1 on chromosomes so far is histone H3, the phosphorylation and dephosphorylation of which may modulate chromosome condensation (Goto et al., 2002; Hsu et al., 2000; Murnion et al., 2001). However, several studies have identified other functions attributable to the enzyme. One of the earliest indications of the specific roles PP1 might play in mitosis, specifically at the kinetochore, comes from the fact that PP1 opposes Aurora B, as mutants in each protein rescue each other (Francisco et al., 1994). Not surprisingly, it has been shown that PP1 plays precisely the opposite role to Aurora B. PP1 can both stabilize kinetochore-microtubule attachments (Sassoon et al., 1999), and is necessary to silence SAC signaling (Pinsky et al., 2009; Vanoosthuyse and Hardwick, 2009). This SAC silencing function is particularly intriguing since it may play a role in the “spatial separation” model of Aurora B substrates that activate the SAC.

How these functions are modulated and the substrates necessary to carry them out remain mysterious. Interestingly, though, there is evidence that localization to the kinetochore can be dynamically regulated and correlated with SAC activation. PP1 chromatin immunoprecipitation with centromeric DNA in fission yeast, as well as kinetochore localization of GFP-PP1 in human cells, both decrease upon treatment with microtubule destabilizing drugs, concurrent with SAC activation (Liu et al., 2010; Meadows et al., 2011)

The role PP1 plays in mitosis is evident yet enigmatic. It was once thought that most phosphatases, including PP1, worked only passively. It was assumed that only the kinase was regulated, and once the kinase was inhibited the phosphorylation was reversed by ubiquitous, soluble phosphatase activity (Virshup and Shenolikar, 2009). It has now become increasingly clear that this is not the case. Phosphatases are regulated in precise networks that work in conjunction with kinases to accurately control the phosphorylation level of any given substrate, both in time and space. Deciphering the role of PP1 in mitosis, therefore, comes down to determination of the mechanism that controls each diverse function.

Regulation of PP1

PP1 regulatory subunits

Although early attempts were made to characterize the substrate specificity of PP1 using techniques similar to those that identified the sequence

specificity of kinases (Antoniw et al., 1977), it soon became clear that PP1 is highly promiscuous *in vitro*. It also became clear that PP1 serves a plethora of distinct, but highly specific functions *in vivo*. The first clue to reconciling these observations came with the isolation of the first PP1 regulatory subunit, also from muscle tissue (Alessi et al., 1992). Since then, biochemical and structural work has established a paradigm for the regulation of PP1.

In the cell, a host of proteins, now called regulatory subunits, bind PP1 through an RVxF motif on the regulatory subunit that fits into a binding pocket on PP1 that is remote from the catalytic pocket (Egloff et al., 1997) (figure 1-5). Notably, though, not all regulatory subunits utilize this method of binding to PP1 (Ceulemans et al., 2002). In addition, there exists a secondary binding site, called the SILK motif, on some regulatory subunits, which confers higher affinity between the regulatory subunit and PP1 (Hendrickx et al., 2009). These regulatory subunits confer specific properties to the catalytic core of PP1 which facilitate its performance of a particular cellular function.

Since the establishment of this regulatory paradigm, large-scale screens have been carried out to catalogue known PP1 regulatory subunits and discover new ones both *in vivo* (Moorhead et al., 2008; Walsh et al., 2002) and *in silico* (Hendrickx et al., 2009; Meiselbach et al., 2006). These efforts represent a shift in perspective of PP1 from one enzyme to many holoenzymes, each with distinct properties and functions. The study of the function of PP1 in any given process,

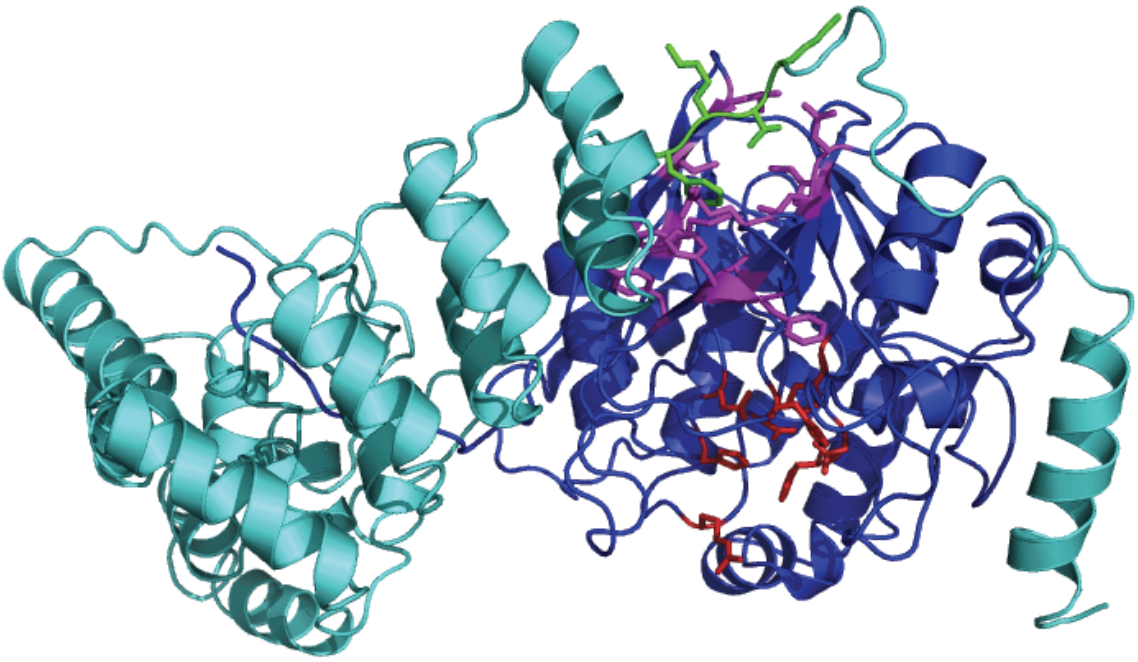

Figure 1-5: Structure of a PP1 holoenzyme. The structure of PP1 (blue) in complex with the regulatory subunit MYPT1 (cyan) was adapted from Terrak et al., 2004. The RVxF motif of MYPT1 is in green and the RVxF binding pocket of PP1 is in magenta. Residues that conjugate metal ions in the catalytic pocket are in red (Egloff et al., 1995).

therefore, can be thought of as the compilation of the effects of several holoenzymes.

What is substrate specificity?

Although there were early attempts to characterize the substrate specificity of phosphatases *in vitro* in a similar manner used to characterize kinases (Antoniw et al., 1977), it soon became clear that kinases and phosphatases are enzymatically quite distinct. Indeed, the first crystal structure of PP1 revealed that the catalytic pocket is significantly shallower than that of most kinases (Egloff et al., 1995). Consequently, the catalytic subunit of most phosphatases, especially PP1, is highly promiscuous with little substrate specificity *in vitro*. Regulatory subunits are commonly viewed as conferring substrate specificity to the catalytic core of PP1, but what does this mean in practice?

Localization is probably the most important consideration when determining the substrates of a certain PP1 holoenzyme. By targeting PP1 to a particular region of the cell, a regulatory subunit automatically restricts the access of the catalytic core to substrates. But this is not the only mechanism through which a regulatory subunit can confer substrate specificity. A regulatory subunit may confer binding sites for specific substrates, thus acting as a scaffold to bring together enzyme and substrate, or the regulatory subunit may be a substrate itself (reviewed in Bollen et al., 2010). Other regulatory subunits act as general inhibitors of PP1 catalytic activity by blocking or perturbing the active site, such

as Inhibitor-1 (Nimmo and Cohen, 1978). Finally, there is structural evidence that at least one PP1 regulatory subunit, MYPT1, does slightly change the shape of the catalytic cleft of PP1 upon binding (Terrak et al., 2004). Whether this change is enough to confer substrate specificity, however, is unclear. Ultimately, the relationship between PP1 and each of its regulatory subunits must be elucidated in order to fully understand how PP1 functions in the cell.

Isoforms of PP1

Although budding yeast only have one gene that encodes a PP1 homologue, *GLC7*, many higher eukaryotes have multiple isoforms of the enzyme. In mammals, there are three isoforms of PP1; PP1α, PP1β, and PP1γ; which primarily differ in their C-terminal 30 residues. To date, it is unclear how their functions differ in the cell. It is known that no one mammalian isoform can completely replace *GLC7*, and that each replacement shows a different phenotype throughout the cell cycle (Gibbons et al., 2007). For two neuronal PP1 regulators, it was shown that the sequences that flank the RVxF motif are important for preferential binding of one isoform over others (Carmody et al., 2004; Terry-Lorenzo et al., 2002), but these sequences are not conserved in other PP1 regulatory subunits. In mitosis, Repo-man preferentially binds PP1γ; however, when it is overexpressed in the cell it also binds PP1α (Trinkle-Mulcahy et al., 2006). It is likely that these isoforms serve some overlapping functions in the cell, but subtle distinctions between each may prove to be significant.

Potential non-catalytic roles of PP1

The closely related phosphatase PP2A has been shown to play a role in chromosome condensation through binding condensin that is independent of its catalytic activity (Takemoto et al., 2009). PP1 itself is a highly structured protein. Structural studies of one PP1 holoenzyme revealed that the regulatory subunit by itself was highly unstructured, but upon binding to PP1, it folds into a rigid conformation (Ragusa et al., 2010). This mechanism of a conformational change of a regulatory subunit upon binding to PP1 may play a role in the function of the regulatory subunit that does not necessarily depend on the catalytic activity of PP1. More detailed structural studies of specific PP1 holoenzymes may elucidate new modes of regulation in this process.

Rationale and significance of this project

Questions to be addressed

The question at the heart of this project is the spatial and temporal regulation of PP1 in mitosis, particularly at the kinetochore. To begin, I sought to simply establish that PP1 localizes to the kinetochore and that this localization is regulated. Once this was established, I searched for a PP1 regulatory subunit that may be responsible for this localization. Finally, I asked how PP1 localization to the kinetochore might be related to the established functions of PP1 in mitosis.

The study of the phosphatase activity controlling mitotic events has the same significance traditionally associated with the study of mitotic kinases. It is the balance of kinase and phosphatase activity that establishes the precise temporal and spatial domains of the phosphoproteins that carry out essential mitotic functions. Without this balance, mitotic defects such as aneuplody occur. Therefore, the study of phosphatases and that of kinases are equally essential to our understanding of how the cell faithfully segregates its genome in each cell cycle.

Initial challenges

The discrepancy in timelines of discovery and elucidation between kinases and phosphatases is not without reason. Simply put, with the tools available to cellular biologists and biochemists today, it is easier to visualize and quantify the appearance of something (i.e. phosphorylation) than the disappearance (i.e. dephosphorylation). In addition, the fact that PP1 functions as many distinct holoenzymes has made any significant insight into its function impossible until the regulatory protein or proteins involved have been identified.

At the onset of this project, we knew only a rough approximation of the localization of PP1 in mitosis and nothing of whether any specific site of localization was functionally significant, let alone what that function may have been. There was little known about the functional domains of PP1, both in time and space. In particular, it was unclear in most systems whether PP1 localized

to the kinetochore at all, and no regulatory subunits acting at the kinetochore had been identified. To this end, the goals of this project started with the most basic, with more detailed aims to be guided by the data.

Systems and approaches

To answer the questions outline above, I used two complementary model systems. First, I used the *Xenopus* egg extract system (Murray, 1991; Murray and Kirschner, 1989) as a biochemical approach for looking at protein interactions. In this system, *Xenopus laevis* eggs are harvested and fractionated by centrifugation. The cytoplasmic fraction, which contains no endogenous nuclear DNA, is collected. These extracts are prepared so that they are arrested in meiotic metaphase II (analogous to mitosis) and called CSF (cytosolic factor) extracts. Upon induction with calcium, the extracts can biochemically recapitulate a full cell cycle. They can also form mitotic spindles around exogenous DNA in the form of purified sperm chromosomes or DNA coated beads. The system is easily manipulated by immunodepletion and addition of recombinant proteins and drugs, and it is ideal for biochemical assays such as co-immunoprecipitation.

One disadvantage of the *Xenopus* egg extract system is that very large proteins are difficult to work with biochemically. Also, because the system is *ex vivo* and easily manipulated, certain aspects of the biochemistry may be different than they would be in a cellular context. Therefore, I also used the budding yeast

Saccharomyces cerevisiae as a genetic system. Using this system, I was able to easily examine the physiological consequences of mutant proteins. The use of these two systems allowed me to approach the problem both from a biochemical and a genetic perspective and thus get a broader understanding of the phenomenon at hand.

CHAPTER 2: PP1 AT KINETOCHORES OF *Xenopus laevis*

Introduction

As discussed in the previous chapter, research progress on the regulation of phosphatases has historically lagged far behind that of kinases, and the mitosis field is no exception. At the onset of this project, the kinases that control specific mitotic events were well characterized, and their substrates and regulatory mechanisms were starting to be elucidated. On the contrary, very little was known about the phosphatases antagonizing these kinases. There were some indications of the functions that PP1 may play, particularly involving processes at the kinetochore, but virtually nothing was known about its substrates and regulation.

Therefore, the first questions to be addressed by this project were if and how PP1 is localized to the kinetochore in mitosis. To answer these questions, I used the biochemical and cellular biology tools available in the *Xenopus laevis* egg extract system. I first used immunoflorescence (IF) to visualize PP1 on the mitotic spindles, and then used co-immunoprecipitation (co-IP) to elucidate the regulation of the visualized localization.

PP1 localization

Development of an RVxF binding mutant

To begin to elucidate the role of PP1 in mitosis, I set out to examine the effect of regulatory subunits on the PP1 catalytic core. Therefore, I started by creating a mutant that could no longer bind to the RVxF motif. An important use of this mutant would be to purify recombinant protein and compare its localization on mitotic spindles with that of wild type PP1 by adding it to *Xenopus* egg extracts. This data would allow me to distinguish to which structures PP1 is localizing through a regulatory subunit that contains an RVxF motif, and from there perform a targeted search for the specific protein.

To design this mutant, I utilized the crystal structure of PP1 bound to an RVxF containing regulatory subunit, MYPT1 (Terrak et al., 2004, figure 2-1A), to delineate the residues on PP1 important for this interaction. In addition, I took advantage of the fact that PP1 is very similar to protein phosphatase 2A (PP2A). Although the two phosphatases share almost identical catalytic pockets, PP2A does not interact with the RVxF motif. Putting these data together, I chose three residues in the RVxF binding pocket of *Xenopus laevis* PP1γ (xPP1γ) to mutate to the corresponding residues in *Xenopus laevis* PP2A (xPP2A).

The first mutation was of the residue D242, which form electrostatic interactions with the argenine of the RVxF motif. Second, I mutated C291 because it forms the base of the valine binding pocket. I mutated these two residues to the corresponding residues of PP2A (Figure 2-1B), making the

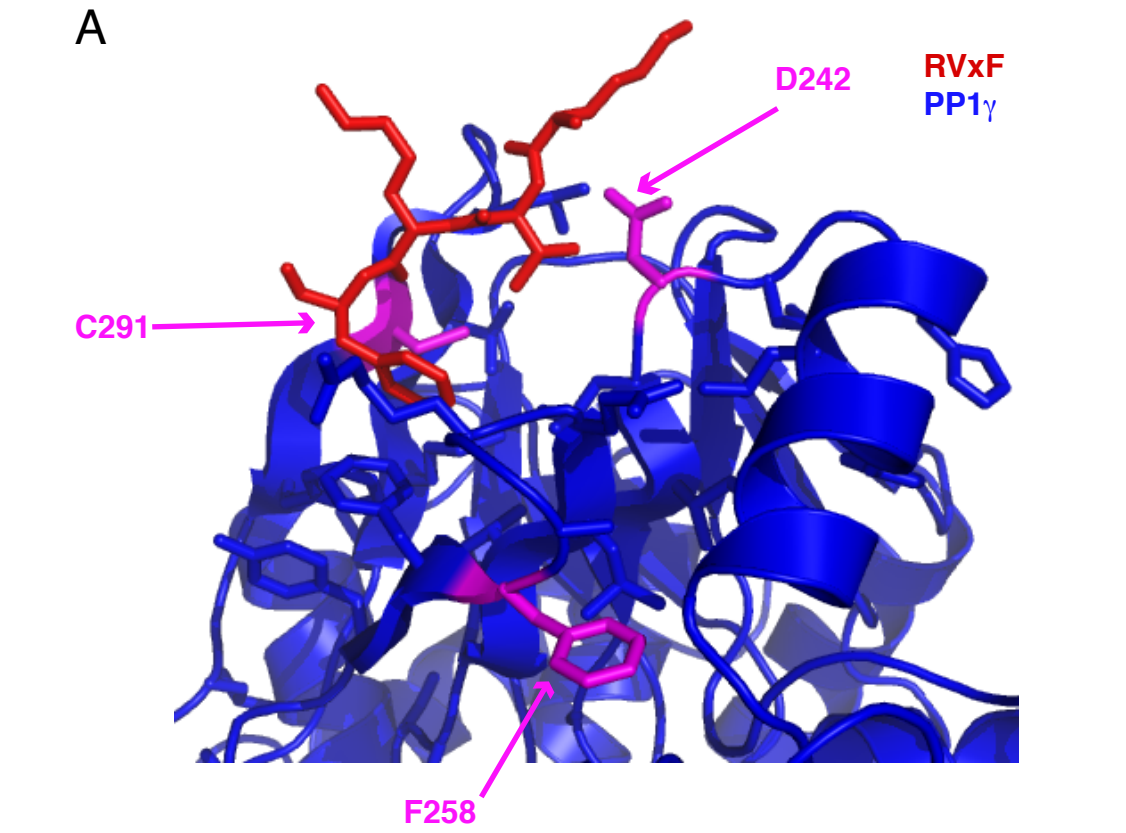

Figure 2-1: Design of a PP1 RVxF binding mutant. (A) Crystal structure of the RVxF binding pocket of PP1 (adapted from Terrak et al., 2004). The RVxF domain of MYPT1 is in red, PP1 is in blue, and the residues mutated in MBP-xPP1γ to perturb the interaction are in magenta. (B) Alignment between *Xenopus laevis* PP1γ and PP2A. Magenta asterisks correspond to the mutated residues of PP1 in A.

mutations D242T, and C291Y. Finally, I attempted to collapse the hydrophobic interactions that form the phenylalanine binding pocket through the mutation F258A.

I mutated these residues in recombinant MBP-xPP1γ, individually and in combination. I first did small-scale preparations of all the mutants on amylose resin and tested their ability to bind a peptide containing the RVxF motif of an established PP1 regulatory subunit, Repo-man (Trinkle-Mulcahy et al., 2006; Vagnarelli et al., 2006). As controls, I used both wild type xPP1γ and a previously described catalytic mutant, D95A (hereafter referred to as xPP1γ^{cat}) (Huang et al., 1997). Three MBP-xPP1γ mutants showed promise in abolishing the interaction with the RVxF peptide when compared to wild type and the catalytic mutant: C291Y, D242T F258A, and D242T C291Y (Figure 2-2A). I carried out large-scale purifications of these proteins. Titrations with the RVxF containing peptide revealed that the best binding mutant was D242T C291Y, hereafter referred to as xPP1γ^{RMB} (RVxF binding mutant) (Figure 2-2B).

To ensure that the recombinant MBP-xPP1γ proteins maintained their native structure, I performed an *in vitro* phosphatase assay using *p*-nitrophenyl phosphate (pNPP), a small molecule substrate of PP1 that turns yellow, and thus absorbs light at 405 nm when dephosphorylated (Figure 2-3). As expected, the wild type MBP-xPP1γ showed strong phosphatase activity, while MBP-xPP1γ^{cat} showed very little activity. Surprisingly, though, MBP-xPP1γ^{RBM} showed enhanced phosphatase activity over wild type. This may be evidence of an

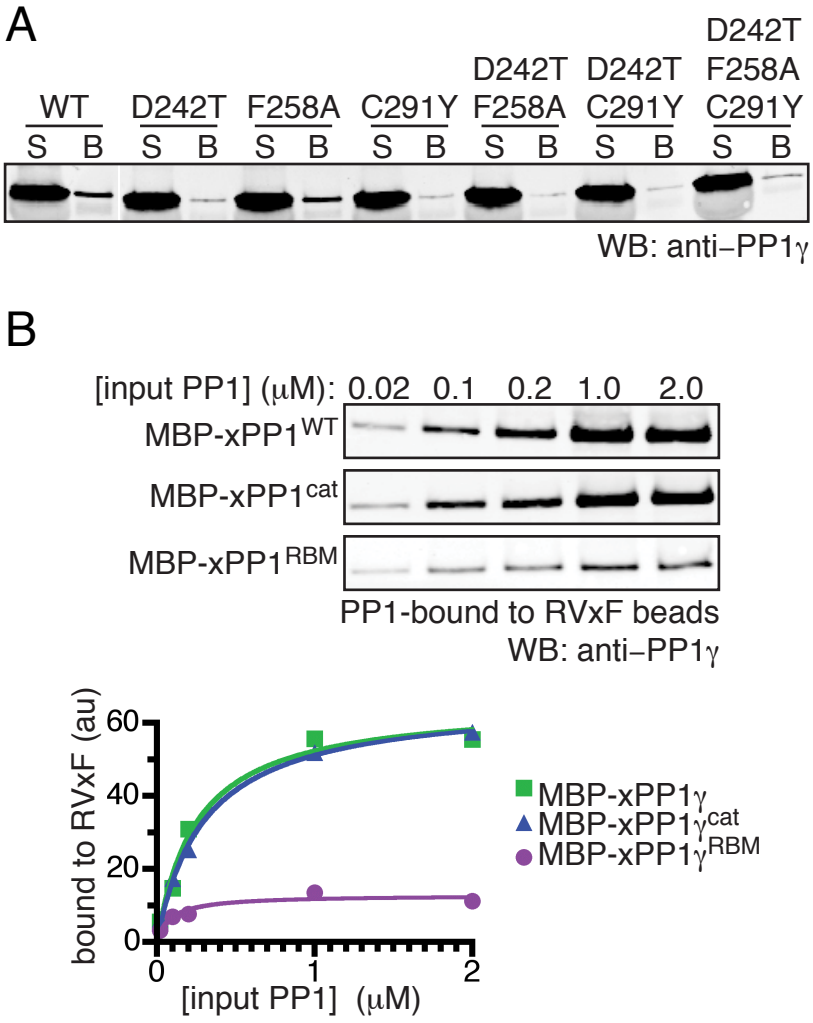

Figure 2-2: Characterization of MBP-xPP1γ^{RBM}. (A) Small-scale prep of each MBP-xPP1γ mutant was incubated with beads coated with peptides containing the RVxF motif. Supernatant and bound proteins were detected by Western blotting using anti-PP1γ antibody. (B) Purified wild-type or mutant MBP-xPP1γ protein at the indicated concentrations was bound to peptide beads as in A, detected by anti-PP1γ Western blot (top), and quantified (bottom).

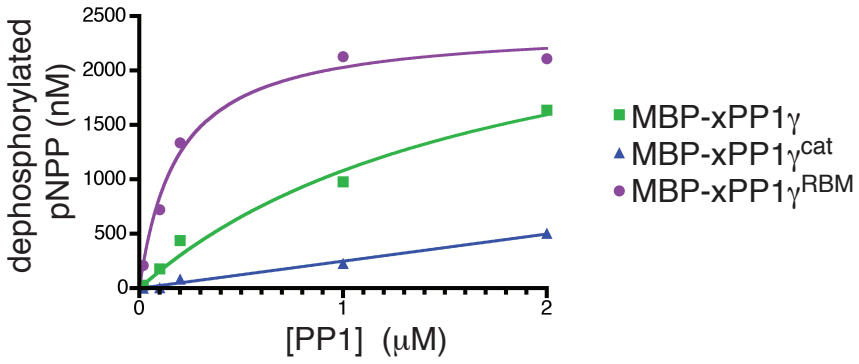

Figure 2-3: Catalytic activity of recombinant MBP-xPP1γ: An *in vitro* phosphatase assay using *p*-nitrophenyl phosphate (pNPP) as a substrate was performed with the indicated concentrations of purified MBP-xPP1γ, MBP-xPP1γ^{cat}, or MBP-xPP1γ^{RBM}. Concentration of dephosphorylated pNPP was assessed after 30 minutes by spectrophotometry.

allosteric effect between the RVxF binding pocket and the catalytic pocket of PP1. Nevertheless, the presence of any catalytic activity indicates that the structural integrity of MBP-xPP1γ is maintained in the RVxF binding mutant.

MBP-xPP1γ on mitotic spindles

I next examined the localization of PP1 on mitotic spindles assembled in *Xenopus* egg extracts. I added wild type and mutant MBP-xPP1γ to extracts along with purified sperm chromosomes, cycled them through interphase into metaphase, and processed them for IF with antibodies against MBP and BubR1 to mark kinetochore. Rhodamine labeled tubulin and DAPI stain were used to visualize the spindle and the DNA, respectively (Figure 2-4).

MBP-xPP1γ showed ubiquitous localization on the spindle and chromosomes, but deconvolution of confocal z-stacks revealed a strong enrichment at the kinetochores. While MBP-xPP1γ^{cat} showed a similar localization pattern, MBP-xPP1γ^{RBM} failed to enrich at kinetochores. Interestingly, MBP-xPP1γ^{RBM} retained faint localization on chromosomes, indicating there may be a non-RVxF regulatory subunit that is at least partially responsible for targeting PP1 to chromatin.

KNL1: a PP1 regulatory subunit

The localization data suggested that there is an RVxF containing protein that is responsible for targeting PP1 to the kinetochores. Based on this, I

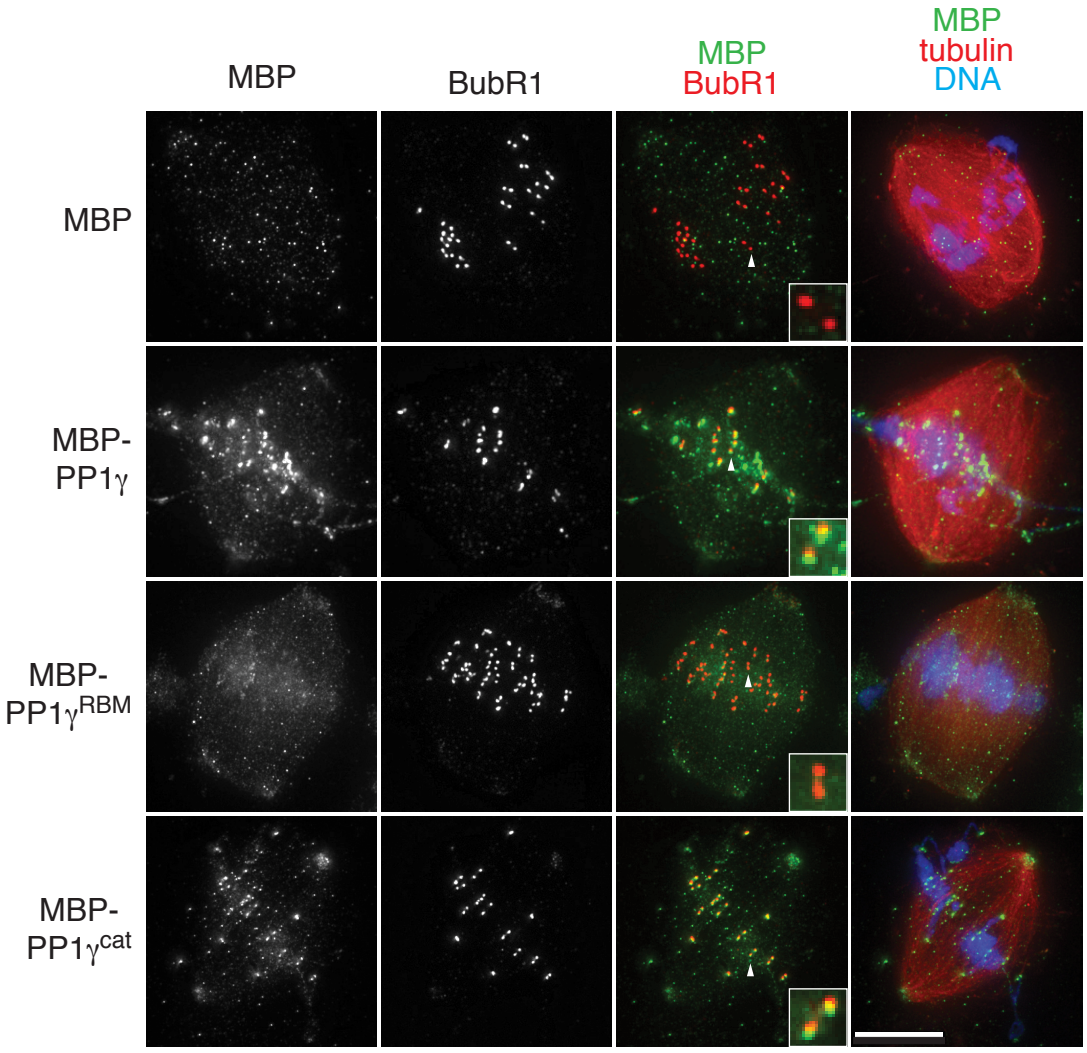

Figure 2-4: MBP-xPP1γ localization on mitotic spindles. Spindles assembled on replicated sperm chromosomes in *Xenopus* metaphase extracts containing the indicated MBP-xPP1γ recombinant proteins and rhodamine-tubulin were processed for immunoflorescence and stained with Hoechst 33258 (DNA), anti-MBP, and anti-BubR1 antibodies. Scale bar, 15 μm. Insets, higher magnifications of the regions indicated by arrowheads.

examined all of the known kinetochore proteins to determine which ones have evolutionarily conserved RVxF motifs, and tested their interaction with PP1 in *Xenopus* egg extracts. The proteins I first focused on were KNL1, CENP-E, EB1, and Ki67. Due to difficulties such as low expression in an *in vitro* translation reaction or high background in the co-immunoprecipitation, however, none of the full-length proteins could be verified to interact with PP1.

Once I obtained and sequenced the full-length *Xenopus laevis* clone of KNL1 (see Figure A-3), I found that it contained evolutionarily conserved RVxF (here RVSF) and SILK motifs close to its N-terminus (Figure 2-5). Because full-length KNL1 is very large (approximately 312 KDa), it also did not express well in an *in vitro* translation reaction. However, I was able to create two N-terminal fragments that contained the RVxF motif, xKNL1^{300} and xKNL1^{790}, comprising the first 300 and 790 residues, respectively. Both of these truncated proteins expressed well, so I was able to use them to focus on assessing the interaction between KNL1 and PP1.

To determine whether KNL1 and PP1 interact in extract, I added ^{35}S labeled *in vitro* translated proteins to extract and looked for co-immunoprecipitation using an anti-xPP1 antibody, which binds to both PP1α and PP1γ. Both truncations showed robust co-immunoprecipitation with PP1 in extract both in interphase and mitosis (Figure 2-6). When the RVSF motif was mutated to RASA, the interaction with PP1 was abolished. These data indicate

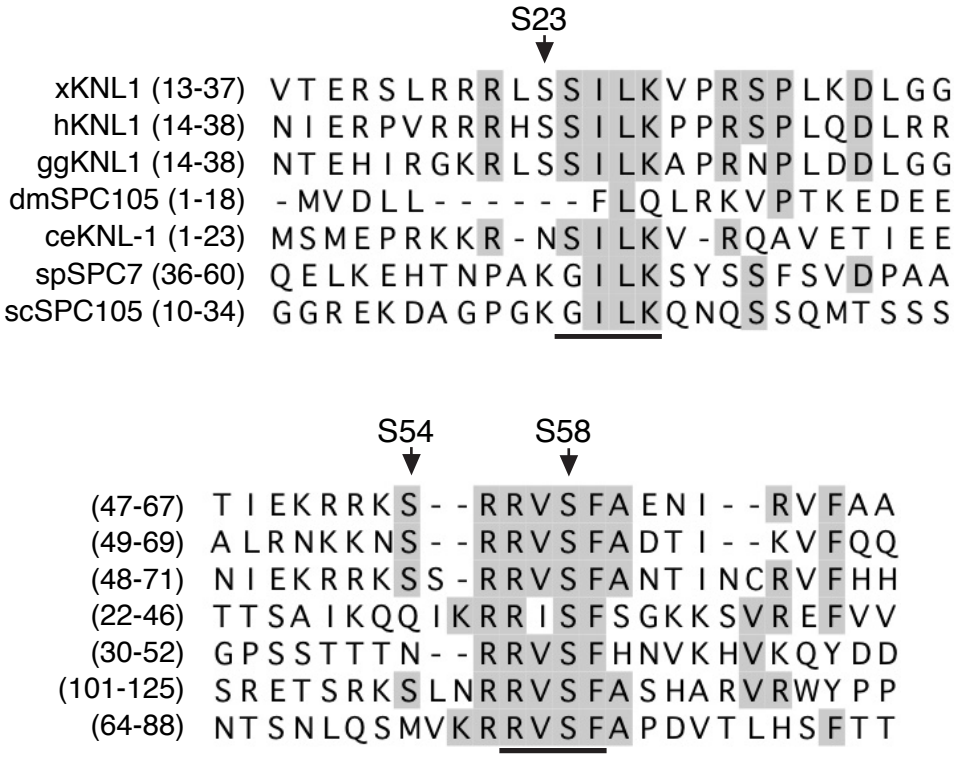

Figure2-5: KNL1 contains conserved PP1 binding motifs. (A) Alignment of the SILK (top) and RVxF (bottom) motifs of KNL1 from *X. laevis* (xKNL1), *H. sapiens* (hKNL1), *G. gallus* (ggKNL1), *D. melanogaster* (dmSPC105), *C. elegans* (ceKNL-1), *S. pombe* (spSPC7), and *S. cerevisiae* (scSPC105). Arrows indicate S23, S54, and S58 of xKNL1.

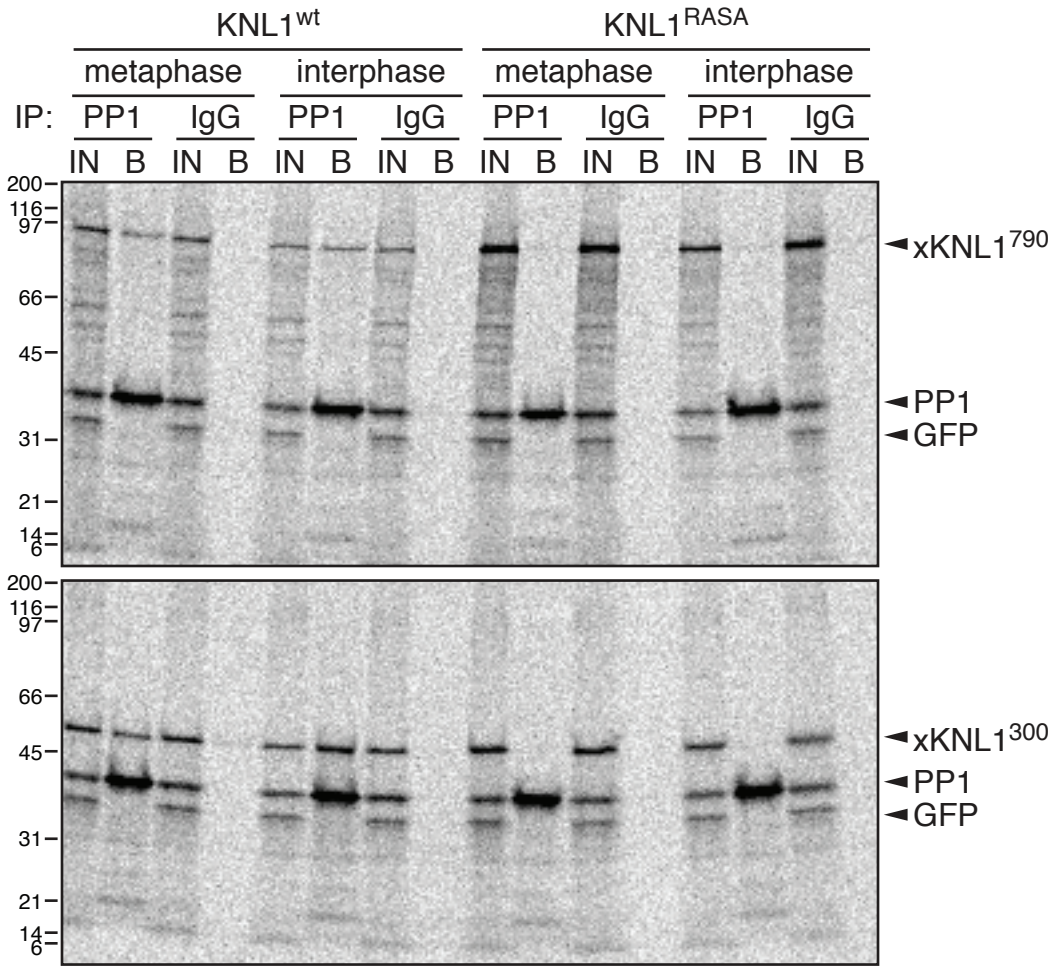

Figure 2-6: xKNL1 interacts with PP1 in *Xenopus* extract. ^{35}S-labeled PP1 (positive control), GFP (negative control), and wild type or the RASA mutant of xKNL1^{790} (top) or xKNL1^{300} (bottom) were added to metaphase or interphase extracts. ^{35}S-labeled proteins in extract (IN) and co-immunoprecipitated with anti-PP1 or control anti-GFP antibody beads (B) were visualized by autoradiography.

that the RVSF motif of KNL1 is functional, and that KNL1 is a good candidate for a PP1 regulatory subunit at the kinetochore.

Phosphorylation of KNL1

The KNL1-PP1 interaction is sensitive to phosphorylation

It had previously been reported that Aurora B phosphorylates KNL1, and this phosphorylation mediates the affinity of the KMN network for microtubules (Welburn et al., 2010). The exact residues that are phosphorylated by Aurora B, however, had not been established. There are three conserved Aurora B consensus sites in and near the SILK and RVxF PP1-binding motifs (see Figure 2-5), which are S23, S54, and S58 in the *Xenopus laevis* protein. Notably, the "x" of the RVxF motif is one such serine (S58), and this is the only one of the three that is conserved in budding yeast.

I hypothesized that phosphorylation of one or all of these residues might impair the interaction between KNL1 and PP1. This could serve as a mechanism for proper temporal regulation of PP1 recruitment to the kinetochore (Figure 2-7), and in fact I had already established phosphorylation of the RVxF motif as a mechanism to regulate PP1 binding using the Repo-Man regulatory subunit (see Appendix, Figure A-2). In this model, early in mitosis, when error correction is occurring and the SAC needs to be active, Aurora B phosphorylates several substrates to achieve these activities. In addition, Aurora B may phosphorylate KNL1 on the SILK and RVxF motifs in order to exclude PP1 from the kinetochore,

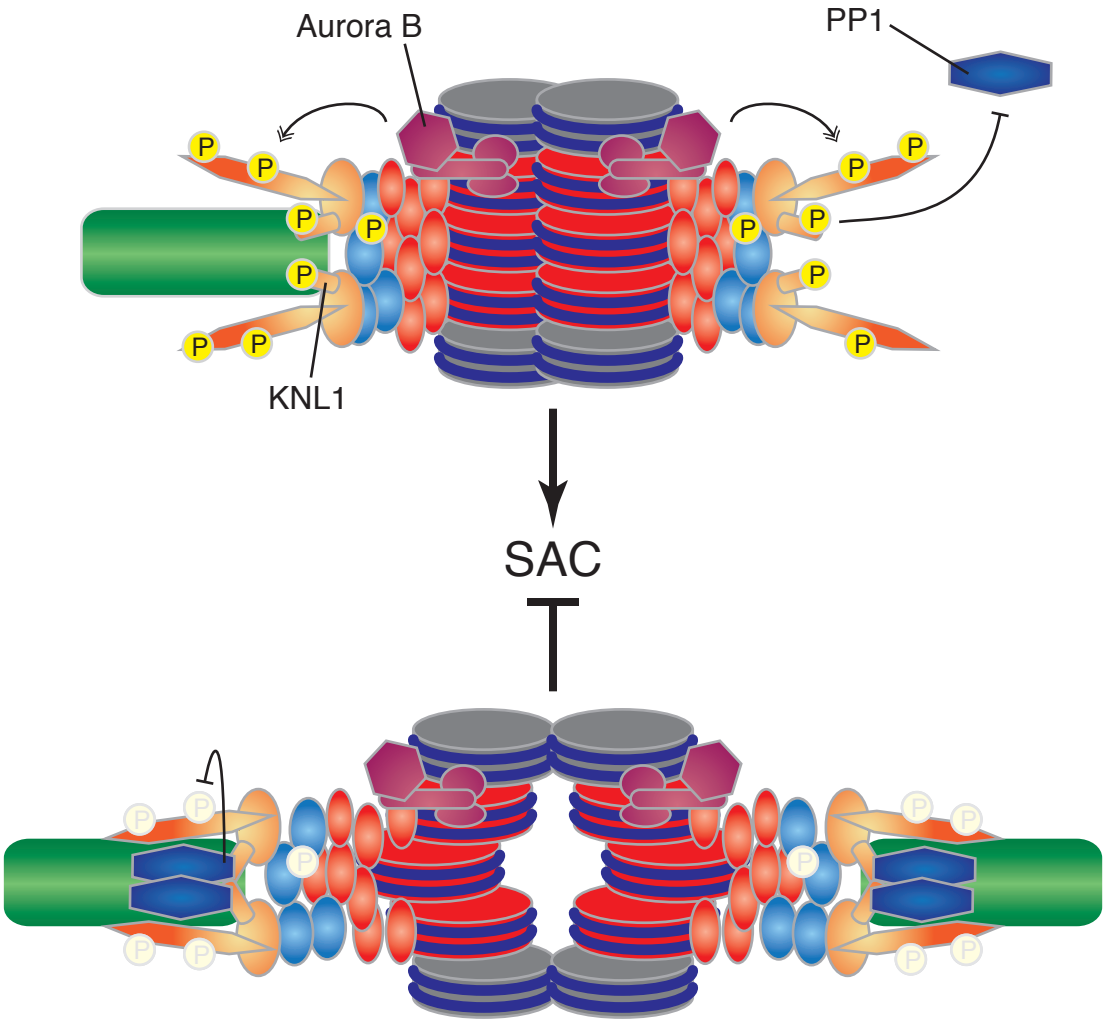

Figure 2-7: Possible model for regulating the KNL1-PP1 interaction. With incorrect attachment (top), Aurora B phosphorylates substrates that activate the SAC and the KNL1 RVxF motif, which prevents targeting of PP1 to the kinetochore. With bipolar attachment (bottom), phosphorylation of substrates at the kinetochore is reduced, including the RVxF motif of KNL1. This promotes recruitment of PP1, reinforcing low phosphorylation levels.

thus allowing Aurora B substrate phosphorylation levels to remain high by eliminating the counteracting phosphatase activity. Once biorientation has been achieved and phosphorylation levels of Aurora B substrates, including KNL1, are reduced, then PP1 is recruited to the kinetochore to ensure that phosphorylation levels remain low and anaphase can proceed.

To test this hypothesis, I examined the interaction of KNL1 (using the truncated xKNL1^{300} protein) and PP1 in extracts treated with okadaic acid. Okadaic acid is a phosphatase inhibitor that acts on both PP1 and PP2A, the major phosphatases working in the extract, and thus stabilizes many phosphorylation marks. In addition, since Aurora B is activated by autophosphorylation, treatment of the extracts with okadaic acid causes hyperactivation of Aurora B. In CSF (mitotic) extracts treated with okadaic acid, the interaction between KNL1 and PP1 is indeed abolished (figure 2-8A). This sensitivity is dependent on the three Aurora B consensus sites, since when all three are mutated to alanine (xKNL1^{300,AAA}) co-immunoprecipitation with PP1 persists even in the presence of okadaic acid. All three serines contribute to this sensitivity, since when any one serine remains the sensitivity is still present to varying degrees (Figure 2-8B). This indicates that phosphorylation on KNL1 can in fact abolish its interaction with PP1.

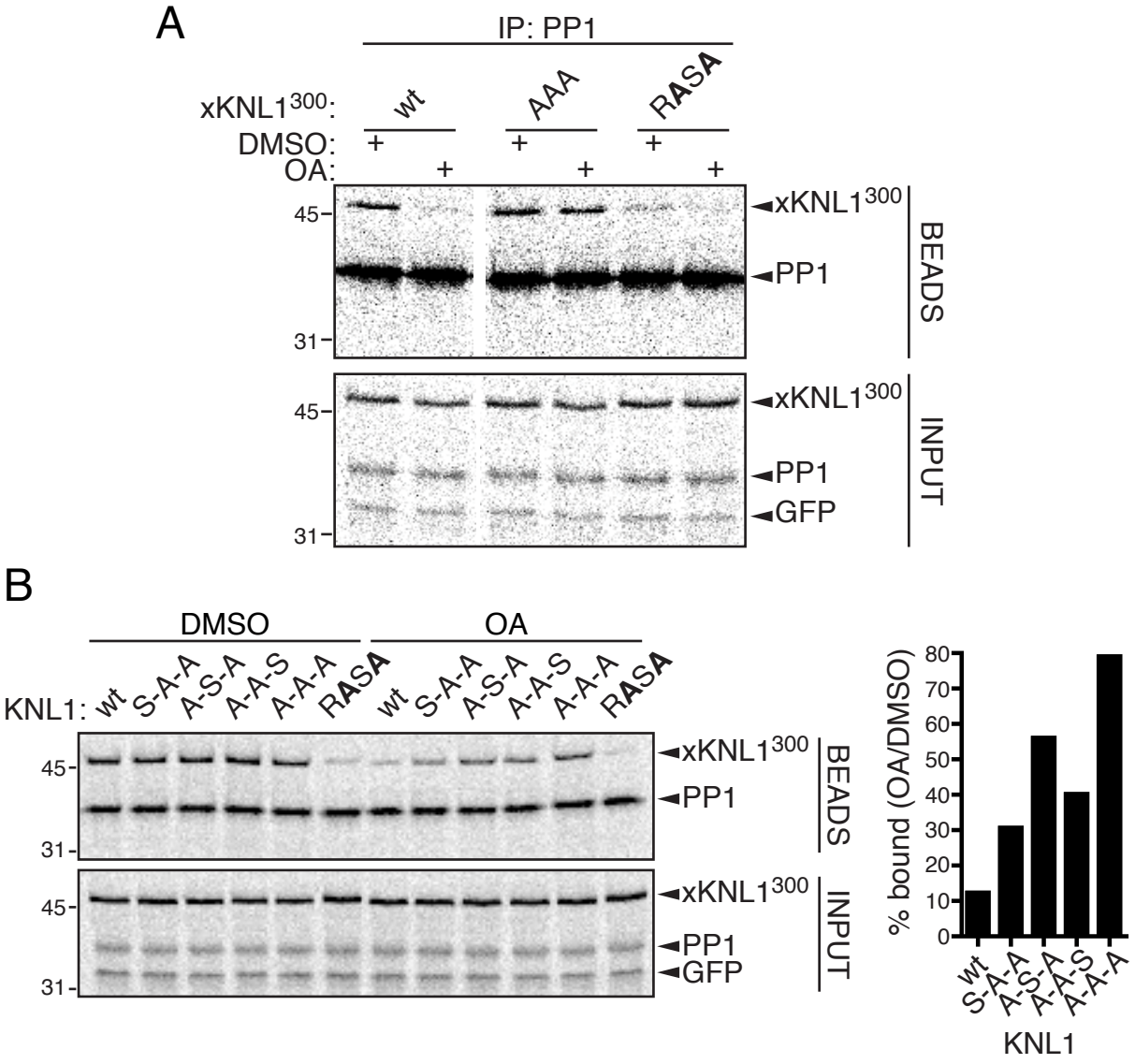

Figure 2-8: The KNL1-PP1 interaction is sensitive to KNL1 phosphorylation. (A) Metaphase egg extracts, containing ^{35}S-labeled PP1 (positive control), GFP (negative control), and either xKNL11^{300}, xKNL11^{300,AAA}, or xKNL11^{300,RASA}, were treated with 0.4 μM okadaic acid (OA), or with DMSO for 30 minutes at 20°C. ^{35}S-labeled proteins in extract (INPUT) and co-immunoprecipitated with anti-PP1 antibody (BEADS) were visualized by autoradiography. (B) ^{35}S-labeled PP1, GFP, and xKNL11^{300} with the indicated alanine mutants of S23, S54 or S54, were co-immunoprecipitated from metaphase egg extracts treated as in A. ^{35}S-labeled proteins were visualized by autoradiography (left), and the relative, normalized % ratios of KNL1 proteins copurified with PP1 were calculated as [(KNL1^{OA}/PP1^{OA})/(KNL1^{DMSO}/PP1^{DMSO})] x 100 (right).

Aurora B-mediated phosphorylation of KNL1

To facilitate *in vitro* examination of the phosphorylation of KNL1 by Aurora B, I purified a bacterially expressed recombinant protein containing the first 100 residues of xKNL1, which includes the SILK and RVSF motifs and all three Aurora B consensus sites, with a FLAG tag (xKNL1^{100}-FLAG). I purified wild type protein and all possible serine-to-alanine mutant combinations. A ^{32}P-ATP *in vitro* kinase assay revealed that xKNL1^{100}-FLAG was phosphorylated by Aurora B, but not by Polo or Haspin kinases (figure 2-9A). I then used the serine-to-alanine mutants to examine which sites are phosphorylated, and found that Aurora B can phosphorylate all three residues. However, when all three are mutated to alanine, the ^{32}P-phosphorylation signal is completely eliminated (Figure 2-9B), indicating that there are no other Aurora B target sites in this region of the protein.

To examine the activity of Aurora B towards KNL1 in a biological context, I added xKNL1^{100}-FLAG to extracts. Taking advantage of the overlapping substrate specificities of Aurora B and protein kinase A (PKA), I used a commercially available anti-PKA substrate antibody against the RRXS/Tph phospho-motif. This antibody will recognize any of the three Aurora B sites on xKNL1^{100}-FLAG. In CSF extract, xKNL1^{100}-FLAG, but not xKNL1^{100,AAA}-FLAG, was phosphorylated in response to okadaic acid treatment. When the CPC was depleted, the phosphorylation signal was mostly, but not entirely, eliminated (Figure 2-10A).

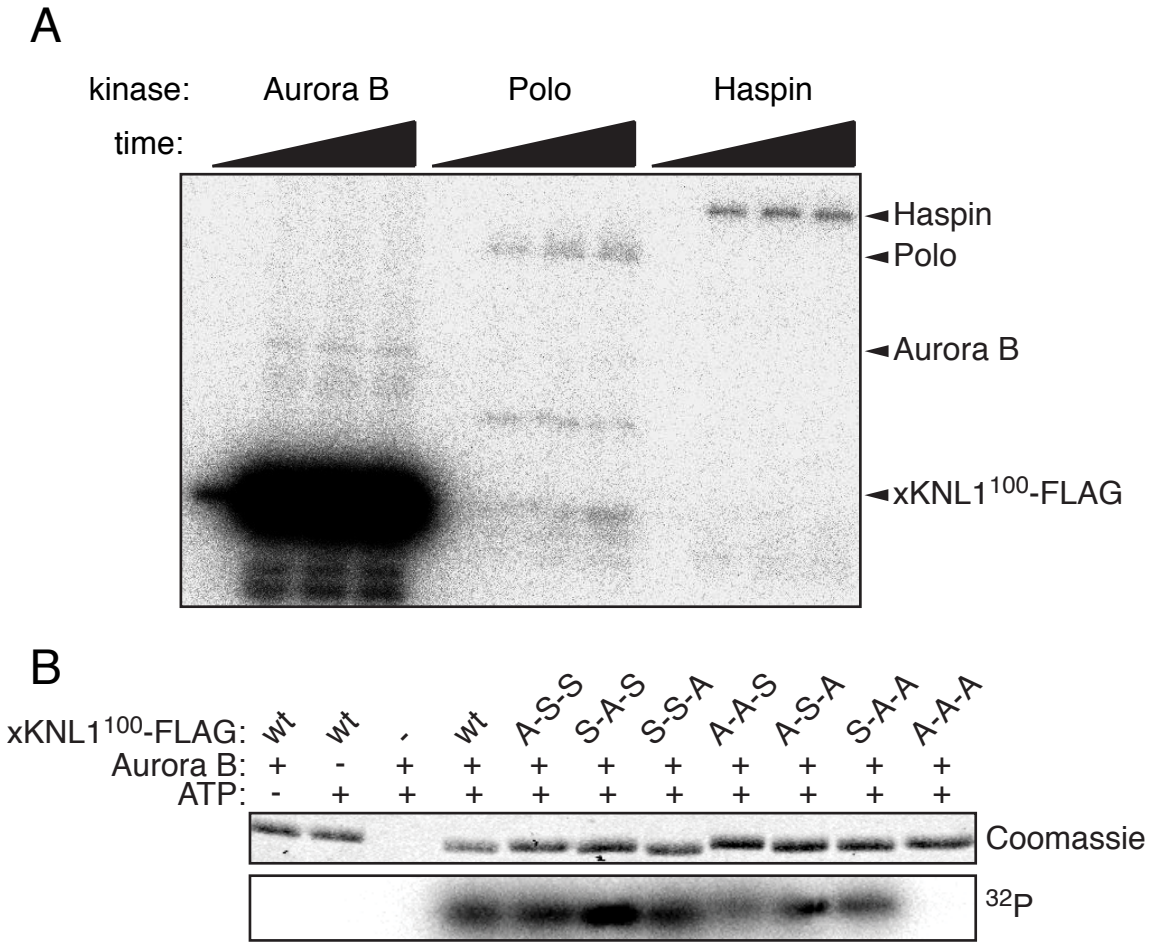

Figure 2-9: Aurora B phosphorylates xKNL1. (A) xKNL1^{100}-FLAG was incubated with the indicated kinases and γ-^{32}P-ATP. Samples were taken at 0, 20, 40, and 60 minutes and visualized for ^{32}P-ATP incorporation by autoradiography. (B) xKNL1^{100}-FLAG containing various serine (S) to alanine (A) mutations as indicated at residues 23, 54, and 58 respectively were incubated with recombinant Aurora B-INCENP$^{790\text{-}871}$ and γ-^{32}P-ATP. Coomassie staining of xKNL1^{100}-FLAG and autography are shown.

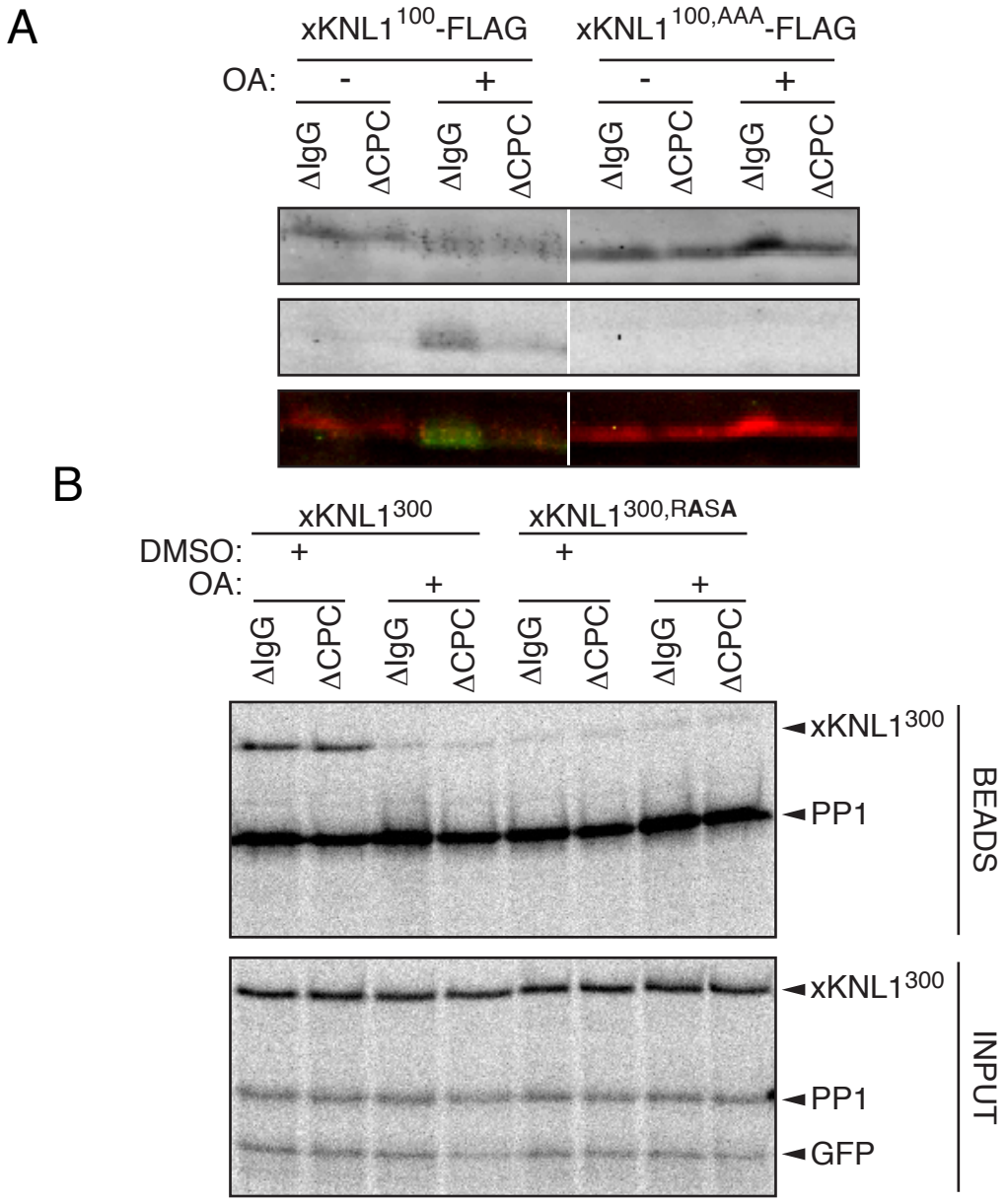

Figure 2-10: Phosphorylation of xKNL1 by Aurora B in extract. (A) Recombinant xKNL1^{100}-FLAG or xKNL1^{100,AAA}-FLAG proteins were added to metaphase control extracts (ΔIgG) or to those depleted of the CPC using anti-INCENP antibody (ΔCPC). 0.4 μM okadaic acid (OA) was added to these extracts and incubated for 60 minutes. Extracts were analyzed by Western blotting using anti-FLAG (red) and anti-RRxS/Tph (green) antibodies. (B) Co-immunoprecipitation was performed between PP1 and xKNL1^{300} or xKNL1^{300,RASA} as in figure 2-8A in metaphase ΔIgG or ΔCPC extracts.

Based on these data and the working hypothesis, if Aurora B is not present to phosphorylate these residues of KNL1, then KNL1 would consistently interact with PP1 independent of any stimuli. This was not the case, however, and the co-immunoprecipitation of KNL1 and PP1 is still sensitive to okadaic acid even when Aurora B is depleted (Figure 2-10B). This could be attributed to the residual phosphorylation of xKNL1^{100}-FLAG seen in the presence of okadaic acid. Since these N-terminal truncations of KNL1 lack the domain necessary to target it to the kinetochore (Kerres et al., 2007) and would therefore be cytoplasmic, other baso-directed kinases (such as Aurora A or PKA) may be phosphorylating these residues that would not normally have access to KNL1 at the kinetochore. This is particularly relevant since a single phosphorylation event is sufficient to cause reduction of the KNL1-PP1 interaction. I therefore sought to test this model without interference of other, likely irrelevant, kinases.

To definitively show that Aurora B phosphorylation of KNL1 can impair its interaction with PP1, I recapitulated the KNL1-PP1 interaction *in vitro*. When xKNL1^{100}-FLAG was incubated with MBP-xPP1γ *in vitro* and isolated using anti-FLAG antibody beads, it interacted with MBP-xPP1γ and MBP-xPP1γ^{cat}, but not with MBP-xPP1γ^{RBM} (Figure 2-11A). I then tested the interaction between xKNL1^{100}-FLAG and MBP-xPP1γ^{cat} when the xKNL1^{100}-FLAG was pre-treated with Aurora B in the presence of ATP. The catalytic mutant of MBP-xPP1γ was used to ensure that the phosphatase would not remove the marks placed by Aurora B, since even at 4°C PP1 retains some enzymatic activity. Indeed,

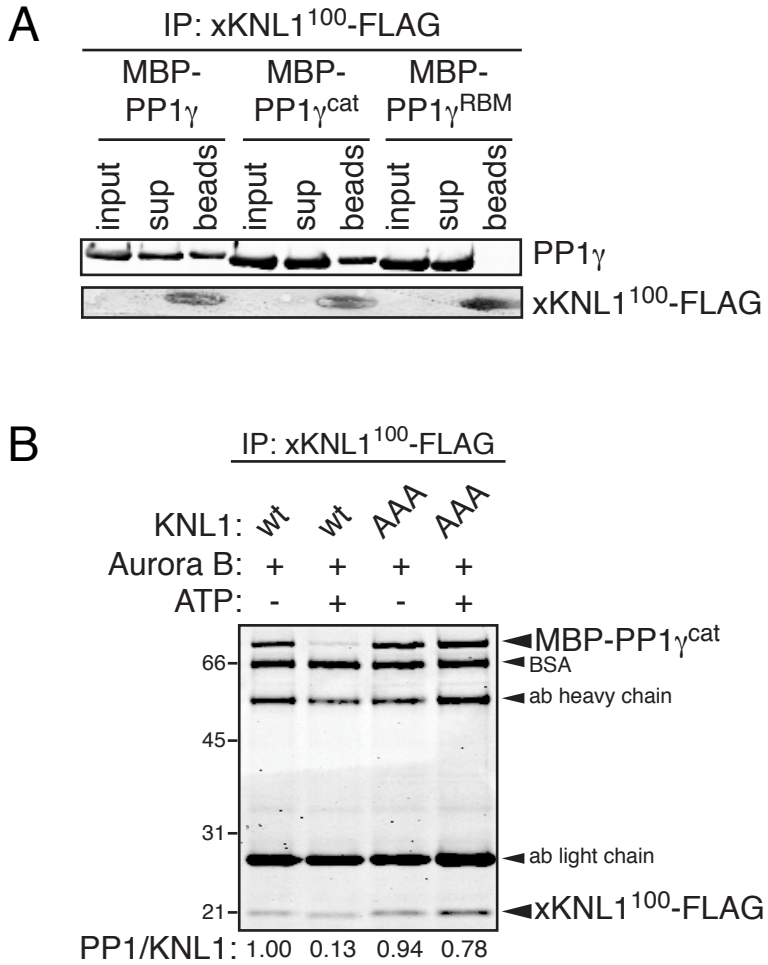

Figure 2-11: Regulation of the KNL1-PP1 interaction by Aurora B *in vitro*. (A) MBP-xPP1γ or MBP-xPP1γ^{RBM} was incubated with xKNL1^{100}-FLAG, followed by immunoprecipitation using anti-FLAG antibody, and analyzed by Western blots. (B) xKNL1^{100}-FLAG was treated with recombinant Aurora B-INCENP$^{790-871}$, in the presence or absence of ATP. xKNL1^{100}-FLAG was then isolated with anti-FLAG beads and incubated with 1 μM MBP-xPP1γ^{cat}. Fractions bound to the beads were visualized with Coomassie. Normalized PP1/KNL1 ratio is indicated below.

prephosphorylation of xKNL1^{100}-FLAG by Aurora B abolished its interaction with MBP-xPP1γ^{cat}. The interaction between xKNL1^{100,AAA}-FLAG and MBP-xPP1γ, however, was insensitive to Aurora B treatment (Figure 2-11B).

Nocodazole treatment causes PP1 redistribution

One prediction that can be made based on the biochemical data is that when the SAC is active, PP1 should be excluded from the kinetochore. A practical consequence of this is that when spindles assembled in *Xenopus* egg extracts are treated with nocodazole to generate unattached kinetochores, PP1 should no longer be visible on the kinetochore by immunofluorescence. Indeed, this phenomenon had been observed previously in human cells (Liu et al., 2010). To avoid any perturbation of the system by the addition of excess phosphatase activity, I observed the localization of MBP-xPP1γ^{cat} on mitotic spindles with and without nocodazole treatment. Surprisingly, even upon nocodazole treatment, PP1 was still targeted to kinetochores (Figure 2-12A).

Upon closer inspection, the localization pattern of MBP-xPP1γ^{cat} around the kinetochore is different in control and nocodazole treated samples. Qualitatively, the signal appears to be more diffuse around the CENP-A marked kinetochores. To quantitate this, I used the Pearson's coefficient, which measures the co-localization of two signals by measuring the degree of overlap of each signal. This measurement for CENP-A and MBP-xPP1γ^{cat} was decreased in the nocodazole treated sample when compared with the control

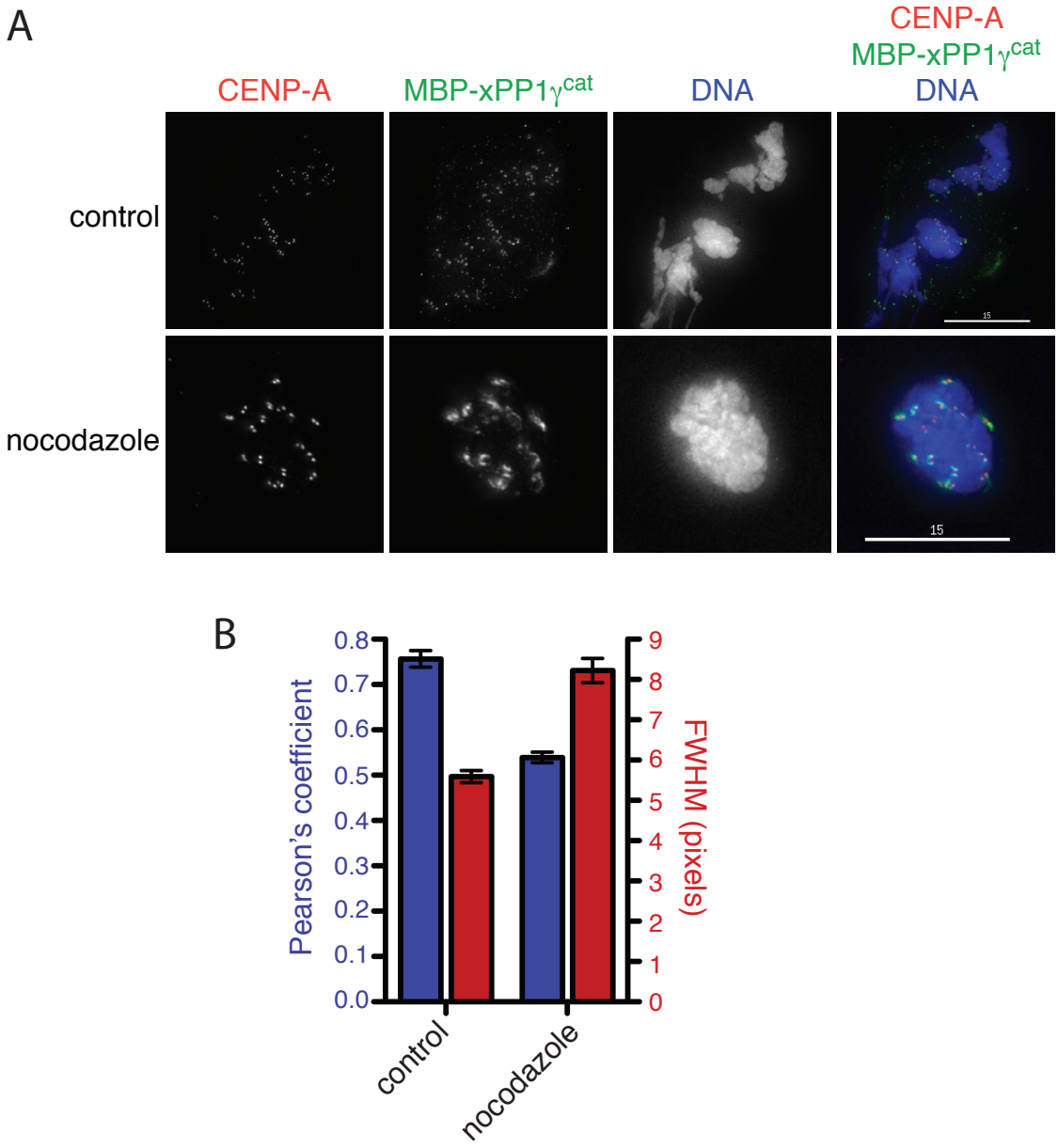

Figure 2-12: Redistribution of PP1 on unattached kinetochores. (A) Metaphase spindles were assembled in *Xenopus* egg extracts, treated with either DMSO (control) or nocodazole, processed for immunofluorescence, and stained with Hoechst 33258 (DNA), anti-MBP, and anti-CENP-A antibodies. Scale bar, 15 μm. (B) The mean ± SEM of the Pearson's coefficient (blue) and FWHM of the Van Steensel's curve (red) between CENP-A and MBP-PP1γ^{cat} are shown for control and nocodazole-treated spindles. n = 5 spindles each.

(Figure 2-12B). Practically, this measurement means that there is more PP1 present that is not perfectly overlapping with CENP-A in the nocodazole treated samples. Additionally, the Van Steensel analysis calculates the Pearson's coefficient of co-localization when one channel is offset relative to the other (Bolte and Cordelieres, 2006). This analysis generates a bell curve, and the full-width-half-maximum (FWHM) of this curve was increased upon nocodazole treatment. This means that the width of the MBP-xPP1γ^{cat} signal relative to the CENP-A foci is larger, representing a change in the localization pattern of PP1.

Discussion

A mechanism for temporal regulation of PP1

Taken together, these data strongly suggest that KNL1 can interact with PP1 in mitosis, and that Aurora B phosphorylation of KNL1 abrogates this interaction. Given that KNL1 is a known kinetochore component, this presented a logical mechanism for the temporal and spatial regulation of PP1 at the kinetochore. This mechanism could potentially act as a bistable switch such that when Aurora B is active, it ensures high substrate phosphorylation by also preventing localization of the counteracting phosphatase. Once the activity of Aurora B is decreased just enough such that PP1 can be recruited by KNL1, the phosphorylation level would be further suppressed.

PP1 on unattached kinetochores

Grossly speaking, my data clearly indicates that PP1 is not completely excluded from unattached kinetochores in this system. Similar experiments in human cells have produced conflicting results. Examination of endogenous PP1γ indicates that PP1 localization to the kinetochore does not change upon treatment with nocodazole (Trinkle-Mulcahy et al., 2003); however, ectopically expressed GFP-PP1 does show a reduction (Liu et al., 2010). These differences may be a result of methodology or detection limits, or may represent a physiological difference between cell types and systems. Further study would be needed to determine the exact dynamics of PP1 on unattached kinetochores.

What is also apparent from my data is a redistribution of PP1 upon nocodazole treatment. It appears that PP1 may be targeted to the pericentromeric region, which may function to keep PP1 in proximity to the kinetochore so that it can be rapidly recruited upon biorientation. Since PP1 has already been shown to be involved in heterochromatin formation (Goto et al., 2002; Hsu et al., 2000), a similar targeting mechanism may be involved here. However, it is also possible that this difference is simply an artifact. In *Xenopus* egg extracts, the chromatin structure is rearranged upon nocodazole treatment, as shown by the shape of the DNA staining. This rearrangement alone may be causing the difference in PP1 localization pattern, and more careful studies would need to be done to determine whether it is indeed being targeted to pericentromeric heterochromatin.

Physiological significance of the KNL1-PP1 interaction

From the data presented here, it is clear that the RVxF motif of KNL1 is capable of binding PP1 and that this interaction can be abrogated by phosphorylation on KNL1 by Aurora B. From these considerations emerged a very attractive model to precisely regulate the phosphorylation status of kinetochore proteins. However, the limitations of *Xenopus* egg extracts as a model system forced me to use small, truncated proteins that were not even targeted to the kinetochore. Therefore, I had no way of knowing whether these interaction and modifications occurred in the context of the kinetochore.

Another limitation to these data is addressing the functional significance of the KNL1-PP1 interaction and its regulation. This regulatory mechanism could affect one or both of the known functions of the PP1-Aurora B balance, namely kinetochore microtubule stability and SAC signaling; or it could represent a completely novel function for these enzymes at the kinetochore. In *Xenopus* egg extracts it is normally possible to immunodeplete and add back mutant proteins to probe their effects on spindle assembly, kinetochore-microtubule attachment, and SAC activation. However, the size and abundance of KNL1 was again a limiting factor. I could not detect the endogenous protein by Western blot, and I could never get full-length protein to express either in extract or bacteria.

For these reason, I chose to continue this project in the budding yeast *Saccharomyces cerevisiae*. In this genetic system, issues such as very large

proteins and low abundance that impair biochemical studies are not a problem. Thus, I was able to probe the physiological consequences of abrogating the KNL1-PP1 interaction and its regulation.

CHAPTER 3: THE KNL1/SPC105-PP1 INTERACTION IN BUDDING YEAST

Introduction

Kinetochore structure and sub-complexes are highly conserved from mammals down to yeast. In fact, the budding yeast kinetochore, which binds a single microtubule, is thought represent the basic repeated unit that makes up the mammalian kinetochore, which binds 15 to 20 microtubules. To this end, I continued my examination of the KNL1-PP1 interaction in budding yeast.

In this system, the homologue of KNL1 is Spc105. Although it was originally identified as a spindle pole component, it is now known to function in the same KMN network as in mammals that works at the kinetochore to form the microtubule interface (Nekrasov et al., 2003). In budding yeast, the *GLC7* gene encodes the single PP1 homologue and *IPL1* is the homologue of Aurora B. For the remainder of this chapter, I will refer to KNL1, PP1, and Aurora B as Spc105, Glc7, and Ipl1 respectively.

Generation of Spc105 mutants

Inducible gene replacement

The genetic tools of budding yeast are vast. However, generating targeted, physiologically relevant mutants is subtly challenging. Most methods utilize non-endogenous promoters or protein degradation that may be incomplete. Furthermore, examination of the terminal phenotype of lethal alleles

was also difficult. To circumvent these issues, I utilized a new method developed in the Cross lab for the inducible generation of a point mutant at the endogenous locus of a gene (Cross and Pecani, 2010). This method relies on the endogenous double strand break repair machinery of the cell, and does not require auxotrophic selection to obtain mutants (Figure 3-1).

To employ this method, called here HGR (HO-induced gene replacement), I first inserted a cassette (*spc105*^{NT}) consisting of a partial gene encoding the N-terminal region of Spc105 containing a specific mutation that is marked with a restriction site, followed by an HO endonuclease cut site (HOcs) and the *URA3* gene, at the promoter region of *SPC105*. All strains are *MATa-inc*, in which the HO cut site in the *MATa* locus has been mutated. Consequently, the HO-site in this cassette is the only one in the genome. Generation of a double strand DNA break at the HO-site by induction of *GAL-HO* stimulates homologous recombination between the truncated *spc105* from the cassette and the full-length endogenous *SPC105* gene. This results in essentially all cells in the culture undergoing recombination to produce either wild-type or mutant *spc105*, depending on the site of crossover, which can be distinguished by the presence of the restriction site. The greatest advantages of this method come with lethal mutations, since the consequences of introducing the mutation can be observed in the first few cell cycles following recombination.

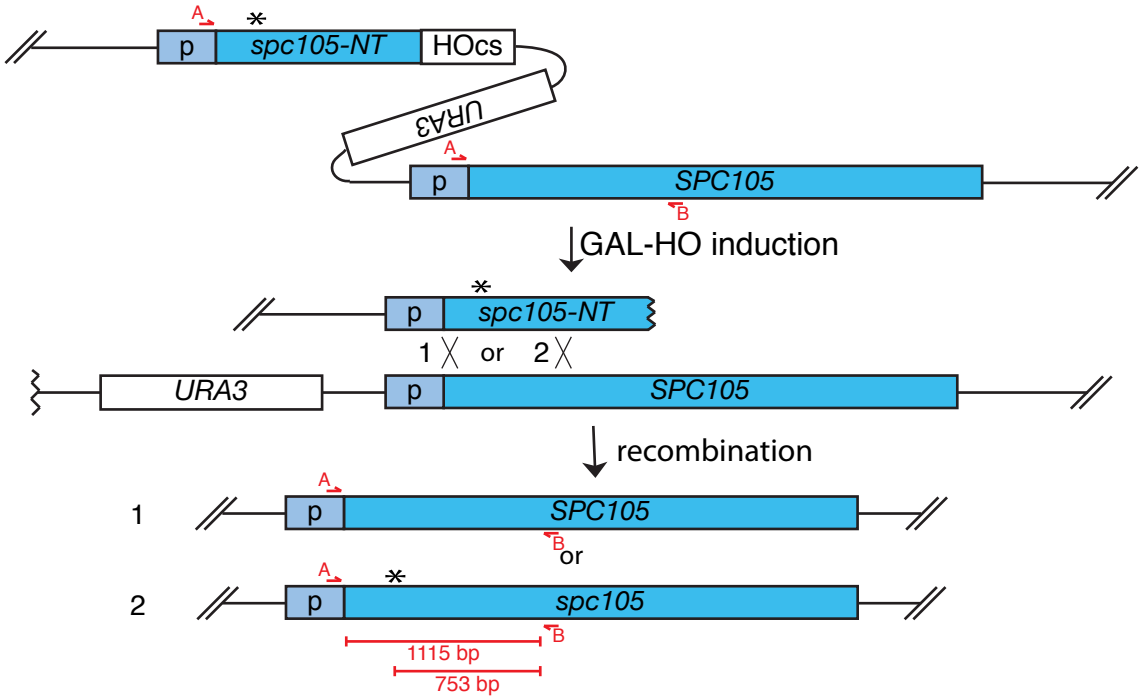

Figure 3-1: The HO-induced Gene Replacement (HGR) method. (A) Schematic of the HGR method. Asterisk indicates the desired mutation, arrows indicate primers used for genotyping. Homologous recombination after HO-induced DNA breaks generates full-length wild-type *SPC105* (1) or mutant *spc105* (2)

Spc105 RVxF mutants

Based on the biochemical experiments carried out in *Xenopus* egg extracts, I hypothesized that Spc105 targets Glc7 to the kinetochore, and that Ipl1 can regulate Glc7 recruitment by phosphorylating Spc105 and abrogating this interaction. To test this hypothesis, I sought to examine the effects of three mutants of the Spc105 RVSF motif using the HGR method. The first was a PP1 binding mutant, R**A**S**A**. The second was an unphosphorylatable mutant, RV**A**F. This mutation represents the only conserved Aurora B consensus site studied in *Xenopus* and therefore with this mutant, Ipl1 would be unable to regulate to Spc105-Glc7 interaction. The third mutant was a negative control that introduced the STOP codon ochre at the start of the RVSF motif (R75ochre). Since Spc105 is an essential gene (Wigge et al., 1998), and this small truncation (the N-terminal 74 residues) does not include the domain necessary to localize to kinetochores (Kerres et al., 2007), I expected this mutation to be lethal. Finally, as a control for the new method, I used a cassette without any mutation that should simply produce wild type cells independent of the recombination site.

To initially examine the viability of each mutant, I incubated the parent strains (*SPC105*^{NT}) on galactose for 6 hours, which is sufficient time to ensure that almost all cells have undergone recombination. I then isolated single cells, and let them grow into colonies. Once grown, I isolated DNA from each viable colony and determined the genotype by PCR and restriction digest. This is the single cell colony assay (SCA) (Figure 3-2). Parent cells containing the wild type-

A

parent	recombinant				
	SPC105	*SPC105^{RVAF}*	*SPC105^{R75ochre}*	*SPC105^{RASA}*	DEAD
NT-WT	20				0
*NT-RV**A**F*	8	11			0
NT-R75ochre	12		8		0
*NT-R**A**S**A***	12			0	8

B

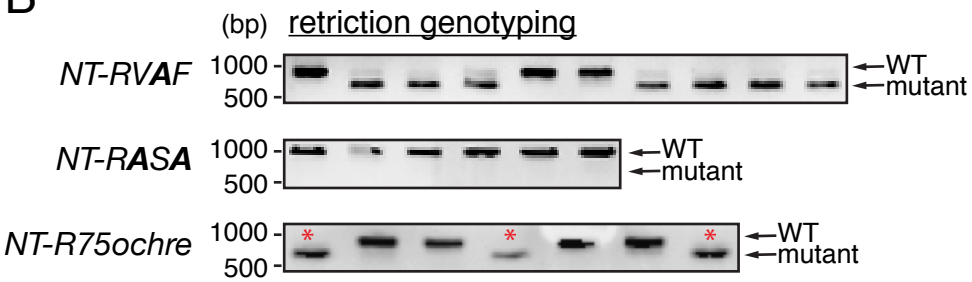

Figure 3-2: Viability of Spc105 mutants. (A) Single cell colony assay of *spc105^{NT-WT}*, *spc105$^{NT-RVAF}$*, *spc105$^{NT-R75ochre}$*, and *spc105$^{NT-RASA}$* parent cells. Six hours after *GAL-HO* induction, single cells were isolated, allowed to grow to isogenic colonies, and genotyped. Number of colonies with the indicated genotypes or those that failed to form macroscopic colonies (DEAD) is shown. (B) Representative genotyping of generated recombinant colonies. The genomic *SPC105* locus was PCR amplified from recombinant colonies using primers A and B in Figure 3-1, digested with mutation-specific restriction enzymes, and resolved on an agarose gel. Red asterisks indicate colonies with growth defects.

or RV**A**F-inducing cassette (*SPC105*$^{NT\text{-}WT}$ and *SPC105*$^{NT\text{-}RV\mathbf{A}F}$, respectively) produced cells that all grew up with wild-type kinetics. Genotyping revealed that all the colonies produced from the *SPC105*$^{NT\text{-}WT}$ parent were *SPC105*. The *SPC105*$^{NT\text{-}RV\mathbf{A}F}$ parent, on the other hand, produced colonies that were both *SPC105* and *spc105*$^{RV\mathbf{A}F}$, with indistinguishable rates of colony growth. From the R75ochre-inducing cassette (*SPC105*$^{NT\text{-}R75ochre}$), two populations of colonies were formed: one with wild type kinetics, and one viable but with a growth defect. The cells with wild type growth were indeed *SPC105*, while the slow-growing cells were *spc105*^{R75ochre}. The viability of these cells at all was surprising, since *SPC105* is an essential gene. I speculate that this viability is due to the read-through of the single STOP codon, making this allele a hypomorph.

In contrast, only a subset of the cells resulting from the RASA-inducing cassette (*SPC105*$^{NT\text{-}R\mathbf{ASA}}$) grew to form viable colonies, and these were all *SPC105*. The rest of the cells died as clumps and strings of large budded cells (Figure 3-3B). Using the methods available, I could not extract DNA from these cells for genotyping. However, when I induced recombination in liquid culture and extracted DNA from the mixed population for genotyping 6 hours later, I could detect the generation of the *spc105*$^{R\mathbf{ASA}}$ allele (Figure 3-3A). I could therefore infer that the death of this subpopulation was due to the *spc105*$^{R\mathbf{ASA}}$ mutation.

To determine the cell cycle status of these cells as they die, I used live imaging of GFP-tubulin (Figure 3-3C). Imaging *spc105*$^{NT\text{-}R\mathbf{ASA}}$ cells from 6 hours

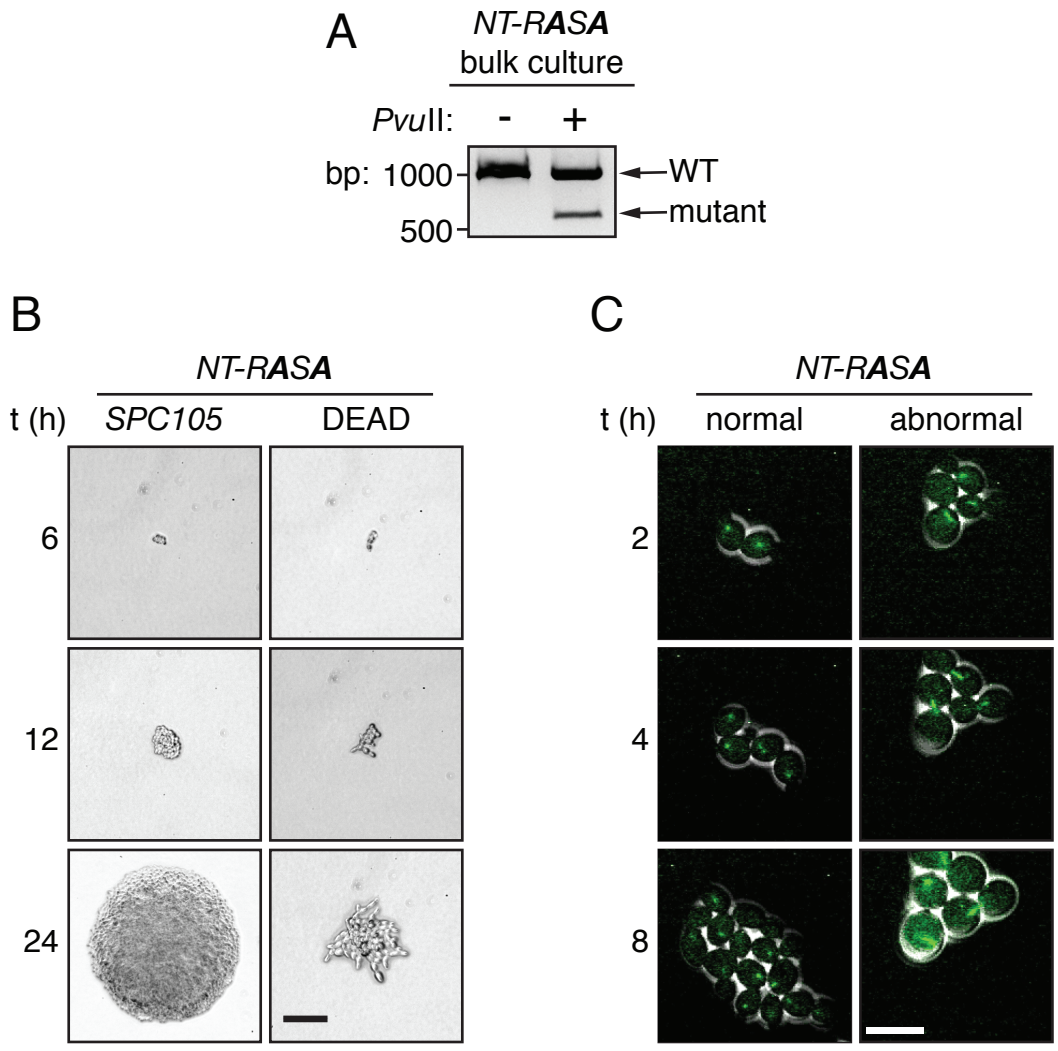

Figure 3-3: The terminal phenotype of *spc105^{RASA}*. (A) Six hours after induction of HGR in the parent strain harboring the *NT-RASA* cassette, the genomic *SPC105* locus was PCR amplified from bulk culture and digested with *Pvu*II to detect generation of *spc105^{RASA}*. (B) Representative colonies of the two classes of recombinants resulting from the R**A**S**A**-inducing cassette were imaged at the times indicated after single cell isolation. The colony on the left harbors wild-type *SPC105* as confirmed by genotyping analysis. Scale bar, 50 μm. (C) Time-lapse microscopy of GFP-Tub1 (green) was performed on *spc105$^{NT\text{-}RASA}$* cells beginning 6 hours after *GAL-HO* induction. Scale bar, 10 μm.

after galactose induction for a duration of 12 hours revealed cells with very prolonged metaphase delays (more than 4 hours in most cases), followed by a sudden anaphase, while other cells, likely the *SPC105* wild type recombinants, divided with normal kinetics. Pedigree analysis of cells exhibiting long mitotic delays revealed that some of the daughter cells attempted to divide again, with another metaphase delay, while others simply stopped growing (Figure 3-4). By contrast, all of the *spc105*$^{NT\text{-}RVAF}$ cells showed normal division kinetics after recombination, so the abnormal divisions seen in the *spc105*$^{NT\text{-}RASA}$ population is not due to the recombination events. This suggests that the terminal phenotype of the *spc105*^{RASA} mutation is a mitotic arrest, although the penetrance of this arrest is not complete. Perhaps the few cellular divisions that these cells go through are due to stochastic drops in CDK1 levels, which induce anaphase.

Rescuing *spc105*^{RASA}

Interaction with *IPL1*

To further study the *spc105*^{RASA} mutant, I searched for suppressor mutations. Suppressor mutations can both give insight into the physiological consequences of the mutation as well as enable further study by producing a viable strain with the mutation. If the phenotype of *spc105*^{RASA} was truly due to a loss of Glc7 phosphatase activity at the kinetochore, then I hypothesized that impaired kinase activity might ameliorate this loss and even out the phosphorylation balance. The mutation *ipl1-1* had already been shown to

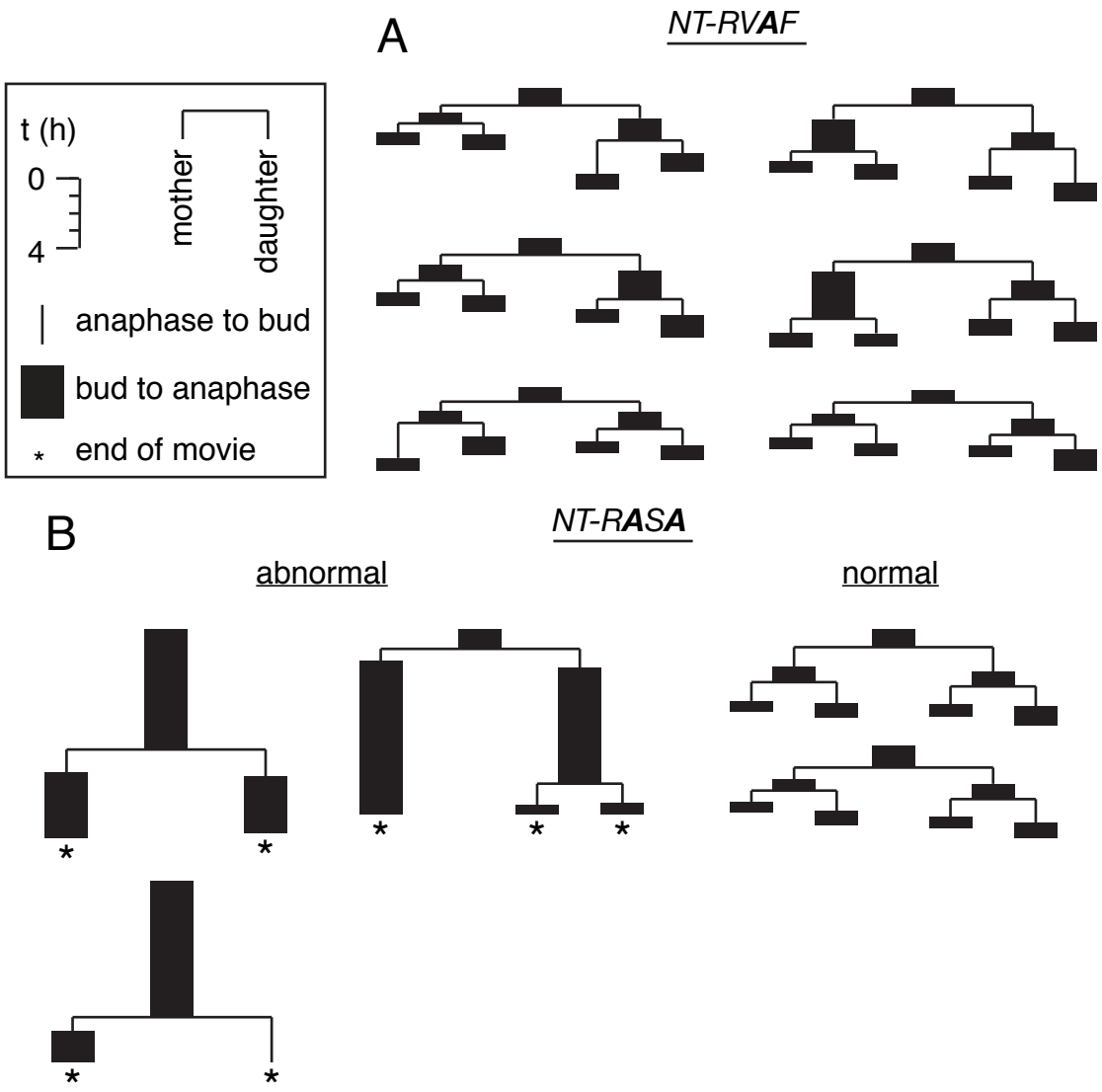

Figure 3-4: Pedigree analysis of *SPC105* mutants. Pedigree analysis of recombinants generated from the cells harboring the *NT-RV**A**F* or *NT-R**A**S**A*** cassettes during live cell imaging. Each lineage starts from a single unbudded cell and the duration of budding to anaphase (black rectangle) and anaphase to budding (line) was measured. Cells were followed for three generations or until the end of the movie (asterisks). When the lineage splits at each division, fates of the mother cell and the daughter cell are shown on the left and right, respectively. (A) Representative pedigrees for cells resulting from the *NT-RV**A**F* cassette. (B) Pedigree analysis of recombinants generated from the cells harboring the *NT-R**A**S**A*** cassette. Representative lineages showing abnormal cell divisions (left 3 examples) and normal cell divisions (right 2 examples) are shown.

partially rescue the *glc7-1* mutation, so I tested whether *ipl1-1* could also rescue *spc105^{RASA}*. Indeed, at the semipermissive temperature for *ipl1-1*, 30°C, viable *spc105^{RASA}* cells were recovered from the SCA in the *ipl1-1* background (Figure 3-5A). The cells are viable, albeit with a slight growth defect. When they were shifted to 23°C and full Ipl1 function was restored, the *ipl1-1 spc105^{RASA}* cells were again lethal (Figure 3-5B). On the other hand, when the double mutant cells were shifted closer to the non-permissive temperature for *ipl1-1*, the *spc105^{RASA}* mutation partially rescued the growth of *ipl1-1*. These results indicate that the Spc105-recruited Glc7 functions to balance the kinase activity of Ipl1 at the kinetochore.

spc105^{RASA} and the SAC

Based on previous research, Glc7 has two known functions at the kinetochore: to stabilize kinetochore microtubule attachments and to silence the SAC (Pinsky et al., 2009; Sassoon et al., 1999; Vanoosthuyse and Hardwick, 2009). Both of these functions act in opposition to Ipl1. To elucidate the function of the Spc105-Glc7 interaction, I decided to examine the interaction of the *spc105^{RASA}* mutation with *MAD2*. In budding yeast, *mad2Δ* cells are viable while exhibiting some chromosome segregation defects, but they do not arrest in response to microtubule poisons (Li and Murray, 1991). This indicates that the SAC is not essential in this system. On the other hand, many mutants that cause structural defects in kinetochore architecture or the kinetochore-microtubule

A

parent	recombinant			
	SPC105	*SPC105 -RASA*	*SPC105 -RVAF*	DEAD
ipl1-1 NT-RASA	15	4		0
ipl1-1 NT-RVAF	14		6	0

B

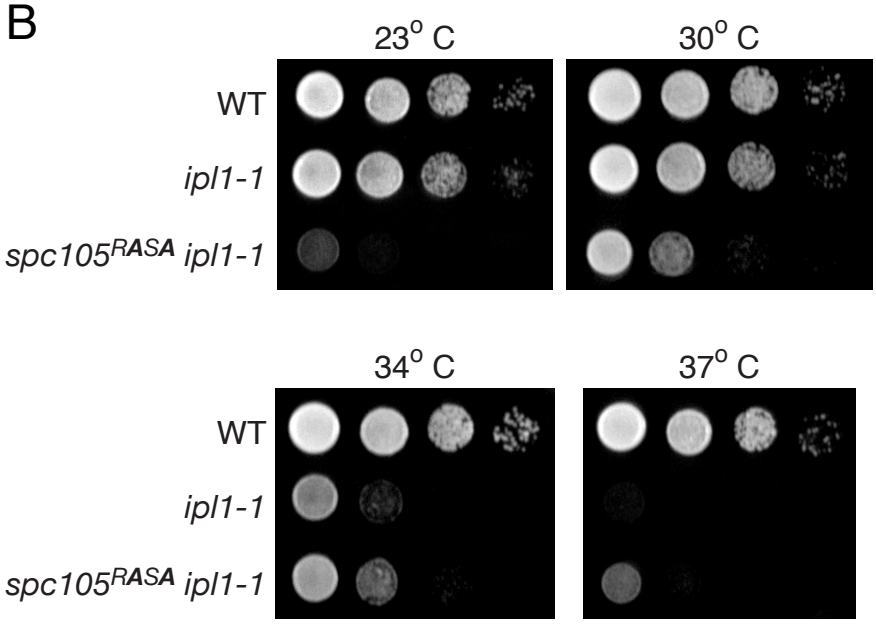

Figure 3-5: *ipl1-1* rescues *spc105^{RASA}*. (A) Single cell colony assay of *ipl1-1 spc105$^{NT\text{-}RASA}$* and *ipl1-1 spc105$^{NT\text{-}RVAF}$* parent cells. Number of colonies with the indicated genotypes or those that failed to form macroscopic colonies (DEAD) is shown. (B) Ten-fold serial dilutions of WT, *ipl1-1*, and *ipl1-1 spc105^{RASA}* were plated on YEPD at 23, 30, 34, and 37°C.

interface are synthetically lethal with *mad2Δ* (Cheeseman et al., 2001b; Daniel et al., 2006; Hardwick et al., 1999; Montpetit et al., 2005; Tong et al., 2004). This negative interaction is presumably because cells that have perturbed kinetochores need the SAC to allow enough time to form bipolar attachments.

Based on these ideas, there are two possible hypotheses for the *spc105^{RASA} mad2Δ* double mutant. If Spc105-recruited Glc7 is responsible for silencing the checkpoint, then elimination of the checkpoint would make silencing no longer essential and the double mutant should consequently be viable. Conversely, if this pool of Glc7 were responsible for kinetochore-microtubule stabilization, then the *spc105^{RASA}* mutation would cause unstable kinetochore-microtubule attachments and should still be lethal in a *mad2Δ* background. The first hypothesis was borne out: in a *mad2Δ* background, completely viable *spc105^{RASA}* cells were recovered from the SCA (Figure 3-6). By contrast, *spc105^{R75ochre}*, which is sick in a wild type background (see above), is lethal in a *mad2Δ* background. This likely reflects an effect of this mutant on kinetochore stability, analogous to the kinetochore structural mutants discussed above.

The *spc105^{RASA} mad2Δ* cells showed no cell cycle defects when assayed by budding index after a G1 arrest or kinetics of Pds1 degradation in mitosis (Figure 3-7). The double mutant did, however, show a slightly reduced growth rate compared to *mad2Δ* cells (Figure 3-8A). This may be due to another function of the Spc105-recruited Glc7. To examine whether the *spc105^{RASA}* mutation had a subtle effect on kinetochore function, I looked at chromosome

parent	recombinant			
	SPC105	*SPC105 -R**A**S**A***	*SPC105 -R75ochre*	DEAD
*mad2*Δ *NT-R**A**S**A***	13	5		0
*mad2*Δ *NT-R75ochre*	14		0	6

Figure 3-6: Viability of *SPC105* mutants in *mad2*Δ background. Single cell colony assay of *mad2*Δ *spc105*$^{NT\text{-}R\mathbf{A}S\mathbf{A}}$ and *mad2*Δ *spc105*$^{NT\text{-}R75ochre}$ parent cells. Number of colonies with the indicated genotypes or those that failed to form macroscopic colonies (DEAD) is shown.

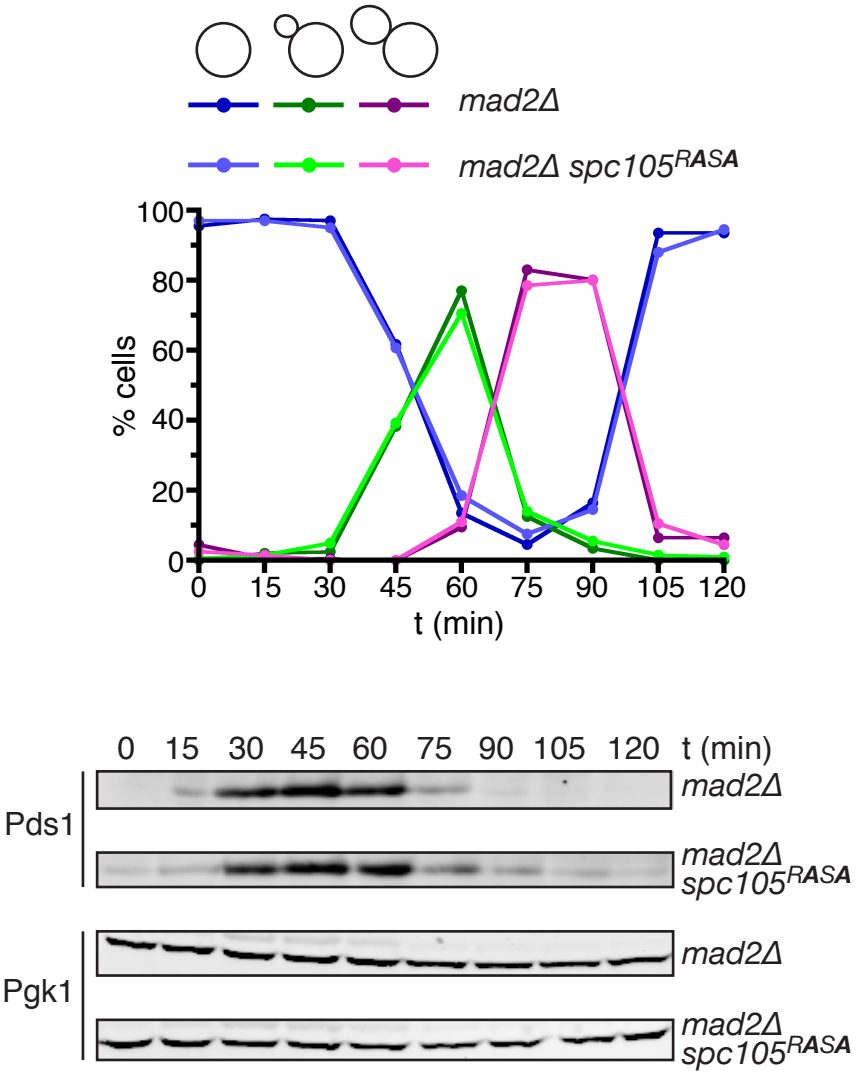

Figure 3-7: Without the SAC, *spc105^{RASA}* has normal cell cycle dynamics. *mad2Δ* and *mad2Δ spc105^{RASA}* cells were released from G1. Budding index (top, n > 200 cells each) and Pds1 and Pgk1 (loading control) levels (bottom, Western blots) were monitored.

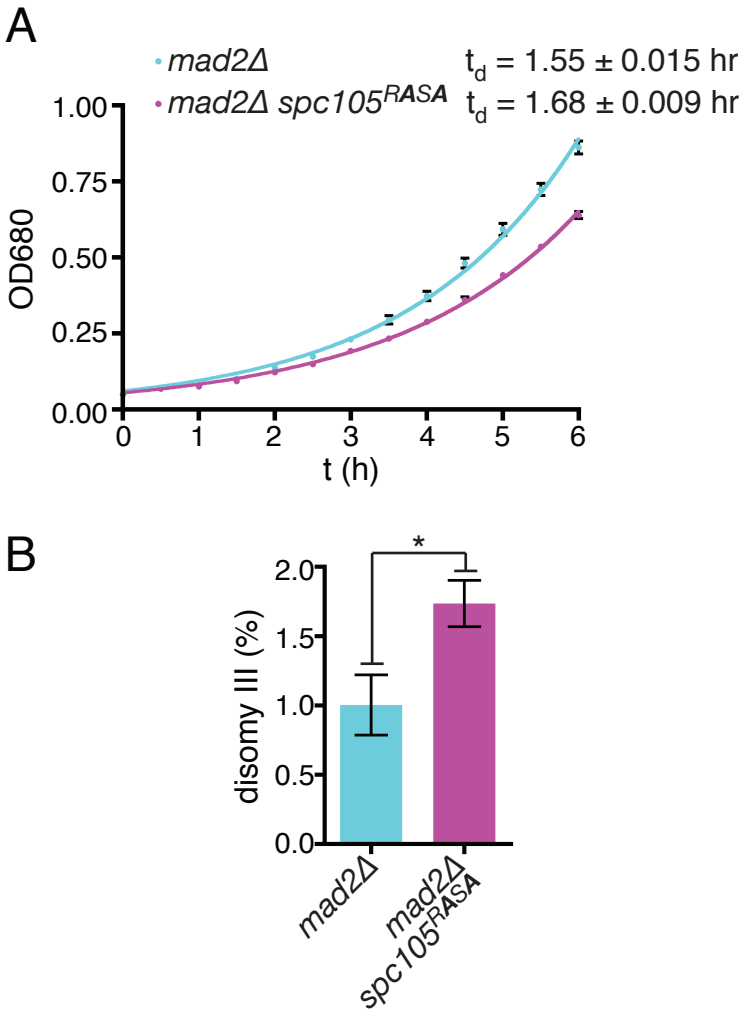

Figure 3-8: *spc105^{RASA}* causes a minor effect on chromosome segregation. (A) Growth curve of *mad2Δ* and *mad2Δ spc105^{RASA}* at 30°C in YEPD medium. Average ± SEM of the doubling time of three independent experiments are also shown. (B) IPL assay of *mad2Δ* and *mad2Δ spc105^{RASA}* cells containing a chromosome III marked with a *leu2* locus disrupted by *URA3*. The mean frequency ± SEM of disomy formation (assessed by generation Leu+, Ura+ colonies) from ten independent cultures are shown.

segregation using an increase in ploidy (IPL) assay. This assay, originally used to characterize Ipl1 for its role in chromosome segregation, assesses the occurrence of disomy of chromosome III using auxotrophic markers (Chan and Botstein, 1993). When compared to *mad2Δ* cells, which have an elevated missegregation occurrence over wild type cells, *spc105*^{RASA} *mad2Δ* cells showed a very slight, though statistically significant, increase in disomy III (Figure 3-8B). This may explain the slightly slower growth rate observed for the double mutant. Taken together, these data indicate that the Spc105-Glc7 interaction is essential for its role in silencing the SAC, and that it plays an auxiliary, non-essential role in physical chromosome segregation, likely through stabilization of kinetochore-microtubule attachments.

Since Mad2 is localized to the kinetochore, the deletion of the protein may result in other structural perturbations of the kinetochore that affect the Spc105-Glc7 interaction. To alleviate this concern, I sought to manipulate SAC signaling without any possible effect on kinetochore structure. To achieve this, I used the dominant mutant *CDC20-127* (figure 3-9). This mutant is insensitive to Mad2 due to a mutation in the Mad2 binding site (Hwang et al., 1998; Indjeian et al., 2005). When this protein is expressed under a tetracycline repressible promoter (*tet*^{R}-*CDC20-127*), the MCC cannot sequester it even when the SAC is signaled and it will constitutively activate the APC/C. When the cells are put on doxycycline, the expression of this dominant protein is repressed and the SAC becomes responsive to signaling again. Consistent with the interaction with *mad2Δ*,

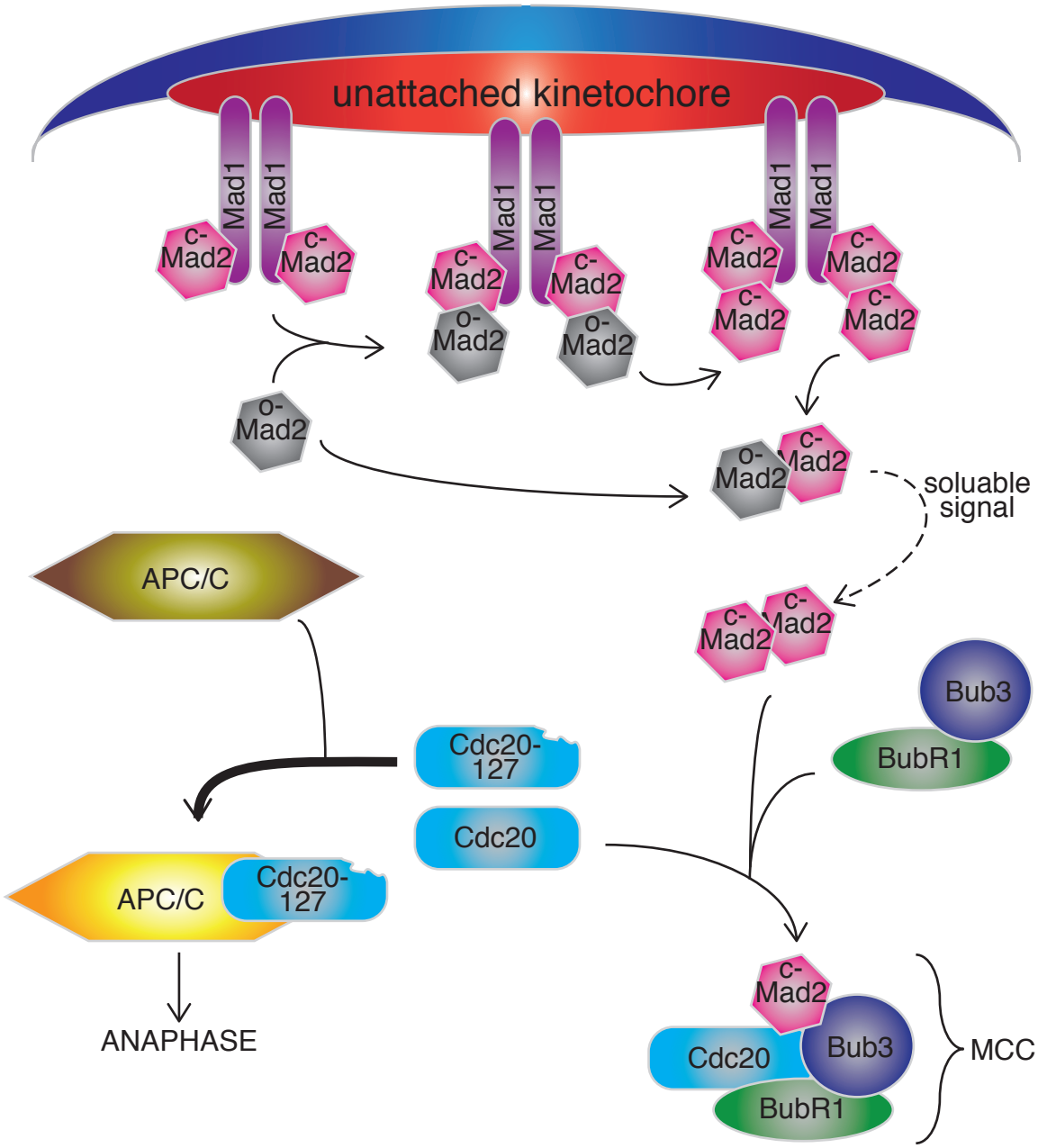

Figure 3-9: The molecular mechanism of Cdc20-127. The dominant protein Cdc20-127 lacks the domain required to bind Mad2. Therefore, even when the SAC is signaled from incorrectly attached kinetochores, the MCC cannot sequester Cdc20-127, the ACP/C gets activated, and anaphase proceeds. However, the wild type Cdc20 can still be bound by the MCC, so that when expression of *CDC20-127* is repressed and only wild type Cdc20 remains, the cells are again responsive to SAC signaling.

spc105^{RASA} is viable in the *tet*^{R}*-CDC20-127* background. When these cells are treated with doxycycline, they die with a similar morphology as previously described for *spc105*^{RASA} (Figure 3-10A). Biochemically, when released from G1 in the presence of doxycycline, they show prolonged stabilization of Pds1 levels and hyperphosphorylation of Mad1, indicative of SAC activation (Figure 3-10B). This data confirms that the terminal phenotype of the *spc105*^{RASA} mutation is prolonged activation of the SAC with a consequent severe mitotic delay, and ultimate failure of proliferation.

Phenotype of *spc105*^{RVAF}

spc105^{RVAF} supports SAC activation

Results in *Xenopus* discussed above suggested that Aurora B/Ipl1 phosphorylates Spc105 in order to prevent premature association of Glc7 to the kinetochore. In this model, the *spc105*^{RVAF} mutation would not be under this regulation and would prematurely recruit Glc7 to the kinetochore. Since I showed that Spc105-recruited Glc7 is necessary to silence the SAC, this premature Glc7 recruitment might impair SAC activation. From the initial SCA, I showed that *spc105*^{RVAF} is viable. The mutation causes no growth defects, and it does not affect chromosome segregation as assayed by the IPL assay (Figure 3-11). In addition, *spc105*^{RVAF} shows no negative interaction with *ipl1-1* (see Figure 3-5A), which might be suspected if there was an increase in phosphatase activity.

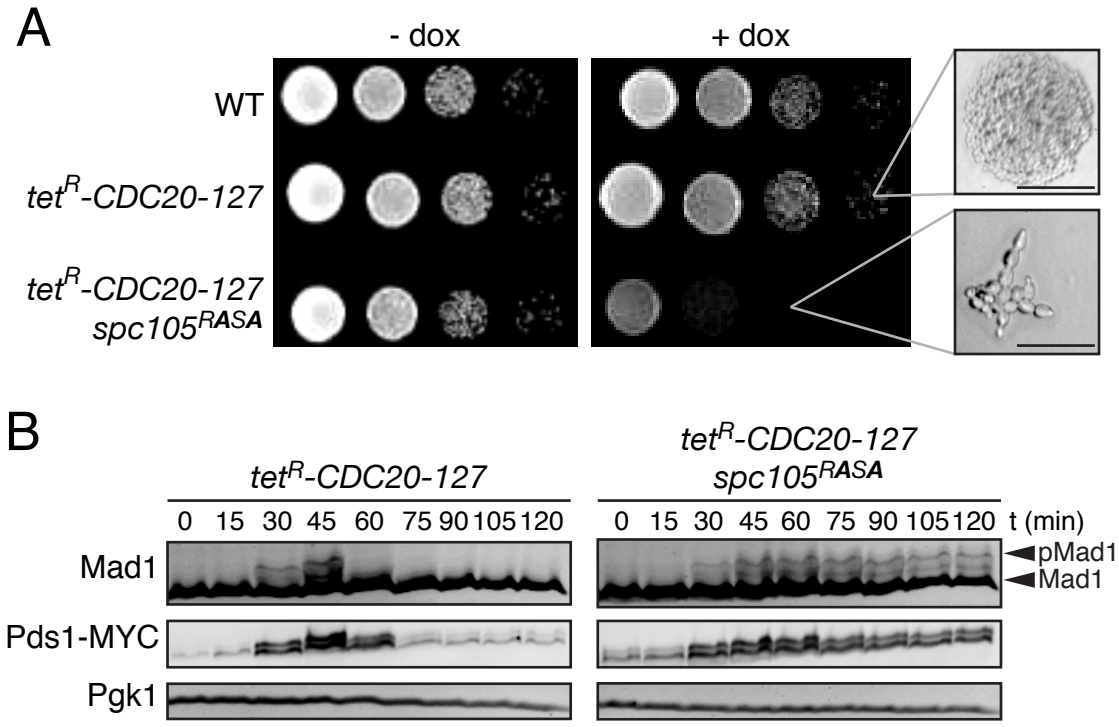

Figure 3-10: *spc105^{RASA}* dies from prolonged SAC activation. (A) Ten-fold serial dilutions of WT, *tet^{R}-CDC20-127*, and *tet^{R}-CDC20-127 spc105^{RASA}* were plated on YEPD with or without 5 μg/ml doxycycline at 30°C. High magnification images of microcolonies are also shown. Scale bar, 50 μm. (B) *tet^{R}-CDC20-127* and *tet^{R}-CDC20-127 spc105^{RASA}* cells were released from G1 arrest in the presence of doxycycline. Pds1-MYC, Mad1, and Pgk1 (loading control) levels were analyzed by Western blots at the indicated timepoints after release.

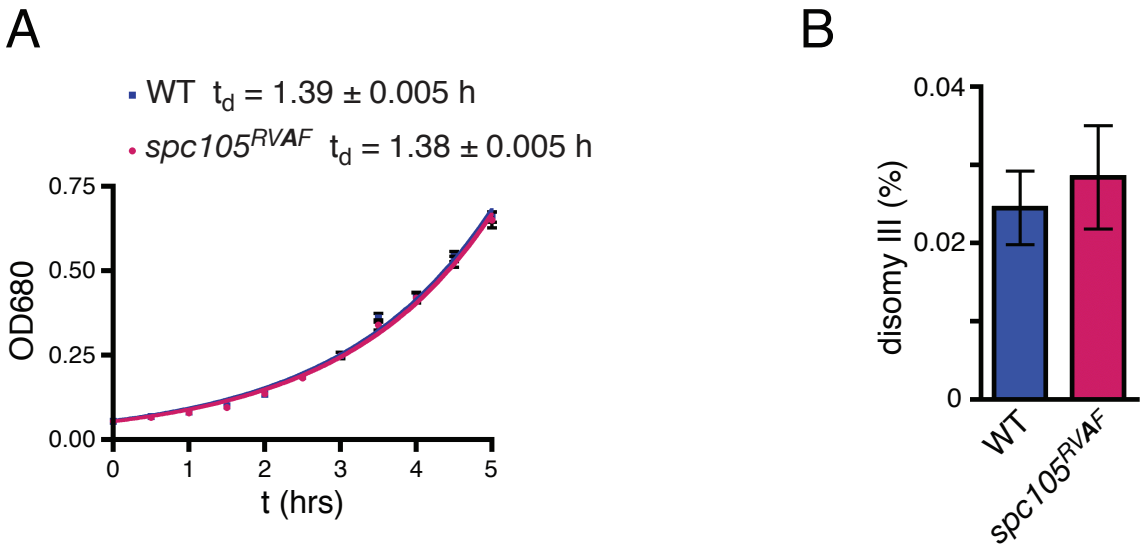

Figure 3-11: *spc105*^{RVAF} does not affect cell growth. (A) Growth curve of WT and *SPC105*^{RVAF} at 30°C in YEPD medium. Average ± SEM of the doubling time of three independent experiments are also shown. (B) IPL assay of wild type and *spc105*^{RVAF} cells containing a chromosome III marked with a *leu2* locus disrupted by *URA3*. The mean frequency ± SEM of disomy formation (assessed by generation Leu+, Ura+ colonies) from five independent cultures are shown.

However, since the SAC is non-essential in this system, *spc105*^{RVAF} may still specifically show a SAC signaling defect caused by an increase in PP1 recruitment. I therefore tested the ability of the *spc105*^{RVAF} cells to respond to SAC signaling. The SAC responds to both a lack of microtubule attachment at a single kinetochore and a lack of tension across kinetochores. I first tested signaling in response to lack of attachment by treating cells with microtubule poisons. In the presence of nocodazole, the majority of both wild type and *spc105*^{RVAF} cells arrested as dumbbell-shaped cells with large buds (Figure 3-12A). This morphology is indicative of a metaphase arrest induced by active SAC signaling. In addition, *spc105*^{RVAF} shows no sensitivity to benomyl, while the true SAC mutant *mad2Δ* shows a significant sensitivity (Figure 3-12B). Taken together, I concluded that *spc105*^{RVAF} cells could signal the SAC in the presence of unattached kinetochores.

In budding yeast, Aurora B is required for SAC signaling in response to lack of tension, but not attachment (Biggins and Murray, 2001). I therefore assayed the ability of *spc105*^{RVAF} cells to activate the SAC in response to tension by examining its effect on the mitotic delay exhibited by a cohesin mutant, *scc1-73*. This mutant has defective sister chromatid cohesion at the centromere, and consequently these cells show a mitotic delay due to SAC activation because tension cannot be generated (Biggins and Murray, 2001). This mitotic delay can be observed as a delay in Pds1 degradation at metaphase. This delay is

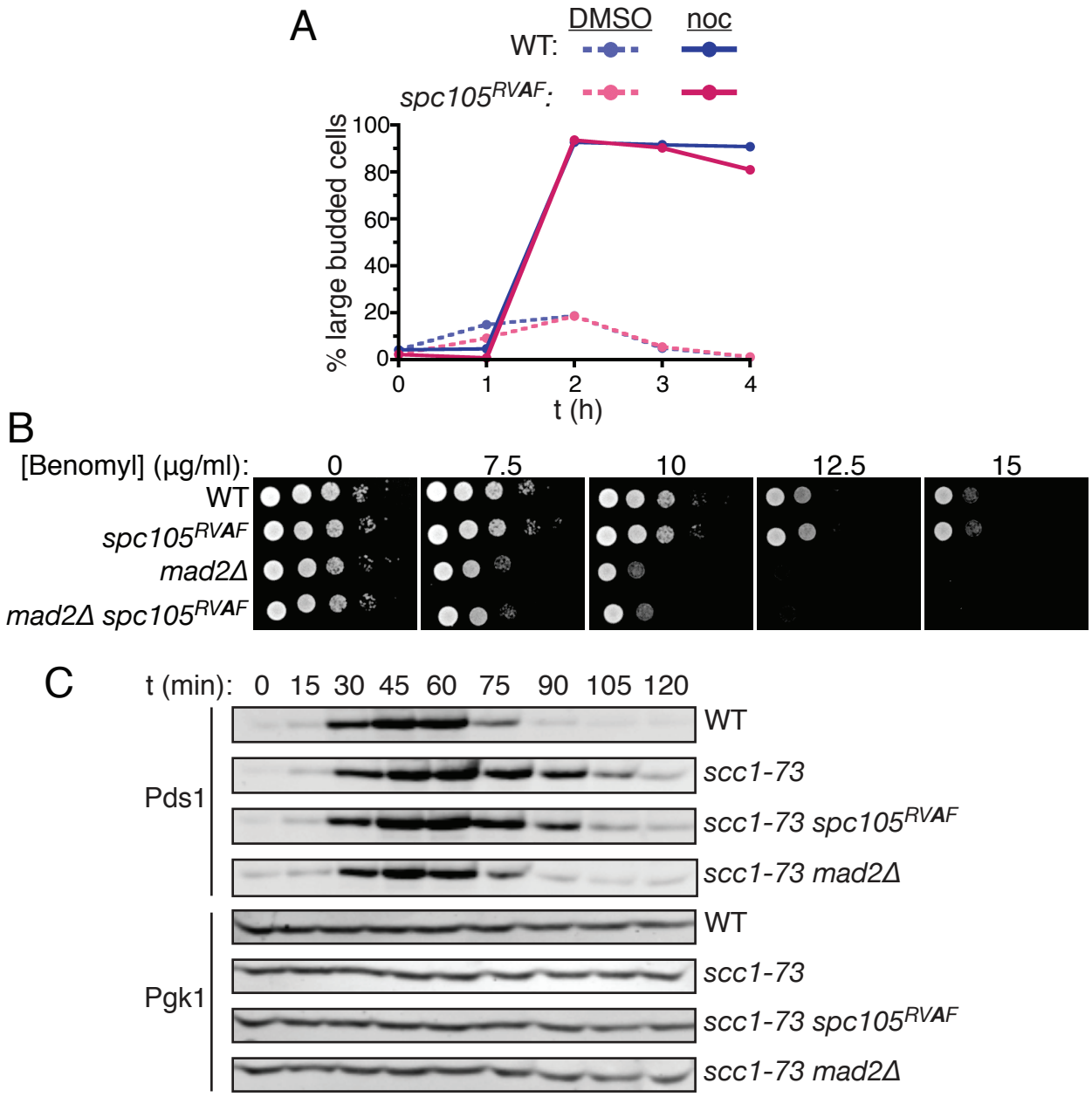

Figure 3-12: *spc105*^{RVAF} supports SAC activation. (A) G1 synchronized WT and *spc105*^{RVAF} cells were released into nocodazole. The number of large budded cells was counted at the indicated timepoints, n > 500 cells each. (B) Ten-fold serial dilutions of WT, *spc105*^{RVAF}, *mad2Δ*, and *mad2Δ spc105*^{RVAF} were plated on YEPD with the indicated concentrations of benomyl. (C) WT, *scc1-73*, *scc1-73 spc105*^{RVAF}, and *scc1-73 mad2Δ* cells were G1 synchronized at the permissive temperature (23°C), released to the restrictive temperature (37°), and Pds1 and Pgk1 (loading control) levels were monitored by Western blotting at the indicated timepoints after release.

abolished in a *mad2Δ* mutant, but the delay persists in the *spc105*^{RVAF} mutant (Figure 3-12C), indicating proper activation of the SAC.

These data are consistent with the IPL assay that showed that *spc105*^{RVAF} does not cause chromosome missegregation. As previously reported, this is not the case with a true SAC deficient mutant such as *mad2Δ*. Taken together, these data demonstrate that prevention of Ipl1 phosphorylation of Spc105 near the Glc7 binding motifs does not affect SAC signaling.

spc105^{RVAF} affects chromosome segregation

Although the double mutant *spc105*^{RVAF} *scc1-73* showed a delay in Pds1 degradation at the non-permissive temperature (37°C), compared to the *scc1-73* single mutant, *spc105*^{RVAF} does partially rescue the viability of the *scc1-73* mutation at the semi-permissive temperature (35°C) (Figure 3-13A). To determine the reason for this rescue, I examined the chromosome dynamics in these cells using a GFP tag at the URA3 locus on chromosome 5.

The characteristic phenotype of cohesin mutants is premature sister chromatid separation in prophase (Michaelis et al., 1997). A consequence of this premature separation is improper kinetochore-microtubule attachments and chromosome missegregation, observable as cells in anaphase with both chromosomes in the same cell. Both of these phenotypes are observed in *scc1-73* cells. In the *spc105*^{RVAF} *scc1-73* cells, the occurrence of premature sister

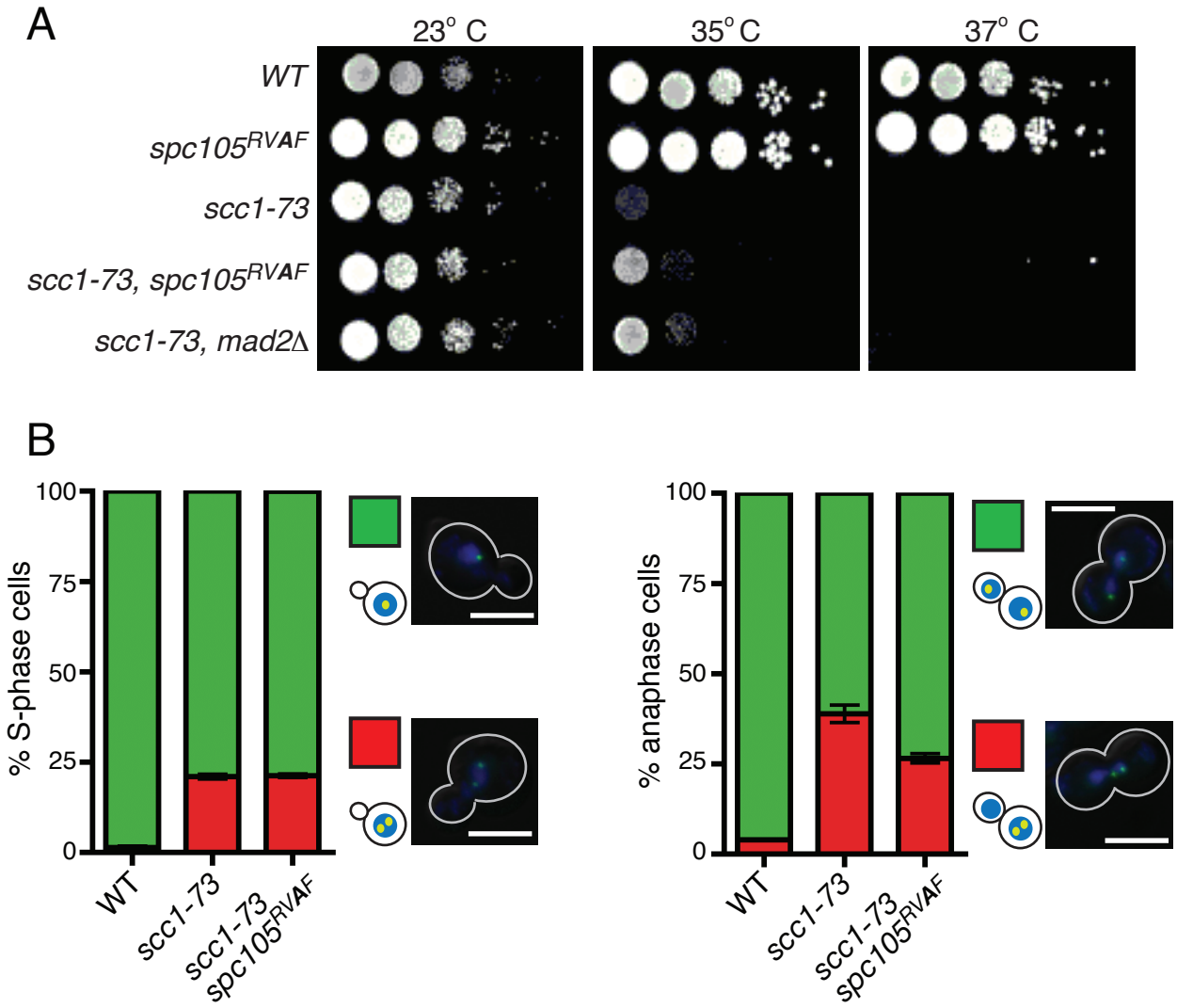

Figure 3-13: *spc105*^{RVAF} affects chromosome segregation in the *scc1-73* background. (A) Ten-fold serial dilutions of WT, *spc105*^{RVAF}, *scc1-73*, and *scc1-73 spc105*^{RVAF} were plated on YEPD at 23, 35, and 37°C. (B) WT, *scc1-73*, and *scc1-73 spc105*^{RVAF} cells with the *URA3* locus marked with GFP were G1 synchronized at the permissive temperature (23°C) and released to the semi-permissive temperature (34°). S-phase cells were fixed and counted for premature sister chromatid separation (left), and anaphase cells were fixed and counted for proper chromosome segregation (right) based on the location of GFP. Average ± SEM of three independent experiments are shown, n = 200 cells each. Representative images of each cell type are shown. Scale bar, 5 μm.

chromatid separation is unaffected. However, the incidence of chromosome missegregation is reduced (Figure 3-13B).

Consequences of constitutive Glc7-Spc105 interaction

GLC7 fusion rescues *spc105^{RASA}*

I have assumed that the *spc105^{RASA}* phenotype is due to the perturbation of the Spc105-Glc7 interaction. However, the N-terminus of Spc105 may have other functions that are sensitive to the R**A**S**A** mutation, independent of Glc7 binding. To alleviate this concern, I attempted to rescue the *spc105^{RASA}* mutant by genetic fusion of the protein to Glc7.

To make this fusion protein, I utilized a modified HGR approach (Figure 3-14). Into the *SPC105$^{NT,\ RASA}$* cassette, I inserted the *GLC7* gene, either wild type or a catalytically dead mutant (*glc7^{cat}*), with a linker N-terminal to the *SPC105* fragment. From the SCA, I obtained viable *GLC7-spc105^{RASA}* cells (Figure 3-15). Conversely, I obtained no viable *glc7^{cat}-spc105^{RASA}* cells, all viable colonies were *SPC105* and a subset of cells died with the *spc105^{RASA}* morphology. The *GLC7* fusion completely rescued the *spc105^{RASA}* mutation, with identical growth rate to wild type and no effect on chromosome segregation as measured by the IPL assay (Figure 3-16). From this data, I concluded that the phenotype observed in

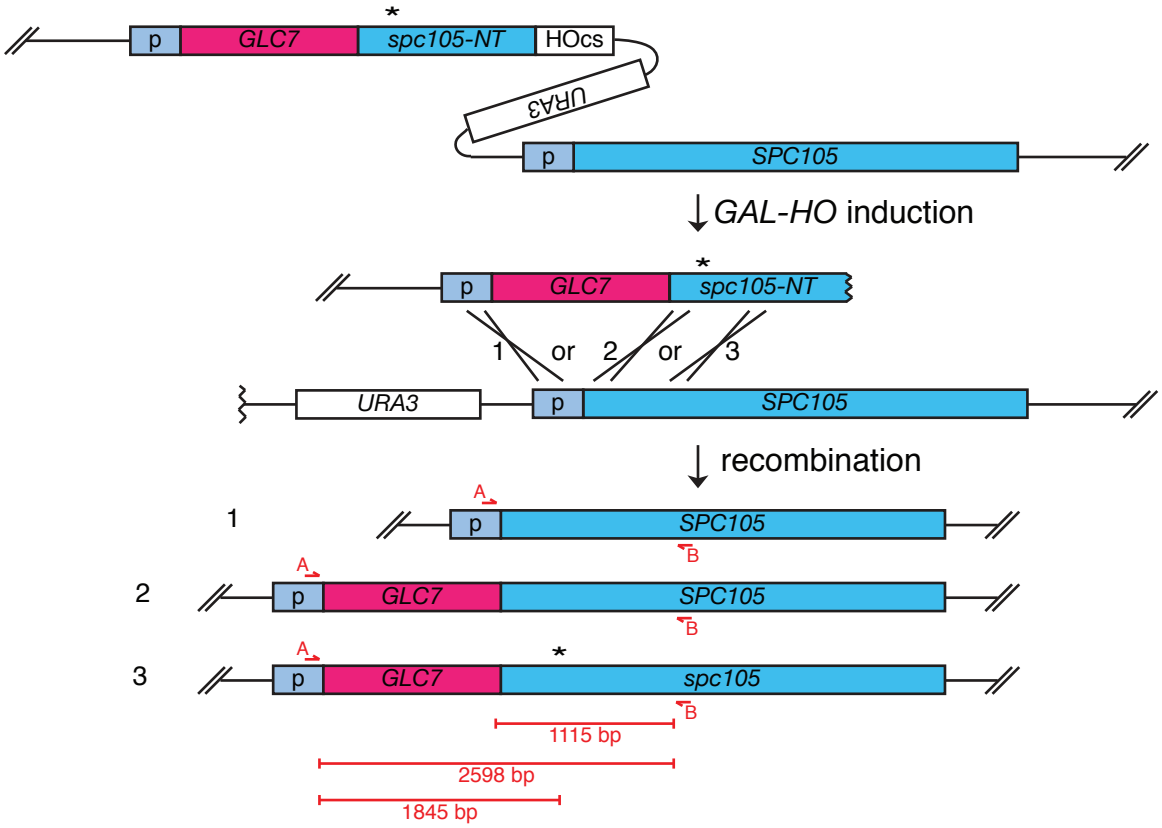

Figure 3-14: Using HGR to generate Glc7-Spc105 fusion proteins. The full length *GLC7* gene, either wild type or with a catalytically dead mutation, was inserted N-terminal to the mutation generating *spc105*^{NT} cassette. Upon repair, three genotypes are possible depending on the site of recombination: regeneration of wild type *SPC105* (1); *GLC7* fused to wild type *SPC105* (2); or *GLC7* fused to mutant *spc105* (3).

A

parent	recombinant					
	SPC105	*GLC7 -SPC105*	*GLC7 -spc105^{RASA}*	*glc7^{cat} -SPC105*	*glc7^{cat} -spc105^{RASA}*	DEAD
NT-GLC7-spc105^{RASA}	15	0	6			3
NT-glc7^{cat}-spc105^{RASA}	11			7	0	10
NT-GLC7-SPC105	14	0				15
NT-glc7^{cat}-SPC105	14			8		0
NT-GLC7-SPC105 mad2Δ	13	0				9

B

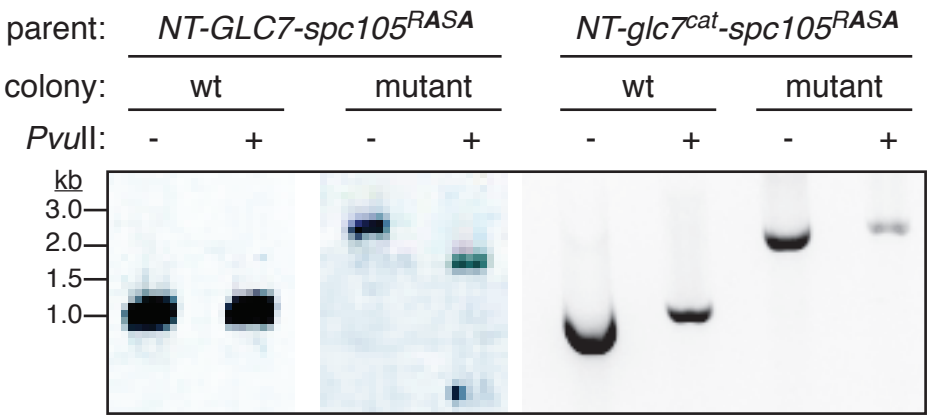

Figure 3-15: Viability of Glc7-Spc105 fusion proteins. (A) Single cell colony assay of cells harboring *GLC7-SPC105* producing cassettes. Number of colonies with the indicated genotypes or those that failed to form macroscopic colonies (DEAD) derived from single cells isolated after HGR of the strain harboring the indicted cassettes is shown. (B) Representative genotyping of colonies produced from the *NT-GLC7-spc105^{RASA}* and *NT-glc7^{cat}-spc105^{RASA}*. The genomic *SPC105* locus was PCR amplified from recombinant colonies using primers A and B in Figure 3-14. Larger fragments include the *GLC7* or *glc7^{cat}* fusion, and digestion with *Pvu*I detects the R**A**S**A** mutation.

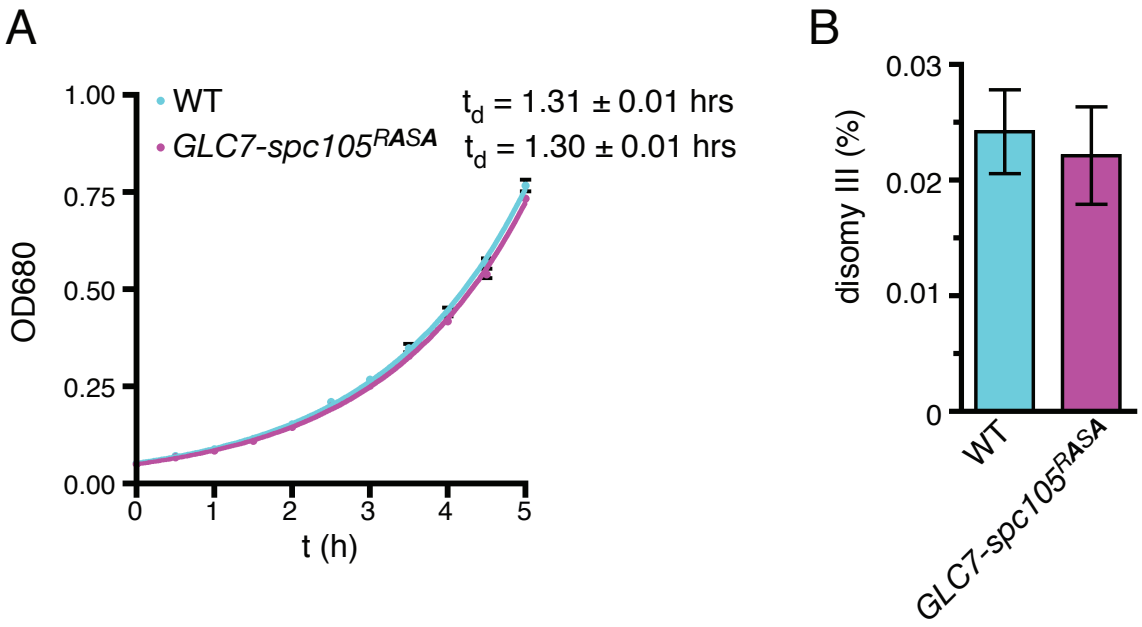

Figure 3-16: Fusing Glc7 to spc105^{RASA} rescues viability. (A) Growth curve of WT and *GLC7-spc105^{RASA}* cells at 30°C in YEPD medium. Average ± SEM of the doubling time of three independent experiments are also shown. (B) IPL assay of WT and *GLC7-spc105^{RASA}* cells containing a chromosome III marked with a *leu2* locus disrupted by *URA3*. The mean frequency ± SEM of disomy III formation (assessed by generation Leu+, Ura+ colonies) from 15 independent cultures are shown.

the *spc105*^{RASA} mutant is due to the loss of Glc7 catalytic activity at the kinetochore.

Using the *GLC7-spc105*^{RASA} mutant, I was able to investigate the consequences of constitutive recruitment of Glc7 to Spc105. As explained above, I hypothesized that constitutive recruitment of Glc7 might prematurely silence the SAC, causing a SAC-deficient phenotype. However, *GLC7-spc105*^{RASA} cells showed no sensitivity to benomyl (Figure 3-17A). In addition, when treated with nocodazole, *GLC7-spc105*^{RASA} cells showed a complete metaphase arrest, analogous to wild type cells (Figure 3-17B). It has previously been shown that impaired Ipl1 activity, despite showing no effect on SAC activation in response to nocodazole, does diminish the cell's ability to recover after nocodazole treatment (Francisco et al., 1994). On the other hand, *GLC7-spc105*^{RASA} cells showed no such sensitivity. This indicates that SAC signaling can be activated even with constitutively recruited Glc7, and that phosphorylation levels of Ipl1 targets are not appreciably affected.

To determine whether premature recruitment of Glc7 to Spc105 had any physiological consequences, I attempted to sensitize the system to phosphatase activity. To do this, I used the *ipl1-1* mutation, reasoning that if the kinase activity is impaired it might be more sensitive early in mitosis to Glc7 recruitment. Indeed, at semipermissive temperature for *ipl1-1* (30°C), *GLC7-spc105*^{RASA} further impairs growth (Figure 3-18A), indicating a negative interaction between these two mutations. Although neither mutant impairs the activation of the SAC

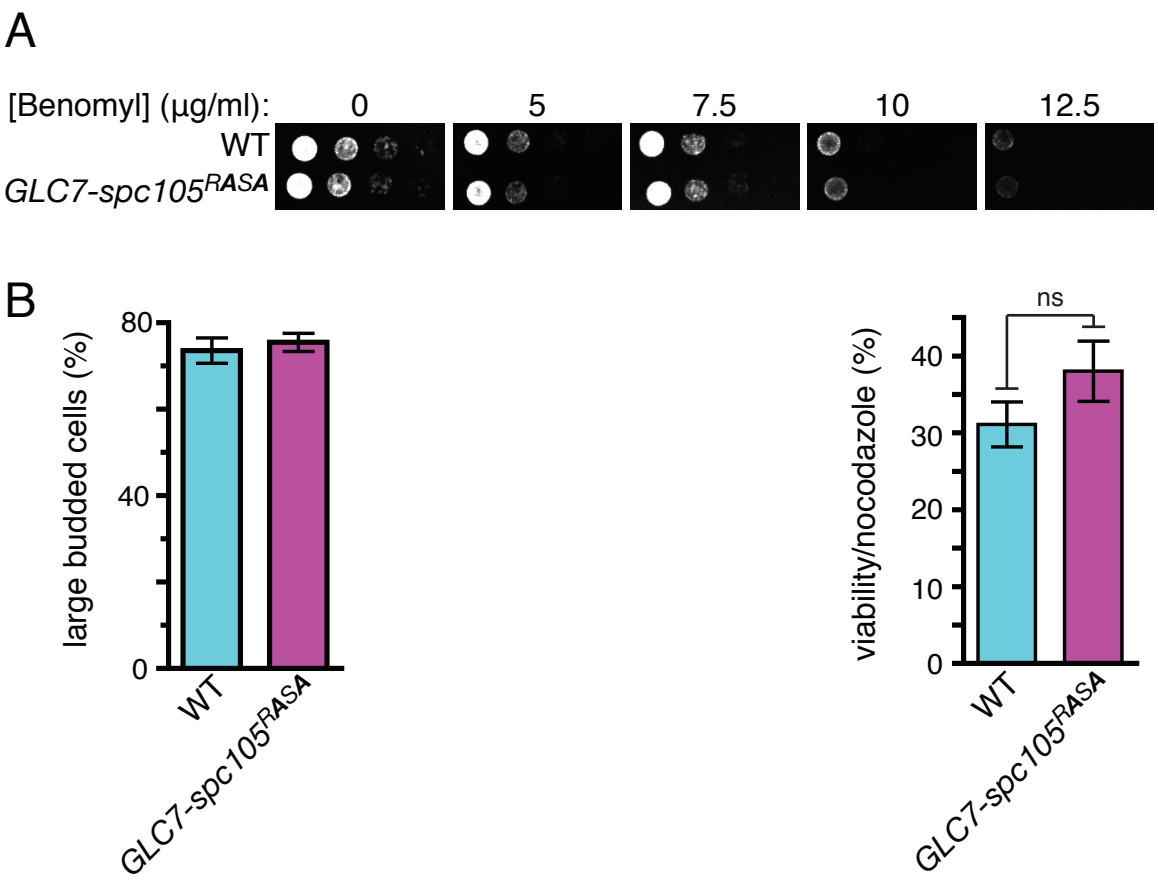

Figure 3-17: *GLC7-spc105^{RASA}* supports SAC activation. (A) 10-fold serial dilutions of WT and *GLC7-spc105^{RASA}* on YEPD with the indicated concentrations of benomyl. (B) WT and *GLC7-spc105^{RASA}* strains were treated with nocodazole and benomyl for 3 hours, cell morphology was counted (left), and cells were washed and plated on YEPD to count colony formation (right). Average ± SEM for 3 separate experiments are shown; n > 400 cells each; ns: not significant, p = 0.23.

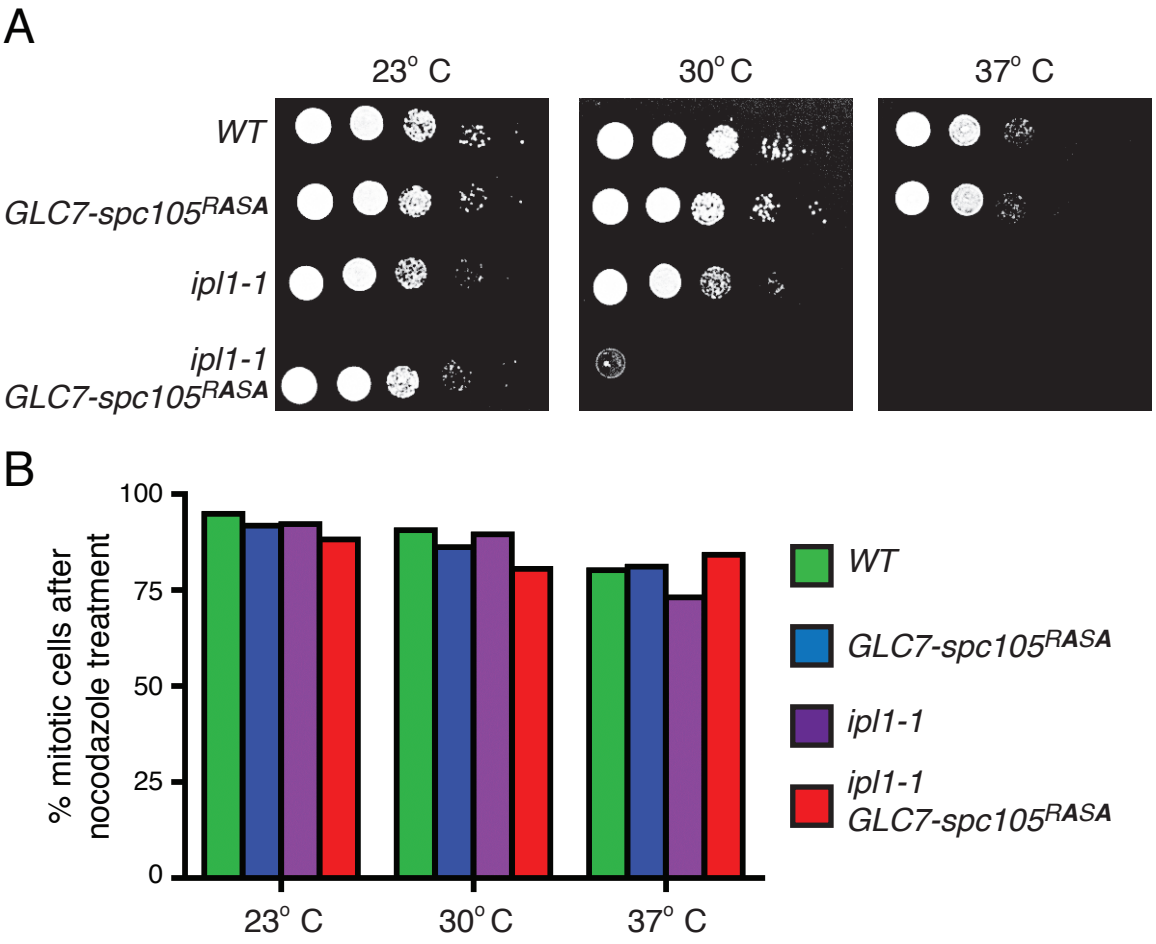

Figure 3-18: *GLC7-spc105^{RASA}* negatively interacts with *ipl1-1*. (A) Ten-fold serial dilutions of WT, *GLC7-spc105^{RASA}*, *ipl1-1*, and *ipl1-1 GLC7-spc105^{RASA}* were plated on YEPD at 23, 30, and 37°C. (B) WT, *GLC7-spc105^{RASA}*, *ipl1-1*, and *ipl1-1 GLC7-spc105^{RASA}* cells were grown to log phase at the permissive temperature, treated with nocodazole and benomyl at the indicated temperatures for 3 hours, and cell morphology was counted.

when cells are treated with nocodazole, I tested the double mutant to see whether the additive effect caused a deficient SAC response. However, at all temperatures tested, the *GLC7-spc105^{RASA} ipl1-1* cells still arrested in metaphase when treated with nocodazole. Therefore, although the constitutive recruitment of the phosphatase does not mimic the effects of the impaired kinase, they do still show an additive effect.

GLC7-SPC105 is lethal

The HGR from the *GLC7-spc105^{RASA}* inducing cassette had three possible outcomes, depending on the site of recombination (see Figure 3-14). The possible genotypes are *GLC7-spc105^{RASA}*, *SPC105*, and *GLC7-SPC105*. However, the only colonies recovered were either *SPC105* or *GLC7-spc105^{RASA}*, and a few cells died upon recombination. When the *glc7^{cat}* mutant was used, I recovered viable *glc7^{cat}-SPC105* clones, but no *glc7^{cat}-spc105^{RASA}* cells (see Figure 3-15). This led me to suspect that *GLC7-SPC105* is a lethal mutation.

Indeed, when I used a cassette without the RASA mutation to simply induce *GLC7-SPC105*, the only viable colonies were *SPC105*. As a control, a similar cassette with the *glc7^{cat}* mutant generated both *SPC105* and *glc7^{cat}-SPC105* cells that were completely viable. Using live imaging of GFP-tubulin and performing pedigree analysis on mutant cells, I observed that the terminal phenotype of *GLC7-SPC105* is highly variable (Figure 3-19). Some cells arrested in G1 as unbudded cells, while others showed a long mitotic delay.

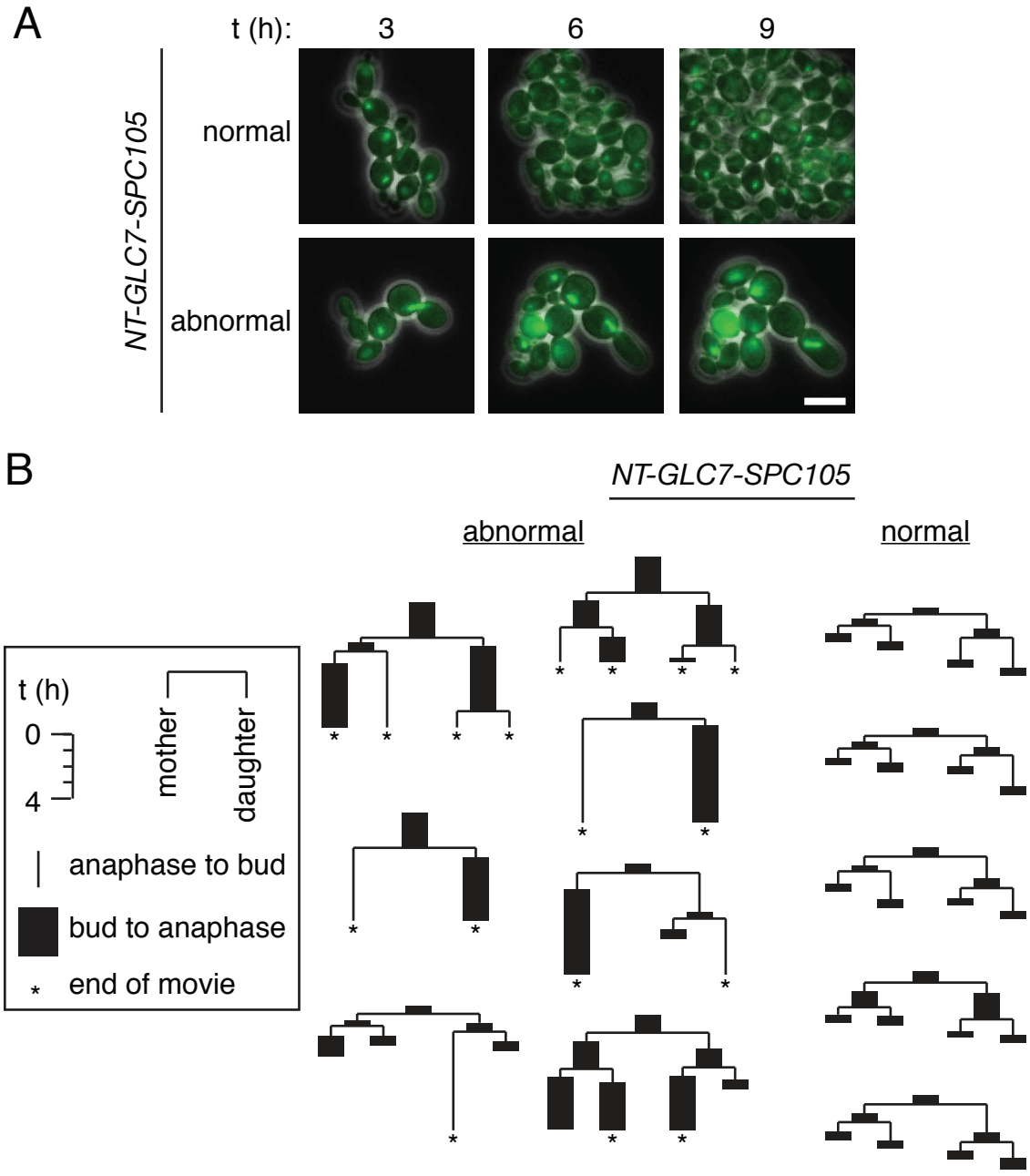

Figure 3-19: *GLC7-SPC105* is lethal. (A) Time-lapse microscopy of GFP-Tub1 (green) was performed on cells harboring the *NT-GLC7-SPC105* cassette beginning 6 hours after *GAL-HO* induction. Scale bar, 10 μm. (B) Pedigree analysis as described in Figure 3-4 of cells harboring the *NT-GLC7-SPC105* cassette. Representative lineages showing abnormal cell divisions (left 7 examples) and normal cell divisions (right 5 examples) are shown.

However, *GLC7-SPC105* is not rescued by *mad2Δ* (see Figure 3-15), indicating that the lethality was not solely due to SAC activation.

Discussion

spc105^{RVAF} affects kinetochore-microtubule stability

The *spc105*^{RVAF} mutant showed a partial rescue of *scc1-73*, but not for the predicted reason. Instead of perturbing SAC signaling, it appeared to rescue chromosome missegregation. Phosphorylation of the KMN network, and specifically KNL1/Spc105, does regulate the stability of kinetochore-microtubule attachments by reducing the direct affinity of the proteins for microtubules (Welburn et al., 2010). A lack of tension across the kinetochore would activate the error correction mechanism, thus promoting this phosphorylation even when the attachment is correct. However, perhaps when Spc105 cannot be phosphorylated at this one site, the kinetochore-microtubule attachment may be slightly more stable, facilitating proper chromosome segregation. This might indiscriminately stabilize all attachments, correct and incorrect, which is why the rescue would not be complete. The *spc105*^{RVAF} mutation alone, however, shows no effect on chromosome missegregation as judged by the IPL assay. This marginal hyperstabilization of kinetochore-microtubule attachments, therefore, possibly only manifests a physiological effect in stressed situations such as in the *scc1-73* mutant background. In conclusion, the partial rescue of *scc1-73* by

spc105^{RVAF} is probably independent of Glc7 recruitment and its effect on SAC silencing.

Sensitivity of the kinetochore to PP1 levels

It is not inherently obvious why *GLC7-SPC105* might be lethal. The viability of *GLC7-spc105*^{RASA} indicates that a fixed Glc7:Spc105 ratio of 1:1 is tolerated. Assuming the endogenous RVSF motif is functionally recruiting Glc7, the Glc-Spc105 fusion is recruiting at most twice the amount of Glc7 catalytic activity. This means that somewhere between 1:1 and 1:2 lies an increased level of Glc7 that cannot be tolerated. This fine sensitivity is highly unusual for an enzyme. Overexpression of GLC7 from a GAL1 promoter in budding yeast causes growth and morphology defects, but it is viable (Black et al., 1995). This might imply that the kinetochore is unique in its sensitivity to phosphatase activity level. Based on the pleiotropic cell cycle phenotype of the mutant, it is possible that the excess Glc7 is dephosphorylating targets other than those it normally would that are required for SAC silencing. These could include targets required for kinetochore-microtubule stability, or targets that affect chromatin structure. These data point to the importance of precise regulation of phosphatase activity at the kinetochore.

Implications of the *spc105^{RASA} ipl1-1* genetic interaction

The viability of *spc105^{RASA} ipl1-1* double mutant indicates that reduction of kinase activity via the temperature sensitive allele rescues the lack of phosphatase recruitment, thus restoring the phosphorylation balance. This is in accordance with the data indicating that Spc105-recruited Glc7 is responsible for silencing the SAC: with reduced Ipl1 levels, the SAC cannot be efficiently activated and therefore might not necessitate silencing. However, this model is contradicted by the fact that at higher temperatures *spc105^{RASA}* actually partially rescues *ipl1-1*. Effects of the SAC cannot explain this data; the Ipl1-1 mutant cannot activate the SAC at the restrictive temperatures, and an impairment in SAC silencing would not cause a rescue in growth. Ipl1 has several other necessary functions, and this indicates that Spc105-recruited Glc7 probably also has other roles at the kinetochore. This may be correlated with the slight increase in chromosome missegregation of the *spc105^{RASA} mad2Δ* double mutant, which points to a potential role in kinetochore-microtubule stabilization. It is possible that under normal circumstances this role is very minor, but in the very stressed conditions caused by the *ipl1-1* mutation, it has a larger impact on the viability of the cells.

Is the Spc105-Glc7 interaction regulated?

Based on biochemical data from *Xenopus* egg extracts, I had hypothesized that the Spc105-Glc7 interaction is temporally regulated by Ipl1-

mediated phosphorylation of Spc105. This would mean that without this regulation Glc7 would be prematurely recruited to the kinetochore and impair SAC signaling. However, the mutant of Spc105 that would eliminate this regulatory mechanism and cause this unregulated recruitment, *spc105*^{RVAF}, did not show the expected phenotype. This could be for two reasons. First, there is a different mechanism that temporally regulates the association of Glc7 with the kinetochore, and even in the phosphorylation mutant this true regulatory pathway still temporally regulates the Spc105-Glc7 interaction. Second, this regulation method is functional and Glc7 is prematurely recruited to the kinetochore in the *spc105*^{RVAF} mutant, but this premature recruitment alone cannot silence the SAC.

Based on observations of the *GLC7-spc105*^{RASA} mutant, I can conclude that constitutive recruitment of Glc7 by Spc105 is insufficient to prematurely silence the SAC. This deduction can help to more accurately interpret the phenotype of the *spc105*^{RVAF} mutant. The reason the *spc105*^{RVAF} mutant shows no SAC deficiency phenotype may be that even if this mutant causes premature recruitment of Glc7, I now know that this is insufficient to silence the SAC. Therefore, although Ipl1 phosphorylation of Spc105 to abrogate its interaction with Glc7 may still be a functional regulatory mechanism, it is not the only mechanism working at the kinetochore to prevent Glc7 from silencing the SAC until biorientation is achieved.

The dynamicity of the Glc7-Spc105 interaction is not essential for timely activation and silencing of the SAC. However, directly fusing Glc7 to Spc105 is

detrimental in an *ipl1-1* background, indicating that there is a functional significance to the dynamicity of the interaction. Impairing the counteracting kinase sensitized the system to inappropriate recruitment of the phosphatase. It may be that the minor effect that this interaction could have on kinetochore-microtubule stability is exacerbated in this situation.

CHAPTER 4: DISCUSSION AND PERSPECTIVE

Function of the KNL1/Spc105-PP1/Glc7 interaction

Coupling SAC silencing to microtubule attachment

The majority of the work presented here was published in Rosenberg et al., 2011. Based on this data, I proposed a model in which the Spc105-Glc7 interaction is necessary to couple the proper attachment of microtubules to kinetochores with SAC silencing (Figure 4-1). When Glc7 is not targeted to Spc105, the SAC cannot be silenced. On the other hand, even if Glc7 is present at the kinetochore but there is no microtubule, the SAC still cannot be silenced. This is most likely because Glc7 cannot effectively dephosphorylate the substrates necessary to silence the SAC. Only with concurrent Glc7 recruitment and microtubule attachment will the SAC be silenced.

This coupling between microtubule attachment and Glc7/PP1 activity could occur in a number of ways. The presence of microtubules may be necessary to bring Spc105/KNL1-bound PP1 in proximity to its critical substrates. This would make the most sense if the substrates were microtubule associated proteins, and thus only localized to kinetochores through microtubules. A different, though not mutually exclusive, mechanism may involve a conformational change in the proteins involved upon microtubule attachment. Under this purview falls the theory of “spatial separation” in which tension across kinetochores caused by bioriented microtubule attachment pulls outer

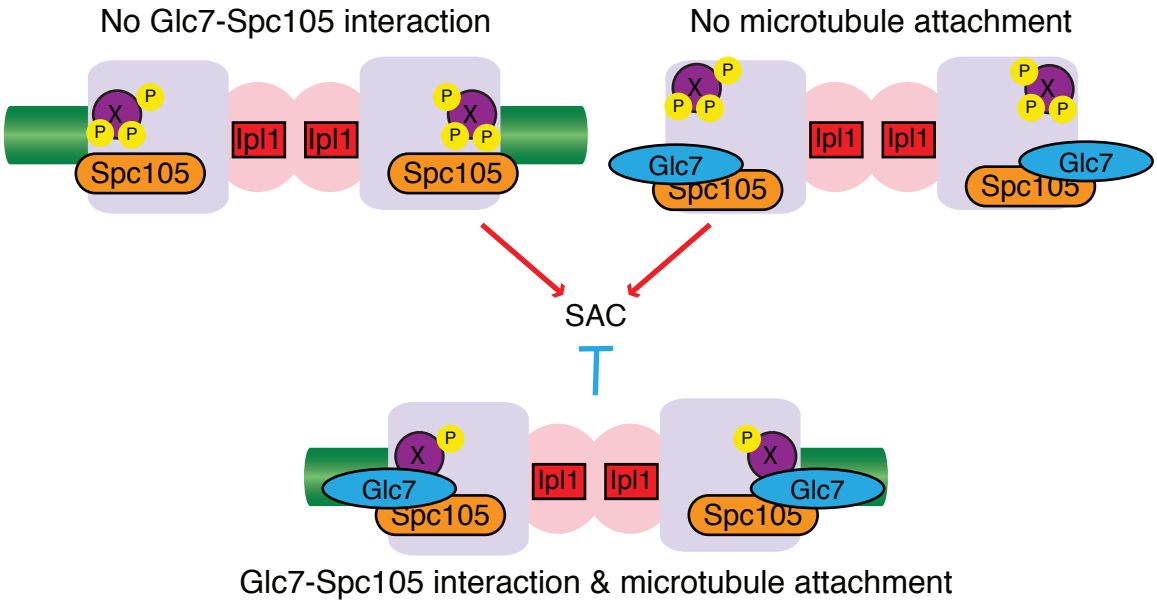

Figure 4-1: PP1/Glc7 couples microtubule attachment to SAC silencing. Model. In the absence of Glc7-Spc105 interaction (top left), or without microtubule attachment (top right), putative kinetochore proteins (X) are efficiently phosphorylated in an Ipl1-dependent manner and the SAC is turned on. Only when Glc7 is recruited to Spc105 and microtubules are attached to the kinetochore, X is dephosphorylated and the SAC becomes silenced.

kinetochore substrates away from the kinase (Aurora B/Ipl1) localized to the inner centromere, thus tipping the balance towards dephosphorylation (Liu et al., 2009).

Domain structure of KNL1

This model implies that KNL1 simply occupies the correct spatial domain for the function of PP1 to counteract Aurora B. However, examination of the domain structure of KNL1 (Figure 4-2) indicates that it may play a more direct role in regulating the function of PP1. The C-terminus of KNL1 is primarily responsible for binding Mis12, and the binding site contains a putative coiled-coil domain that may be essential for this interaction. The N-terminus, on the other hand, contains a variety of sequence and structural motifs, which are not yet fully understood, that may point to potential mechanistic properties.

First, the N-terminus of KNL1 itself binds microtubules directly (Pagliuca et al., 2009; Welburn et al., 2010), and in *C. elegans* the exact binding motif has been mapped to a basic patch adjacent to the RVxF motif (Espeut et al., 2012). Through this interaction, it is possible that there is a more direct and dramatic conformation change induced by microtubule binding that facilitates dephosphorylation by the KNL1-PP1 holoenzyme. In addition, there is evidence that KNL1 directly binds the SAC signaling proteins Bub1 and BubR1, and these binding sites have also been mapped to the N-terminus (Bolanos-Garcia et al., 2009; Bolanos-Garcia et al., 2011; Kiyomitsu et al., 2011; Kiyomitsu et al., 2007;

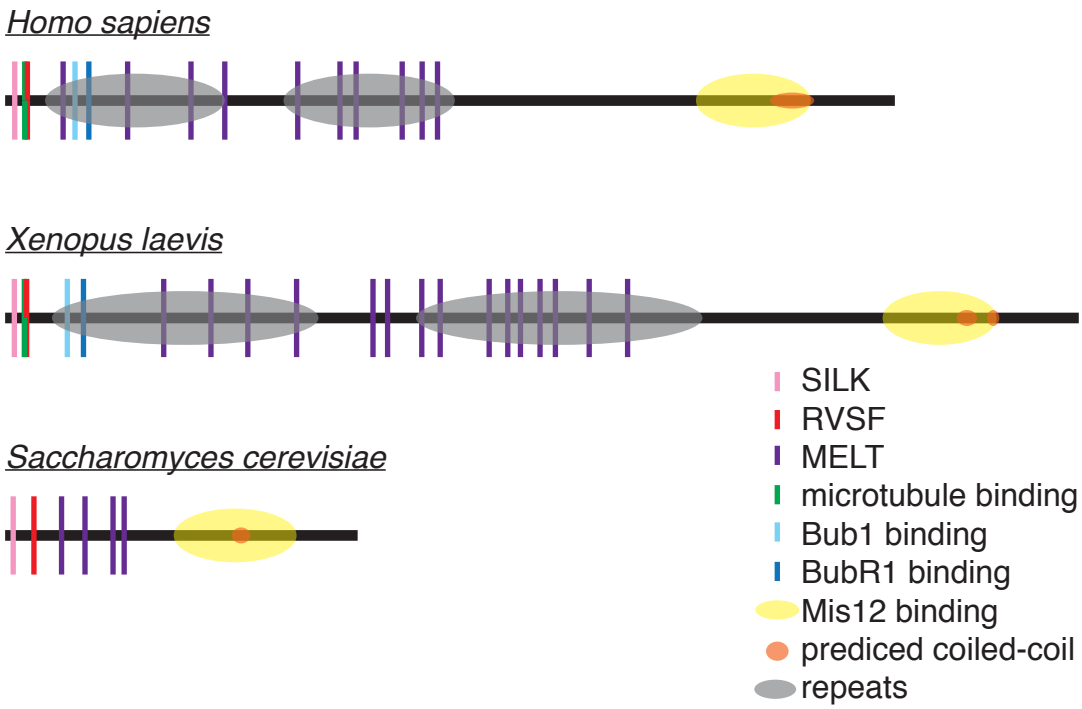

Figure 4-2: Domain structure of KNL1/Spc105. Schematic of sequence motifs and predicted structural and functional domains of KNL1/Spc105 from *Homo sapiens*, *Xenopus laevis*, and *Saaccharomyces Cerevisiae*. The SILK and RVxF motifs are defined previously. MELT repeats are defined by M[E/D][I/L][S/T] (Cheeseman et al., 2004). The microtubule binding motif was identified by sequence homology to the sites identified in *C. elegans* (Espeut et al., 2012). The Bub1 and BubR1 binding motifs were mapped in the human homologue (Kiyomitsu et al., 2011), and the Mis12 binding motif was mapped in S. pombe (Kerres et al., 2007). Repeat sequences and coiled-coil domains were predicted using the SMART databases (Letunic et al., 2012; Schultz et al., 1998).

Krenn et al., 2012). Finally, there is a series of MELT repeats (defined as M [E/D] [I/V] T) that are highly conserved across the evolutionary spectrum. The phosphorylation of these repeats by Mps1 has been implicated in recruitment of SAC proteins, and they may be dephosphorylated by PP1 directly (London et al., 2012; Shepperd et al., 2012). In higher eukaryotes such as frogs and humans, these sequence domains are located in two large internal repeats. These repeats may in part contribute to the gross size difference between these proteins and the yeast homologues, which do not contain the repeats.

The interactions of KNL1 with PP1, microtubules, and SAC proteins may be significantly intertwined to coordinate the SAC silencing activity of PP1 upon microtubule attachment. Definition of the critical substrates as well as more precise structural data on the consequences of microtubule binding at the kinetochore are both necessary to begin to elucidate a possible mechanism for this coupling phenomenon.

Mechanisms of silencing the SAC

Mechanisms to activate SAC signaling have long been scrutinized, as the SAC is considered critical for maintaining genomic integrity. Indeed, in most systems other than budding yeast, all SAC components are essential for maintained growth. Silencing of the SAC, on the other hand, has only recently been considered. It is in fact counterintuitive that a mechanism for SAC silencing should be essential in an unperturbed cell cycle when the SAC is thought of as

an emergency mechanism engaged only upon mitotic malfunction. However, there is evidence that SAC components are recruited to kinetochores in the course of every cell cycle (Gillett et al., 2004). It is therefore logical to conclude that in the course of prometaphase, when kinetochores are formed but not yet attached, SAC signaling is activated to some degree. The "normal" cell cycle timing, then, is dictated by the rate of action of the mechanism to silence the SAC.

How, then, is the SAC silenced? Obviously, reversal of the phosphorylation signal that triggers SAC activation and formation of the MCC by phosphatases is necessary. This is the part of the process for which the KNL1-PP1 holoenzyme is critical. Additionally, the motor protein dynein has been shown to facilitate the ejection of SAC proteins, including Mad2, from the kinetochore upon establishment of bipolar attachment (Howell et al., 2001). This would facilitate the cessation of the SAC signal emanating from the kinetochore. Simply silencing the activation, however, may not be enough. The diffusible c-Mad2 signal would still be present in the cytoplasm and the MCC would still be intact. The stochastic breakdown of this complex is likely not fast enough to account for the observed timing of transition to anaphase once all kinetochores are bioriented.

The protein P31^{comet} has been implicated as a direct silencer of the SAC. P31^{comet} localizes to unattached kinetochores, but it also shows a rapid turnover and is present in the cytoplasm. When P31^{comet} is depleted, cells arrest in

metaphase with stable, bipolar attachments that are under tension (Hagan et al., 2011). In this situation, SAC signaling originating at the kinetochore would be turned off (possibly via KNL1-recruited PP1 activity), however, that is insufficient to silence the SAC without P31^{comet}. Mechanistically, P31^{comet} preferentially binds c-Mad2, but not o-Mad2, and dissociates the MCC, facilitating Cdc20-mediated activation of the APC/C (Westhorpe et al., 2011; Xia et al., 2004; Yang et al., 2007). The dissolving of the MCC mediated by P31^{comet} requires the hydrolysis of ATP (Teichner et al., 2011), pointing to an active process.

It is clear that KNL1-PP1 and P31^{comet} play critical roles in silencing the SAC. How, then, are they related? One possibility is that P31^{comet} is a passive antagonizing force to SAC activation and once the initiating signal at the kinetochore is silenced by KNL1-PP1, the balance of c-Mad2 binding is tipped from the MCC to P31^{comet}. The other possibility is that P31^{comet} is regulated to activate upon biorientation of all chromosomes by the activity of KNL1-PP1, although a potential signaling mechanism is not yet apparent. A third possibility, given that there has not yet been a homologue of P31^{comet} found in yeast, is that these represent two independent essential mechanisms for SAC silencing. Elucidating the critical substrates of KNL1-PP1 for SAC silencing would help to distinguish between these alternatives, and possible point to a molecular mechanism for translating biorientation into SAC silencing.

Other work on KNL1/Spc105

Concurrent with this work, several other efforts to identify PP1 regulatory subunits at the kinetochore were reported. Other studies focused on KNL1 in fission yeast, human cells, and worms. The fission yeast homologue, Spc7, also shows an interaction with PP1 that is essential for silencing the SAC (Meadows et al., 2011). In human cells, the PP1 binding mutant of KNL1 causes a decrease in kinetochore-microtubule stability, although the SAC was not examined. In *C. elegans*, the PP1 binding mutant of KNL1 showed a delay in forming stable kinetochore-microtubule attachments as well, although no lagging chromosomes were observed. Similar to my data in budding yeast, the mutant also causes a significant cell cycle delay after SAC activation, which was alleviated by depletion of the Mad2 homologue. However, in stark contrast to my results, the PP1 binding mutant is synthetically lethal with depletion of Mad2 (Espeut et al., 2012).

The data from human cells and worms is in contradiction with my results in budding yeast that indicate the Spc105/KNL1-PP1 interaction does not play a significant role in kinetochore-microtubule stability. One potential reason for this discrepancy is the robustness of the system. The human cells were cold-treated, and perhaps in this stressed situation perturbation of the KNL1-PP1 holoenzyme causes a decrease in kinetochore-microtubule stability, but in a normal cell cycle this dysfunction is not enough to cause a visible phenotype in the functional

assay I used (the increase in ploidy assay). The *C.* elegans data represents embryonic lethality, a system in which there may be different requirements for both kinetochore-microtubule attachment and SAC signaling and silencing.

Another possibility is that these discrepancies represent an evolutionary difference between human cells, worms, and budding yeast. It may be that in yeast the Spc105-Glc7 holoenzyme represents the major SAC silencing factor, but in humans it plays more of a role in kinetochore-microtubule attachment and a separate mechanism, such as $P31^{comet}$ discussed above, functions to silence the SAC. In this case, the data from worms may represent an intermediate situation where the KNL1-PP1 holoenzyme plays a role in both mechanisms.

Additional PP1 holoenzymes at the kinetochore

In addition to KNL1/Spc105, there have been several other PP1 holoenzymes at the kinetochore examined recently. PP1 interacts with the microtubule motor protein CENP-E in human cells through a conserved RVTF motif, and this motif is regulated by phosphorylation by both Aurora A and Aurora B in a similar manner as I hypothesized for KNL1. This holoenzyme and its regulation are required for proper chromosome congression to the metaphase plate and establishment of bioriented attachments (Kim et al., 2010). In fission yeast, PP1 associates with the kinesin 8-like motors Klp5 and Klp6, and this interaction is also necessary to silence the SAC (Meadows et al., 2011).

Fin1 is a PP1 regulatory subunit described in budding yeast (but for which no homologue in other organisms has yet been found) that localizes to microtubules and kinetochores at anaphase onset. Premature targeting of this complex results in monopolar spindles but a suppression of SAC activation (Akiyoshi et al., 2009b). Repo-man recruits PP1 to chromosome arms, but it is responsible for the centromeric localization of Aurora B because it dephosphorylates the Aurora B-recruiting mark histone H3-threonine 3 phosphorylation, thus limiting Aurora B to centromeres (Qian et al., 2011; Trinkle-Mulcahy et al., 2006; Vagnarelli et al., 2006).

Finally, Sds22 is the most studied mitotic PP1 regulatory subunit, although its function is the least well understood. It does not interact through a canonical RVxF motif but rather through interaction of α-helices on both surfaces (Ceulemans et al., 2002). It was discovered in fission yeast, where deletion of the gene causes mitotic arrest (Ohkura and Yanagida, 1991). In budding yeast, Sds22 is required for the nuclear localization of PP1, and mutation of the gene causes mitotic arrest and chromosome instability (Pedelini et al., 2007; Peggie et al., 2002). In addition, it was independently identified as a suppressor of an Aurora B/Ipl1 mutation (Pinsky et al., 2006). In human cells, however, it is not necessary for nuclear accumulation of PP1 (Lesage et al., 2004), but rather for kinetochore localization of PP1, where it may modulate the kinase activity of Aurora B directly (Posch et al., 2010). Interestingly, in all organisms studied, Sds22 forms an inhibitory complex with PP1 that impairs its enzymatic activity

(Daher et al., 2006a; Daher et al., 2006b; Lesage et al., 2007; Pedelini et al., 2007). How this inhibition relates to its function at the kinetochore, however, remains unclear.

Perspective: The many faces of PP1

Why so many?

At the onset of this project, a major struggle came from the fact that we knew very little about the function of PP1 at the kinetochore, and nothing of the mechanism of localization. Now at the conclusion there appears to be an excess of regulatory subunits for the functions we know PP1 plays. There is likely a separation of function such that some PP1 regulatory subunits are responsible for the kinetochore-microtubule attachment stabilizing function of PP1, while others are responsible for the SAC silencing function. This is consistent with the view that each regulatory subunit represents a different holoenzyme with unique localization and function. However, there still appear to be up to six holoenzymes for only two major functions, and this may not even be a complete list since *in vivo* and *in silico* screens have generated large lists of uncharacterized PP1 binding proteins.

This is reminiscent of the "kinase paradox" discussed earlier. The specific properties of the holoenzymes might necessitate an overlap of function, such that each holoenzyme might have distinct timing, spatial range, or substrate specificity. This would create a situation in which several enzymes are needed

but at different times or in different places. But this also raises the question of whether the PP1 holoenzymes and the pathways that they are a part of interact with each other in a similar manner as those of the kinetochore kinases. Indeed, in the case of the PP1-CENP-E interaction, CENP-E needs to be dephosphorylated in order to bind PP1 at all. Might this be the function of another PP1 holoenzyme at the kinetochore? Also, similar to some current models for kinases, certain PP1 holoenzymes might carry out the same function and even act on the same target, but in response to different stimuli. These are just some of the many ways these pathways can interact, and a full understanding of kinetochore function will not be complete until we examine the relationships between enzymes beyond linear pathways.

Discovery Methods

There appear to be two major methods used to discover a "novel" PP1 holoenzyme. First, PP1 is co-purified with a previously uncharacterized protein, and then the localization and function of this protein is examined as it relates to how it regulates PP1. Second, previously studied proteins are found to have a conserved RVxF motif, and then an additional role for this protein in regulating PP1 emerges. This raises the question of whether the proteins solely discovered for their ability to bind PP1 actually have other roles in the cell as well. An in-depth look at these proteins independent of their roles in regulating PP1 may reveal novel regulatory pathways.

Another question that arises from these considerations is whether the "dual roles" of some of these proteins come up out of convenience or necessity. In other words, is the PP1-recruiting role of a protein somehow related to a seemingly PP1-independent role? This question is particularly relevant to the work I have presented here, as discussed above. Is it only that KNL1/Spc105 occupies the right position to optimize the SAC silencing function of PP1, or is it critical for the function of the holoenzyme that KNL1/Spc105 also binds to microtubules and interacts with Bub1 and BubR1? Our data indicating that the KNL1/Spc105-PP1 interaction is necessary for the coupling of microtubule attachment to SAC silencing make attractive the hypothesis that there is a functional connection between these three seemingly independent roles of KNL1/Spc105, but further studies are necessary to elucidate this connection.

Evolution of the RVxF motif

The RVxF motif is strikingly simple. One of the strictest accepted variations of this motif are [R/K] [V/I] {P} [F/W], and any random twelve-nucleotide sequence has a 0.057 % chance of encoding this sequence. This means that a human protein of "average" size (485 amino acids, or 1455 base pairs) has a 56 % chance of containing an RVxF motif at random. This high rate of random occurrence can be practically observed in the *in silico* screen done for novel PP1 regulatory subunits (Hendrickx et al., 2009). Of the 397 proteins found to have an RVxF motif conserved in mice, rats, and humans, 65% of these RVxF motifs

were in globular or extracellular domains, and were obviously not functional PP1 binding motifs, but simply occurring at random.

This random occurrence of the PP1 binding motif may represent a significant evolutionary force, especially considering the diversity of the cellular roles of PP1. Given the high chance of random mutations generating an RVxF motif, once PP1 had this binding pocket it could have quickly obtained new roles in the cell. This gives an evolutionary explanation for the discrepancy in numbers of kinases and phosphatases. It would take far fewer steps of random mutation for an independent protein to obtain an RVxF motif and thus recruit PP1 for a specific purpose than for PP1 itself to duplicate and evolve a new targeting domain or substrate specificity necessary for a specific function.

The potential rapid evolution of RVxF-containing PP1 regulatory subunits must also be considered when examining data from different model systems. For example, the Sds22-PP1 holoenzyme discussed above exhibits rather different localization and behaviors in yeast and human cells. PP1 also binds motor proteins in both human (Cenp-E) and fission yeast (kinesin-8), but they are not the same motor proteins and do not appear to be evolutionarily linked. In this case it is possible that it was evolutionarily advantageous for a microtubule motor protein to bind PP1, but because of the high chance of random occurrence it ended up as different motor proteins in different evolutionary lineages.

The many kinetochore-associated PP1 holoenzymes may represent a very interesting case of co-evolution and cooperation of functions. Data from more

diverse species, especially in plants, is necessary to construct an accurate picture of how this network of kinetochore dephosphorylation has evolved. This may reveal evidence of the functions of each part of this network in a way that studying any individual system could not.

Future perspective

Major outstanding questions

The work presented here furthers our understanding of the phosphorylation balance at the kinetochore, both in terms of function and regulation. However, there are many more questions that stem from this data, and they fall into two main categories. First, what are the critical substrates of PP1 at the kinetochore? Since we know that, at least in budding yeast, the KNL1-PP1 holoenzyme is primarily responsible for silencing the SAC, we can narrow down possible targets in terms of spatial range and function. Two good candidates are Ndc80 and Mad3. Both are phosphorylated upon checkpoint activation and need to be dephosphorylated in order to facilitate SAC silencing, and both are localized to the kinetochore in close proximity to KNL1 (Akiyoshi et al., 2009a; King et al., 2007). In addition, Dam1 in yeast shares these same characteristics and represents another potential substrate in this system (Keating et al., 2009). However, to definitively show that a particular protein is a substrate of PP1 *in vivo* is very difficult. To answer this question requires better *in vivo* biochemical techniques and detection mechanisms.

Aside from KNL1-recruited PP1, there are broader considerations for PP1 at the kinetochore given the number of PP1 holoenzymes that have some function at this structure. To fully understand the mechanism of targeted dephosphorylation as it relates to the kinetochore, we must not only identify the critical substrates of each PP1 holoenzyme, but also how this substrate specificity comes about. In addition, we must consider how the different PP1 populations interact, whether they have overlapping sets of substrates and whether they are targeted in response to different stimuli. A full consideration of kinetochore function is not complete without understanding how the phosphatase pathways interact with each other and with the kinases in order to converge on critical targets.

The second class of outstanding problems focuses on the kinetochore itself. Specifically, what are the structural changes that occur to the kinetochore upon microtubule attachment? It has been shown that there occurs both intrakinetochore and interkinetochore stretching upon attachment due to the tension created by the pulling forces of the microtubules. But this simple spatial separation might not be enough to elicit all of the precise biochemical changes that need to occur upon biorientation. It is likely that there are other, smaller scale changes that occur, both to multi-subunit complexes and even to an individual protein conformation. These changes may be crucial not only for PP1 function but also for all the other factors that contribute to successful anaphase.

New advances in structural microscopy may in the future be able to more precisely visualize these transitions and help answer some of these questions.

PP1 as a therapeutic target

Due to its ubiquitous functions in the cell, PP1 has attracted much interest in the field of medical pharmacology. Originally, small molecule modulators of the activity of the PP1 catalytic subunit, such as okadaic acid and microcystin, appeared promising as therapeutics for several diseases. However, because the PP1 catalytic subunit plays so many roles in the cell, these drugs could have enormous off-target effects and are observed to be extremely toxic to cells.

The next generation of phosphatase targeting drugs, therefore, is focused on specifically affecting PP1 regulatory subunits to generate a specific effect on a particular holoenzyme (reviewed in Fardilha et al., 2010 and Tsaytler and Bertolotti, 2012). For example, the drug salubrinal inhibits the GADD34-PP1 holoenzyme, which dephosphorylates the transcription factor eIF2α. The ultimate effect of this is to inhibit the viral transcription of HERPES, and it has therefore been used as an effective treatment. In the heart, there is a phosphorylation cascade that increases the heart rate in response to hormonal stimuli, and PP1 is responsible for return of the heart rate to basal levels. The inhibitor I-1 modulates this function to act at the appropriate time, and I-1 dysfunction has been linked to heart disease and ischemia. In mice, the expression of a constitutively active I-1 alleviates overload-induced heart failure

and ischemia, and there is currently work to develop a synthetic molecule with similar actions (Nicolaou et al., 2009).

We ultimately study the fine-tuned mechanisms that regulate the cell cycle and chromosome segregation for their links to aneuploidy and cancer. PP1 is not unique in the fact that if we understand its mechanism of action in mitosis, it may lead to a better understanding of cancer-causing events and even to a potential therapy. But understanding the mechanism of PP1 substrate specificity, localization, and activity has broader implications to many aspects of human health and disease. Therefore, every study, including this one, that elucidates the specific mechanism of action of a PP1 holoenzyme adds to our understanding of the human system as a whole.

CHAPTER 5: MATERIALS AND METHODS

Biochemistry and *Xenopus* extracts

Plasmids and constructs

For a full list of plasmids used in this study see table 5-1. MBP-xPP1γ was made by cloning PP1γ from a *X. laevis* cDNA library into pMAL-c4g using the *Bam*HI and *Hin*DIII sites. cDNA encoding *X. laevis* KNL1, Repo-Man1, and Repo-Man2 were purchased from Open Biosystems (IMAGE clone numbers 7794105, 4084144, and 8329563 respectively) and the full-length sequence was determined (xKNL1 Genbank Accession JF804775). xKNL1^{100}-FLAG was made by cloning *X. laevis* KNL1 into PGEX-6p2 using the *Bam*HI and *Eco*RI sites and inserting a C-terminal FLAG tag by PCR. xKNL1^{300} was made by splicing the endogenous *HinD*III site in KNL1 at residue 300 and the *HinD*III site in the polylinker, and xKNL1^{790} was made in a the same way using *Xho*I sites. All point mutants were made using Quikchange site-directed mutagenesis (Agilent). For primers used see table 5-2.

Recombinant proteins

All proteins were expressed in BL-21 rosetta cells.

For PP1γ-HIS, protein was first purified on an SP FF sepharose FPLC column according to manufacturers directions (Amersham Biosciences). Peak fractions were further purified on NiNTA resin according to manufacturers

Table 5-1: plasmids used in this study (pages 118 to 119)

Plasmid	Description
pJR021	MBP-xPP1α
pJR022	MBP-xPP1γ
pJR023	MBP-xPP1γ^{D95A} = MBP-xPP1γ^{cat}
pJR025	MBP-xPP1γ^{D242T}
pJR026	MBP-xPP1γ^{F258A}
pJR027	MBP-xPP1γ^{C291Y}
pJR028	MBP-xPP1$\gamma^{D242T\ F258A}$
pJR029	MBP-xPP1$\gamma^{D242T\ C291Y}$ = MBP-xPP1γ^{RBM}
pJR030	MBP-xPP1$\gamma^{D242T\ F258A\ C291Y}$
pJR031	xKNL1^{300}
pJR032	xKNL1^{790}
pJR033	xKNL1$^{300,\ RASA}$
pJR034	xKNL1$^{790,\ RASA}$
pJR050	xKNL1$^{300,\ S54A,\ S58A}$ = xKNL1^{SAA}
pJR062	xKNL1$^{300,\ S23A,\ S58A}$ = xKNL1^{ASA}
pJR061	xKNL1$^{300,\ S23A,\ S54A}$ = xKNL1^{AAS}
pJR059	xKNL1$^{300,\ S23A,\ S54A,\ S58A}$ = xKNL1^{AAA}

pJR051 GST-xKNL1^{100}-FLAG

pJR063 GST-xKNL1$^{100, S23A}$-FLAG = GST-xKNL1$^{100, ASS}$

pJR052 GST-xKNL1$^{100, S54A}$-FLAG = GST-xKNL1$^{100, SAS}$

pJR053 GST-xKNL1$^{100, S58A}$-FLAG = GST-xKNL1$^{100, SSA}$

pJR064 GST-xKNL1$^{100, S23A\ S54A}$-FLAG = GST-xKNL1$^{100, AAS}$

pJR065 GST-xKNL1$^{100, S23A\ S58A}$-FLAG = GST-xKNL1$^{100, ASA}$

pJR054 GST-xKNL1$^{100, S54A\ S58A}$-FLAG = GST-xKNL1$^{100, SAA}$

pJR066 GST-xKNL1$^{100, S23A\ S54A\ S58A}$-FLAG = GST-xKNL1$^{100, AAA}$

pJR067 spc105$^{wt\text{-}NT}$

pJR056 spc105$^{R\mathbf{A}S\mathbf{A}\text{-}NT}$

pJR057 spc105$^{RV\mathbf{A}F\text{-}NT}$

pJR058 spc105$^{ochre\text{-}NT}$

pJR070 spc105$^{GLC7\text{-}R\mathbf{A}S\mathbf{A}\text{-}NT}$

pJR073 spc105$^{glc7cat\text{-}R\mathbf{A}S\mathbf{A}\text{-}NT}$

pJR071 spc105$^{GLC7\text{-}SPC105\text{-}NT}$

pJR072 spc105$^{glc7cat\text{-}SPC105\text{-}NT}$

pJR007 PP!γ-HIS

Table 5-2: primers used in this study (pages 120 to 121)

Name	Sequence	Purpose
PP1g_D95A_s	CCTAGGAGACTATGTAGCTCGAG GCAAGCAGTCT	PP1γ D95A mutation (sense)
PP1g_D95A_as	AGACTGCTTGCCTCGAGCTACATA GTCTCCTAGG	PP1γ D95A mutation (antisense)
PP1g_D242T_s	ATTTCTTCACAAACATGATCTGACT CTCATTTGCCGAGCTCATCAG	PP1γ D242T mutation (sense)
PP1g_D242T_as	CTGATGAGCTCGGCAAATGAGAG TCAGATCATGTTTGTGAAGAAAT	PP1γ D242T mutation (antisense)
PP1g_F258A_s	GTTGAAGATGGGTATGAATTCGCT GCCAAGAGACAACTGGTTAC	PP1γ F258A mutation (sense)
PP1g_F258A_as	GTAACCAGTTGTCTCTTGGCAGCG AATTCATACCCATCTTCAAC	PP1γ F258A mutation (antisense)
PP1g_C291Y_s	GATGAGTGTAGATGAAACATTAAT GTATTCCTTCCAGATTCTAAAACC	PP1γ C291Y mutation (sense)
PP1g_C291Y_as	GGTTTTAGAATCTGGAAGGAATAC ATTAATGTTTCATCTACACTCATC	PP1γ C291Y mutation (antisense)
Blinkin_RASA_sense	GCGGAGAAAAAGTCGTCGAGCTA GCGCTGCTGAGAATATAAGGGTTT	KNL1 R**A**S**A** mutation (sense)
Blinkin_RASA_antisense	AAACCCTTATATTCTCAGCAGCGC TAGCTCGACGACTTTTTCTCCGC	KNL1 R**A**S**A** mutation (antisense)
BlinkinS23A_sense	AGCCTCAGGAGGCGACTTGCCTC TATTTTAAAAGTTC	KNL1 S23A mutation (sense)
BlinkinS23A_antisense	GAACTTTTAAAATAGAGGCAAGTC GCCTCCTGAGGCT	KNL1 S23A mutation (antisense)
BlinkinS54A_	GATTCAACCATTGAAAAGCGGAGA	KNL1 S54A mutation

sense	AAAGCTCGTCGAGTTAGCT	(sense)
BlinkinS54A_ antisense	AGCTAACTCGACGAGCTTTTCTCC GCTTTTCAATGGTTGAATC	KNL1 S54A mutation (antisense)
BlinkinS58A_ sense	GGAGAAAAAGTCGTCGAGTTGCC TTTGCTGAGAATATAAGGG	KNL1 S58A mutation (sense)
BlinkinS58A_ antisense	CCCTTATATTCTCAGCAAAGGCAA CTCGACGACTTTTTCTCC	KNL1 S58A mutation (antisense)
Blinkin_S54_to _DM_sense	GGAGAAAAGCTCGTCGAGTTGCC TTTGCTGAGAAATTAAGGG	KNL1 S54A, S58A mutation (sense)
Blinkin_S54_to _DM_antisense	CCCTTATATTCTCAGCAAAGGCAA CTCGACGAGCTTTTCTCC	KNL1 S45A, S58A mutation (antisense)
spc105_RVAF_ wt_s	TACAGAGTATGGTAAAGAGAAGAG TTTCGTTCGCTCCCGA	Mutating *spc105*^{NT} construct to WT (sense)
spc105_RVAF_ wt_as	TCGGGAGCGAACGAAACTCTTCTC TTTACCATACTCTGTA	Mutating *spc105*^{NT} construct to WT (antisense)
GLC7_sal1_QC _a	CTATTTTTGGGTGATTATGTTGAC CGTGGTAAACAATCC	Eliminating *Sal*I site in *GLC7* (sense)
GLC7_sal1_QC _as	GGATTGTTTACCACGGTCAACATA ATCACCCAAAAATAG	Eliminating *Sal*I site in *GLC7* (antisense)
glc7_D95A_s	CTATTTTTGGGTGATTATGTCGCC CGTGGTAAACAATCCTTAGAG	*GLC7* D94A mutation (sense)
glc7_D95A_as	CTCTAAGGATTGTTTACCACGGGC GACATAATCACCCAAAAATAG	*GLC7* D94A mutation (antisense)
spc105_sg_seq	CGCGAAAGAGAAGGCGCC	Genotyping *spc105* (F)
Spc105_R	CGCATGCTTTTCGCTGGGAG	Genotyping *spc105* (R)

directions (Qiagen) and exchanged into PP1 storage buffer (50 mM TRIS pH 8.0, 200 mM NaCl, 0.1 mM $MnCl_2$, 0.1 mM EDTA, 5 mM DTT).

For MBP-xPP1γ and all related mutants: protein was purified on Amylose Resin according to manufacturers instructions (NEB), and dialyzed into PP1 storage buffer.

For xKNL1^{00}-FLAG and all related mutants: GST-tagged protein was purified on Glutathione Sepharose 4B and cleaved with precision protease according to manufacturers instructions (GE Healthcare), and dialyzed into sperm dilution buffer (5 mM HEPES pH 8.0, 150 mM sucrose, 100 mM KCl, 1mM $MgCl_2$).

***in vitro* phosphatase assay**

Varying concentrations of purified MBP-xPP1γ were incubated protected from light in 50 μl final volume of pNPP reaction buffer [40 mM TRIS pH 7.4, 10 mM KCl, 15 mM $MgCl_2$, 1 mM DTT, 0.5 mg/mL BSA, 0.5 mM $MnCl_2$, 20 mM pNPP (NEB), adapted from (Takai and Mieskes, 1991)]. After 30 minutes, the reaction was quenched with 1 ml 0.5 M EDTA. The 20 fold diluted reaction was read by spectrophotometry for generation of dephosphorylated pNPP, molar extinction coefficient at 405 nM, e=16,000/M*cm. The concentration of dephosphorylated pNPP was calculated as $c=(20*A_{405})/.016$ nM.

in vitro kinase assay and immunoprecipitation

KNL1$^{1\text{-}100}$-FLAG (10 μM) was incubated with AuroraB-INCENP$_{790\text{-}871}$ (A gift from A. Kelly), Polo, or Haspin (Gifts from C. Ghenoiu) (0.2 μM) for 30 minutes at 20°C in kinase buffer (20 mM HEPES, 150 mM NaCl, 10 mM MgCl2, 1 mM DTT, 1 mM MnCl2, .025% Tween-20) with either 1 mM ATP or 30 μM ATP plus 0.02 μM ^{32}P-ATP (approx. 6000 Ci/mmol).

In vitro immunoprecipitation was performed in binding buffer (BB = PBS, 0.01% NP-40, 0.1 mg/ml BSA, 0.25 mM TCEP, 10 % glycerol). For Figure 2-2A, 20 μl Dynabeads M-280 streptavidin beads (Invitrogen) coupled to peptide containing the RVxF motif of human Repo-Man (biotin-NMRKRK**RVTF**GEDLSPEVFD) were incubated in 50 μl with 6.25 pmol of the indicated MBP-xPP1γ mutants for 1 hour at room temperature. For Figure 2-2B, 10 μl RVxF peptide beads were incubated in 50 μl with the indicated concentrations of MBP-xPP1γ for 2 hours at 4°C. For Figure 2-11A, 0.8 μM MBP-xPP1γ and 0.4 μM xKNL1^{100}-FLAG were incubated in 50 μl for 1 hour at 4 °C, then added to an equal volume of protein A antibody beads (Sigma) coupled to anti-FLAG antibody and incubated for 1 hour at 4°C. For Figure 2-11B, 5 μl of a non-radioactive *in vitro* kinase reaction (see above) was added to 10 μl of anti-FLAG M2 agarose (Sigma) in 50 μl TBS and incubated for 30 minutes at room temperature. The agarose was washed 2 times in TBS, 2 times in BB, resuspended in BB with 1 μM MBP-xPP1γ^{cat}, and incubated 2 hours at 4°C. For

all experiments, beads were washed 3 times in BB and eluted with SDS sample buffer.

Generation of peptide antibodies

Methods previously described (Field et al., 1998) were followed. Peptides corresponding to the C termini of PP1γ (RPVTPPRGIITKQAKK), and PP1α (QSRPVTPPRNKNKQSK) were synthesized (Tufts University Core Facility) and conjugated to KLH, and polyclonal antibodies were raised in rabbits (Covance). Antibodies were affinity purified using SulfoLink Coupling Gel (Pierce) according to the manufacturer's directions. PP1γ antibody recognizes PP1γ but not PP1α, and is therefore used as an isoform specific antibody (anti-PP1γ). PP1α antibody recognizes both PP1α and PP1γ, and is therefore used as a pan-PP1 antibody (anti-PP1) (Figure 5-1).

***Xenopus laevis* egg extracts**

Meiotic metaphase II (CSF)-arrested extracts were prepared as previously described (Murray, 1991).

Spindle assembly and immunofluorescence

CSF extracts were supplemented with rhodamine labeled tubulin, demembrenated sperm to a final concentration of 500 nuclei/μl, and 2 μM MBP-xPP1γ. $CaCl_2$ was added to 0.3 μM, and the extract was incubated for 90

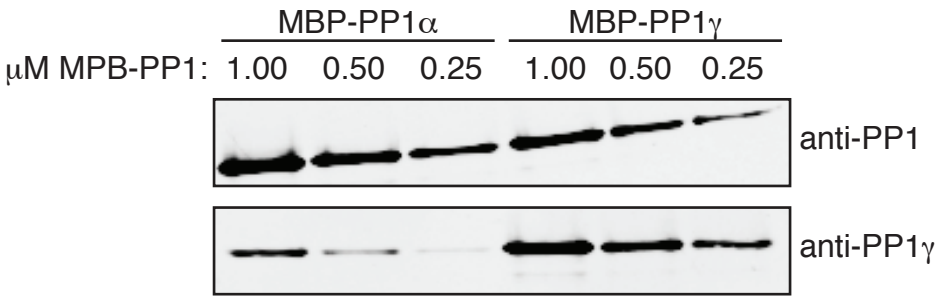

Figure 5-1: Specificity of newly generated PP1 antibodies. The indicated amounts of MBP-xPP1α or MBP-xPP1γ were blotted with purified PP1 antibodies. The antibody raised against the C-terminus of PP1α (top) recognizes both MBP-xPP1α and MBP-xPP1γ, and is therefore referred to as anti-PP1. The antibody raised against the C-terminus of PP1γ (bottom) is isoform specific and referred to as anti-PP1γ.

minutes at 20 °C to induce interphase. Fresh CSF extract was added at a ratio of 2:1, and incubated for 60 minutes. For Figure 2-12, 10 μg/ml nocodazole or DMSO control was added and incubated for an additional 10 minutes.

Spindles were processed for immunofluorescence as previously described (Desai et al., 1999). Anti-MBP (Sigma, 1/1000), or anti-BubR1 (a gift from Rey-Huei Chen, 0.1 μg/mL) primary antibodies and Alexa 488-conjugated goat anti-mouse (Invitrogen) and cy3-conjugated donkey anti-rabbit (Jackson) secondary antibodies were used for detection. 10 μm stacks were taken using a DeltaVision Image Restoration Microscope and deconvolved using SoftWoRx software (Applied Precision). Co-localization analysis was performed using JACoP in ImageJ. Pearson's coefficient of co-localization between CENP-A and MBP-PP1γ was determined, and Van Steensel's analysis was performed to yield the CCF curve (Bolte and Cordelieres, 2006).

Immunodepletion and immunoprecipitation from extract

Control rabbit IgG, anti-INCENP (Sampath et al., 2004), or anti-PP1 antibodies were crosslinked to protein A Dynabeads (Invitrogen) using BS^3 (Pierce) according to the manufacturer's directions. For Immunodepletion, antibody-crosslinked beads were incubated with an equal volume of extract for 75 minutes at 4° C and then removed to yield the depleted extracts. For Immunoprecipitation, GFP, PP1, and $xKNL1^{300}$ or $xKNL1^{790}$ were translated and ^{35}S-labeled in rabbit reticulocyte lysate with SP6 RNA polymerase according to

manufactures directions (Promega). Proteins were added to extract (1/10 of total extract volume, approx 1:1:6 PP1:GFP:xKNL1 by volume) and incubated for 1 hour at 20°C, then added to an equal volume of antibody crosslinked beads and incubated for 30 minutes at 4° C. Beads were washed 6 times with PBS + 0.1 % triton and eluted with SDS sample buffer.

Immunoblots

Primary antibodies were diluted in PBS + 4% milk, autoclaved or Blocking Buffer (Li-Cor) + 0.05% Tween-20. IRDye 800 goat anti-rabbit or donkey anti-goat or IRDye 680 goat anti-mouse secondary antibodies were used according to manufacturers instructions. Blots were detected and quantified using the Odyssey Infrared Imaging System (Li-Cor).

Saccharomyces cerevisiae methods

Yeast strains

All strains are derivative of the W303 background, see table 5-3. *spc105*$^{NT\text{-}RV\mathbf{A}F}$, *spc105*$^{NT\text{-}R\mathbf{ASA}}$, and *spc105*$^{NT\text{-}R75ochre}$ constructs were synthesized with a *Sal*I site in the promoter for integrating (Epoch Biolabs) and cloned into RS406 using the *Sac*II and *Kpn*I sites. For *spc105*$^{NT\text{-}WT}$, the RVAF mutation was eliminated from *spc105*$^{NT\text{-}RV\mathbf{A}F}$ using site-directed mutagenesis. For Glc7 fusion constructs: An *Asc*I site and a linker (GDGAGL) were inserted into the *spc105*$^{NT\text{-}WT}$ or *spc105*$^{NT\text{-}R\mathbf{ASA}}$ plasmids via PCR, *GLC7* was PCR amplified from genomic

Table 5-3: Yeast strains (pages 128 to 130)

Strain	Genotype
JSR070	*MATa-inc lys2::GAL-HO-LYS2 SPC105::spc105$^{WT\text{-}NT}$-URA3*
JSR002	*MATa-inc lys2::GAL-HO-LYS2 his3::TUB1-GFP-HIS3 SPC105::spc105$^{RV\mathbf{A}F\text{-}NT}$-URA3 ADE2*
JSR001	*MATa-inc lys2::GAL-HO-LYS2 his3::TUB1-GFP-HIS3 SPC105::spc105$^{R\mathbf{A}S\mathbf{A}\text{-}NT}$-URA3 ADE2*
JSR003	*MATa-inc lys2::GAL-HO-LYS2 his3::TUB1-GFP-HIS3 SPC105::spc105$^{ochre\text{-}NT}$-URA3 ADE2*
JSR057	*MATa-inc lys2::GAL-HO-LYS2 SPC105::spc105$^{R\mathbf{A}S\mathbf{A}\text{-}NT}$-URA3 ipl1-1 TRP1*
JSR069	*MATa-inc lys2::GAL-HO-LYS2 spc105-R**A**S**A** ipl1-1 TRP1*
JSR069-1	*MATa-inc lys2::GAL-HO-LYS2 SPC105 ipl1-1 TRP1*
JSR006	*MATa-inc mad2Δ::KanMX lys2::GAL-HO-LYS2 his3::TUB1-GFP-HIS3 SPC105::spc105$^{R\mathbf{A}S\mathbf{A}\text{-}NT}$-URA3 ADE2*
JSR083	*MATa-inc bar1Δ his3::TUB1-GFP-HIS3 PDS1-18MYC-LEU2 LYS2**
JSR084	*MATa-inc bar1Δ his3::TUB1-GFP-HIS3 PDS1-18MYC-LEU2 LYS2* trp1::tet^{off}-CDC20-127-TRP1*
JSR085	*MATa-inc bar1Δ his3::TUB1-GFP-HIS3 PDS1-18MYC-LEU2 LYS2* trp1::tet^{off}-CDC20-127-TRP1 spc105-R**A**S**A***
JSR004	*MATa-inc lys2::GAL-HO-LYS2 his3::TUB1-GFP-HIS3 spc105-RV**A**F ADE2*
JSR004-1	*MATa-inc lys2::GAL-HO-LYS2 his3::TUB1-GFP-HIS3 SPC105 ADE2*

JSR049	*MATa-inc mad2Δ::KanMX lys2::GAL-HO-LYS2 his3::TUB1-GFP-HIS3 spc105-RV**A**F*
JSR078	*MATa-inc bar1Δ leu2::tetR-GFP-LEU2 ura3::TetOs-URA3 LYS2**
JSR079	*MATa-inc bar1Δ leu2::tetR-GFP-LEU2 ura3::TetOs-URA3 LYS2* SPC105-RV**A**F ADE2*
JSR080	*MATa-inc bar1Δ leu2::tetR-GFP-LEU2 ura3::TetOs-URA3 LYS2* scc1-73 TRP1 ADE2*
JSR081	*MATa-inc bar1Δ leu2::tetR-GFP-LEU2 ura3::TetOs-URA3 LYS2* spc105-RV**A**F scc1-73 TRP1 ADE2*
YL044	*MATa-inc bar1Δ mad2::KanMX scc1-73 leu2::GAL-PDS1-mdb-LEU2*
JSR103	*MATa-inc mad2Δ::KanMX lys2::GAL-HO-LYS2 his3::TUB1-GFP-HIS3 spc105-R**A**S**A** ADE2*
JSR103-1	*MATa-inc mad2Δ::KanMX lys2::GAL-HO-LYS2 his3::TUB1-GFP-HIS3 SPC105 ADE2*
JSR093	*MATa-inc bar1Δ mad2::KanMX leu2::tetR-GFP-LEU2 ura3::TetOs-URA3*
JSR094	*MATa-inc bar1Δ mad2::KanMX leu2::tetR-GFP-LEU2 ura3::TetOs-URA3 spc105-R**A**S**A***
JSR096	*MATα lys2::GAL-HO-LYS2 mad2::kanMX leu2-Δ101::URA3::leu2-Δ102 ADE2*
JSR097	*MATα spc105-R**A**S**A** lys2::LYS2-GAL-HO mad2::kanMX leu2-Δ101::URA3::leu2-Δ102 ADE2*
JSR102	*MATa-inc lys2:: GAL-HO-LYS2 SPC105::spc105$^{GLC7\text{-}R\mathbf{A}S\mathbf{A}\text{-}NT}$-URA3*
JSR113	*MATa-inc lys2:: GAL-HO-LYS2 SPC105::spc105$^{glc7cat\text{-}R\mathbf{A}S\mathbf{A}\text{-}NT}$-URA3*

JSR112	*MATa-inc lys2:: GAL-HO-LYS2 SPC105::spc105$^{GLC7\text{-}SPC105\text{-}NT}$-URA3*
JSR114	*MATa-inc lys2:: GAL-HO-LYS2 SPC105::spc105$^{glc7cat7\text{-}SPC105\text{-}NT}$-URA3*
JSR128	*MATa-inc lys2:: GAL-HO-LYS2 SPC105::spc105$^{GLC7\text{-}SPC105\text{-}NT}$-URA3 mad2::KanMX his3::TUB1-GFP-HIS3 ADE2*
JSR105	*MATa-inc lys2::GAL-HO-LYS2 Glc7-spc105-R**A**S**A***
JSR105-1	*MATa-inc lys2::GAL-HO-LYS2 SPC105*
JSR106	*MATa-inc lys2 leu2-Δ101::URA3::leu2-Δ102*
JSR107	*MATa-inc lys2 leu2-Δ101::URA3::leu2-Δ102 GLC7-spc105$^{R\mathbf{A}S\mathbf{A}}$*
JSR127	*MATa-inc lys2:: GAL-HO-LYS2 SPC105::spc105$^{GLC7\text{-}SPC105\text{-}NT}$-URA3 his3::TUB1-GFP-HIS3 ADE2*

Yeast strains used in this study. All strains are W303 background. Asterisks indicates either *LYS2* or *lys2::GAL-HO-LYS2*.

DNA and inserted into the *Asc*I site, and the *Sal*I site in *GLC7* was eliminated and the catalytically dead mutation D94A was created using site directed mutagenesis. For all site directed mutagenesis, primers used are listed in table 5-2.

HO-induced Gene Replacement (HGR) and Single-Cell Colony Assay (SCA)

For live cell imaging and bulk culture genotyping, parent cells were grown to log phase before *GAL-HO* induction for 6 hours, the time needed to guarantee cells have performed recombination (Cross and Pecani, 2010). Cells were then prepared for live cell imaging or DNA extraction. For the single cell colony assay, *spc105*^{NT} strains were streaked on galactose plates and left for 6 hours at 30°C. Single budded cells were isolated and allowed to grow to colonies. In cases where macroscopic colonies formed, DNA was isolated by standard protocol. The genotype was assessed by PCR amplification (for primers used see table 5-2) and restriction digestion with an enzyme specific to each mutation.

IPL assay

Cells containing *ura3-52* and *leu2-Δ101::URA3::leu2-Δ102* at the endogenous *LEU2* locus on chromosome 3 (Chan and Botstein, 1993) were grown in unselective YEPD for 48 hours, diluted appropriately and plated on selective medium lacking leucine, or that lacking both leucine and uracil. Percent disomy III is defined as frequency of Leu^+, Ura^+ cell formation.

Time courses

Cells were arrested in G1 in YEPD + 10 nM α-factor for 1.5 (30°C) or 2 (23°C) hours. For *tet^{R}-CDC20-127* experiments, 10 μg/ml doxycycline (sigma-aldirch) was added for 2 hours, and cells were washed into YEPD with doxycycline and without α-factor. For all others, after arrest cells were washed into YEPD without α-factor at 30°C or the indicated temperatures. Samples for florescent microscopy and/or Western blotting were prepared as previously described (Bean et al., 2006) every 15 minutes for 2 hours after release, and 10 nM α-factor was added 45 minutes after release to prevent cells from entering the next cell cycle.

Nocodazole block

For Figures 3-16B and 3-17B, asynchronous cultures grown to log phase in YEPD were treated with 15 μg/ml nocodazole and 10 μg/ml benomyl or an equivalent amount of DMSO for 3 hours, and cell morphology was counted. For figure 3-16B, cells were then washed 2 times in YEPD, plated onto YEPD, and colony formation was counted after 48 hours. For Figure 3-11A, cultures were arrested in G1 in YEPD + 10 nM α-factor for 1.5 hours, then washed into YEPD without α-factor with 15 μg/ml nocodazole and 10 μg/ml benomyl or an equivalent amount of DMSO, and cell morphology was counted every hour.

Time-lapse microscopy

Parent strains (*spc105*^{NT}) were grown to log phase in SCR-URA (synthetic media with raffinose and without uracil). Galactose and uracil were added, and cells were further incubated for 6 hours. Cells were then plated on agarose, and a previously described method (Drapkin et al., 2009) was used for 12 hour time-lapse microscopy.

APPENDIX

Identification of the *Xenopus laevis* KNL1 homologue

Since the *Xenopus laevis* genome has not yet been sequenced, the first task in this study was to identify and sequence the KNL1 homologue. I identified a potential homologue from a cDNA library using 5'EST homology and sequentially sequenced the full-length coding region. The encoded protein was 37.5 % similar to the human homologue, and contained the conserved RVxF motif (Figure A-1). This is the protein used for all *Xenopus* egg extract experiments.

Figure A-1: Alignment of KNL1 homologues. KNL1 from *Xenopus laevis* was identified from the IMAGE clone library by 5'EST homology and sequentially sequenced (xKNL1, IMAGE clone number 7794105, Genbank Accession JF804775). The full-length sequence is compared to the published sequences from *Homo sapiens* (hKNL1). Identical residues are marked in dark grey, similar residues in light grey, and red bar indicates the conserved RVxF motif.

Figure A1: pages 137 to 147

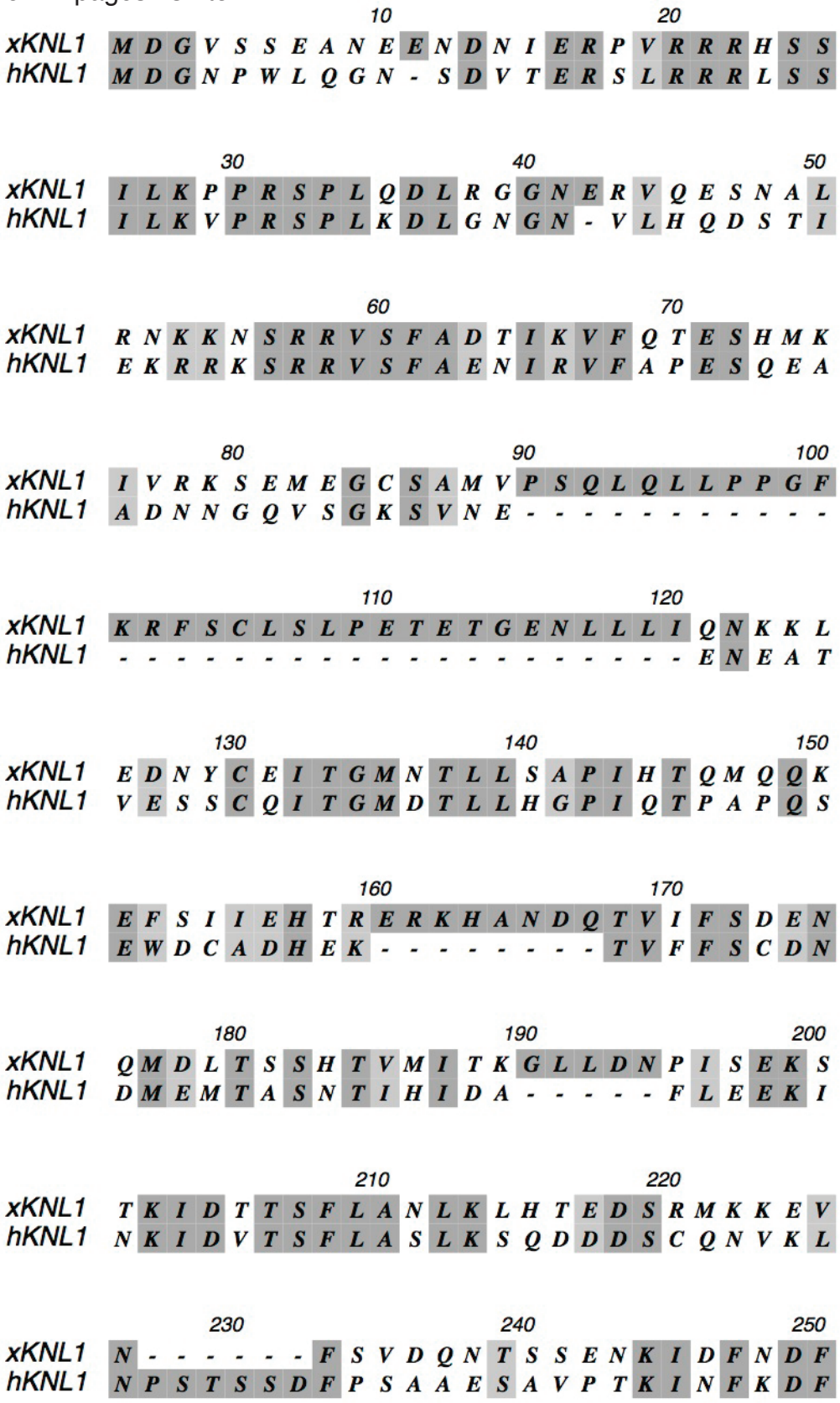

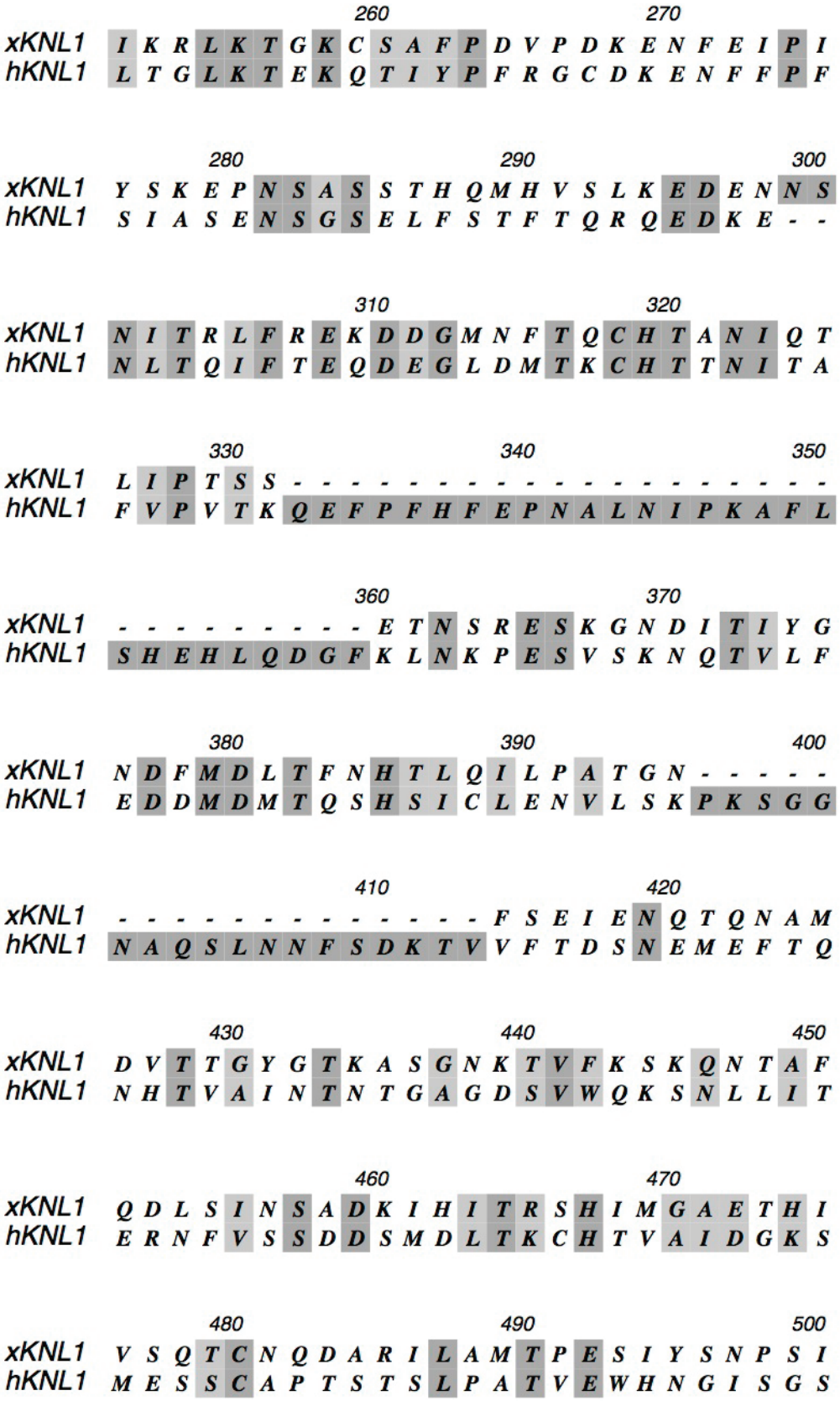
260 270
xKNL1 I K R L K T G K C S A F P D V P D K E N F E I P I
hKNL1 L T G L K T E K Q T I Y P F R G C D K E N F F P F
280 290 300
xKNL1 Y S K E P N S A S S T H Q M H V S L K E D E N N S
hKNL1 S I A S E N S G S E L F S T F T Q R Q E D K E - -
310 320
xKNL1 N I T R L F R E K D D G M N F T Q C H T A N I Q T
hKNL1 N L T Q I F T E Q D E G L D M T K C H T T N I T A
330 340 350
xKNL1 L I P T S S - - - - - - - - - - - - - - - - - - -
hKNL1 F V P V T K Q E F P F H F E P N A L N I P K A F L
360 370
xKNL1 - - - - - - - - - E T N S R E S K G N D I T I Y G
hKNL1 S H E H L Q D G F K L N K P E S V S K N Q T V L F
380 390 400
xKNL1 N D F M D L T F N H T L Q I L P A T G N - - - - -
hKNL1 E D D M D M T Q S H S I C L E N V L S K P K S G G
410 420
xKNL1 - - - - - - - - - - - - - F S E I E N Q T Q N A M
hKNL1 N A Q S L N N F S D K T V V F T D S N E M E F T Q
430 440 450
xKNL1 D V T T G Y G T K A S G N K T V F K S K Q N T A F
hKNL1 N H T V A I N T N T G A G D S V W Q K S N L L I T
460 470
xKNL1 Q D L S I N S A D K I H I T R S H I M G A E T H I
hKNL1 E R N F V S S D D S M D L T K C H T V A I D G K S
480 490 500
xKNL1 V S Q T C N Q D A R I L A M T P E S I Y S N P S I
hKNL1 M E S S C A P T S T S L P A T V E W H N G I S G S

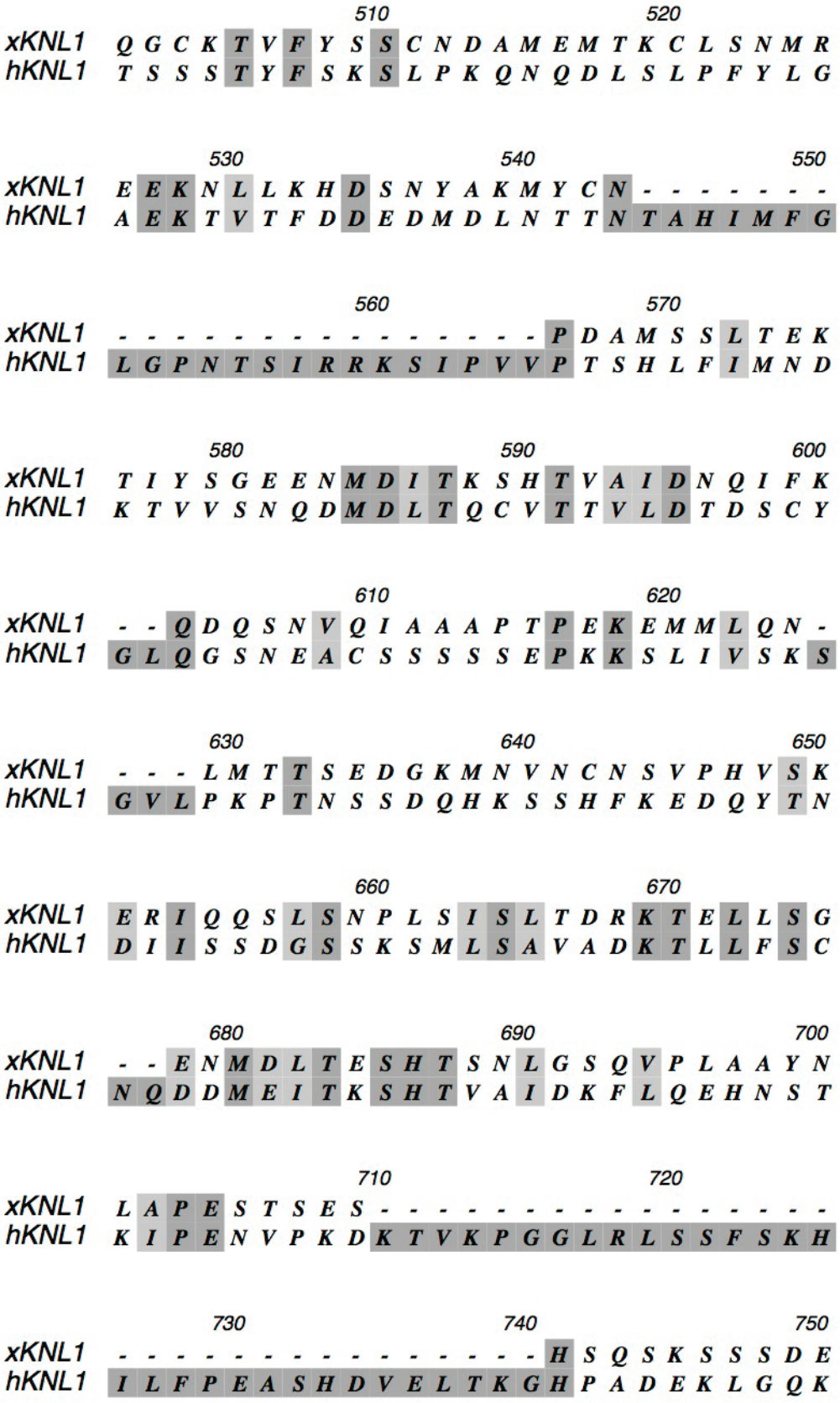
510 520
xKNL1 Q G C K T V F Y S S C N D A M E M T K C L S N M R
hKNL1 T S S S T Y F S K S L P K Q N Q D L S L P F Y L G
530 540 550
xKNL1 E E K N L L K H D S N Y A K M Y C N - - - - - - - -
hKNL1 A E K T V T F D D E D M D L N T T N T A H I M F G
560 570
xKNL1 - - - - - - - - - - - - - - - - P D A M S S L T E K
hKNL1 L G P N T S I R R K S I P V V P T S H L F I M N D
580 590 600
xKNL1 T I Y S G E E N M D I T K S H T V A I D N Q I F K
hKNL1 K T V V S N Q D M D L T Q C V T T V L D T D S C Y
610 620
xKNL1 - - Q D Q S N V Q I A A A P T P E K E M M L Q N -
hKNL1 G L Q G S N E A C S S S S S E P K K S L I V S K S
630 640 650
xKNL1 - - - L M T T S E D G K M N V N C N S V P H V S K
hKNL1 G V L P K P T N S S D Q H K S S H F K E D Q Y T N
660 670
xKNL1 E R I Q Q S L S N P L S I S L T D R K T E L L S G
hKNL1 D I I S S D G S S K S M L S A V A D K T L L F S C
680 690 700
xKNL1 - - E N M D L T E S H T S N L G S Q V P L A A Y N
hKNL1 N Q D D M E I T K S H T V A I D K F L Q E H N S T
710 720
xKNL1 L A P E S T S E S - - - - - - - - - - - - - - - - -
hKNL1 K I P E N V P K D K T V K P G G L R L S S F S K H
730 740 750
xKNL1 - - - - - - - - - - - - - - - - H S Q S K S S S D E
hKNL1 I L F P E A S H D V E L T K G H P A D E K L G Q K

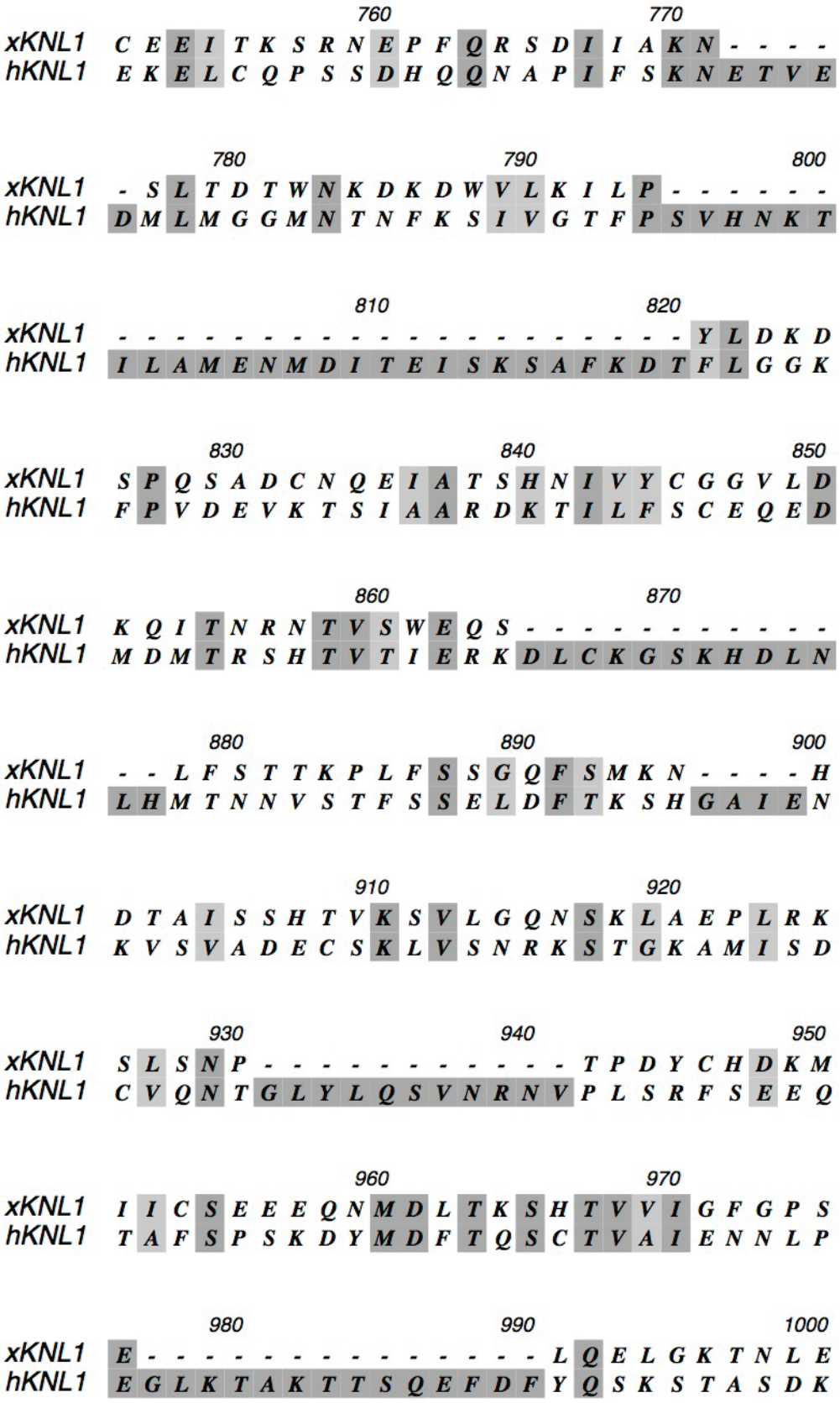
760 770
xKNL1 C E E I T K S R N E P F Q R S D I I A K N - - - -
hKNL1 E K E L C Q P S S D H Q Q N A P I F S K N E T V E
780 790 800
xKNL1 - S L T D T W N K D K D W V L K I L P - - - - - -
hKNL1 D M L M G G M N T N F K S I V G T F P S V H N K T
810 820
xKNL1 - Y L D K D
hKNL1 I L A M E N M D I T E I S K S A F K D T F L G G K
830 840 850
xKNL1 S P Q S A D C N Q E I A T S H N I V Y C G G V L D
hKNL1 F P V D E V K T S I A A R D K T I L F S C E Q E D
860 870
xKNL1 K Q I T N R N T V S W E Q S - - - - - - - - - - -
hKNL1 M D M T R S H T V T I E R K D L C K G S K H D L N
880 890 900
xKNL1 - - L F S T T K P L F S S G Q F S M K N - - - - H
hKNL1 L H M T N N V S T F S S E L D F T K S H G A I E N
910 920
xKNL1 D T A I S S H T V K S V L G Q N S K L A E P L R K
hKNL1 K V S V A D E C S K L V S N R K S T G K A M I S D
930 940 950
xKNL1 S L S N P - - - - - - - - - - - T P D Y C H D K M
hKNL1 C V Q N T G L Y L Q S V N R N V P L S R F S E E Q
960 970
xKNL1 I I C S E E E Q N M D L T K S H T V V I G F G P S
hKNL1 T A F S P S K D Y M D F T Q S C T V A I E N N L P
980 990 1000
xKNL1 E - - - - - - - - - - - - - - - L Q E L G K T N L E
hKNL1 E G L K T A K T T S Q E F D F Y Q S K S T A S D K

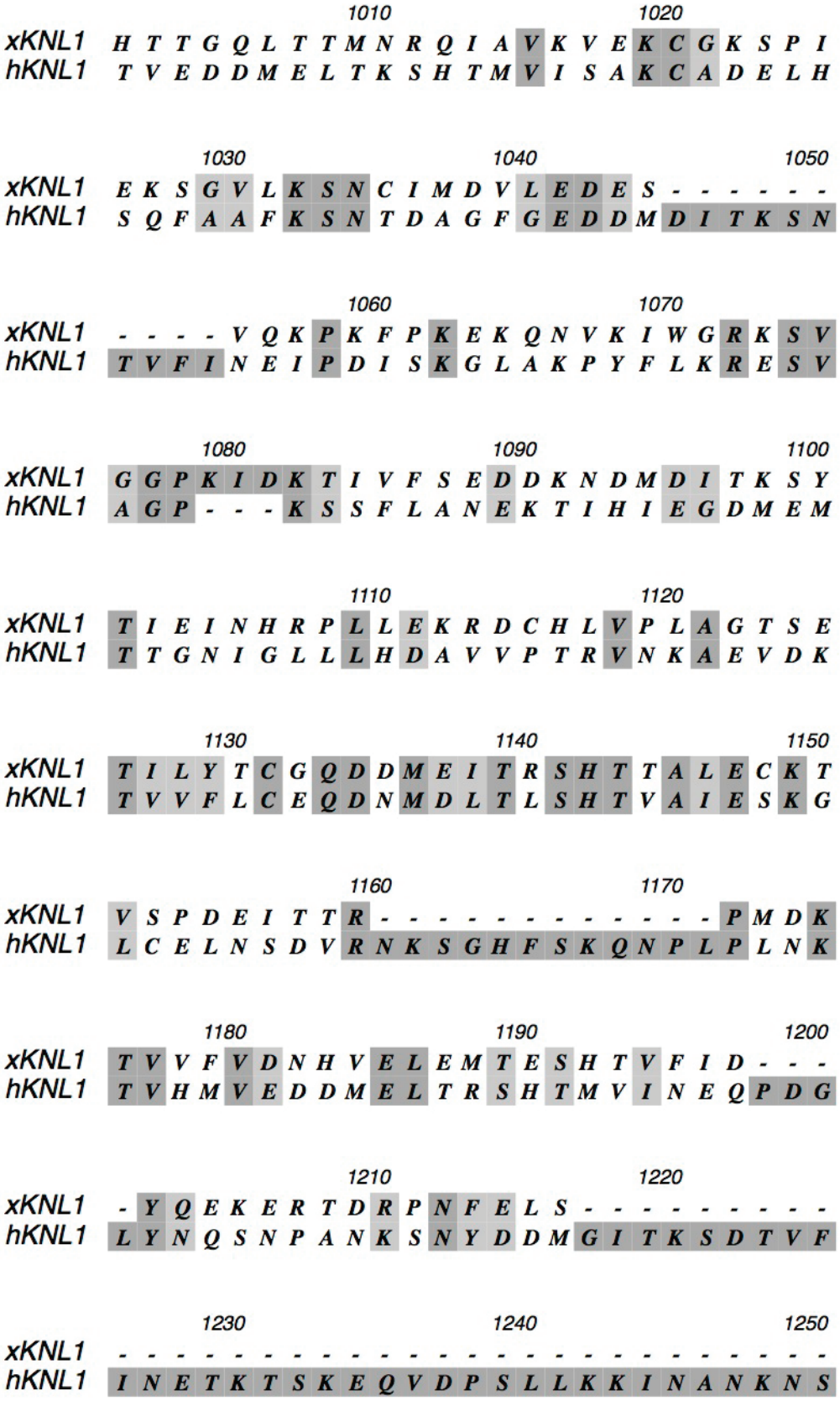
1010 1020
xKNL1 H T T G Q L T T M N R Q I A V K V E K C G K S P I
hKNL1 T V E D D M E L T K S H T M V I S A K C A D E L H
1030 1040 1050
xKNL1 E K S G V L K S N C I M D V L E D E S - - - - - - -
hKNL1 S Q F A A F K S N T D A G F G E D D M D I T K S N
1060 1070
xKNL1 - - - - V Q K P K F P K E K Q N V K I W G R K S V
hKNL1 T V F I N E I P D I S K G L A K P Y F L K R E S V
1080 1090 1100
xKNL1 G G P K I D K T I V F S E D D K N D M D I T K S Y
hKNL1 A G P - - - K S S F L A N E K T I H I E G D M E M
1110 1120
xKNL1 T I E I N H R P L L E K R D C H L V P L A G T S E
hKNL1 T T G N I G L L L H D A V V P T R V N K A E V D K
1130 1140 1150
xKNL1 T I L Y T C G Q D D M E I T R S H T T A L E C K T
hKNL1 T V V F L C E Q D N M D L T L S H T V A I E S K G
1160 1170
xKNL1 V S P D E I T T R - - - - - - - - - - - - P M D K
hKNL1 L C E L N S D V R N K S G H F S K Q N P L P L N K
1180 1190 1200
xKNL1 T V V F V D N H V E L E M T E S H T V F I D - - -
hKNL1 T V H M V E D D M E L T R S H T M V I N E Q P D G
1210 1220
xKNL1 - Y Q E K E R T D R P N F E L S - - - - - - - - -
hKNL1 L Y N Q S N P A N K S N Y D D M G I T K S D T V F
1230 1240 1250
xKNL1 -
hKNL1 I N E T K T S K E Q V D P S L L K K I N A N K N S

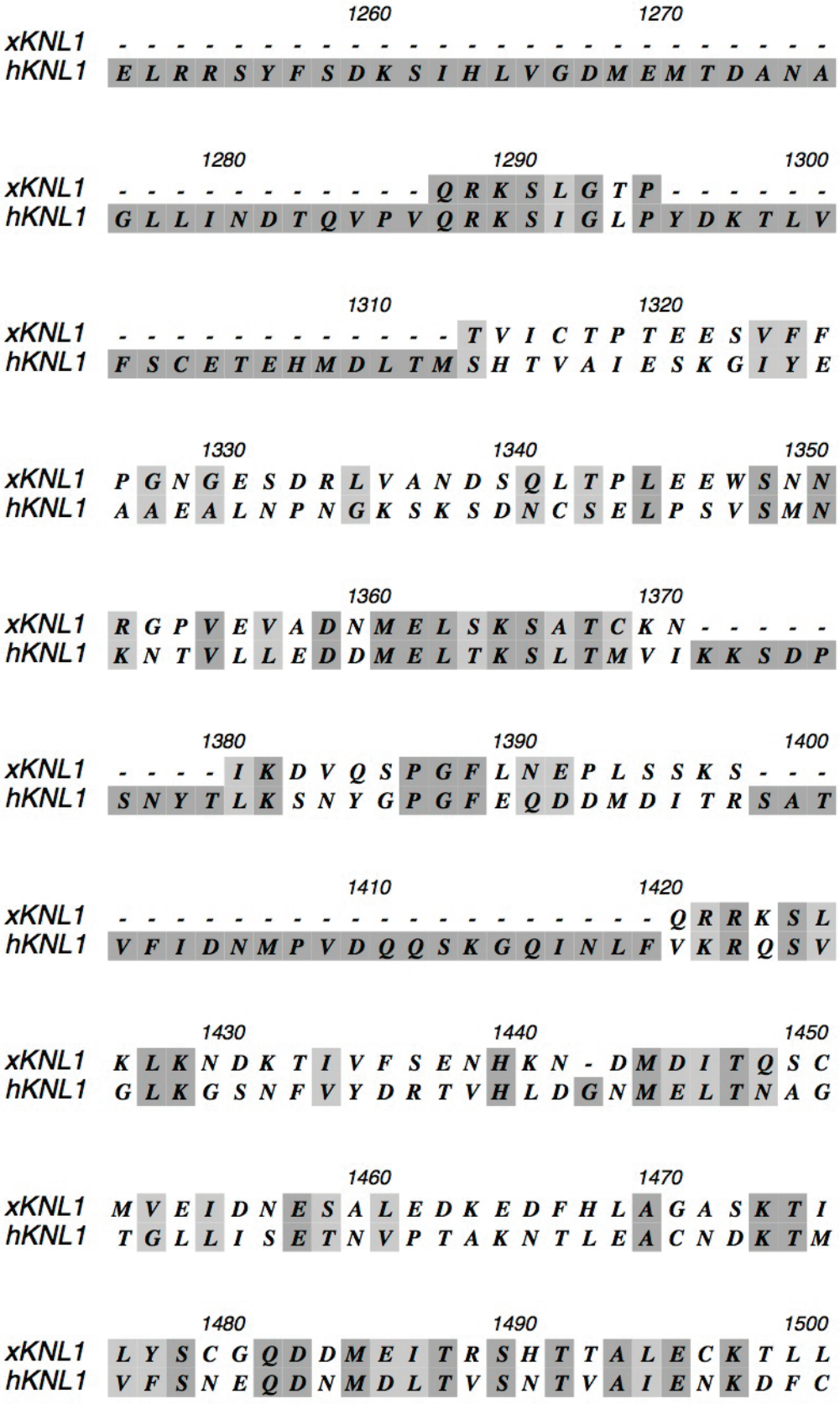
1260 1270
xKNL1 -
hKNL1 E L R R S Y F S D K S I H L V G D M E M T D A N A
1280 1290 1300
xKNL1 - - - - - - - - - - - - Q R K S L G T P - - - - - - -
hKNL1 G L L I N D T Q V P V Q R K S I G L P Y D K T L V
1310 1320
xKNL1 - - - - - - - - - - - - - T V I C T P T E E S V F F
hKNL1 F S C E T E H M D L T M S H T V A I E S K G I Y E
1330 1340 1350
xKNL1 P G N G E S D R L V A N D S Q L T P L E E W S N N
hKNL1 A A E A L N P N G K S K S D N C S E L P S V S M N
1360 1370
xKNL1 R G P V E V A D N M E L S K S A T C K N - - - - - -
hKNL1 K N T V L L E D D M E L T K S L T M V I K K S D P
1380 1390 1400
xKNL1 - - - - I K D V Q S P G F L N E P L S S K S - - -
hKNL1 S N Y T L K S N Y G P G F E Q D D M D I T R S A T
1410 1420
xKNL1 - Q R R K S L
hKNL1 V F I D N M P V D Q Q S K G Q I N L F V K R Q S V
1430 1440 1450
xKNL1 K L K N D K T I V F S E N H K N - D M D I T Q S C
hKNL1 G L K G S N F V Y D R T V H L D G N M E L T N A G
1460 1470
xKNL1 M V E I D N E S A L E D K E D F H L A G A S K T I
hKNL1 T G L L I S E T N V P T A K N T L E A C N D K T M
1480 1490 1500
xKNL1 L Y S C G Q D D M E I T R S H T T A L E C K T L L
hKNL1 V F S N E Q D N M D L T V S N T V A I E N K D F C

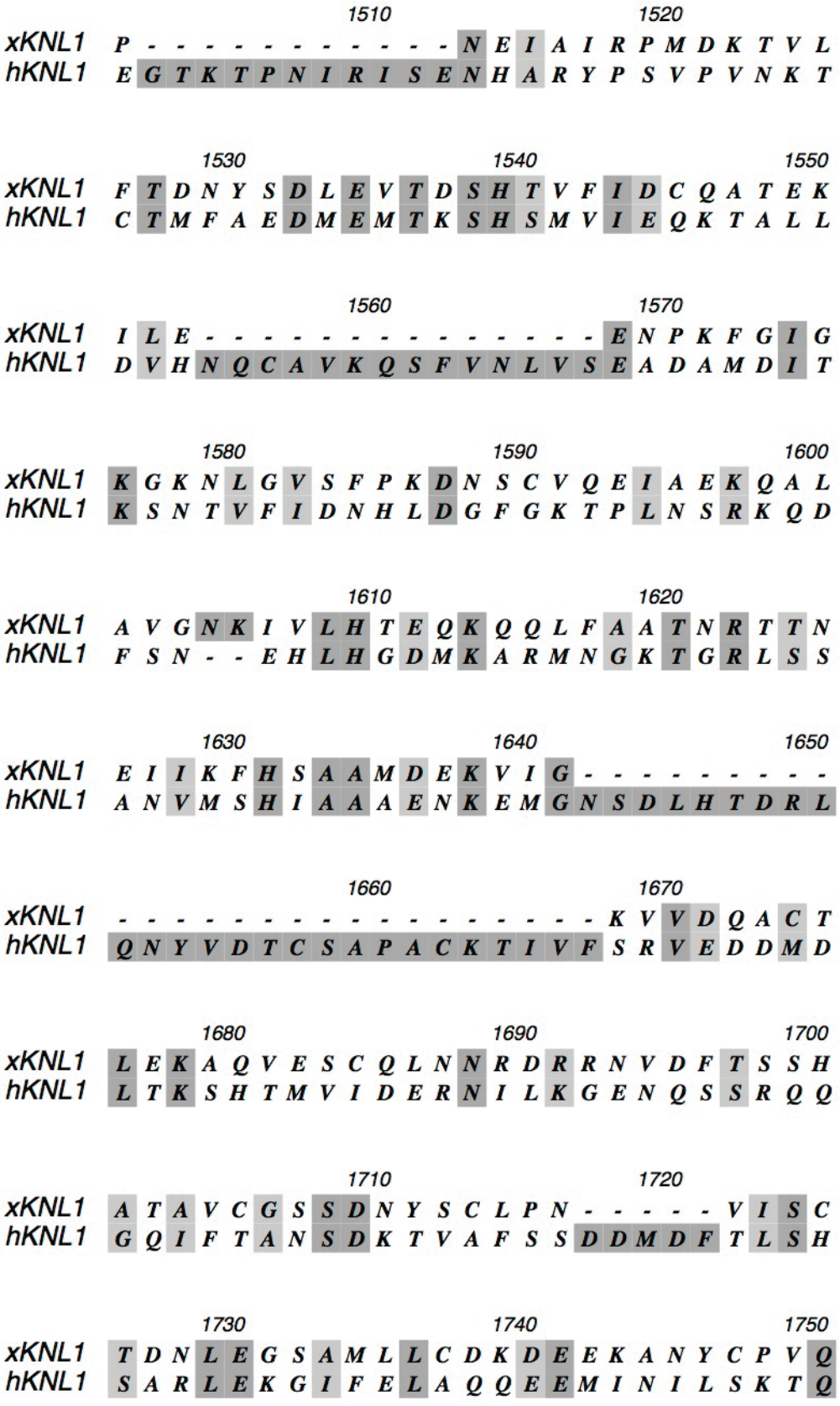
1510
1520
xKNL1 P - - - - - - - - - - - - N E I A I R P M D K T V L
hKNL1 E G T K T P N I R I S E N H A R Y P S V P V N K T
1530
1540
1550
xKNL1 F T D N Y S D L E V T D S H T V F I D C Q A T E K
hKNL1 C T M F A E D M E M T K S H S M V I E Q K T A L L
1560
1570
xKNL1 I L E - - - - - - - - - - - - - - - E N P K F G I G
hKNL1 D V H N Q C A V K Q S F V N L V S E A D A M D I T
1580
1590
1600
xKNL1 K G K N L G V S F P K D N S C V Q E I A E K Q A L
hKNL1 K S N T V F I D N H L D G F G K T P L N S R K Q D
1610
1620
xKNL1 A V G N K I V L H T E Q K Q Q L F A A T N R T T N
hKNL1 F S N - - E H L H G D M K A R M N G K T G R L S S
1630
1640
1650
xKNL1 E I I K F H S A A M D E K V I G - - - - - - - - -
hKNL1 A N V M S H I A A A E N K E M G N S D L H T D R L
1660
1670
xKNL1 - - - - - - - - - - - - - - - - - - K V V D Q A C T
hKNL1 Q N Y V D T C S A P A C K T I V F S R V E D D M D
1680
1690
1700
xKNL1 L E K A Q V E S C Q L N N R D R R N V D F T S S H
hKNL1 L T K S H T M V I D E R N I L K G E N Q S S R Q Q
1710
1720
xKNL1 A T A V C G S S D N Y S C L P N - - - - - V I S C
hKNL1 G Q I F T A N S D K T V A F S S D D M D F T L S H
1730
1740
1750
xKNL1 T D N L E G S A M L L C D K D E E K A N Y C P V Q
hKNL1 S A R L E K G I F E L A Q Q E E M I N I L S K T Q

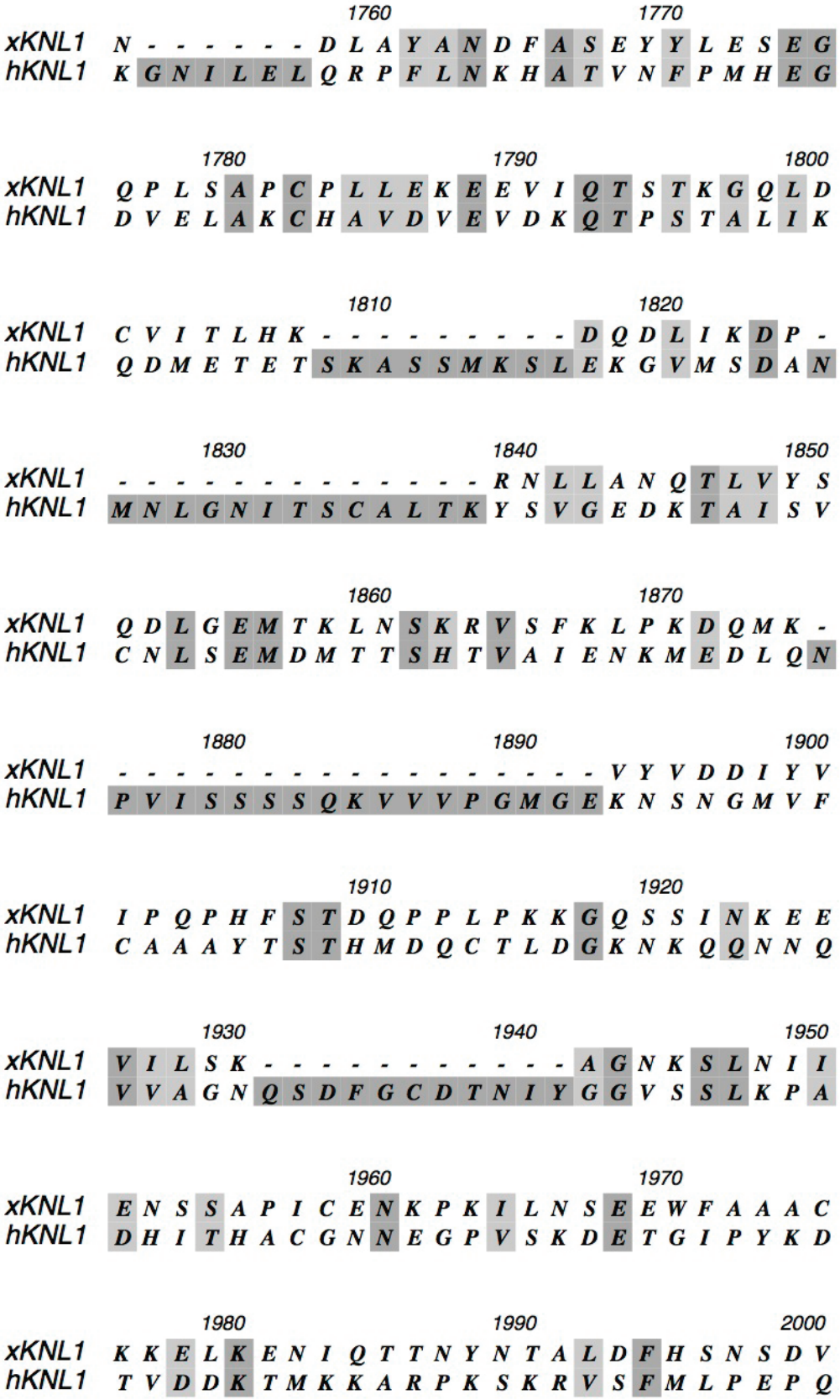
1760
1770
xKNL1 N - - - - - - - D L A Y A N D F A S E Y Y L E S E G
hKNL1 K G N I L E L Q R P F L N K H A T V N F P M H E G
1780
1790
1800
xKNL1 Q P L S A P C P L L E K E E V I Q T S T K G Q L D
hKNL1 D V E L A K C H A V D V E V D K Q T P S T A L I K
1810
1820
xKNL1 C V I T L H K - - - - - - - - - - D Q D L I K D P -
hKNL1 Q D M E T E T S K A S S M K S L E K G V M S D A N
1830
1840
1850
xKNL1 - - - - - - - - - - - - - - - R N L L A N Q T L V Y S
hKNL1 M N L G N I T S C A L T K Y S V G E D K T A I S V
1860
1870
xKNL1 Q D L G E M T K L N S K R V S F K L P K D Q M K -
hKNL1 C N L S E M D M T T S H T V A I E N K M E D L Q N
1880
1890
1900
xKNL1 - - - - - - - - - - - - - - - - - - V Y V D D I Y V
hKNL1 P V I S S S S Q K V V V P G M G E K N S N G M V F
1910
1920
xKNL1 I P Q P H F S T D Q P P L P K K G Q S S I N K E E
hKNL1 C A A A Y T S T H M D Q C T L D G K N K Q Q N N Q
1930
1940
1950
xKNL1 V I L S K - - - - - - - - - - - - A G N K S L N I I
hKNL1 V V A G N Q S D F G C D T N I Y G G V S S L K P A
1960
1970
xKNL1 E N S S A P I C E N K P K I L N S E E W F A A A C
hKNL1 D H I T H A C G N N E G P V S K D E T G I P Y K D
1980
1990
2000
xKNL1 K K E L K E N I Q T T N Y N T A L D F H S N S D V
hKNL1 T V D D K T M K K A R P K S K R V S F M L P E P Q

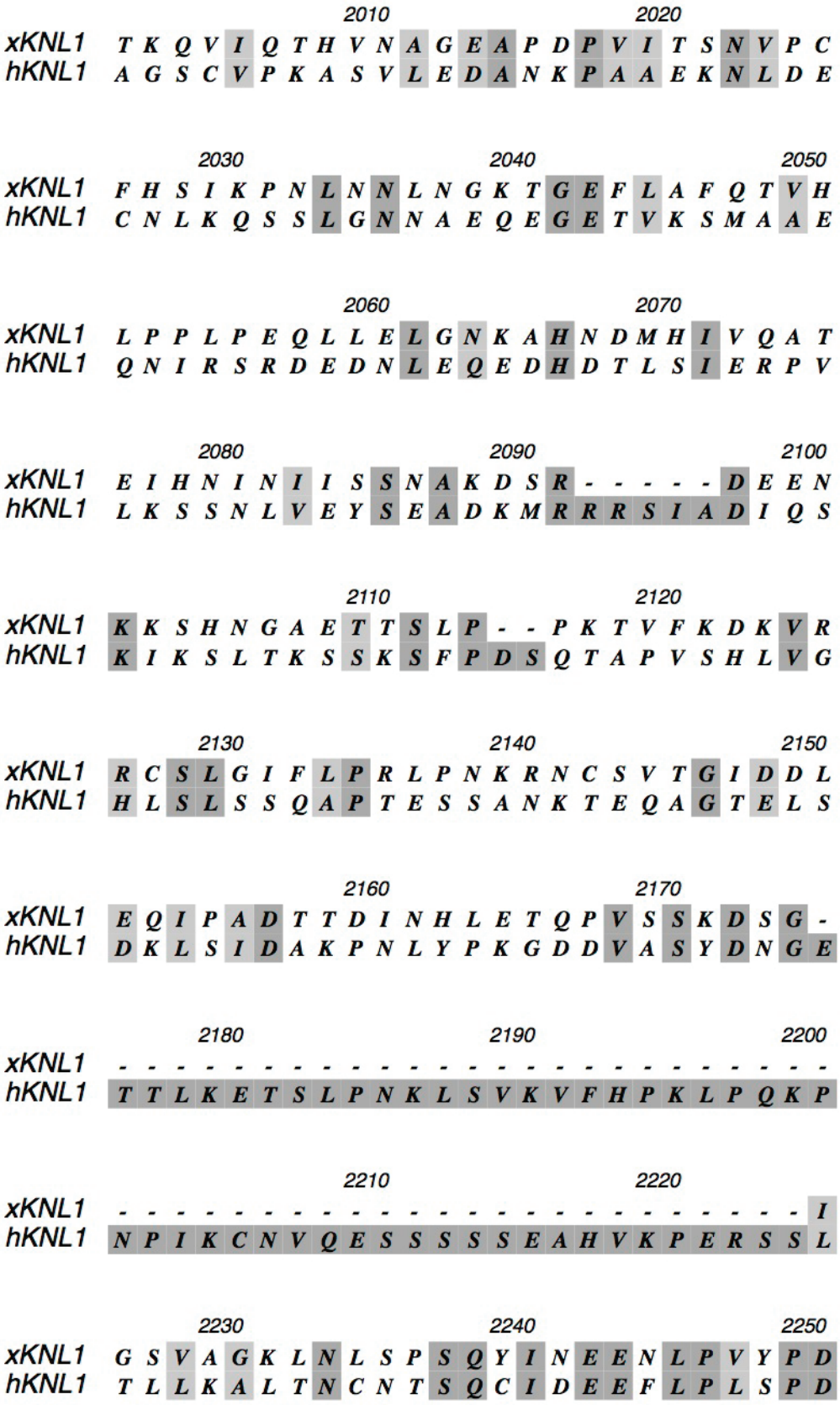
2010
2020
xKNL1 T K Q V I Q T H V N A G E A P D P V I T S N V P C
hKNL1 A G S C V P K A S V L E D A N K P A A E K N L D E
2030
2040
2050
xKNL1 F H S I K P N L N N L N G K T G E F L A F Q T V H
hKNL1 C N L K Q S S L G N N A E Q E G E T V K S M A A E
2060
2070
xKNL1 L P P L P E Q L L E L G N K A H N D M H I V Q A T
hKNL1 Q N I R S R D E D N L E Q E D H D T L S I E R P V
2080
2090
2100
xKNL1 E I H N I N I I S S N A K D S R - - - - - D E E N
hKNL1 L K S S N L V E Y S E A D K M R R R S I A D I Q S
2110
2120
xKNL1 K K S H N G A E T T S L P - - P K T V F K D K V R
hKNL1 K I K S L T K S S K S F P D S Q T A P V S H L V G
2130
2140
2150
xKNL1 R C S L G I F L P R L P N K R N C S V T G I D D L
hKNL1 H L S L S S Q A P T E S S A N K T E Q A G T E L S
2160
2170
xKNL1 E Q I P A D T T D I N H L E T Q P V S S K D S G -
hKNL1 D K L S I D A K P N L Y P K G D D V A S Y D N G E
2180
2190
2200
xKNL1 -
hKNL1 T T L K E T S L P N K L S V K V F H P K L P Q K P
2210
2220
xKNL1 - I
hKNL1 N P I K C N V Q E S S S S S S E A H V K P E R S S L
2230
2240
2250
xKNL1 G S V A G K L N L S P S Q Y I N E E N L P V Y P D
hKNL1 T L L K A L T N C N T S Q C I D E E F L P L S P D

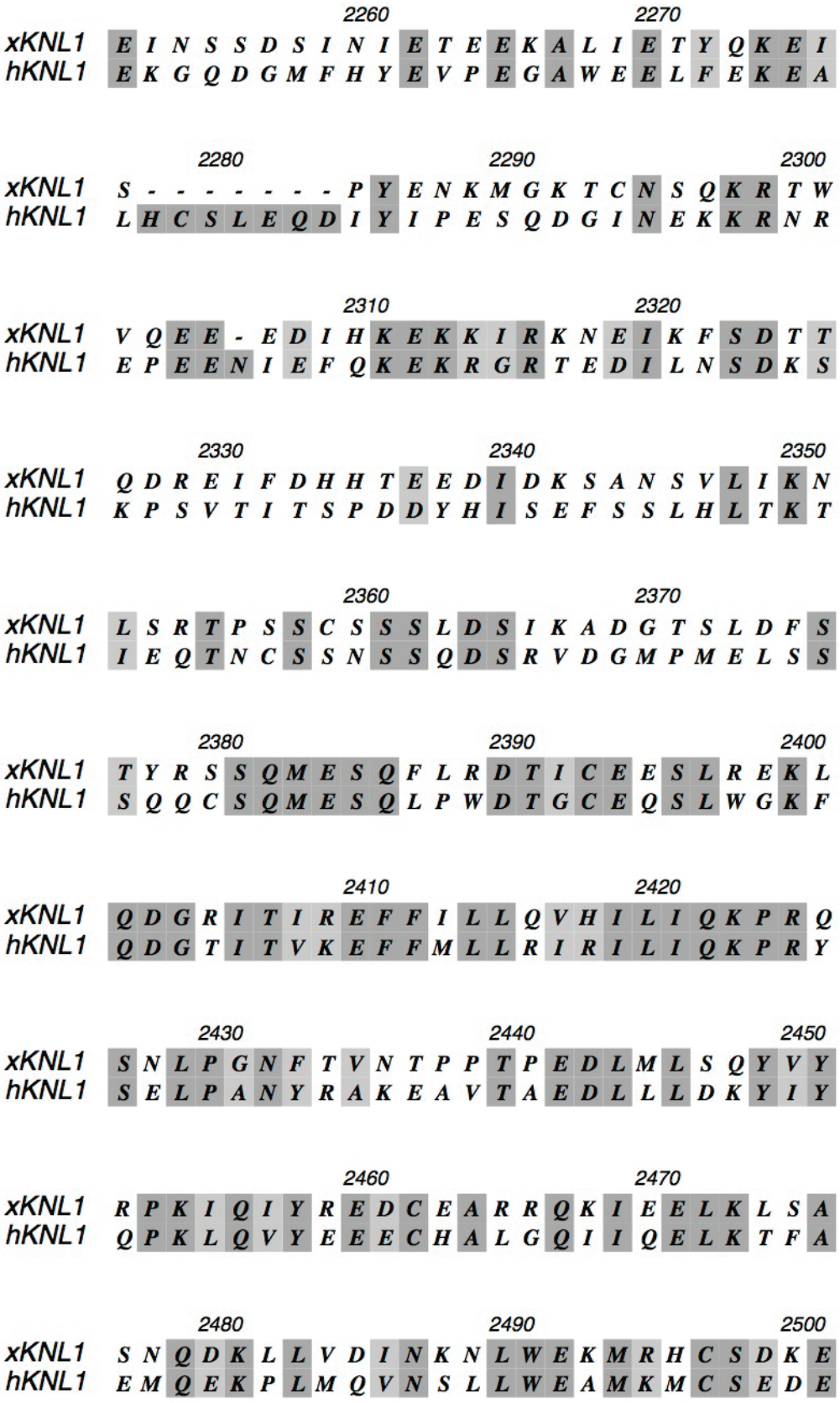
2260
2270
xKNL1 E I N S S D S I N I E T E E K A L I E T Y Q K E I
hKNL1 E K G Q D G M F H Y E V P E G A W E E L F E K E A
2280
2290
2300
xKNL1 S - - - - - - - P Y E N K M G K T C N S Q K R T W
hKNL1 L H C S L E Q D I Y I P E S Q D G I N E K K R N R
2310
2320
xKNL1 V Q E E - E D I H K E K K I R K N E I K F S D T T
hKNL1 E P E E N I E F Q K E K R G R T E D I L N S D K S
2330
2340
2350
xKNL1 Q D R E I F D H H T E E D I D K S A N S V L I K N
hKNL1 K P S V T I T S P D D Y H I S E F S S L H L T K T
2360
2370
xKNL1 L S R T P S S C S S S L D S I K A D G T S L D F S
hKNL1 I E Q T N C S S N S S Q D S R V D G M P M E L S S
2380
2390
2400
xKNL1 T Y R S S Q M E S Q F L R D T I C E E S L R E K L
hKNL1 S Q Q C S Q M E S Q L P W D T G C E Q S L W G K F
2410
2420
xKNL1 Q D G R I T I R E F F I L L Q V H I L I Q K P R Q
hKNL1 Q D G T I T V K E F F M L L R I R I L I Q K P R Y
2430
2440
2450
xKNL1 S N L P G N F T V N T P P T P E D L M L S Q Y V Y
hKNL1 S E L P A N Y R A K E A V T A E D L L L D K Y I Y
2460
2470
xKNL1 R P K I Q I Y R E D C E A R R Q K I E E L K L S A
hKNL1 Q P K L Q V Y E E E C H A L G Q I I Q E L K T F A
2480
2490
2500
xKNL1 S N Q D K L L V D I N K N L W E K M R H C S D K E
hKNL1 E M Q E K P L M Q V N S L L W E A M K M C S E D E

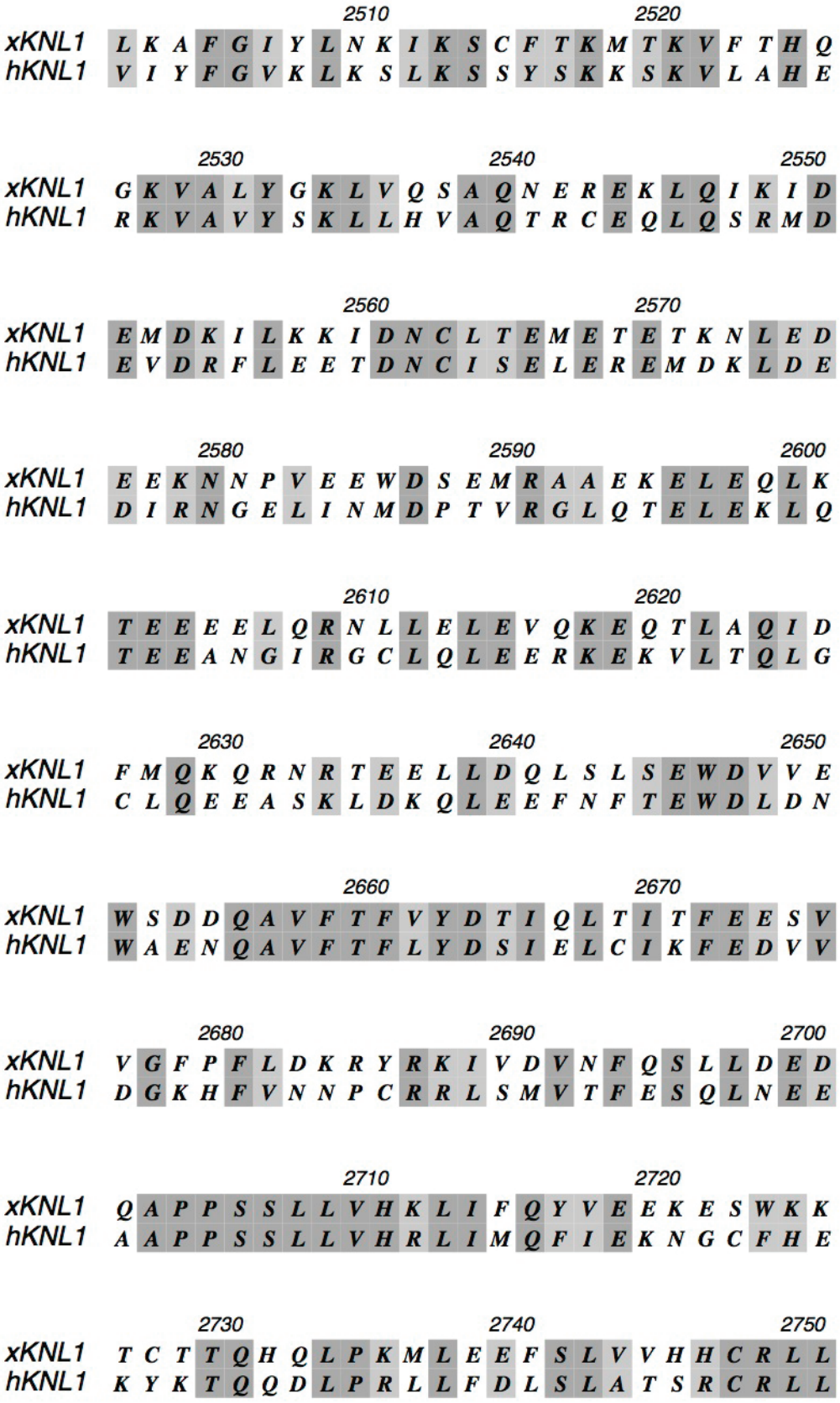
2510
2520
xKNL1 L K A F G I Y L N K I K S C F T K M T K V F T H Q
hKNL1 V I Y F G V K L K S L K S S Y S K K S K V L A H E
2530
2540
2550
xKNL1 G K V A L Y G K L V Q S A Q N E R E K L Q I K I D
hKNL1 R K V A V Y S K L L H V A Q T R C E Q L Q S R M D
2560
2570
xKNL1 E M D K I L K K I D N C L T E M E T E T K N L E D
hKNL1 E V D R F L E E T D N C I S E L E R E M D K L D E
2580
2590
2600
xKNL1 E E K N N P V E E W D S E M R A A E K E L E Q L K
hKNL1 D I R N G E L I N M D P T V R G L Q T E L E K L Q
2610
2620
xKNL1 T E E E E L Q R N L L E L E V Q K E Q T L A Q I D
hKNL1 T E E A N G I R G C L Q L E E R K E K V L T Q L G
2630
2640
2650
xKNL1 F M Q K Q R N R T E E L L D Q L S L S E W D V V E
hKNL1 C L Q E E A S K L D K Q L E E F N F T E W D L D N
2660
2670
xKNL1 W S D D Q A V F T F V Y D T I Q L T I T F E E S V
hKNL1 W A E N Q A V F T F L Y D S I E L C I K F E D V V
2680
2690
2700
xKNL1 V G F P F L D K R Y R K I V D V N F Q S L L D E D
hKNL1 D G K H F V N N P C R R L S M V T F E S Q L N E E
2710
2720
xKNL1 Q A P P S S L L V H K L I F Q Y V E E K E S W K K
hKNL1 A A P P S S L L V H R L I M Q F I E K N G C F H E
2730
2740
2750
xKNL1 T C T T Q H Q L P K M L E E F S L V V H H C R L L
hKNL1 K Y K T Q Q D L P R L L F D L S L A T S R C R L L

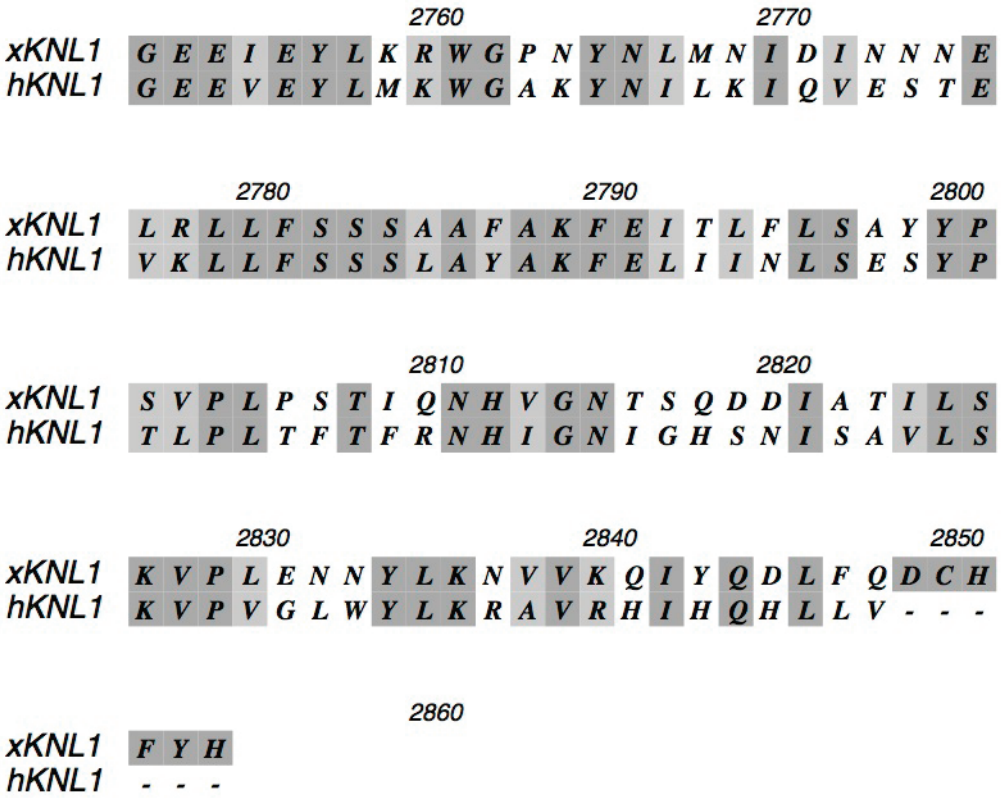
2760
2770
xKNL1 G E E I E Y L K R W G P N Y N L M N I D I N N N E
hKNL1 G E E V E Y L M K W G A K Y N I L K I Q V E S T E
2780
2790
2800
xKNL1 L R L L F S S S A A F A K F E I T L F L S A Y Y P
hKNL1 V K L L F S S S L A Y A K F E L I I N L S E S Y P
2810
2820
xKNL1 S V P L P S T I Q N H V G N T S Q D D I A T I L S
hKNL1 T L P L T F T F R N H I G N I G H S N I S A V L S
2830
2840
2850
xKNL1 K V P L E N N Y L K N V V K Q I Y Q D L F Q D C H
hKNL1 K V P V G L W Y L K R A V R H I H Q H L L V - - -
2860
xKNL1 F Y H
hKNL1 - - -

Regulation of the Repo-Man-PP1 interaction

Identification of *Xenopus laevis* Repo-Man

At the onset of this project, Repo-Man was one of the few known chromatin-associated PP1 regulatory subunits (Trinkle-Mulcahy et al., 2006; Vagnarelli et al., 2006). The regulation of this interaction, however, had not yet been explored. I therefore initially set out to study this regulatory mechanism in *Xenopus laevis* egg extracts. Since all previous studies of Repo-Man had been done in human cells, I first had to identify the homologue in this system.

Using homology between the 5'EST sequences of a *Xenopus laevis* cDNA library and the *Xenopus tropicalis* Repo-Man homologue, I identified two potential homologues. I sequentially sequenced these cDNA clones, and indeed they code for two distinct, full-length Repo-Man homologues with 79.8 % homology to each other, hereafter referred to as Repo-Man1 and Repo-Man2 (Figure A-2). Repo-Man2 is more similar to *Xenopus tropicalis* Repo-Man than is Repo-Man1 (74.2 and 68.3 % homology, respectively). Consistent with this, Repo-Man2 contains the conserved RVxF motif, while Repo-Man1 does not. All *Xenopus* homologues have approximately 31.5 % homology to human Repo-Man.

Effects of phosphorylation of the RVxF motif

I hypothesized that this interaction may be temporally regulated throughout mitosis. The "x" of the RVxF motif in this case is a strikingly conserved threonine. I therefore sought to test whether phosphorylation of this

Figure A-2: Alignment of Repo-Man homologues. Alignment of the full-length sequences of Repo-Man. Two isoforms from *Xenopus laevis* were identified from the IMAGE clone library and sequentially sequenced (Xl_Repo-Man1, IMAGE clone number 4084144, and Xl_Repo-Man2, IMAGE clone number 8329563). They are compared to published sequences from *Xenopus tropicalis* (Xt_Repo-Man) and *Homo sapiens* (Hs_Repo-Man). Identical residues are marked in dark grey, similar residues in light grey, and red bar indicates the conserved RVxF motif.

Figure A2: pages 150 to 157

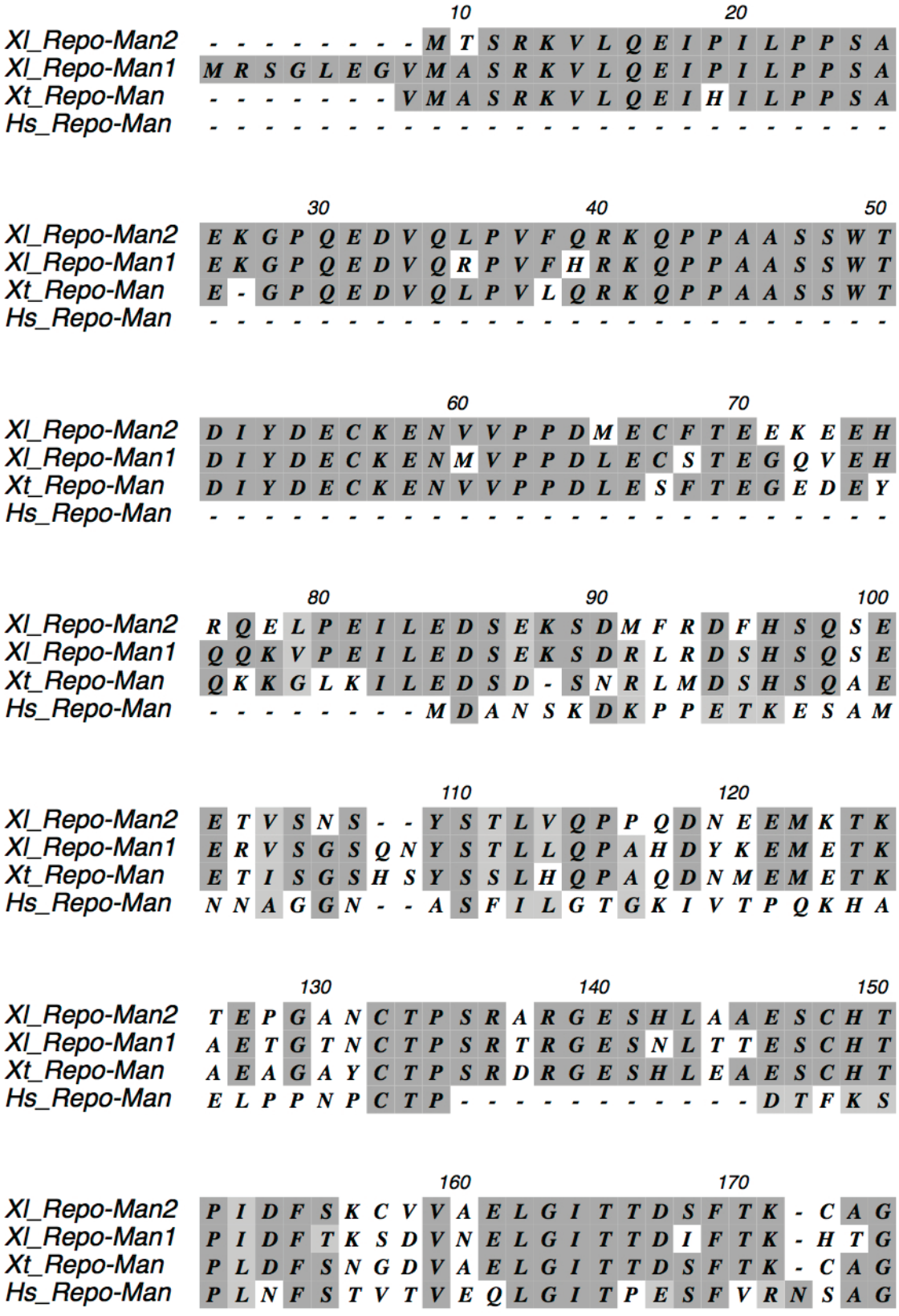

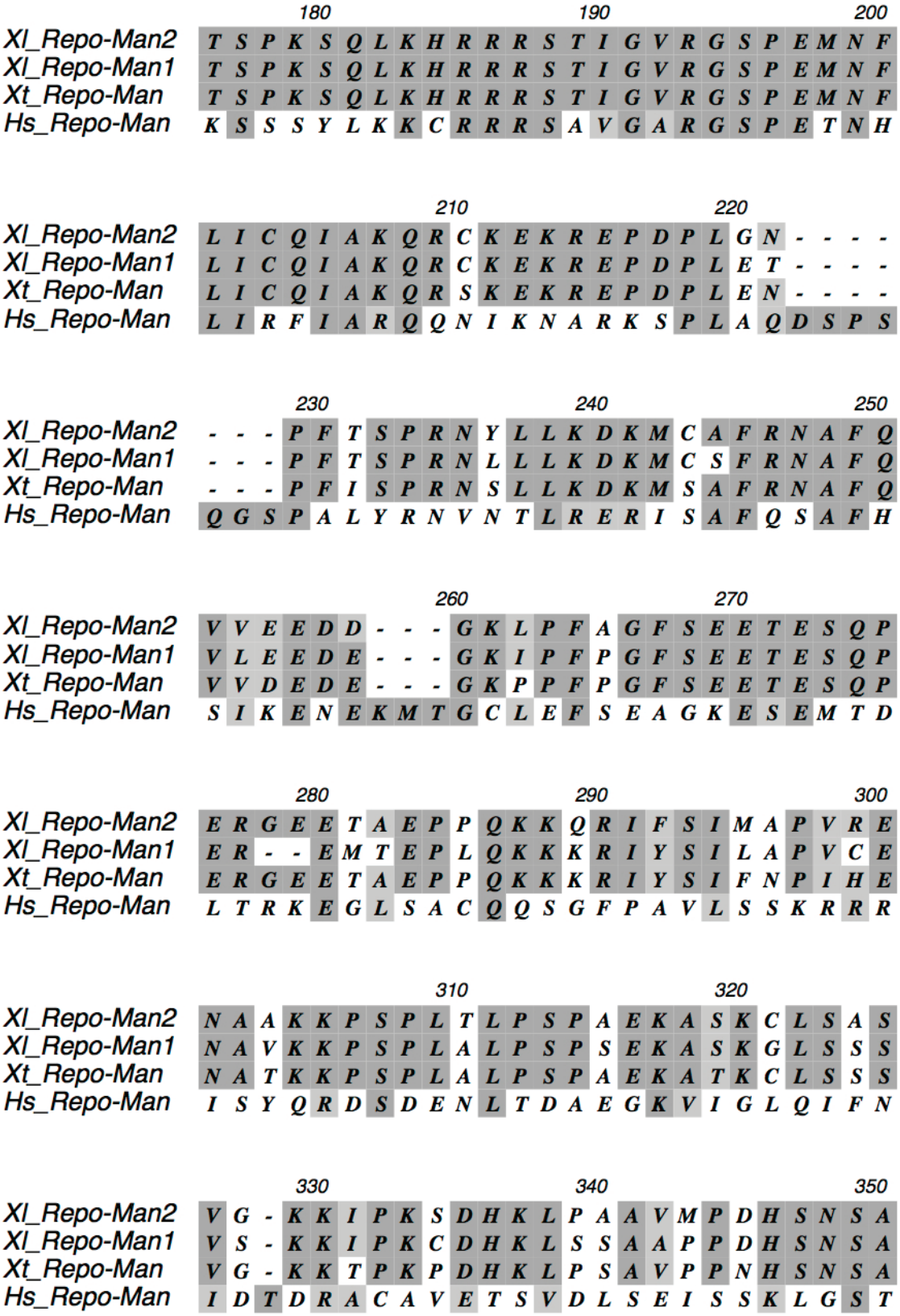
180 190 200
Xl_Repo-Man2 T S P K S Q L K H R R R S T I G V R G S P E M N F
Xl_Repo-Man1 T S P K S Q L K H R R R S T I G V R G S P E M N F
Xt_Repo-Man T S P K S Q L K H R R R S T I G V R G S P E M N F
Hs_Repo-Man K S S S Y L K K C R R R S A V G A R G S P E T N H
210 220
Xl_Repo-Man2 L I C Q I A K Q R C K E K R E P D P L G N - - - -
Xl_Repo-Man1 L I C Q I A K Q R C K E K R E P D P L E T - - - -
Xt_Repo-Man L I C Q I A K Q R S K E K R E P D P L E N - - - -
Hs_Repo-Man L I R F I A R Q Q N I K N A R K S P L A Q D S P S
230 240 250
Xl_Repo-Man2 - - - P F T S P R N Y L L K D K M C A F R N A F Q
Xl_Repo-Man1 - - - P F T S P R N L L L K D K M C S F R N A F Q
Xt_Repo-Man - - - P F I S P R N S L L K D K M S A F R N A F Q
Hs_Repo-Man Q G S P A L Y R N V N T L R E R I S A F Q S A F H
260 270
Xl_Repo-Man2 V V E E D D - - - G K L P F A G F S E E T E S Q P
Xl_Repo-Man1 V L E E D E - - - G K I P F P G F S E E T E S Q P
Xt_Repo-Man V V D E D E - - - G K P P F P G F S E E T E S Q P
Hs_Repo-Man S I K E N E K M T G C L E F S E A G K E S E M T D
280 290 300
Xl_Repo-Man2 E R G E E T A E P P Q K K Q R I F S I M A P V R E
Xl_Repo-Man1 E R - - E M T E P L Q K K K R I Y S I L A P V C E
Xt_Repo-Man E R G E E T A E P P Q K K K R I Y S I F N P I H E
Hs_Repo-Man L T R K E G L S A C Q Q S G F P A V L S S K R R R
310 320
Xl_Repo-Man2 N A A K K P S P L T L P S P A E K A S K C L S A S
Xl_Repo-Man1 N A V K K P S P L A L P S P S E K A S K G L S S S
Xt_Repo-Man N A T K K P S P L A L P S P A E K A T K C L S S S
Hs_Repo-Man I S Y Q R D S D E N L T D A E G K V I G L Q I F N
330 340 350
Xl_Repo-Man2 V G - K K I P K S D H K L P A A V M P D H S N S A
Xl_Repo-Man1 V S - K K I P K C D H K L S S A A P P D H S N S A
Xt_Repo-Man V G - K K T P K P D H K L P S A V P P N H S N S A
Hs_Repo-Man I D T D R A C A V E T S V D L S E I S S K L G S T

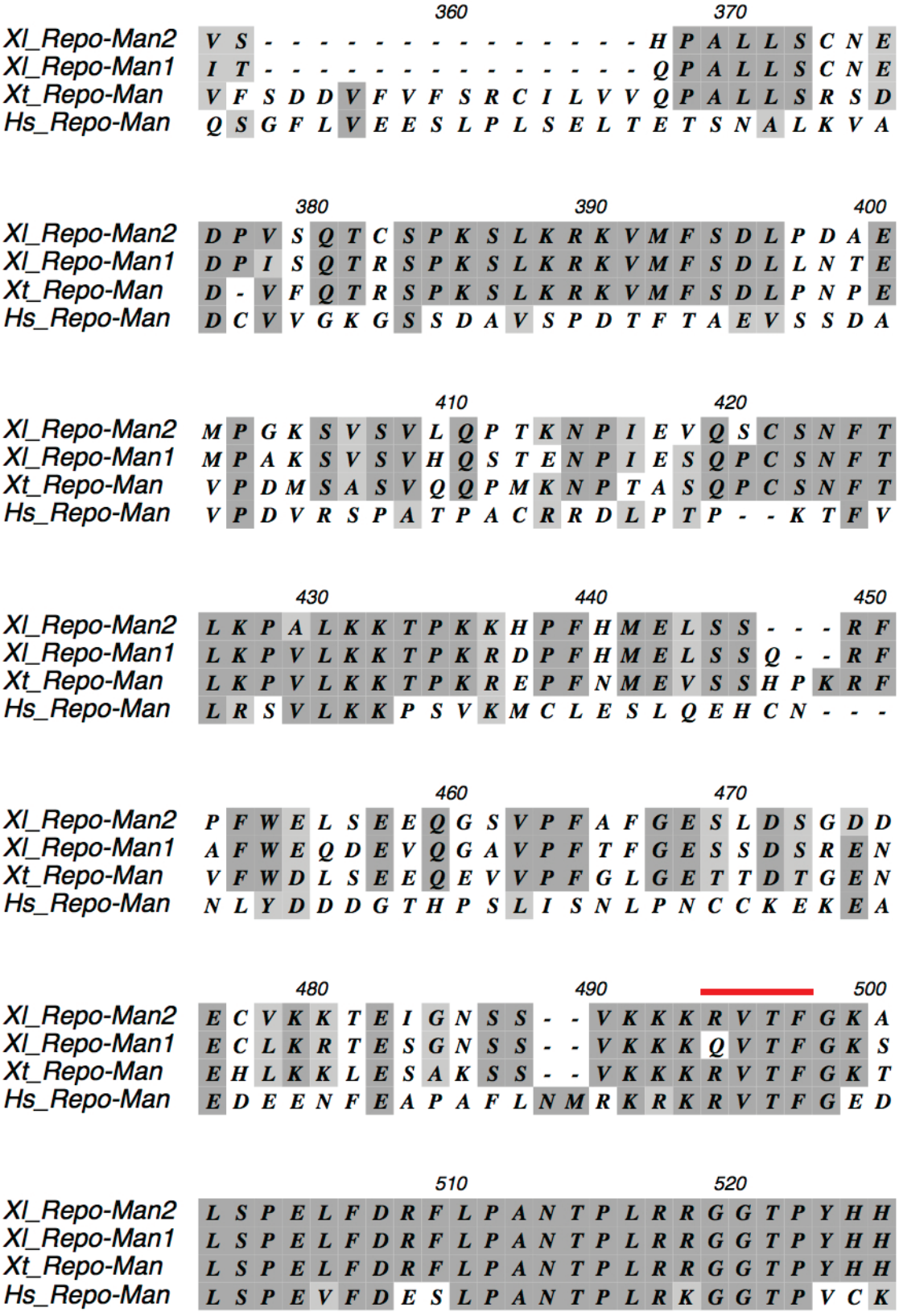
360
370
Xl_Repo-Man2 V S - - - - - - - - - - - - - - H P A L L S C N E
Xl_Repo-Man1 I T - - - - - - - - - - - - - - Q P A L L S C N E
Xt_Repo-Man V F S D D V F V F S R C I L V V Q P A L L S R S D
Hs_Repo-Man Q S G F L V E E S L P L S E L T E T S N A L K V A
380
390
400
Xl_Repo-Man2 D P V S Q T C S P K S L K R K V M F S D L P D A E
Xl_Repo-Man1 D P I S Q T R S P K S L K R K V M F S D L L N T E
Xt_Repo-Man D - V F Q T R S P K S L K R K V M F S D L P N P E
Hs_Repo-Man D C V V G K G S S D A V S P D T F T A E V S S D A
410
420
Xl_Repo-Man2 M P G K S V S V L Q P T K N P I E V Q S C S N F T
Xl_Repo-Man1 M P A K S V S V H Q S T E N P I E S Q P C S N F T
Xt_Repo-Man V P D M S A S V Q Q P M K N P T A S Q P C S N F T
Hs_Repo-Man V P D V R S P A T P A C R R D L P T P - - K T F V
430
440
450
Xl_Repo-Man2 L K P A L K K T P K K H P F H M E L S S - - - R F
Xl_Repo-Man1 L K P V L K K T P K R D P F H M E L S S Q - - R F
Xt_Repo-Man L K P V L K K T P K R E P F N M E V S S H P K R F
Hs_Repo-Man L R S V L K K P S V K M C L E S L Q E H C N - - -
460
470
Xl_Repo-Man2 P F W E L S E E Q G S V P F A F G E S L D S G D D
Xl_Repo-Man1 A F W E Q D E V Q G A V P F T F G E S S D S R E N
Xt_Repo-Man V F W D L S E E Q E V V P F G L G E T T D T G E N
Hs_Repo-Man N L Y D D D G T H P S L I S N L P N C C K E K E A
480
490
500
Xl_Repo-Man2 E C V K K T E I G N S S - - V K K K R V T F G K A
Xl_Repo-Man1 E C L K R T E S G N S S - - V K K K Q V T F G K S
Xt_Repo-Man E H L K K L E S A K S S - - V K K K R V T F G K T
Hs_Repo-Man E D E E N F E A P A F L N M R K R K R V T F G E D
510
520
Xl_Repo-Man2 L S P E L F D R F L P A N T P L R R G G T P Y H H
Xl_Repo-Man1 L S P E L F D R F L P A N T P L R R G G T P Y H H
Xt_Repo-Man L S P E L F D R F L P A N T P L R R G G T P Y H H
Hs_Repo-Man L S P E V F D E S L P A N T P L R K G G T P V C K

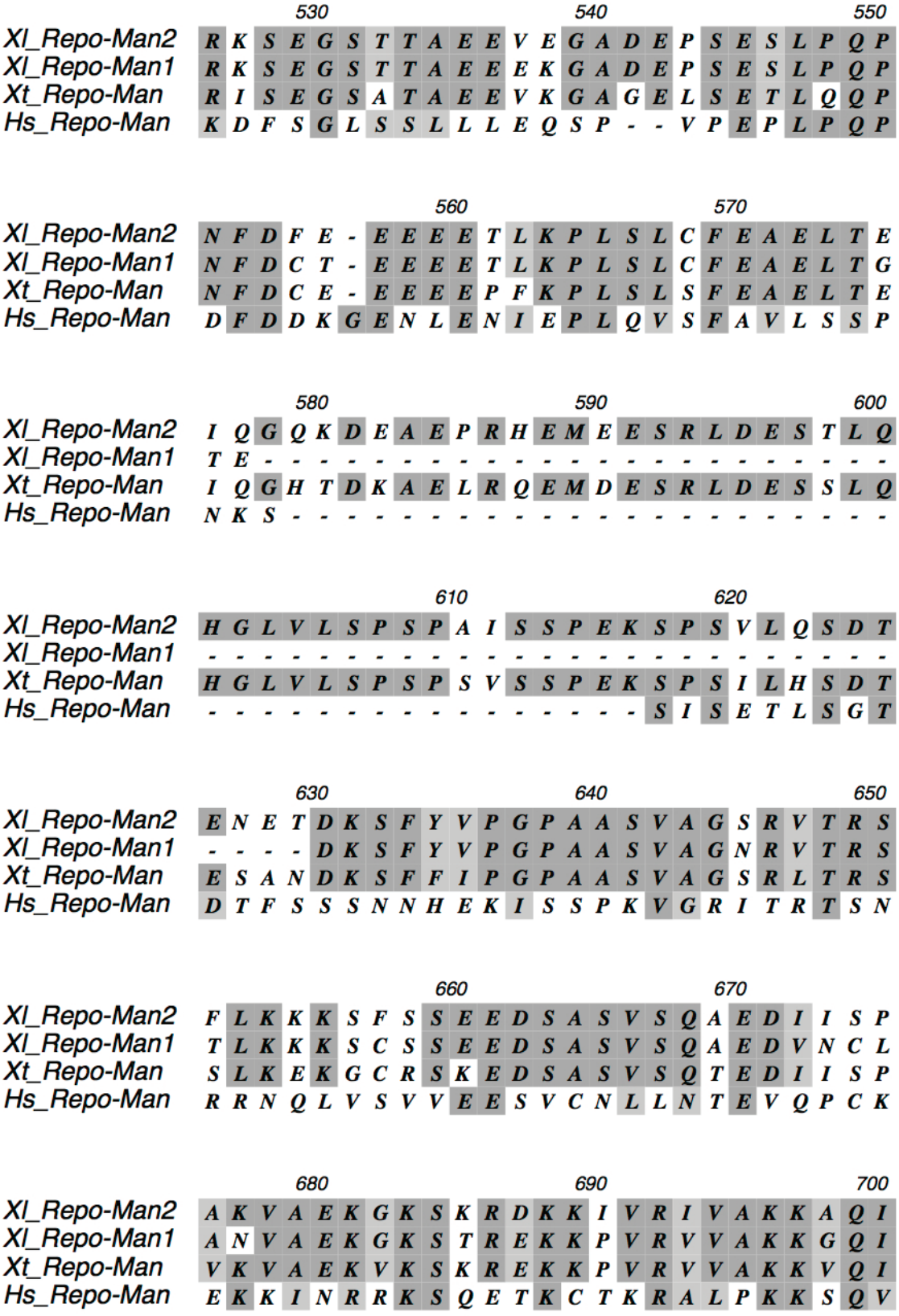
530 540 550
Xl_Repo-Man2 R K S E G S T T A E E V E G A D E P S E S L P Q P
Xl_Repo-Man1 R K S E G S T T A E E E K G A D E P S E S L P Q P
Xt_Repo-Man R I S E G S A T A E E V K G A G E L S E T L Q Q P
Hs_Repo-Man K D F S G L S S L L L E Q S P - - V P E P L P Q P
560 570
Xl_Repo-Man2 N F D F E - E E E E T L K P L S L C F E A E L T E
Xl_Repo-Man1 N F D C T - E E E E T L K P L S L C F E A E L T G
Xt_Repo-Man N F D C E - E E E E P F K P L S L S F E A E L T E
Hs_Repo-Man D F D D K G E N L E N I E P L Q V S F A V L S S P
580 590 600
Xl_Repo-Man2 I Q G Q K D E A E P R H E M E E S R L D E S T L Q
Xl_Repo-Man1 T E -
Xt_Repo-Man I Q G H T D K A E L R Q E M D E S R L D E S S L Q
Hs_Repo-Man N K S -
610 620
Xl_Repo-Man2 H G L V L S P S P A I S S P E K S P S V L Q S D T
Xl_Repo-Man1 -
Xt_Repo-Man H G L V L S P S P S V S S P E K S P S I L H S D T
Hs_Repo-Man - - - - - - - - - - - - - - - - S I S E T L S G T
630 640 650
Xl_Repo-Man2 E N E T D K S F Y V P G P A A S V A G S R V T R S
Xl_Repo-Man1 - - - - D K S F Y V P G P A A S V A G N R V T R S
Xt_Repo-Man E S A N D K S F F I P G P A A S V A G S R L T R S
Hs_Repo-Man D T F S S S N N H E K I S S P K V G R I T R T S N
660 670
Xl_Repo-Man2 F L K K K S F S S E E D S A S V S Q A E D I I S P
Xl_Repo-Man1 T L K K K S C S S E E D S A S V S Q A E D V N C L
Xt_Repo-Man S L K E K G C R S K E D S A S V S Q T E D I I S P
Hs_Repo-Man R R N Q L V S V V E E S V C N L L N T E V Q P C K
680 690 700
Xl_Repo-Man2 A K V A E K G K S K R D K K I V R I V A K K A Q I
Xl_Repo-Man1 A N V A E K G K S T R E K K P V R V V A K K G Q I
Xt_Repo-Man V K V A E K V K S K R E K K P V R V V A K K V Q I
Hs_Repo-Man E K K I N R R K S Q E T K C T K R A L P K K S Q V

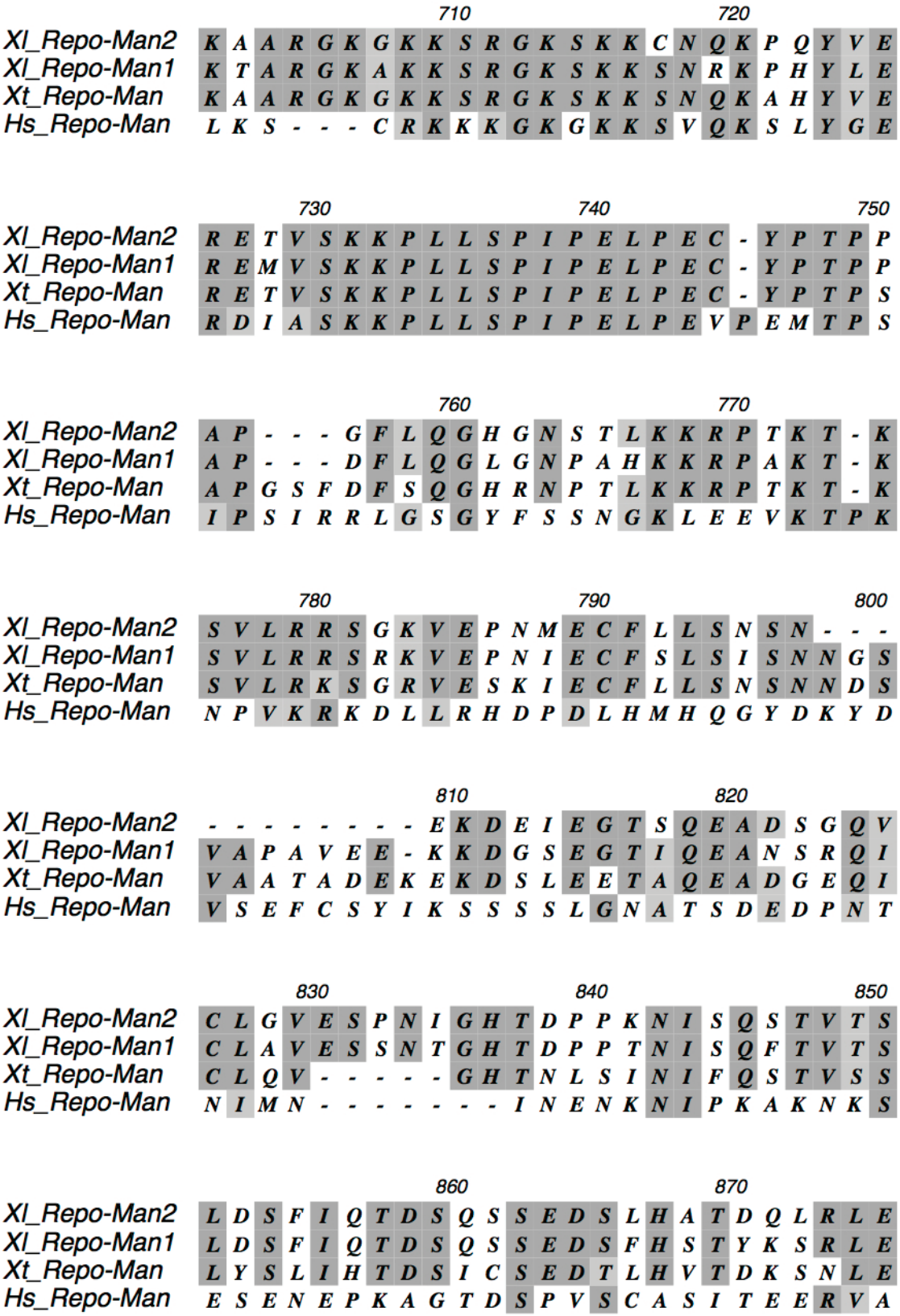
710
720
Xl_Repo-Man2 K A A R G K G K K S R G K S K K C N Q K P Q Y V E
Xl_Repo-Man1 K T A R G K A K K S R G K S K K S N R K P H Y L E
Xt_Repo-Man K A A R G K G K K S R G K S K K S N Q K A H Y V E
Hs_Repo-Man L K S - - - C R K K K G K G K K S V Q K S L Y G E
730
740
750
Xl_Repo-Man2 R E T V S K K P L L S P I P E L P E C - Y P T P P
Xl_Repo-Man1 R E M V S K K P L L S P I P E L P E C - Y P T P P
Xt_Repo-Man R E T V S K K P L L S P I P E L P E C - Y P T P S
Hs_Repo-Man R D I A S K K P L L S P I P E L P E V P E M T P S
760
770
Xl_Repo-Man2 A P - - - G F L Q G H G N S T L K K R P T K T - K
Xl_Repo-Man1 A P - - - D F L Q G L G N P A H K K R P A K T - K
Xt_Repo-Man A P G S F D F S Q G H R N P T L K K R P T K T - K
Hs_Repo-Man I P S I R R L G S G Y F S S N G K L E E V K T P K
780
790
800
Xl_Repo-Man2 S V L R R S G K V E P N M E C F L L S N S N - - -
Xl_Repo-Man1 S V L R R S R K V E P N I E C F S L S I S N N G S
Xt_Repo-Man S V L R K S G R V E S K I E C F L L S N S N N D S
Hs_Repo-Man N P V K R K D L L R H D P D L H M H Q G Y D K Y D
810
820
Xl_Repo-Man2 - - - - - - - - E K D E I E G T S Q E A D S G Q V
Xl_Repo-Man1 V A P A V E E - K K D G S E G T I Q E A N S R Q I
Xt_Repo-Man V A A T A D E K E K D S L E E T A Q E A D G E Q I
Hs_Repo-Man V S E F C S Y I K S S S S L G N A T S D E D P N T
830
840
850
Xl_Repo-Man2 C L G V E S P N I G H T D P P K N I S Q S T V T S
Xl_Repo-Man1 C L A V E S S N T G H T D P P T N I S Q F T V T S
Xt_Repo-Man C L Q V - - - - - G H T N L S I N I F Q S T V S S
Hs_Repo-Man N I M N - - - - - - - I N E N K N I P K A K N K S
860
870
Xl_Repo-Man2 L D S F I Q T D S Q S S E D S L H A T D Q L R L E
Xl_Repo-Man1 L D S F I Q T D S Q S S E D S F H S T Y K S R L E
Xt_Repo-Man L Y S L I H T D S I C S E D T L H V T D K S N L E
Hs_Repo-Man E S E N E P K A G T D S P V S C A S I T E E R V A

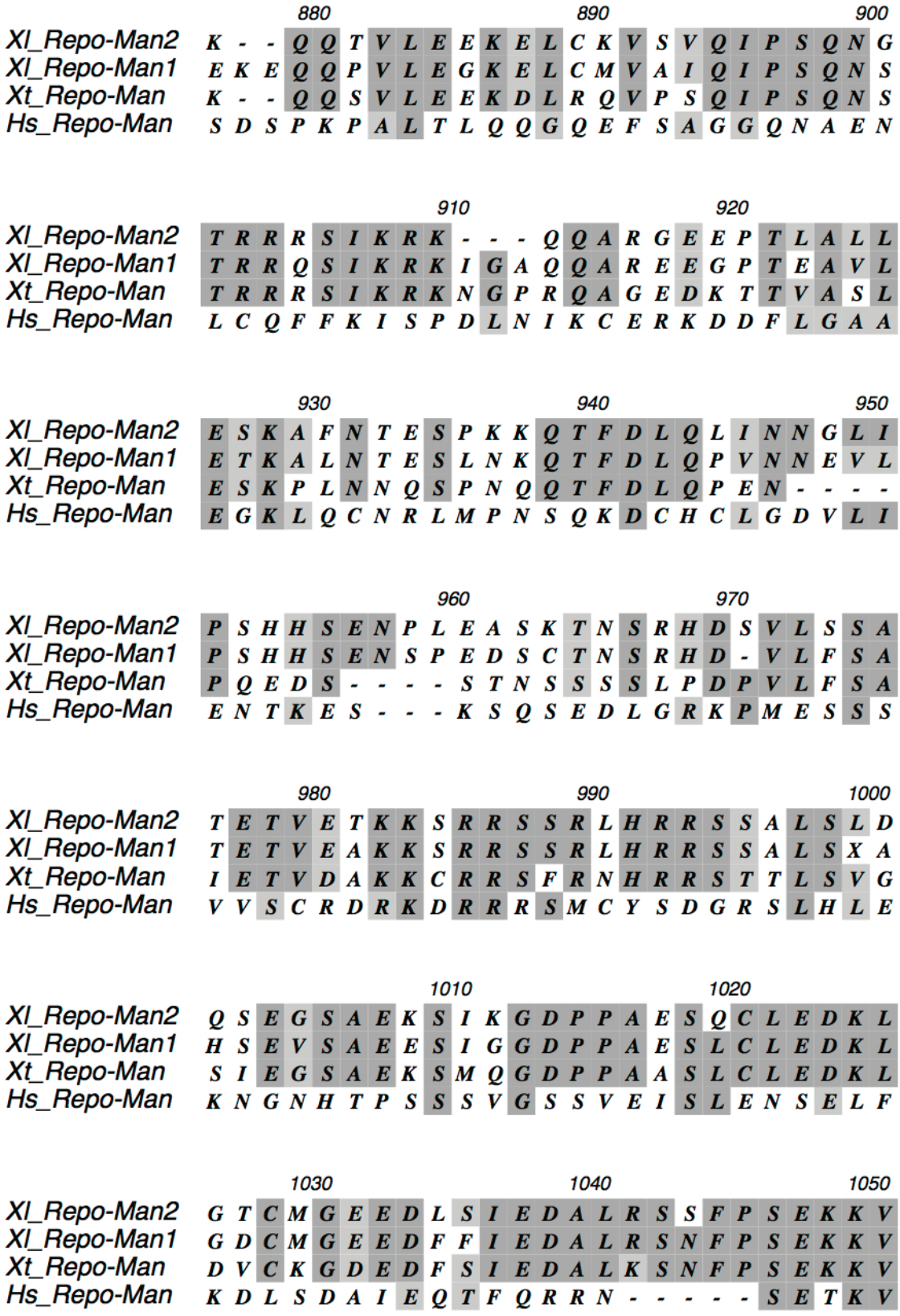
880 890 900
Xl_Repo-Man2 K - - Q Q T V L E E K E L C K V S V Q I P S Q N G
Xl_Repo-Man1 E K E Q Q P V L E G K E L C M V A I Q I P S Q N S
Xt_Repo-Man K - - Q Q S V L E E K D L R Q V P S Q I P S Q N S
Hs_Repo-Man S D S P K P A L T L Q Q G Q E F S A G G Q N A E N
910 920
Xl_Repo-Man2 T R R R S I K R K - - - Q Q A R G E E P T L A L L
Xl_Repo-Man1 T R R Q S I K R K I G A Q Q A R E E G P T E A V L
Xt_Repo-Man T R R R S I K R K N G P R Q A G E D K T T V A S L
Hs_Repo-Man L C Q F F K I S P D L N I K C E R K D D F L G A A
930 940 950
Xl_Repo-Man2 E S K A F N T E S P K K Q T F D L Q L I N N G L I
Xl_Repo-Man1 E T K A L N T E S L N K Q T F D L Q P V N N E V L
Xt_Repo-Man E S K P L N N Q S P N Q Q T F D L Q P E N - - - -
Hs_Repo-Man E G K L Q C N R L M P N S Q K D C H C L G D V L I
960 970
Xl_Repo-Man2 P S H H S E N P L E A S K T N S R H D S V L S S A
Xl_Repo-Man1 P S H H S E N S P E D S C T N S R H D - V L F S A
Xt_Repo-Man P Q E D S - - - - S T N S S S S L P D P V L F S A
Hs_Repo-Man E N T K E S - - - K S Q S E D L G R K P M E S S S
980 990 1000
Xl_Repo-Man2 T E T V E T K K S R R S S R L H R R S S A L S L D
Xl_Repo-Man1 T E T V E A K K S R R S S R L H R R S S A L S X A
Xt_Repo-Man I E T V D A K K C R R S F R N H R R S T T L S V G
Hs_Repo-Man V V S C R D R K D R R R S M C Y S D G R S L H L E
1010 1020
Xl_Repo-Man2 Q S E G S A E K S I K G D P P A E S Q C L E D K L
Xl_Repo-Man1 H S E V S A E E S I G G D P P A E S L C L E D K L
Xt_Repo-Man S I E G S A E K S M Q G D P P A A S L C L E D K L
Hs_Repo-Man K N G N H T P S S S V G S S V E I S L E N S E L F
1030 1040 1050
Xl_Repo-Man2 G T C M G E E D L S I E D A L R S S F P S E K K V
Xl_Repo-Man1 G D C M G E E D F F I E D A L R S N F P S E K K V
Xt_Repo-Man D V C K G D E D F S I E D A L K S N F P S E K K V
Hs_Repo-Man K D L S D A I E Q T F Q R R N - - - - - S E T K V

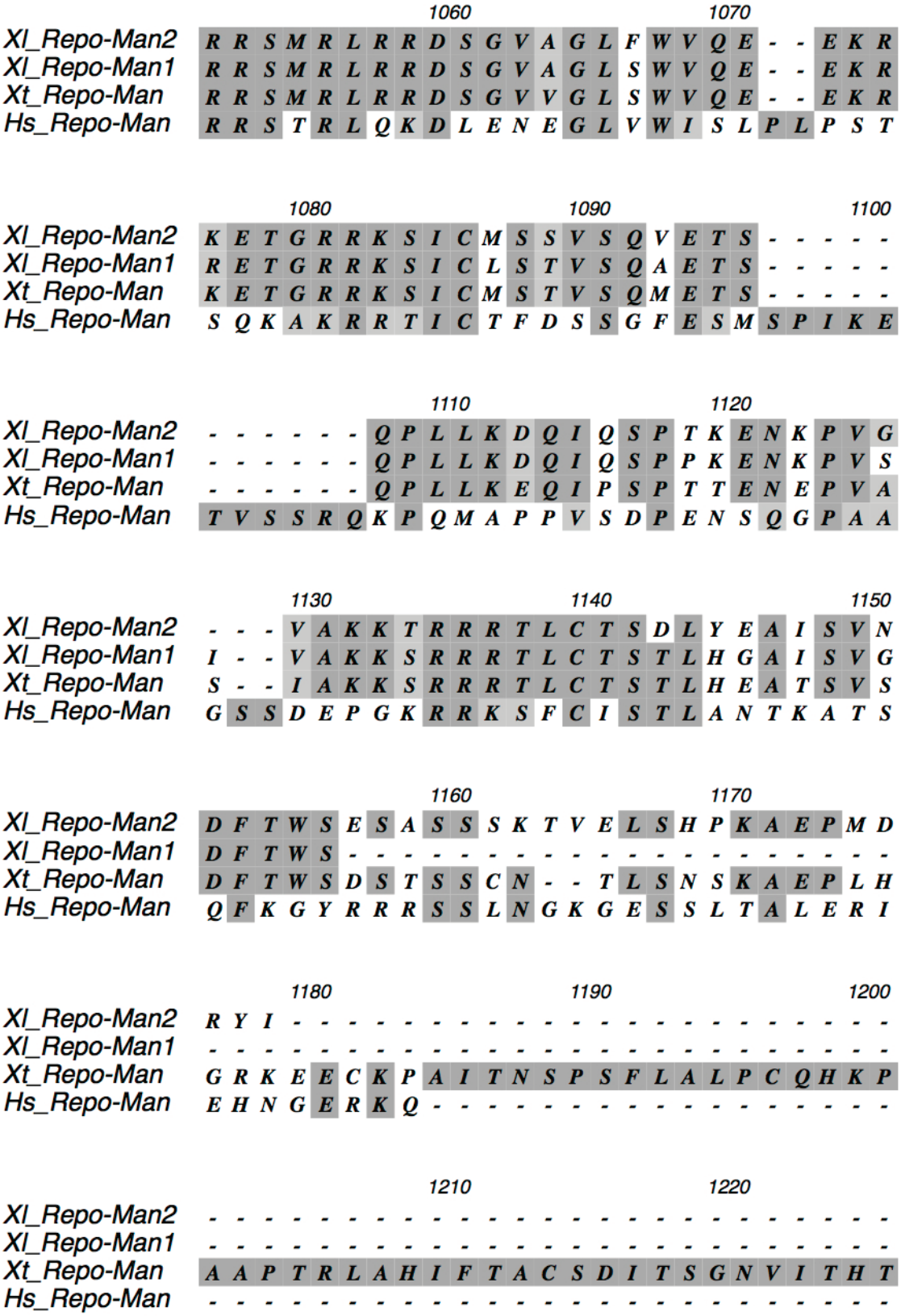
1060
1070
Xl_Repo-Man2 R R S M R L R R D S G V A G L F W V Q E - - E K R
Xl_Repo-Man1 R R S M R L R R D S G V A G L S W V Q E - - E K R
Xt_Repo-Man R R S M R L R R D S G V V G L S W V Q E - - E K R
Hs_Repo-Man R R S T R L Q K D L E N E G L V W I S L P L P S T
1080
1090
1100
Xl_Repo-Man2 K E T G R R K S I C M S S V S Q V E T S - - - - - -
Xl_Repo-Man1 R E T G R R K S I C L S T V S Q A E T S - - - - - -
Xt_Repo-Man K E T G R R K S I C M S T V S Q M E T S - - - - - -
Hs_Repo-Man S Q K A K R R T I C T F D S S G F E S M S P I K E
1110
1120
Xl_Repo-Man2 - - - - - - Q P L L K D Q I Q S P T K E N K P V G
Xl_Repo-Man1 - - - - - - Q P L L K D Q I Q S P P K E N K P V S
Xt_Repo-Man - - - - - - Q P L L K E Q I P S P T T E N E P V A
Hs_Repo-Man T V S S R Q K P Q M A P P V S D P E N S Q G P A A
1130
1140
1150
Xl_Repo-Man2 - - - V A K K T R R R T L C T S D L Y E A I S V N
Xl_Repo-Man1 I - - V A K K S R R R T L C T S T L H G A I S V G
Xt_Repo-Man S - - I A K K S R R R T L C T S T L H E A T S V S
Hs_Repo-Man G S S D E P G K R R K S F C I S T L A N T K A T S
1160
1170
Xl_Repo-Man2 D F T W S E S A S S S K T V E L S H P K A E P M D
Xl_Repo-Man1 D F T W S -
Xt_Repo-Man D F T W S D S T S S C N - - T L S N S K A E P L H
Hs_Repo-Man Q F K G Y R R R S S L N G K G E S S L T A L E R I
1180
1190
1200
Xl_Repo-Man2 R Y I -
Xl_Repo-Man1 -
Xt_Repo-Man G R K E E C K P A I T N S P S F L A L P C Q H K P
Hs_Repo-Man E H N G E R K Q - - - - - - - - - - - - - - - - -
1210
1220
Xl_Repo-Man2 -
Xl_Repo-Man1 -
Xt_Repo-Man A A P T R L A H I F T A C S D I T S G N V I T H T
Hs_Repo-Man -

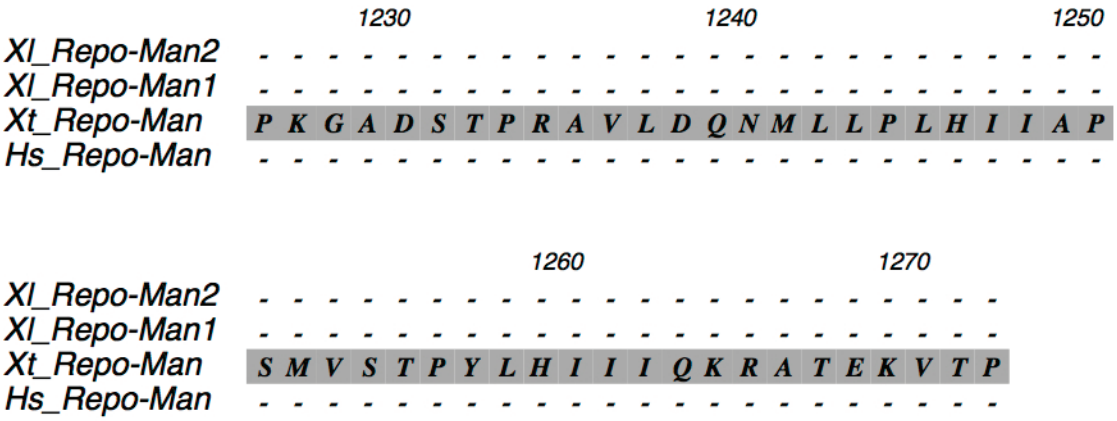
1230
1240
1250
Xl_Repo-Man2
Xl_Repo-Man1
Xt_Repo-Man
Hs_Repo-Man
P K G A D S T P R A V L D Q N M L L P L H I I A P
1260
1270
S M V S T P Y L H I I I Q K R A T E K V T P

residue may provide a mechanism for regulation of the interaction between Repo-Man and PP1. To examine this possibility *in vitro*, I had synthesized biotinylated peptides corresponding to the 20 amino acids surrounding the RVxF motif of the human protein. I had to use the human sequence instead of the *Xenopus* laevis sequence because the protein is so large that it took several rounds of sequencing before I had reached the RVxF motif.

I ordered two versions of this peptide: with and without a phosphorylated RVTF motif. To test the interaction between PP1 and Repo-Man, I incubated peptide-coated beads with purified PP1γ-HIS. To modulate the catalytic activity of the PP1γ-HIS, I supplemented the binding buffer with either $MnCl_2$ (required for full activation of the phosphatase) or phosphatase inhibitors. In either buffer, PP1γ-HIS bound to the unphosphorylated peptide. However, PP1γ-HIS bound to the phosphorylated peptide in the activating buffer but not in the inhibitory buffer (Figure A-3). This difference is most likely due to dephosphorylation of the peptide by active PP1γ-HIS.

From these data, I concluded that the interaction between PP1 and Repo-Man could be abrogated by phosphorylation of the Repo-Man RVTF motif. This mechanism was later shown to be physiologically relevant and essential for regulating the anaphase function of the Repo-Man-PP1 holoenzyme (Vagnarelli et al., 2011).

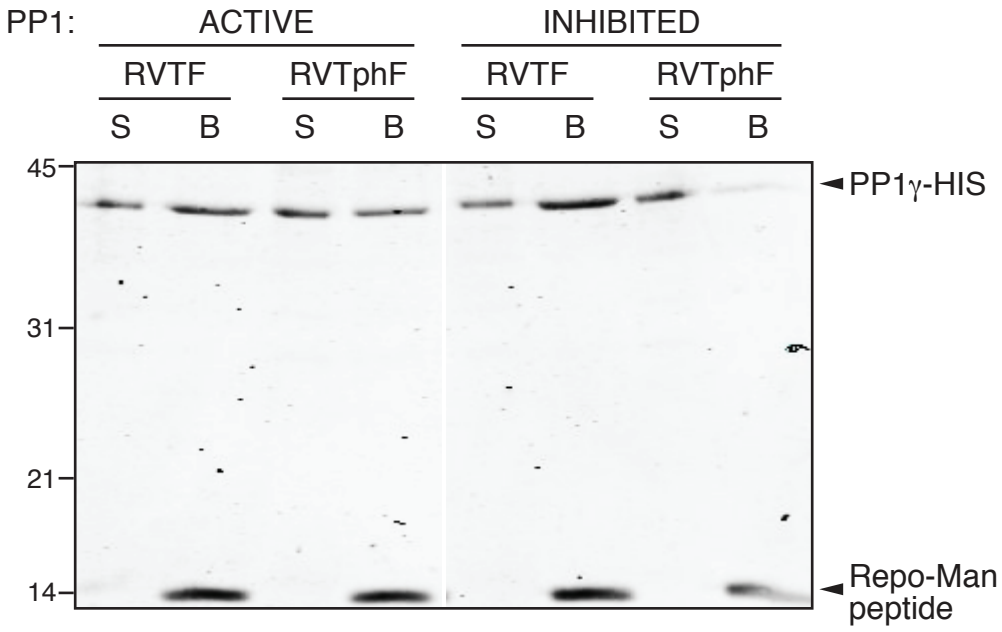

Figure A-3: Phosphorylation on Repo-Man abrogates its interaction with PP1. Peptides corresponding to the 20 amino acids surrounding the human Repo-Man RVTF motif were synthesized with or without threonine phosphorylation. Peptides conjugated to magnetic beads were incubated with PP1γ-HIS in binding buffer supplemented with $MnCl_2$ (ACTIVE), or phosphatase inhibitors (INHIBITED). Proteins in the supernatant (S) and those bound to beads (B) are imaged by Coomassie.

REFERENCES

Ahonen, L.J., Kallio, M.J., Daum, J.R., Bolton, M., Manke, I.A., Yaffe, M.B., Stukenberg, P.T., and Gorbsky, G.J. (2005). Polo-like kinase 1 creates the tension-sensing 3F3/2 phosphoepitope and modulates the association of spindle-checkpoint proteins at kinetochores. Curr Biol *15*, 1078-1089.

Akiyoshi, B., Nelson, C.R., Ranish, J.A., and Biggins, S. (2009a). Analysis of Ipl1-mediated phosphorylation of the Ndc80 kinetochore protein in Saccharomyces cerevisiae. Genetics *183*, 1591-1595.

Akiyoshi, B., Nelson, C.R., Ranish, J.A., and Biggins, S. (2009b). Quantitative proteomic analysis of purified yeast kinetochores identifies a PP1 regulatory subunit. Genes Dev *23*, 2887-2899.

Alessi, D., MacDougall, L.K., Sola, M.M., Ikebe, M., and Cohen, P. (1992). The control of protein phosphatase-1 by targetting subunits. The major myosin phosphatase in avian smooth muscle is a novel form of protein phosphatase-1. Eur J Biochem *210*, 1023-1035.

Andrews, P.D., Ovechkina, Y., Morrice, N., Wagenbach, M., Duncan, K., Wordeman, L., and Swedlow, J.R. (2004). Aurora B regulates MCAK at the mitotic centromere. Dev Cell *6*, 253-268.

Antoniw, J.F., and Cohen, P. (1976). Separation of two phosphorylase kinase phosphatases from rabbit skeletal muscle. Eur J Biochem *68*, 45-54.

Antoniw, J.F., Nimmo, H.G., Yeaman, S.J., and Cohen, P. (1977). Comparison of the substrate specificities of protein phosphatases involved in the regulation of glycogen metabolism in rabbit skeletal muscle. Biochem J *162*, 423-433.

Axton, J.M., Dombrádi, V., Cohen, P.T., and Glover, D.M. (1990). One of the protein phosphatase 1 isoenzymes in Drosophila is essential for mitosis. Cell *63*, 33-46.

Bean, J.M., Siggia, E.D., and Cross, F.R. (2006). Coherence and timing of cell cycle start examined at single-cell resolution. Mol Cell *21*, 3-14.

Beardmore, V.A., Ahonen, L.J., Gorbsky, G.J., and Kallio, M.J. (2004). Survivin dynamics increases at centromeres during G2/M phase transition and is regulated by microtubule-attachment and Aurora B kinase activity. Journal of Cell Science *117*, 4033-4042.

Bergmann, J.H., Rodríguez, M.G., Martins, N.M.C., Kimura, H., Kelly, D.A., Masumoto, H., Larionov, V., Jansen, L.E.T., and Earnshaw, W.C. (2011). Epigenetic engineering shows H3K4me2 is required for HJURP targeting and CENP-A assembly on a synthetic human kinetochore. EMBO J *30*, 328-340.

Biggins, S., and Murray, A.W. (2001). The budding yeast protein kinase Ipl1/Aurora allows the absence of tension to activate the spindle checkpoint. Genes Dev *15*, 3118-3129.

Black, S., Andrews, P.D., Sneddon, A.A., and Stark, M.J. (1995). A regulated MET3-GLC7 gene fusion provides evidence of a mitotic role for Saccharomyces cerevisiae protein phosphatase 1. Yeast *11*, 747-759.

Bloecher, A., and Tatchell, K. (2000). Dynamic localization of protein phosphatase type 1 in the mitotic cell cycle of Saccharomyces cerevisiae. The Journal of Cell Biology *149*, 125-140.

Bolanos-Garcia, V.M., Kiyomitsu, T., D'Arcy, S., Chirgadze, D.Y., Grossmann, J.G., Matak-Vinkovic, D., Venkitaraman, A.R., Yanagida, M., Robinson, C.V., and Blundell, T.L. (2009). The crystal structure of the N-terminal region of BUB1 provides insight into the mechanism of BUB1 recruitment to kinetochores. Structure (London, England : 1993) *17*, 105-116.

Bolanos-Garcia, V.M., Lischetti, T., Matak-Vinkovic, D., Cota, E., Simpson, P.J., Chirgadze, D.Y., Spring, D.R., Robinson, C.V., Nilsson, J., and Blundell, T.L. (2011). Structure of a Blinkin-BUBR1 complex reveals an interaction crucial for kinetochore-mitotic checkpoint regulation via an unanticipated binding Site. Structure (London, England : 1993) *19*, 1691-1700.

Bollen, M., Peti, W., Ragusa, M.J., and Beullens, M. (2010). The extended PP1 toolkit: designed to create specificity. Trends Biochem Sci *35*, 450-458.

Bolte, S., and Cordelieres, F.P. (2006). A guided tour into subcellular colocalization analysis in light microscopy. Journal of microscopy *224*, 213-232.

Carmena, M., Pinson, X., Platani, M., Salloum, Z., Xu, Z., Clark, A., Macisaac, F., Ogawa, H., Eggert, U., Glover, D.M.*, et al.* (2012). The chromosomal passenger complex activates Polo kinase at centromeres. PLoS Biol *10*, e1001250.

Carmody, L.C., Bauman, P.A., Bass, M.A., Mavila, N., DePaoli-Roach, A.A., and Colbran, R.J. (2004). A protein phosphatase-1gamma1 isoform selectivity determinant in dendritic spine-associated neurabin. J Biol Chem *279*, 21714-21723.

Ceulemans, H., Vulsteke, V., De Maeyer, M., Tatchell, K., Stalmans, W., and Bollen, M. (2002). Binding of the concave surface of the Sds22 superhelix to the alpha 4/alpha 5/alpha 6-triangle of protein phosphatase-1. J Biol Chem *277*, 47331-47337.

Chan, C.S., and Botstein, D. (1993). Isolation and characterization of chromosome-gain and increase-in-ploidy mutants in yeast. Genetics *135*, 677-691.

Cheeseman, I.M., Anderson, S., Jwa, M., Green, E.M., Kang, J.s., Yates, J.R., Chan, C.S.M., Drubin, D.G., and Barnes, G. (2002). Phospho-regulation of kinetochore-microtubule attachments by the Aurora kinase Ipl1p. Cell *111*, 163-172.

Cheeseman, I.M., Brew, C., Wolyniak, M., Desai, A., Anderson, S., Muster, N., Yates, J.R., Huffaker, T.C., Drubin, D.G., and Barnes, G. (2001a). Implication of a novel multiprotein Dam1p complex in outer kinetochore function. The Journal of Cell Biology *155*, 1137-1145.

Cheeseman, I.M., Chappie, J.S., Wilson-Kubalek, E.M., and Desai, A. (2006). The conserved KMN network constitutes the core microtubule-binding site of the kinetochore. Cell *127*, 983-997.

Cheeseman, I.M., and Desai, A. (2008). Molecular architecture of the kinetochore-microtubule interface. Nat Rev Mol Cell Biol *9*, 33-46.

Cheeseman, I.M., Enquist-Newman, M., Müller-Reichert, T., Drubin, D.G., and Barnes, G. (2001b). Mitotic spindle integrity and kinetochore function linked by the Duo1p/Dam1p complex. The Journal of Cell Biology *152*, 197-212.

Cheeseman, I.M., Niessen, S., Anderson, S., Hyndman, F., Yates, J.R., Oegema, K., and Desai, A. (2004). A conserved protein network controls assembly of the outer kinetochore and its ability to sustain tension. Genes Dev *18*, 2255-2268.

Choi, S.H., and McCollum, D. (2012). A role for metaphase spindle elongation forces in correction of merotelic kinetochore attachments. Curr Biol *22*, 225-230.

Choo, K.H. (2001). Domain organization at the centromere and neocentromere. Dev Cell *1*, 165-177.

Cimini, D., Cameron, L.A., and Salmon, E.D. (2004). Anaphase spindle mechanics prevent mis-segregation of merotelically oriented chromosomes. Curr Biol *14*, 2149-2155.

Cimini, D., Fioravanti, D., Salmon, E.D., and Degrassi, F. (2002). Merotelic kinetochore orientation versus chromosome mono-orientation in the origin of lagging chromosomes in human primary cells. Journal of Cell Science *115*, 507-515.

Cimini, D., Howell, B., Maddox, P., Khodjakov, A., Degrassi, F., and Salmon, E.D. (2001). Merotelic kinetochore orientation is a major mechanism of aneuploidy in mitotic mammalian tissue cells. The Journal of Cell Biology *153*, 517-527.

Cimini, D., Moree, B., Canman, J.C., and Salmon, E.D. (2003). Merotelic kinetochore orientation occurs frequently during early mitosis in mammalian tissue cells and error correction is achieved by two different mechanisms. J Cell Sci *116*, 4213-4225.

Cimini, D., Wan, X., Hirel, C., and Salmon, E. (2006a). Aurora kinase promotes turnover of kinetochore microtubules to reduce chromosome segregation errors. Current Biology.

Cimini, D., Wan, X., Hirel, C.B., and Salmon, E.D. (2006b). Aurora kinase promotes turnover of kinetochore microtubules to reduce chromosome segregation errors. Curr Biol *16*, 1711-1718.

Ciosk, R., Zachariae, W., Michaelis, C., Shevchenko, A., Mann, M., and Nasmyth, K. (1998). An ESP1/PDS1 complex regulates loss of sister chromatid cohesion at the metaphase to anaphase transition in yeast. Cell *93*, 1067-1076.

Clarke, L., and Carbon, J. (1980). Isolation of a yeast centromere and construction of functional small circular chromosomes. Nature *287*, 504-509.

Clarke, L., and Carbon, J. (1983). Genomic substitutions of centromeres in Saccharomyces cerevisiae. Nature *305*, 23-28.

Corbett, K.D., Yip, C.K., Ee, L.-S., Walz, T., Amon, A., and Harrison, S.C. (2010). The monopolin complex crosslinks kinetochore components to regulate chromosome-microtubule attachments. Cell *142*, 556-567.

Cross, F.R., and Pecani, K. (2010). Efficient and rapid exact gene replacement without selection. Yeast.

Daher, W., Browaeys, E., Pierrot, C., Jouin, H., Dive, D., Meurice, E., Dissous, C., Capron, M., Tomavo, S., Doerig, C.*, et al.* (2006a). Regulation of protein phosphatase type 1 and cell cycle progression by PfLRR1, a novel leucine-rich repeat protein of the human malaria parasite Plasmodium falciparum. Mol Microbiol *60*, 578-590.

Daher, W., Cailliau, K., Takeda, K., Pierrot, C., Khayath, N., Dissous, C., Capron, M., Yanagida, M., Browaeys, E., and Khalife, J. (2006b). Characterization of Schistosoma mansoni Sds homologue, a leucine-rich repeat protein that interacts with protein phosphatase type 1 and interrupts a G2/M cell-cycle checkpoint. Biochem J *395*, 433-441.

Daniel, J.A., Keyes, B.E., Ng, Y.P.Y., Freeman, C.O., and Burke, D.J. (2006). Diverse functions of spindle assembly checkpoint genes in Saccharomyces cerevisiae. Genetics *172*, 53-65.

Date, D., Dreier, M.R., Borton, M.T., Bekier, M.E., and Taylor, W.R. (2012). Effects of Phosphatase and Proteasome Inhibitors on Borealin Phosphorylation and Degradation. J Biochem.

DeLuca, J.G., Gall, W.E., Ciferri, C., Cimini, D., Musacchio, A., and Salmon, E.D. (2006). Kinetochore microtubule dynamics and attachment stability are regulated by Hec1. Cell *127*, 969-982.

Deluca, K.F., Lens, S.M.A., and Deluca, J.G. (2011). Temporal changes in Hec1 phosphorylation control kinetochore-microtubule attachment stability during mitosis. J Cell Sci.

Dephoure, N., Zhou, C., Villén, J., Beausoleil, S.A., Bakalarski, C.E., Elledge, S.J., and Gygi, S.P. (2008). A quantitative atlas of mitotic phosphorylation. Proc Natl Acad Sci USA *105*, 10762-10767.

Desai, A., Murray, A., Mitchison, T.J., and Walczak, C.E. (1999). The use of Xenopus egg extracts to study mitotic spindle assembly and function in vitro. Methods Cell Biol *61*, 385-412.

Desai, A., Rybina, S., Müller-Reichert, T., Shevchenko, A., Shevchenko, A., Hyman, A., and Oegema, K. (2003). KNL-1 directs assembly of the microtubule-binding interface of the kinetochore in C. elegans. Genes Dev *17*, 2421-2435.

Dewar, H., Tanaka, K., Nasmyth, K., and Tanaka, T. (2004). Tension between two kinetochores suffices for their bi-orientation on the mitotic spindle. Nature.

Ditchfield, C., Johnson, V.L., Tighe, A., Ellston, R., Haworth, C., Johnson, T., Mortlock, A., Keen, N., and Taylor, S.S. (2003). Aurora B couples chromosome alignment with anaphase by targeting BubR1, Mad2, and Cenp-E to kinetochores. The Journal of Cell Biology *161*, 267-280.

Dombrádi, V., Axton, J.M., Barker, H.M., and Cohen, P.T. (1990). Protein phosphatase 1 activity in Drosophila mutants with abnormalities in mitosis and chromosome condensation. FEBS Lett *275*, 39-43.

Doonan, J.H., and Morris, N.R. (1989). The bimG gene of Aspergillus nidulans, required for completion of anaphase, encodes a homolog of mammalian phosphoprotein phosphatase 1. Cell *57*, 987-996.

Drapkin, B.J., Lu, Y., Procko, A.L., Timney, B.L., and Cross, F.R. (2009). Analysis of the mitotic exit control system using locked levels of stable mitotic cyclin. Mol Syst Biol *5*, 328.

Du, J., Cai, X., Yao, J., Ding, X., Wu, Q., Pei, S., Jiang, K., Zhang, Y., Wang, W., Shi, Y.*, et al.* (2008). The mitotic checkpoint kinase NEK2A regulates kinetochore microtubule attachment stability. Oncogene *27*, 4107-4114.

Echeverri, C.J., Paschal, B.M., Vaughan, K.T., and Vallee, R.B. (1996). Molecular characterization of the 50-kD subunit of dynactin reveals function for the complex in chromosome alignment and spindle organization during mitosis. The Journal of Cell Biology *132*, 617-633.

Egloff, M.P., Cohen, P.T., Reinemer, P., and Barford, D. (1995). Crystal structure of the catalytic subunit of human protein phosphatase 1 and its complex with tungstate. J Mol Biol *254*, 942-959.

Egloff, M.P., Johnson, D.F., Moorhead, G., Cohen, P.T., and Barford, D. (1997). Structural basis for the recognition of regulatory subunits by the catalytic subunit of protein phosphatase 1. EMBO J *16*, 1876-1887.

Elowe, S., Hümmer, S., Uldschmid, A., Li, X., and Nigg, E.A. (2007). Tension-sensitive Plk1 phosphorylation on BubR1 regulates the stability of kinetochore microtubule interactions. Genes Dev *21*, 2205-2219.

Espeut, J., Cheerambathur, D.K., Krenning, L., Oegema, K., and Desai, A. (2012). Microtubule binding by KNL-1 contributes to spindle checkpoint silencing at the kinetochore. J Cell Biol *196*, 469-482.

Fardilha, M., Esteves, S.L., Korrodi-Gregorio, L., da Cruz e Silva, O.A., and da Cruz e Silva, F.F. (2010). The physiological relevance of protein phosphatase 1 and its interacting proteins to health and disease. Current medicinal chemistry *17*, 3996-4017.

Félix, M.A., Cohen, P.T., and Karsenti, E. (1990). Cdc2 H1 kinase is negatively regulated by a type 2A phosphatase in the Xenopus early embryonic cell cycle: evidence from the effects of okadaic acid. EMBO J *9*, 675-683.

Feng, Z.H., Wilson, S.E., Peng, Z.Y., Schlender, K.K., Reimann, E.M., and Trumbly, R.J. (1991). The yeast GLC7 gene required for glycogen accumulation encodes a type 1 protein phosphatase. J Biol Chem *266*, 23796-23801.

Fernandez, A., Brautigan, D.L., and Lamb, N.J. (1992). Protein phosphatase type 1 in mammalian cell mitosis: chromosomal localization and involvement in mitotic exit. The Journal of Cell Biology *116*, 1421-1430.

Field, C.M., Oegema, K., Zheng, Y., Mitchison, T.J., and Walczak, C.E. (1998). Purification of cytoskeletal proteins using peptide antibodies. Meth Enzymol *298*, 525-541.

Francisco, L., Wang, W., and Chan, C.S. (1994). Type 1 protein phosphatase acts in opposition to IpL1 protein kinase in regulating yeast chromosome segregation. Molecular and Cellular Biology *14*, 4731-4740.

Gibbons, J.A., Kozubowski, L., Tatchell, K., and Shenolikar, S. (2007). Expression of human protein phosphatase-1 in Saccharomyces cerevisiae highlights the role of phosphatase isoforms in regulating eukaryotic functions. J Biol Chem *282*, 21838-21847.

Gillett, E.S., Espelin, C.W., and Sorger, P.K. (2004). Spindle checkpoint proteins and chromosome-microtubule attachment in budding yeast. The Journal of Cell Biology *164*, 535-546.

Goto, H., Kiyono, T., Tomono, Y., Kawajiri, A., Urano, T., Furukawa, K., Nigg, E.A., and Inagaki, M. (2006). Complex formation of Plk1 and INCENP required for metaphase-anaphase transition. Nat Cell Biol *8*, 180-187.

Goto, H., Yasui, Y., Nigg, E.A., and Inagaki, M. (2002). Aurora-B phosphorylates Histone H3 at serine28 with regard to the mitotic chromosome condensation. Genes Cells *7*, 11-17.

Gregan, J., Riedel, C.G., Pidoux, A.L., Katou, Y., Rumpf, C., Schleiffer, A., Kearsey, S.E., Shirahige, K., Allshire, R.C., and Nasmyth, K. (2007). The kinetochore proteins Pcs1 and Mde4 and heterochromatin are required to prevent merotelic orientation. Curr Biol *17*, 1190-1200.

Hagan, R.S., Manak, M.S., Buch, H.K., Meier, M.G., Meraldi, P., Shah, J.V., and Sorger, P.K. (2011). p31(comet) acts to ensure timely spindle checkpoint silencing subsequent to kinetochore attachment. Mol Biol Cell *22*, 4236-4246.

Hardwick, K.G., Li, R., Mistrot, C., Chen, R.H., Dann, P., Rudner, A., and Murray, A.W. (1999). Lesions in many different spindle components activate the spindle checkpoint in the budding yeast Saccharomyces cerevisiae. Genetics *152*, 509-518.

Hauf, S., Cole, R.W., LaTerra, S., Zimmer, C., Schnapp, G., Walter, R., Heckel, A., van Meel, J., Rieder, C.L., and Peters, J.-M. (2003). The small molecule Hesperadin reveals a role for Aurora B in correcting kinetochore-microtubule attachment and in maintaining the spindle assembly checkpoint. The Journal of Cell Biology *161*, 281-294.

Hayden, J.H., Bowser, S.S., and Rieder, C.L. (1990). Kinetochores capture astral microtubules during chromosome attachment to the mitotic spindle: direct visualization in live newt lung cells. The Journal of Cell Biology *111*, 1039-1045.

He, X., Jones, M.H., Winey, M., and Sazer, S. (1998). Mph1, a member of the Mps1-like family of dual specificity protein kinases, is required for the spindle checkpoint in S. pombe. J Cell Sci *111 (Pt 12)*, 1635-1647.

Hendrickx, A., Beullens, M., Ceulemans, H., Den Abt, T., Van Eynde, A., Nicolaescu, E., Lesage, B., and Bollen, M. (2009). Docking motif-guided mapping of the interactome of protein phosphatase-1. Chem Biol *16*, 365-371.

Hewitt, L., Tighe, A., Santaguida, S., White, A.M., Jones, C.D., Musacchio, A., Green, S., and Taylor, S.S. (2010). Sustained Mps1 activity is required in mitosis to recruit O-Mad2 to the Mad1-C-Mad2 core complex. The Journal of Cell Biology *190*, 25-34.

Hisamoto, N., Sugimoto, K., and Matsumoto, K. (1994). The Glc7 type 1 protein phosphatase of Saccharomyces cerevisiae is required for cell cycle progression in G2/M. Molecular and Cellular Biology *14*, 3158-3165.

Howell, B.J., McEwen, B.F., Canman, J.C., Hoffman, D.B., Farrar, E.M., Rieder, C.L., and Salmon, E.D. (2001). Cytoplasmic dynein/dynactin drives kinetochore protein transport to the spindle poles and has a role in mitotic spindle checkpoint inactivation. The Journal of Cell Biology *155*, 1159-1172.

Hoyt, M.A., Totis, L., and Roberts, B.T. (1991). S. cerevisiae genes required for cell cycle arrest in response to loss of microtubule function. Cell *66*, 507-517.

Hsu, J.Y., Sun, Z.W., Li, X., Reuben, M., Tatchell, K., Bishop, D.K., Grushcow, J.M., Brame, C.J., Caldwell, J.A., Hunt, D.F.*, et al.* (2000). Mitotic phosphorylation of histone H3 is governed by Ipl1/aurora kinase and Glc7/PP1 phosphatase in budding yeast and nematodes. Cell *102*, 279-291.

Huang, H.B., Horiuchi, A., Goldberg, J., Greengard, P., and Nairn, A.C. (1997). Site-directed mutagenesis of amino acid residues of protein phosphatase 1 involved in catalysis and inhibitor binding. Proc Natl Acad Sci USA *94*, 3530-3535.

Hwang, L.H., Lau, L.F., Smith, D.L., Mistrot, C.A., Hardwick, K.G., Hwang, E.S., Amon, A., and Murray, A.W. (1998). Budding yeast Cdc20: a target of the spindle checkpoint. Science *279*, 1041-1044.

Indjeian, V.B., Stern, B.M., and Murray, A.W. (2005). The centromeric protein Sgo1 is required to sense lack of tension on mitotic chromosomes. Science *307*, 130-133.

Irniger, S., Piatti, S., Michaelis, C., and Nasmyth, K. (1995). Genes involved in sister chromatid separation are needed for B-type cyclin proteolysis in budding yeast. Cell *81*, 269-278.

Jacobs, C.W., Adams, A.E., Szaniszlo, P.J., and Pringle, J.R. (1988). Functions of microtubules in the Saccharomyces cerevisiae cell cycle. The Journal of Cell Biology *107*, 1409-1426.

Jelluma, N., Brenkman, A.B., van den Broek, N.J.F., Cruijsen, C.W.A., van Osch, M.H.J., Lens, S.M.A., Medema, R.H., and Kops, G.J.P.L. (2008). Mps1 phosphorylates Borealin to control Aurora B activity and chromosome alignment. Cell *132*, 233-246.

Jones, M.H., Huneycutt, B.J., Pearson, C.G., Zhang, C., Morgan, G., Shokat, K., Bloom, K., and Winey, M. (2005). Chemical genetics reveals a role for Mps1 kinase in kinetochore attachment during mitosis. Curr Biol *15*, 160-165.

Kallio, M.J., McCleland, M.L., Stukenberg, P.T., and Gorbsky, G.J. (2002). Inhibition of aurora B kinase blocks chromosome segregation, overrides the spindle checkpoint, and perturbs microtubule dynamics in mitosis. Curr Biol *12*, 900-905.

Kapoor, T.M., Lampson, M.A., Hergert, P., Cameron, L., Cimini, D., Salmon, E.D., McEwen, B.F., and Khodjakov, A. (2006). Chromosomes can congress to the metaphase plate before biorientation. Science *311*, 388-391.

Kawashima, S.A., Yamagishi, Y., Honda, T., Ishiguro, K.-i., and Watanabe, Y. (2010). Phosphorylation of H2A by Bub1 prevents chromosomal instability through localizing shugoshin. Science *327*, 172-177.

Keating, P., Rachidi, N., Tanaka, T.U., and Stark, M.J.R. (2009). Ipl1-dependent phosphorylation of Dam1 is reduced by tension applied on kinetochores. J Cell Sci *122*, 4375-4382.

Kelly, A.E., and Funabiki, H. (2009). Correcting aberrant kinetochore microtubule attachments: an Aurora B-centric view. Curr Opin Cell Biol *21*, 51-58.

Kelly, A.E., Ghenoiu, C., Xue, J.Z., Zierhut, C., Kimura, H., and Funabiki, H. (2010). Survivin Reads Phosphorylated Histone H3 Threonine 3 to Activate the Mitotic Kinase Aurora B. Science.

Kemmler, S., Stach, M., Knapp, M., Ortiz, J., Pfannstiel, J., Ruppert, T., and Lechner, J. (2009). Mimicking Ndc80 phosphorylation triggers spindle assembly checkpoint signalling. EMBO J *28*, 1099-1110.

Kerres, A., Jakopec, V., and Fleig, U. (2007). The conserved Spc7 protein is required for spindle integrity and links kinetochore complexes in fission yeast. Mol Biol Cell *18*, 2441-2454.

Kim, Y., Heuser, J.E., Waterman, C.M., and Cleveland, D.W. (2008). CENP-E combines a slow, processive motor and a flexible coiled coil to produce an essential motile kinetochore tether. The Journal of Cell Biology *181*, 411-419.

Kim, Y., Holland, A.J., Lan, W., and Cleveland, D.W. (2010). Aurora kinases and protein phosphatase 1 mediate chromosome congression through regulation of CENP-E. Cell *142*, 444-455.

King, E.M.J., Rachidi, N., Morrice, N., Hardwick, K.G., and Stark, M.J.R. (2007). Ipl1p-dependent phosphorylation of Mad3p is required for the spindle checkpoint response to lack of tension at kinetochores. Genes Dev *21*, 1163-1168.

King, J.M., and Nicklas, R.B. (2000). Tension on chromosomes increases the number of kinetochore microtubules but only within limits. J Cell Sci *113 Pt 21*, 3815-3823.

Kiyomitsu, T., Murakami, H., and Yanagida, M. (2011). Protein interaction domain mapping of human kinetochore protein Blinkin reveals a consensus motif for binding of spindle assembly checkpoint proteins Bub1 and BubR1. Mol Cell Biol *31*, 998-1011.

Kiyomitsu, T., Obuse, C., and Yanagida, M. (2007). Human Blinkin/AF15q14 is required for chromosome alignment and the mitotic checkpoint through direct interaction with Bub1 and BubR1. Dev Cell *13*, 663-676.

Knowlton, A.L., Lan, W., and Stukenberg, P.T. (2006). Aurora B is enriched at merotelic attachment sites, where it regulates MCAK. Curr Biol *16*, 1705-1710.

Krenn, V., Wehenkel, A., Li, X., Santaguida, S., and Musacchio, A. (2012). Structural analysis reveals features of the spindle checkpoint kinase Bub1-kinetochore subunit Knl1 interaction. J Cell Biol *196*, 451-467.

Lampson, M.A., and Kapoor, T.M. (2005). The human mitotic checkpoint protein BubR1 regulates chromosome-spindle attachments. Nat Cell Biol *7*, 93-98.

Lesage, B., Beullens, M., Nuytten, M., Van Eynde, A., Keppens, S., Himpens, B., and Bollen, M. (2004). Interactor-mediated nuclear translocation and retention of protein phosphatase-1. J Biol Chem *279*, 55978-55984.

Lesage, B., Beullens, M., Pedelini, L., Garcia-Gimeno, M.A., Waelkens, E., Sanz, P., and Bollen, M. (2007). A complex of catalytically inactive protein phosphatase-1 sandwiched between Sds22 and inhibitor-3. Biochemistry *46*, 8909-8919.

Letunic, I., Doerks, T., and Bork, P. (2012). SMART 7: recent updates to the protein domain annotation resource. Nucleic Acids Res *40*, D302-305.

Li, R., and Murray, A.W. (1991). Feedback control of mitosis in budding yeast. Cell *66*, 519-531.

Li, X., and Nicklas, R.B. (1995). Mitotic forces control a cell-cycle checkpoint. Nature *373*, 630-632.

Liu, D., Vader, G., Vromans, M.J.M., Lampson, M.A., and Lens, S.M.A. (2009). Sensing chromosome bi-orientation by spatial separation of aurora B kinase from kinetochore substrates. Science *323*, 1350-1353.

Liu, D., Vleugel, M., Backer, C.B., Hori, T., Fukagawa, T., Cheeseman, I.M., and Lampson, M.A. (2010). Regulated targeting of protein phosphatase 1 to the outer kinetochore by KNL1 opposes Aurora B kinase. The Journal of Cell Biology *188*, 809-820.

Liu, X., McLeod, I., Anderson, S., Yates, J.R., and He, X. (2005). Molecular analysis of kinetochore architecture in fission yeast. EMBO J *24*, 2919-2930.

Logarinho, E., and Bousbaa, H. (2008). Kinetochore-microtubule interactions "in check" by Bub1, Bub3 and BubR1: The dual task of attaching and signalling. Cell Cycle *7*, 1763-1768.

London, N., Ceto, S., Ranish, J.A., and Biggins, S. (2012). Phosphoregulation of Spc105 by Mps1 and PP1 Regulates Bub1 Localization to Kinetochores. Current biology : CB.

Lou, Y., Yao, J., Zereshki, A., Dou, Z., Ahmed, K., Wang, H., Hu, J., Wang, Y., and Yao, X. (2004). NEK2A interacts with MAD1 and possibly functions as a novel integrator of the spindle checkpoint signaling. J Biol Chem *279*, 20049-20057.

Luo, X., Tang, Z., Rizo, J., and Yu, H. (2002). The Mad2 spindle checkpoint protein undergoes similar major conformational changes upon binding to either Mad1 or Cdc20. Mol Cell *9*, 59-71.

Ma, H.T., and Poon, R.Y.C. (2011). How protein kinases co-ordinate mitosis in animal cells. Biochem J *435*, 17-31.

Maldonado, M., and Kapoor, T.M. (2011). Constitutive Mad1 targeting to kinetochores uncouples checkpoint signalling from chromosome biorientation. Nat Cell Biol *13*, 475-482.

Maresca, T.J., and Salmon, E.D. (2009). Intrakinetochore stretch is associated with changes in kinetochore phosphorylation and spindle assembly checkpoint activity. The Journal of Cell Biology *184*, 373-381.

Maresca, T.J., and Salmon, E.D. (2010). Welcome to a new kind of tension: translating kinetochore mechanics into a wait-anaphase signal. J Cell Sci *123*, 825-835.

Matsumura, S., Toyoshima, F., and Nishida, E. (2007). Polo-like kinase 1 facilitates chromosome alignment during prometaphase through BubR1. J Biol Chem *282*, 15217-15227.

Maure, J.-F., Kitamura, E., and Tanaka, T.U. (2007). Mps1 kinase promotes sister-kinetochore bi-orientation by a tension-dependent mechanism. Curr Biol *17*, 2175-2182.

McEwen, B.F., Heagle, A.B., Cassels, G.O., Buttle, K.F., and Rieder, C.L. (1997). Kinetochore fiber maturation in PtK1 cells and its implications for the

mechanisms of chromosome congression and anaphase onset. The Journal of Cell Biology *137*, 1567-1580.

Meadows, John C., Shepperd, Lindsey A., Vanoosthuyse, V., Lancaster, Theresa C., Sochaj, Alicja M., Buttrick, Graham J., Hardwick, Kevin G., and Millar, Jonathan B.A. (2011). Spindle Checkpoint Silencing Requires Association of PP1 to Both Spc7 and Kinesin-8 Motors. Dev Cell *20*, 739-750.

Meiselbach, H., Sticht, H., and Enz, R. (2006). Structural analysis of the protein phosphatase 1 docking motif: molecular description of binding specificities identifies interacting proteins. Chem Biol *13*, 49-59.

Meraldi, P., and Sorger, P.K. (2005). A dual role for Bub1 in the spindle checkpoint and chromosome congression. EMBO J *24*, 1621-1633.

Michaelis, C., Ciosk, R., and Nasmyth, K. (1997). Cohesins: chromosomal proteins that prevent premature separation of sister chromatids. Cell *91*, 35-45.

Montpetit, B., Thorne, K., Barrett, I., Andrews, K., Jadusingh, R., Hieter, P., and Measday, V. (2005). Genome-wide synthetic lethal screens identify an interaction between the nuclear envelope protein, Apq12p, and the kinetochore in Saccharomyces cerevisiae. Genetics *171*, 489-501.

Moorhead, G.B.G., Trinkle-Mulcahy, L., Nimick, M., De Wever, V., Campbell, D.G., Gourlay, R., Lam, Y.W., and Lamond, A.I. (2008). Displacement affinity chromatography of protein phosphatase one (PP1) complexes. BMC Biochem *9*, 28.

Murnion, M.E., Adams, R.R., Callister, D.M., Allis, C.D., Earnshaw, W.C., and Swedlow, J.R. (2001). Chromatin-associated protein phosphatase 1 regulates aurora-B and histone H3 phosphorylation. J Biol Chem *276*, 26656-26665.

Murray, A.W. (1991). Cell cycle extracts. Methods Cell Biol *36*, 581-605.

Murray, A.W., and Kirschner, M.W. (1989). Cyclin synthesis drives the early embryonic cell cycle. Nature *339*, 275-280.

Musacchio, A., and Salmon, E.D. (2007). The spindle-assembly checkpoint in space and time. Nat Rev Mol Cell Biol *8*, 379-393.

Nasmyth, K. (2005). How do so few control so many? Cell *120*, 739-746.

Nekrasov, V.S., Smith, M.A., Peak-Chew, S., and Kilmartin, J.V. (2003). Interactions between centromere complexes in Saccharomyces cerevisiae. Mol Biol Cell *14*, 4931-4946.

Nicklas, R.B., and Ward, S.C. (1994). Elements of error correction in mitosis: microtubule capture, release, and tension. The Journal of Cell Biology *126*, 1241-1253.

Nicolaou, P., Hajjar, R.J., and Kranias, E.G. (2009). Role of protein phosphatase-1 inhibitor-1 in cardiac physiology and pathophysiology. Journal of molecular and cellular cardiology *47*, 365-371.

Nimmo, G.A., and Cohen, P. (1978). The regulation of glycogen metabolism. Purification and characterisation of protein phosphatase inhibitor-1 from rabbit skeletal muscle. Eur J Biochem *87*, 341-351.

Norbury, C., and Nurse, P. (1992). Animal cell cycles and their control. Annu Rev Biochem *61*, 441-470.

Nousiainen, M., Silljé, H.H.W., Sauer, G., Nigg, E.A., and Körner, R. (2006). Phosphoproteome analysis of the human mitotic spindle. Proc Natl Acad Sci USA *103*, 5391-5396.

O'Toole, E.T., Winey, M., and McIntosh, J.R. (1999). High-voltage electron tomography of spindle pole bodies and early mitotic spindles in the yeast Saccharomyces cerevisiae. Mol Biol Cell *10*, 2017-2031.

Ohkura, H., Adachi, Y., Kinoshita, N., Niwa, O., Toda, T., and Yanagida, M. (1988). Cold-sensitive and caffeine-supersensitive mutants of the Schizosaccharomyces pombe dis genes implicated in sister chromatid separation during mitosis. EMBO J *7*, 1465-1473.

Ohkura, H., Kinoshita, N., Miyatani, S., Toda, T., and Yanagida, M. (1989). The fission yeast dis2+ gene required for chromosome disjoining encodes one of two putative type 1 protein phosphatases. Cell *57*, 997-1007.

Ohkura, H., and Yanagida, M. (1991). S. pombe gene sds22+ essential for a midmitotic transition encodes a leucine-rich repeat protein that positively modulates protein phosphatase-1. Cell *64*, 149-157.

Pagliuca, C., Draviam, V.M., Marco, E., Sorger, P.K., and De Wulf, P. (2009). Roles for the conserved spc105p/kre28p complex in kinetochore-microtubule binding and the spindle assembly checkpoint. PLoS ONE *4*, e7640.

Pedelini, L., Marquina, M., Ariño, J., Casamayor, A., Sanz, L., Bollen, M., Sanz, P., and Garcia-Gimeno, M.A. (2007). YPI1 and SDS22 proteins regulate the nuclear localization and function of yeast type 1 phosphatase Glc7. J Biol Chem *282*, 3282-3292.

Peggie, M.W., MacKelvie, S.H., Bloecher, A., Knatko, E.V., Tatchell, K., and Stark, M.J.R. (2002). Essential functions of Sds22p in chromosome stability and nuclear localization of PP1. J Cell Sci *115*, 195-206.

Peterson, J.B., and Ris, H. (1976). Electron-microscopic study of the spindle and chromosome movement in the yeast Saccharomyces cerevisiae. J Cell Sci *22*, 219-242.

Pinsky, B.A., and Biggins, S. (2005). The spindle checkpoint: tension versus attachment. Trends Cell Biol *15*, 486-493.

Pinsky, B.A., Kung, C., Shokat, K.M., and Biggins, S. (2006). The Ipl1-Aurora protein kinase activates the spindle checkpoint by creating unattached kinetochores. Nat Cell Biol *8*, 78-83.

Pinsky, B.A., Nelson, C.R., and Biggins, S. (2009). Protein phosphatase 1 regulates exit from the spindle checkpoint in budding yeast. Curr Biol *19*, 1182-1187.

Posch, M., Khoudoli, G.A., Swift, S., King, E.M., Deluca, J.G., and Swedlow, J.R. (2010). Sds22 regulates aurora B activity and microtubule-kinetochore interactions at mitosis. The Journal of Cell Biology *191*, 61-74.

Qian, J., Lesage, B., Beullens, M., Van Eynde, A., and Bollen, M. (2011). PP1/Repo-Man Dephosphorylates Mitotic Histone H3 at T3 and Regulates Chromosomal Aurora B Targeting. Curr Biol.

Rabitsch, K.P., Petronczki, M., Javerzat, J.P., Genier, S., Chwalla, B., Schleiffer, A., Tanaka, T.U., and Nasmyth, K. (2003). Kinetochore recruitment of two nucleolar proteins is required for homolog segregation in meiosis I. Dev Cell *4*, 535-548.

Ragusa, M.J., Dancheck, B., Critton, D.A., Nairn, A.C., Page, R., and Peti, W. (2010). Spinophilin directs protein phosphatase 1 specificity by blocking substrate binding sites. Nat Struct Mol Biol *17*, 459-464.

Rancati, G., Crispo, V., Lucchini, G., and Piatti, S. (2005). Mad3/BubR1 phosphorylation during spindle checkpoint activation depends on both Polo and Aurora kinases in budding yeast. Cell Cycle *4*, 972-980.

Rieder, C., Cole, R., and Khodjakov, A. (1995). The checkpoint delaying anaphase in response to chromosome monoorientation is mediated by an inhibitory signal produced by unattached kinetochores. Journal of Cell Biology.

Rieder, C.L., and Alexander, S.P. (1990). Kinetochores are transported poleward along a single astral microtubule during chromosome attachment to the spindle in newt lung cells. The Journal of Cell Biology *110*, 81-95.

Rieder, C.L., Schultz, A., Cole, R., and Sluder, G. (1994). Anaphase onset in vertebrate somatic cells is controlled by a checkpoint that monitors sister kinetochore attachment to the spindle. The Journal of Cell Biology *127*, 1301-1310.

Rosenberg, Jessica S., Cross, Frederick R., and Funabiki, H. (2011). KNL1/Spc105 Recruits PP1 to Silence the Spindle Assembly Checkpoint. Current Biology *21*, 942-947.

Ruchaud, S., Carmena, M., and Earnshaw, W.C. (2007). Chromosomal passengers: conducting cell division. Nat Rev Mol Cell Biol *8*, 798-812.

Rumpf, C., Cipak, L., Schleiffer, A., Pidoux, A., Mechtler, K., Tolić-Nørrelykke, I.M., and Gregan, J. (2010). Laser microsurgery provides evidence for merotelic kinetochore attachments in fission yeast cells lacking Pcs1 or Clr4. Cell Cycle *9*, 3997-4004.

Sakuno, T., Tada, K., and Watanabe, Y. (2009). Kinetochore geometry defined by cohesion within the centromere. Nature *458*, 852-858.

Sampath, S.C., Ohi, R., Leismann, O., Salic, A., Pozniakovski, A., and Funabiki, H. (2004). The chromosomal passenger complex is required for chromatin-induced microtubule stabilization and spindle assembly. Cell *118*, 187-202.

Sandall, S., Severin, F., McLeod, I.X., Yates, J.R., Oegema, K., Hyman, A., and Desai, A. (2006). A Bir1-Sli15 complex connects centromeres to microtubules and is required to sense kinetochore tension. Cell *127*, 1179-1191.

Santaguida, S., and Musacchio, A. (2009). The life and miracles of kinetochores. EMBO J *28*, 2511-2531.

Santaguida, S., Vernieri, C., Villa, F., Ciliberto, A., and Musacchio, A. (2011). Evidence that Aurora B is implicated in spindle checkpoint signalling independently of error correction. EMBO J.

Sassoon, I., Severin, F.F., Andrews, P.D., Taba, M.R., Kaplan, K.B., Ashford, A.J., Stark, M.J.R., Sorger, P.K., and Hyman, A.A. (1999). Regulation of Saccharomyces cerevisiae kinetochores by the type 1 phosphatase Glc7p. Genes Dev *13*, 545-555.

Schueler, M.G., Higgins, A.W., Rudd, M.K., Gustashaw, K., and Willard, H.F. (2001). Genomic and genetic definition of a functional human centromere. Science *294*, 109-115.

Schultz, J., Milpetz, F., Bork, P., and Ponting, C.P. (1998). SMART, a simple modular architecture research tool: identification of signaling domains. Proc Natl Acad Sci USA *95*, 5857-5864.

Shepperd, L.A., Meadows, J.C., Sochaj, A.M., Lancaster, T.C., Zou, J., Buttrick, G.J., Rappsilber, J., Hardwick, K.G., and Millar, J.B.A. (2012). Phosphodependent Recruitment of Bub1 and Bub3 to Spc7/KNL1 by Mph1 Kinase Maintains the Spindle Checkpoint. Current biology : CB.

Sironi, L., Mapelli, M., Knapp, S., De Antoni, A., Jeang, K.-T., and Musacchio, A. (2002). Crystal structure of the tetrameric Mad1-Mad2 core complex: implications of a 'safety belt' binding mechanism for the spindle checkpoint. EMBO J *21*, 2496-2506.

Sudakin, V., Chan, G.K., and Yen, T.J. (2001). Checkpoint inhibition of the APC/C in HeLa cells is mediated by a complex of BUBR1, BUB3, CDC20, and MAD2. The Journal of Cell Biology *154*, 925-936.

Sullivan, K.F., Hechenberger, M., and Masri, K. (1994). Human CENP-A contains a histone H3 related histone fold domain that is required for targeting to the centromere. The Journal of Cell Biology *127*, 581-592.

Sumara, I., Giménez-Abián, J.F., Gerlich, D., Hirota, T., Kraft, C., de la Torre, C., Ellenberg, J., and Peters, J.-M. (2004). Roles of polo-like kinase 1 in the assembly of functional mitotic spindles. Curr Biol *14*, 1712-1722.

Takai, A., and Mieskes, G. (1991). Inhibitory effect of okadaic acid on the p-nitrophenyl phosphate phosphatase activity of protein phosphatases. Biochem J *275 (Pt 1)*, 233-239.

Takemoto, A., Maeshima, K., Ikehara, T., Yamaguchi, K., Murayama, A., Imamura, S., Imamoto, N., Yokoyama, S., Hirano, T., Watanabe, Y*., et al.* (2009). The chromosomal association of condensin II is regulated by a noncatalytic function of PP2A. Nat Struct Mol Biol *16*, 1302-1308.

Tanaka, K., Mukae, N., Dewar, H., van Breugel, M., James, E.K., Prescott, A.R., Antony, C., and Tanaka, T.U. (2005). Molecular mechanisms of kinetochore capture by spindle microtubules. Nature *434*, 987-994.

Tanaka, T., Rachidi, N., Janke, C., Pereira, G., and Galova, M. (2002). Evidence that the Ipl1-Sli15 (Aurora kinase-INCENP) complex promotes chromosome bi-orientation by altering kinetochore-spindle pole connections. Cell.

Teichner, A., Eytan, E., Sitry-Shevah, D., Miniowitz-Shemtov, S., Dumin, E., Gromis, J., and Hershko, A. (2011). p31comet Promotes disassembly of the mitotic checkpoint complex in an ATP-dependent process. Proc Natl Acad Sci U S A *108*, 3187-3192.

Terrak, M., Kerff, F., Langsetmo, K., Tao, T., and Dominguez, R. (2004). Structural basis of protein phosphatase 1 regulation. Nature *429*, 780-784.

Terry-Lorenzo, R.T., Carmody, L.C., Voltz, J.W., Connor, J.H., Li, S., Smith, F.D., Milgram, S.L., Colbran, R.J., and Shenolikar, S. (2002). The neuronal actin-binding proteins, neurabin I and neurabin II, recruit specific isoforms of protein phosphatase-1 catalytic subunits. J Biol Chem *277*, 27716-27724.

Tighe, A., Staples, O., and Taylor, S. (2008). Mps1 kinase activity restrains anaphase during an unperturbed mitosis and targets Mad2 to kinetochores. The Journal of Cell Biology *181*, 893-901.

Tipton, A.R., Wang, K., Link, L., Bellizzi, J.J., Huang, H., Yen, T., and Liu, S.-T. (2011). BUBR1 and Closed MAD2 (C-MAD2) Interact Directly to Assemble a Functional Mitotic Checkpoint Complex. Journal of Biological Chemistry *286*, 21173-21179.

Tong, A.H.Y., Lesage, G., Bader, G.D., Ding, H., Xu, H., Xin, X., Young, J., Berriz, G.F., Brost, R.L., Chang, M.*, et al.* (2004). Global mapping of the yeast genetic interaction network. Science *303*, 808-813.

Trinkle-Mulcahy, L., Andersen, J., Lam, Y.W., Moorhead, G., Mann, M., and Lamond, A.I. (2006). Repo-Man recruits PP1 gamma to chromatin and is essential for cell viability. The Journal of Cell Biology *172*, 679-692.

Trinkle-Mulcahy, L., Andrews, P.D., Wickramasinghe, S., Sleeman, J., Prescott, A., Lam, Y.W., Lyon, C., Swedlow, J.R., and Lamond, A.I. (2003). Time-lapse imaging reveals dynamic relocalization of PP1gamma throughout the mammalian cell cycle. Mol Biol Cell *14*, 107-117.

Trinkle-Mulcahy, L., Sleeman, J.E., and Lamond, A.I. (2001). Dynamic targeting of protein phosphatase 1 within the nuclei of living mammalian cells. J Cell Sci *114*, 4219-4228.

Tsaytler, P., and Bertolotti, A. (2012). Exploiting the selectivity of protein phosphatase 1 for pharmacological intervention. The FEBS journal.

Tsukahara, T., Tanno, Y., and Watanabe, Y. (2010). Phosphorylation of the CPC by Cdk1 promotes chromosome bi-orientation. Nature.

Uchida, K.S.K., Takagaki, K., Kumada, K., Hirayama, Y., Noda, T., and Hirota, T. (2009). Kinetochore stretching inactivates the spindle assembly checkpoint. The Journal of Cell Biology *184*, 383-390.

Vader, G., Cruijsen, C., Van Harn, T., Vromans, M., Medema, R., and Lens, S. (2007). The Chromosomal Passenger Complex Controls Spindle Checkpoint Function Independent from Its Role in Correcting Microtubule Kinetochore Interactions. Mol Biol Cell *18*, 4553.

Vagnarelli, P., Hudson, D.F., Ribeiro, S.A., Trinkle-Mulcahy, L., Spence, J.M., Lai, F., Farr, C.J., Lamond, A.I., and Earnshaw, W.C. (2006). Condensin and Repo-Man-PP1 co-operate in the regulation of chromosome architecture during mitosis. Nat Cell Biol *8*, 1133-1142.

Vagnarelli, P., Ribeiro, S., Sennels, L., Sanchez-Pulido, L., de Lima Alves, F., Verheyen, T., Kelly, D.A., Ponting, C.P., Rappsilber, J., and Earnshaw, W.C. (2011). Repo-Man coordinates chromosomal reorganization with nuclear envelope reassembly during mitotic exit. Dev Cell *21*, 328-342.

van Vugt, M.A.T.M., van de Weerdt, B.C.M., Vader, G., Janssen, H., Calafat, J., Klompmaker, R., Wolthuis, R.M.F., and Medema, R.H. (2004). Polo-like kinase-1 is required for bipolar spindle formation but is dispensable for anaphase promoting complex/Cdc20 activation and initiation of cytokinesis. J Biol Chem *279*, 36841-36854.

Vanoosthuyse, V., and Hardwick, K.G. (2009). A novel protein phosphatase 1-dependent spindle checkpoint silencing mechanism. Curr Biol *19*, 1176-1181.

Vázquez-Novelle, M.D., and Petronczki, M. (2010). Relocation of the chromosomal passenger complex prevents mitotic checkpoint engagement at anaphase. Curr Biol *20*, 1402-1407.

Verdaasdonk, J.S., and Bloom, K. (2011). Centromeres: unique chromatin structures that drive chromosome segregation. Nat Rev Mol Cell Biol *12*, 320-332.

Vigneron, S., Prieto, S., Bernis, C., Labbé, J.-C., Castro, A., and Lorca, T. (2004). Kinetochore localization of spindle checkpoint proteins: who controls whom? Mol Biol Cell *15*, 4584-4596.

Virshup, D.M., and Shenolikar, S. (2009). From promiscuity to precision: protein phosphatases get a makeover. Mol Cell *33*, 537-545.

Walsh, E.P., Lamont, D.J., Beattie, K.A., and Stark, M.J.R. (2002). Novel interactions of Saccharomyces cerevisiae type 1 protein phosphatase identified by single-step affinity purification and mass spectrometry. Biochemistry *41*, 2409-2420.

Wan, X., O'Quinn, R.P., Pierce, H.L., Joglekar, A.P., Gall, W.E., Deluca, J.G., Carroll, C.W., Liu, S.-T., Yen, T.J., McEwen, B.F.*, et al.* (2009). Protein architecture of the human kinetochore microtubule attachment site. Cell *137*, 672-684.

Wang, F., Dai, J., Daum, J.R., Niedzialkowska, E., Banerjee, B., Stukenberg, P.T., Gorbsky, G.J., and Higgins, J.M.G. (2010). Histone H3 Thr-3 phosphorylation by Haspin positions Aurora B at centromeres in mitosis. Science *330*, 231-235.

Wei, R., Ngo, B., Wu, G., and Lee, W.H. (2011). Phosphorylation of the Ndc80 complex protein, HEC1, by Nek2 kinase modulates chromosome alignment and signaling of the spindle assembly checkpoint. Mol Biol Cell *22*, 3584-3594.

Weiss, E., and Winey, M. (1996). The Saccharomyces cerevisiae spindle pole body duplication gene MPS1 is part of a mitotic checkpoint. The Journal of Cell Biology *132*, 111-123.

Welburn, J.P.I., Vleugel, M., Liu, D., Iii, J.R.Y., Lampson, M.A., Fukagawa, T., and Cheeseman, I.M. (2010). Aurora B Phosphorylates Spatially Distinct Targets to Differentially Regulate the Kinetochore-Microtubule Interface. Mol Cell *38*, 383-392.

Westermann, S., Avila-Sakar, A., Wang, H.-W., Niederstrasser, H., Wong, J., Drubin, D.G., Nogales, E., and Barnes, G. (2005). Formation of a dynamic kinetochore- microtubule interface through assembly of the Dam1 ring complex. Mol Cell *17*, 277-290.

Westhorpe, F.G., Tighe, A., Lara-Gonzalez, P., and Taylor, S.S. (2011). p31comet-mediated extraction of Mad2 from the MCC promotes efficient mitotic exit. J Cell Sci *124*, 3905-3916.

Wigge, P.A., Jensen, O.N., Holmes, S., Souès, S., Mann, M., and Kilmartin, J.V. (1998). Analysis of the Saccharomyces spindle pole by matrix-assisted laser desorption/ionization (MALDI) mass spectrometry. The Journal of Cell Biology *141*, 967-977.

Wong, O.K., and Fang, G. (2005). Plx1 is the 3F3/2 kinase responsible for targeting spindle checkpoint proteins to kinetochores. The Journal of Cell Biology *170*, 709-719.

Xia, G., Luo, X., Habu, T., Rizo, J., Matsumoto, T., and Yu, H. (2004). Conformation-specific binding of p31(comet) antagonizes the function of Mad2 in the spindle checkpoint. Embo J *23*, 3133-3143.

Yamagishi, Y., Honda, T., Tanno, Y., and Watanabe, Y. (2010). Two histone marks establish the inner centromere and chromosome bi-orientation. Science *330*, 239-243.

Yang, M., Li, B., Tomchick, D.R., Machius, M., Rizo, J., Yu, H., and Luo, X. (2007). p31comet blocks Mad2 activation through structural mimicry. Cell *131*, 744-755.

Zinkowski, R.P., Meyne, J., and Brinkley, B.R. (1991). The centromere-kinetochore complex: a repeat subunit model. The Journal of Cell Biology *113*, 1091-1110.